Diet-responsive gene networks rewire metabolism in the nematode *Caenorhabditis elegans* to provide robustness against vitamin B12 deficiency

A Dissertation Presented

By

EMMA WATSON

Submitted to the Faculty of the University of Massachusetts Graduate School of Biomedical Sciences, Worcester in partial fulfillment of the requirements for the degree of

DOCTOR OF PHILOSOPHY

SEPTEMBER 17th, 2015

Diet-responsive gene networks rewire metabolism in the nematode *Caenorhabditis elegans* to provide robustness against vitamin B12 deficiency

A Dissertation Presented
By
EMMA WATSON

The signatures of the Dissertation Defense Committee signify completion and approval as to style and content of the Dissertation

_____
Marian Walhout, Ph.D., Thesis Advisor

_____
Victor Ambros, Ph.D., Member of Committee

_____
Oliver Rando, M.D., Ph.D., Member of Committee

_____
Read Pukkila-Worley, M.D., Member of Committee

_____
Dennis Kim, M.D., Ph.D., Member of Committee

The signature of the Chair of the Committee signifies that the written dissertation meets the requirements of the Dissertation Committee

_____
Amy Walker, Ph.D., Chair of Committee

The signature of the Dean of the Graduate School of Biomedical Sciences signifies that the student has met all graduation requirements of the school.

_____
Anthony Carruthers, Ph.D., Dean of the Graduate School of Biomedical Sciences

Program in Systems Biology, Interdisciplinary Graduate Program

SEPTEMBER 17th, 2015

DEDICATION

This thesis is dedicated to my mother, Cathy Watson, who taught me how to be brave.

" Nothing in life is to be feared,

it is only to be

understood. "

~Marie Curie

ACKNOWLEDGEMENTS

This thesis would not have been possible without the guidance from my advisor, the support from my talented colleagues and collaborators, and the love from my friends and family.

First I'll acknowledge several lab mates and collaborators who were instrumental in this work. I'll start with Lesley MacNeil, a brilliant geneticist who taught me everything I know in the lab, from how to collect worm eggs to how to think about genetic interaction data. We worked together towards the same goals, each taking a different path through the forest of biological complexity to cover more ground. It worked out brilliantly! She proverbially taught me to fish, with genetic screens, though I preferred when she would just buy me fish, on our many outings to Baba Sushi. I wish Lesley the best of luck in her new PI post – I know she will do great things.

I'll also acknowledge Michael Hoy for all of his hard work and ingenuity when we were faced with challenges of biblical proportions in the lab – like when we had to grow 6 million worms for mass spec experiments. Mike's sense of humor kept me from giving up on the project on several occasions.

Safak Yilmaz has had a huge influence on the way I think about metabolism and has opened my eyes to the world of possibility that is metabolic modeling. Safak has generously offered his time and effort to several projects, in really important ways – for instance, when he reconstructed a bacterial genome from scratch like it was no big deal. Safak's sense of humor also kept me from

burning down the lab on several occasions – interesting fact, once Safak accidentally almost burned down the lab (ok I'm exaggerating… slightly).

Ashlyn Ritter was kind enough to help me out when we needed lifespans for a paper. I'll never forget meeting up in lab, tapping worms' heads at 3AM to count the dead one last time before we flew to L.A. for worm meeting. She taught me what it takes to run endurance experiments. Amy Holdorf, who has been helping us with the propionate shunt project even though she has a million other things to do, has inspired me to persevere through adversity, and to always keep rocking. I'd also like to acknowledge Chi-Hua, a new member of the lab and a very diligent worker, who generated a CRISPR mutant for our paper in record speed, which was greatly appreciated. I'll also mention Juan Fuxman Bass, my bay-mate, who has always been eager to offer advice, support, and help with statistics – he also laughs at my jokes, which I am grateful for. I also want to acknowledge Gabby Giese, who keeps the lab from falling apart, and who has been very patient with my messy desk etc, and who has also been very patient with my dog, Beni, on several occasions when she cared for him – including that one time when he got loose and became famous in the town of Sutton.

There were several collaborators who helped us with targeted metabolomics experiments, who were excessively patient with us. Amy Caudy and Adam Rosebrock at the University of Toronto worked masterfully to measure vitamin B12 levels in our various bacterial species and mutants, and Maria Olin-Sandoval and Markus Ralser figured out how to extract and quantify a difficult-to-

measure intermediate metabolite called 3-hydroxypropionate (3-HP) from *C. elegans*. Vicky Yao and Olga Troyanskaya helped us with bioinformatics that pointed us in the right direction when trying to find the genes downstream of 3-HP in our pathway, which was like trying to find two needles in a genome-scale haystack. The cooperative spirit embodied by each of our collaborators reminds me that science is a community, and gives me a lot of hope for humanity.

Now I'll acknowledge my family and friends, who make me who I am. My brother Anthony (aka "A-Wat") and sister Gina (aka "Ice Plan") have been cheering me through grad school, and I hope that I can make them proud, and maybe even convince them that I'm cool (but probably not). My dad, Ian, taught me the very important lesson that hard work is the key to everything – he taught me how to blaze my own trail and be self-sufficient. At the same time, if I asked him to fly 1000 miles to help me put up blinds, he would drop everything and be here the next day with tools – this actually happened one time. My best friends Shawna and Cara have also always been there for me – like all those times we chatted about experiments over beer or, when experiments weren't working, over bourbon. And of course, my husband Nate Wilson has been a continuous source of support, motivation, and most importantly – hilarious one-liners. He is the most creative person I know, so naturally he is the person who inspires me the most.

Finally I'll acknowledge my advisor, Marian Walhout, who gave me a chance when I walked into her office 5 ½ years ago, despite me knowing nothing about worms, genetics, or systems biology. I first met Marian after she gave a

lecture on systems biology during my first year of graduate school, which opened my eyes to the world of biological networks. I also thought she had a great sense of fashion. Marian's fearless attitude about science made me feel bold enough to try anything, to do wild experiments, and to follow my instinct. Her confidence and trust in me translated into self-confidence, and I quickly achieved success in the lab. She taught me how to work thoroughly, but also efficiently, and how to harness the power of collaboration. She taught me how to have a scientific debate, and how to communicate science. She taught me how to challenge ideas, and in doing so, taught me how to develop good ones.

ABSTRACT

Maintaining cellular homeostasis is a complex task, which involves monitoring energy states and essential nutrients, regulating metabolic fluxes to accommodate energy and biomass needs, and preventing buildup of potentially toxic metabolic intermediates and byproducts. Measures aimed at maintaining a healthy cellular economy inherently depend on the composition of nutrients available to the organism through its diet. We sought to delineate links between dietary composition, metabolic gene regulation, and physiological responses in the model organism *C. elegans*.

As a soil-dwelling bacterivore, *C. elegans* encounters diverse bacterial diets. Compared to a diet of *E. coli* OP50, a diet of *Comamonas aquatica* accelerates *C. elegans* developmental rate, alters egg-laying dynamics and shortens lifespan. These physiological responses are accompanied by gene expression changes. Taking advantage of this natural, genetically tractable predator-prey system, we performed genetic screens i) in *C. elegans* to identify regulators of diet-responsive genes, and ii) in *E. coli* and *Comamonas* to determine dietary factors driving transcriptional responses in *C. elegans*. We identified a *C. elegans* transcriptional program that regulates metabolic genes in response to vitamin B12 content in the bacterial diet. Interestingly, several B12-repressed metabolic genes of unknown function are highly activated when B12-dependent propionyl-CoA breakdown is impaired, and inactivation of these genes

renders animals sensitive to propionate-induced toxicity. We provide genetic and metabolomic evidence in support of the hypothesis that these genes form a parallel, B12-independent, β-oxidation-like propionate breakdown shunt in *C. elegans,* similar to the pathway utilized by organisms like yeast and plants that do not use vitamin B12.

Table of Contents

LIST OF FIGURES

LIST OF TABLES

CHAPTER I: INTRODUCTION

Preface

This introduction chapter is adapted from a review written by myself and Marian Walhout published in the journal *Trends in Endocrinology and Metabolism* in 2014, titled, "*Caenorhabditis elegans* metabolic gene regulatory networks govern the cellular economy." [1]

Introduction

Diet greatly impacts metabolism in health and disease. In response to the presence or absence of specific nutrients, metabolic gene regulatory networks sense the metabolic state of the cell and regulate metabolic flux accordingly, for instance by the transcriptional control of metabolic enzymes. Many diseases are characterized by disruption of metabolic homeostasis, including inborn errors of metabolism (cumulative incidence estimated at 1 in 784 live births [2], as well as multifactorial diseases such as diabetes (2.8% worldwide incidence in 2000, estimated to double by 2030 [3]). For patients with genetic metabolic disorders, diet can be therapeutic or detrimental, depending on the composition and quantities of dietary nutrients and the nature of the metabolic impairment. Diet can also have a primary causal role in diseases such as obesity and type II diabetes [4], however the mechanisms by which diet can lead to metabolic syndrome and insulin resistance are not fully understood.

The bacterivorous nematode *Caenorhabditis elegans* has been used to great effect to elucidate mechanisms of metabolic network regulation. *C. elegans* has similar auxotrophic requirements compared with humans, including the same essential amino acids and vitamins. Additionally, *C. elegans* maintains orthologous metabolic pathways, as well as canonical metabolic regulatory pathways such as insulin signaling and TOR (target of rapamycin) signaling. *C. elegans* provides clear advantages compared to mammals for system-level studies of metabolism. The nematode is small (~1.5 mm), has a transparent body, a short lifespan (~2-3 weeks), and a well-annotated genome [5, 6]. In addition, a variety of genome-wide technologies and resources enable the genome-scale characterization of metabolic phenotypes, for instance in response to dietary changes. These include two genome-wide RNAi libraries [7, 8] and a growing number of deletion mutants generated and maintained by the *Caenorhabditis* Genetics Center (CGC). In addition, large-scale protein-protein and protein-DNA interaction mapping efforts have identified many molecular connections that can be integrated with phenotypic data [9-11]. These tools have in recent years helped researchers gain new insights into metabolic gene regulatory networks.

Several principles have begun to emerge with respect to *C. elegans* metabolic gene regulatory networks – a modular organization of transcription factors (TFs) and targets, an enrichment of nuclear hormone receptors (NHRs) among the transcriptional regulators, feedback between metabolic pathways and

their regulators, and the capacity to sense various metabolite signals, which are dependent on diet and metabolic flux.

Metabolic regulatory networks are enriched for nuclear hormone receptors

Transcriptional regulation provides a major mechanism of metabolic network control, and diet-induced metabolic gene expression changes have been observed in organisms ranging from bacteria to humans. In mammals, many metabolites have regulatory power. For instance, glucose triggers the insulin signaling cascade, which represses the transcription of gluconeogenesis genes [12], and amino acids such as leucine activate the TOR pathway, which controls gene product expression at the translational level [13]. These nutrient-sensing pathways are central to cell survival, growth and proliferation. Other metabolites interact directly with NHRs to modulate their function, such as vitamin A activating the retinoic acid receptor [14], vitamin D activating the vitamin D receptor [15], and free fatty acids and eicosanoids binding to peroxisome proliferator-activated receptor alpha (PPARα) [16]. Aberrant transcriptional control of metabolic pathways and subsequently altered metabolic flux, especially pertaining to fatty acids, are hallmarks of diabetes. Indeed, PPARα, a lipid-sensing NHR that promotes lipid catabolism is a target of anti-diabetic drugs [17].

Interestingly, the NHR family has greatly expanded in nematodes: whereas humans and mice have 48 and 49 NHRs, respectively, the *C. elegans* genome encodes 274 receptors [18]. While ligands have been identified for many

human NHRs, only one ligand has been identified for a *C. elegans* NHR (dafachronic acid, which binds and activates DAF-12 [19, 20]). Thus, all other *C. elegans* NHRs are currently orphan receptors, and the gene targets of the vast majority of NHRs remain undefined. Yeast-one-hybrid assays have identified the repertoire of TFs that can interact with a set of *C. elegans* metabolic gene promoters [21]. These TFs are enriched for NHRs [21], suggesting that, like their mammalian orthologs, *C. elegans* NHRs function in metabolic network control [17].

Protein-DNA interaction networks indicate that the TFs that bind to *C. elegans* metabolic gene promoters tend to separate into densely interconnected modules with overlapping targets [21]. Modularity in biological networks has been proposed to facilitate rapid and robust responses to variable environmental cues [22-25]. In *C. elegans*, the NHR gene family expansion and functional organization into highly interconnected regulatory modules controlling metabolic genes may enable rapid and adaptive metabolic rewiring in response to different conditions, such as diet or environmental toxins. This network organization may provide the animal with a mechanism to ensure robust development and reproductive fitness on diets of highly metabolically diverse bacterial species encountered in its natural habitat (**Figure 1.1**). The current state of knowledge regarding *C. elegans* NHRs in metabolic regulatory roles is reviewed in **Table 1.1**, and several examples are discussed throughout this review.

The role of diet in regulating the metabolic network

C. elegans can be found in temperate climates around the world and is likely to encounter a wide variety of bacterial species in its natural habitat [26]. Therefore, the worm must adjust to potentially large differences in macro- and micronutrients provided by different bacterial diets. *C. elegans* exhibit a range of differences in life history traits, including development rate, fecundity and lifespan, when fed different bacteria [27-30]. For instance, animals fed the soil bacterium *Comamonas* DA1877 develop faster, have fewer progeny, and a shorter lifespan than animals fed the standard *E. coli* OP50 diet. Gene expression profiling of *C. elegans* fed different bacterial diets revealed an enrichment of metabolic genes among differentially expressed genes [29, 31]. The promoter of one of the *Comamonas*-repressed transcripts corresponding to the metabolic gene *acdh-1* was also repressed by the *Comamonas* diet using a transgenic GFP reporter [29], suggesting that the transcriptional regulation of metabolic genes in response to diet may be an important regulatory mechanism.

Relatively little is known about the mechanisms that govern the regulation of *C. elegans* metabolic genes in response to different bacterial diets, or how these changes lead to physiological changes in the animal. To dissect these mechanisms, it is pertinent to: (i) identify which *C. elegans* genes are involved in mediating a dietary response; (ii) determine which bacterial nutrients or metabolites drive the response; and (iii) characterize diet-specific phenotypes for

metabolic and regulatory gene mutants to determine the biological significance of metabolic rewiring events.

(i) Identifying *C. elegans* genes that control the metabolic response to diet

Genetic screens can be used to reveal *C. elegans* factors that control the expression of metabolic genes in response to diet. For instance, genome-scale RNAi and mutagenesis screens can be performed using transgenic animals that express green fluorescent protein (GFP) under control of a diet-responsive gene promoter. Unbiased, reporter-based screening approaches identified factors responsible for the transcriptional activation of xenobiotic metabolism genes in response to specific xenobiotic compounds [32], the repression of xenobiotic metabolism genes under normal conditions [33], and the induction of triglyceride lipases in response to starvation [34]. NHRs have also emerged as important mediators in the response of drug metabolism genes to toxic xenobiotic compounds. For instance, *nhr-176* is required for inducing expression of the cytochrome P450 *cyp-35d1* specifically in response to thiabendazole, an antifungal/antiparasitic drug. Interestingly, knockdown of *nhr-176* by RNAi negatively affects fertility when animals are exposed to thiabendazole, but not under normal conditions [32]. In humans, NHRs including the pregnane X receptor (PXR) and constitutive androstane receptor (CAR) are known to play pivotal roles in the induction of detoxifying cytochrome P450's by xenobiotic compounds [35].

(ii) Identifying metabolite signals that drive responses to different bacterial diets

Bacterial nutrients that induce a response in *C. elegans* can be identified in different ways. For instance, metabolomics might reveal differences in nutrient levels between bacterial diets. However, the number of metabolites that can be measured is rather limited and usually there are multiple differences in nutrient levels, thus identifying the key nutrients driving physiological responses in *C. elegans* is difficult (see below for more discussion on Metabolomics). Another approach is to identify mutant bacterial strains that, when fed to *C. elegans* elicit a distinct response from the wild type diet. For instance, a strain of *E. coli* HT115 with a spontaneous mutation in the *aroD* gene was serendipitously found to extend lifespan when fed to *C. elegans*. This mutation reduces bacterial folate synthesis, which extends lifespan in *C. elegans* [36]. Similarly, by feeding a nitric oxide synthase-deficient *Bacillus subtilis* strain and comparing the effects to a wild type *Bacillus subtilis* diet, it was discovered that bacterially supplemented nitric oxide can impact *C. elegans* longevity [37]. Possibilities for unbiased screening of bacterial mutants are emerging, as bacterial mutant libraries such as the *E. coli* Keio collection have recently been developed [38, 39].

(iii) Characterizing diet-specific phenotypes

Diet-specific phenotypes have been characterized for metabolic gene mutants [31, 40, 41], and can indicate differential requirements for metabolic pathways on different diets. One metabolic gene with a diet-specific phenotype is *alh-6*, which is involved in the breakdown of proline. *alh-6* mutants exhibit normal lifespan

when fed *E. coli* HT115, but exhibit reduced lifespan when fed *E. coli* OP50 or *E. coli* HT115 supplemented with excess proline [40]. Knockdown of the enzyme directly upstream of *alh-6*, *prodh*, eliminated the negative effect of proline on *alh-6* mutant longevity [40]. This suggests that the proline breakdown intermediate and *alh-6* substrate 1-pyrroline-5-carboxylate (P5C) builds up in the *alh-6* mutant, and negative affects longevity in these animals [40].

Diet-specific phenotypes have not only been observed for metabolic genes but also for the regulators of metabolic genes. A diet-specific phenotype can indicate a role for that particular regulator in diet-induced metabolic rewiring. For instance, *nhr-114*, which targets stress response and detoxification genes (including cytochrome P450's, UDP-glucuronosyltransferases and glutathione S-transferases) and lipid metabolism genes (*lipl-2*, *acs-10*) [42], was identified in an RNAi screen for factors that are necessary for germline development [42]. Surprisingly, the associated sterility phenotype was diet-dependent: *nhr-114* mutants fed *E. coli* OP50 were sterile, while mutants fed *E. coli* HT115 were not [42]. Fertility could be restored in *nhr-114* mutants fed *E. coli* OP50 if the diet was supplemented with tryptophan [42]. The rescue by tryptophan is likely due to its conversion by *E. coli* to another as-yet-undetermined bacterial metabolite, as its effect required a living bacterial diet [42].

nhr-8 was also identified in an RNAi screen, this time for enhancers of *daf-36* null mutants, which have reduced dafachronic acid (DA) production and thus impaired *daf-12* function [43]. *nhr-8* mutants exhibit decreased DA production,

enhanced dauer formation and gonad migration defects, and these phenotypes are mitigated by dietary cholesterol supplementation [43]. Gene expression profiling of *nhr-8* mutants revealed differences in lipid and DA metabolism gene expression [43], indicating a regulatory role in maintaining adequate levels of DA synthesis genes that utilize cholesterol as a precursor. Future studies will be required to determine whether *nhr-8* and *nhr-114* are ligand-gated, and whether their ligands are diet-derived.

Metabolomics, transcriptomics, and proteomics– towards understanding regulatory consequences to metabolic flux

The goal of regulating a metabolic gene is to regulate flux through the pathway in which the enzyme encoded by the gene functions. However, not all enzymes are regulated at the level of transcription; many can be regulated allosterically or by post-translational protein modifications. Thus, more directly measuring protein and metabolite levels may be required to uncover the outputs of transcriptional, allosteric and protein-modification changes.

Metabolomics is the simultaneous quantification of many different metabolites in a biological sample. Current technologies enable several hundred metabolites to be detected from biological samples, which is impressive considering the chemical diversity of these molecules. However, it only represents a small fraction of the thousands of metabolites present in the cell. In *C. elegans*, metabolomics using mass spectrometry and/or nuclear magnetic resonance (NMR) spectroscopy has uncovered metabolic signatures of insulin

receptor (*daf-2)* mutants [44-46], a peptide transport (*pept-1*) mutant [45], a histone deacetylase (*sir-2.1*) mutant [46, 47], mitochondrial mutants (*isp-1, clk-1*, *mev-1, ucr-2.3, gas-1*) [46, 48, 49], a TCA cycle (*idh-1*) mutant [46], fatty acid synthesis mutants (*fat-5*, *fat-6*, *fat-7*) [50], as well as wild type animals exposed to anoxic conditions [51]. For metabolic gene mutants, metabolomic profiling can shed light on the block caused by the lack of enzymatic function and its rippling effects throughout the metabolic network. For instance, aqueous and lipid fraction profiling of Δ9 desaturase mutants required for monounsaturated fatty acid (MUFA) synthesis revealed that a lack of these enzymes had far-reaching effects beyond just decreases in MUFAs, and the overall trend was a shift towards a catabolic state [50].

Integration of metabolomic data with transcriptomic and proteomic data can provide a more complete picture of how metabolic gene regulation affects metabolic flux. For instance, proteomic analysis of a peptide transport mutant, *pept-1 (lg601)*, revealed 23 proteins with significantly altered abundance compared to wild type, and four of these were methionine/SAM cycle enzymes, which were all downregulated in the mutant. Metabolomics revealed increased homocysteine and decreased methionine levels accompanying the downregulation of methioine/SAM cycle enzyme expression, indicating reduced flux through this metabolic pathway in *pept-1* mutants [45].

One major challenge when interpreting metabolomics data is overcoming variability that naturally arises within a population of animals and across

experiments. In the study of various MUFA synthesis mutants (*fat-5*, *fat-6*, *fat-7*) the major principle component explaining the largest portion of sample variance in the metabolomics data was not genotype, but rather batch effects [50]. Two studies found that, surprisingly, the metabolomic differences between cohorts of wild type *C. elegans* fed two different *E. coli* strains (OP50 and HT115) were equal to, or greater than the metabolomic differences caused by perturbing *daf-2*/insulin signaling [46, 52]. This suggests that *C. elegans* metabolic profiles are exquisitely sensitive to differences in diet and environment, as well as to genotypic differences. These two *E. coli* diets were previously shown to have different carbohydrate content, but similar protein and fat content [53], however differences in micronutrient content are yet to be determined. Importantly, since wild type animals fed *E. coli* OP50 and those fed *E. coli* HT115 are more-or-less equally fit [29], yet have different metabolomic and transcriptomic profiles [29], we can hypothesize that *C. elegans* may have a range of homeostatic metabolic states that are conducive to healthy development, reproduction and aging.

Concluding remarks

C. elegans is a powerful model to study metabolic regulatory networks, and how they connect diet to gene expression and physiology. The nematode is extremely well suited to provide valuable insights into mammalian metabolic networks, as its core metabolic pathways share significant homology to their human counterparts. *C. elegans* and mammals also share a similar suite of nutrient auxotrophies and thus dietary requirements. Its amenability to genetic

manipulation and high content “omics” data generation makes *C. elegans* a valuable tool in the study of gene networks. Reverse genetics approaches, such as high-throughput RNAi screening with genome-wide or targeted mini-libraries, have been applied to the task of identifying members of metabolic gene regulatory networks. With the emergence of transgenic tools that report transcriptional responses to different diets or metabolites, used in conjunction with high-throughput screening, researchers will be able to map the gene networks responsible for sensing the metabolome and transmitting that information to the genome. Additionally, bacterial mutant collections like the *E. coli* Keio deletion library can be used to identify components within the diet that affect *C. elegans* physiology or metabolic gene expression, in an unbiased fashion.

Figures

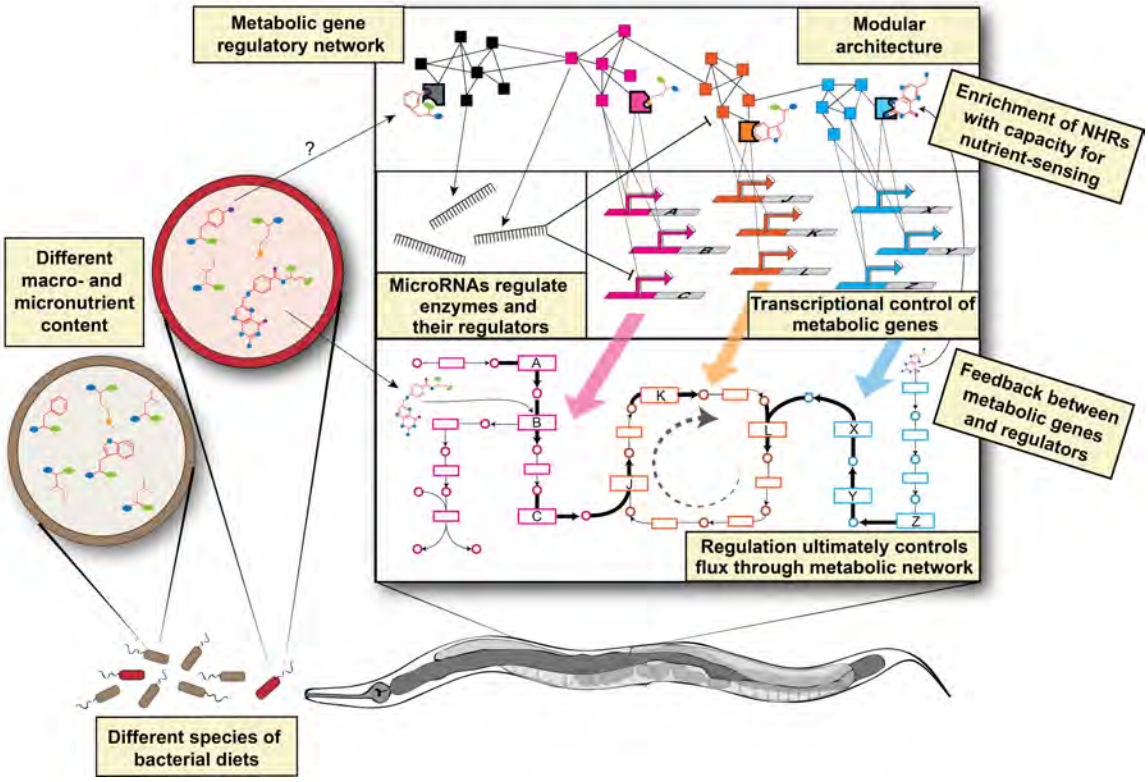

Figure 1.1 – *C. elegans* metabolic gene regulatory networks.
Model illustrating principles of metabolic regulation in the worm. *C. elegans* likely encounters a wide variety of bacterial diets with different nutrient composition in the wild. These nutritional differences trigger transcriptional changes in metabolic genes, mediated by gene regulatory networks enriched for NHRs. Yeast one-hybrid studies have revealed that metabolic gene regulatory networks are highly modular, which may ensure the rapid and coordinated response of metabolic pathways to environmental cues. Metabolic genes can also be regulated post-transcriptionally by microRNAs. Feedback between NHRs and metabolic pathways via metabolite signals may be an important mechanism for regulating metabolic flux and maintaining cellular homeostasis on diverse diets.

NHR	Ref.	Metabolic Targets	Physiological Role
daf-12	[54, 55]	TCA cycle enzymes (e.g. *cts-1*, *aco-1*)*; Fatty acyl-transferases (e.g. *acl-1*, *acl-2* & *acl-4*)* short-chain dehydrogenases/ reductases (e.g. *dhs-21* & *dhs-26)*	Required for proper developmental timing; mutants are heterochronic
nhr-8	[43]	Sterol, lipid and dafachronic acid metabolism genes	On cholesterol-deficient diets, *nhr-8* partial loss-of-function mutants display enhanced dauer formation, gonad migration defects, and larval arrest at high temperatures
nhr-176	[32]	*cyp-35d1*	Knockdown of *nhr-176* causes reduced fertility when animals are exposed to thiabendazole
nhr-49	[56, 57]	fatty acid metabolism genes	Impairment of *nhr-49* results in a high fat phenotype and reduced lifespan, as well as decreased oxygen consumption rates and abnormal mitochondrial morphology.
nhr-80	[57-59]	Fatty acid desaturases *fat-5*, *fat-6* and *fat-7*	Required for increased lifespan induced by loss of the germline; also required for proper mitochondrial morphology and oxygen consumption. Binds *nhr-49* and has overlapping targets.
nhr-66	[57]	Sphingolipid and lipid remodeling genes; carbohydrate metabolic processes	Mutants exhibit reduced basal oxygen consumption and beta-oxidation rates. Binds *nhr-49* and has overlapping targets.
nhr-62	[60]	Fatty acid localization and transport genes	Regulates dietary restriction (DR)-induced genes; overexpression leads to DR-like phenotypes such as small body size, reduced fat and increased longevity
nhr-40	[61, 62]	Lipid binding proteins, ATPases, glycolysis and TCA cycle genes	Required for larval development
nhr-114	[42]	Stress response and detoxification genes and some lipid metabolism genes	Mutant is sterile on the *E. coli* OP50 diet, but fertile on the *E. coli* HT115 diet. Sterility on *E. coli* OP50 is rescued by a tryptophan-derived *E. coli* metabolite
nhr-64	[63]	Fatty acid metabolism genes	Knockdown partially suppressed the developmental delay caused by *sbp-1* mutation. Also partially suppressed developmental delay and reduced fertility of *fat-6;fat-7* double mutant.

*Representative targets of DAF-12 from enriched metabolic GO categories based on ChIP data

Table 1.1 – Nuclear Hormone Receptors that regulate *C. elegans* metabolism

CHAPTER II: INTEGRATION OF METABOLIC AND GENE REGULATORY NETWORKS MODULATES THE *C. ELEGANS* DIETARY RESPONSE

Preface

This research chapter derives from work that Lesley MacNeil and I started in 2010, based on an observation by Efsun Arda that the *Pacdh-1::GFP* transgene was expressed differently on *E. coli* HT115 vs *E. coli* OP50. This prompted Lesley MacNeil to test the transgene on other diets, and found the dramatic effect elicited by *Comamonas* DA1877. Lesley and I worked closely to characterize the response of *C. elegans* to *Comamonas*, and this chapter is adapted from our 2013 publication in *Cell* titled "Integration of metabolic and gene regulatory networks modulates the *C. elegans* dietary response." [64] In this work, Lesley and I share first authorship, and the other authors on the paper are Efsun Arda, Julie Zhu, and Marian Walhout.

Lesley is responsible for the content of Figures 2.1 and 2.2, and Table 2.1, which describe the results of the EMS screen and mutant mapping, sequencing, and characterization, which were done by Lesley. Lesley is also responsible for Figure 2.9c, d, and e, and Table 2.4, which describe the gene expression changes observed in Δ*pcca-1* and Δ*metr-1* mutants. Julie Zhu analyzed the raw microarray data for these experiments, and helped map the genome sequencing data. Lesley and I worked jointly to generate the data in Figure 2.11a.

Abstract

Expression profiles are tailored according to dietary input. However, the networks that control dietary responses remain largely uncharacterized. Here, we combine forward and reverse genetic screens to delineate a network of 184 genes that affect the *C. elegans* dietary response to *Comamonas* DA1877 bacteria. We find that perturbation of a mitochondrial network comprised of enzymes involved in amino acid metabolism and the TCA cycle affects the dietary response. In humans, mutations in the corresponding genes cause inborn diseases of amino acid metabolism, most of which are treated by dietary intervention. We identify several transcription factors (TFs) that mediate the changes in gene expression upon metabolic network perturbations. Altogether, our findings unveil a transcriptional response system that is poised to sense dietary cues and metabolic imbalances, illustrating extensive communication between metabolic networks in the mitochondria and gene regulatory networks in the nucleus.

Introduction

To maintain homeostasis, a cell must be able to sense its own energy state, assess nutrient availability, and modulate metabolic pathways in a coordinated fashion. Organisms utilize and integrate endocrine, allosteric and transcriptional mechanisms to respond to nutrients and activate or repress appropriate metabolic pathways accordingly. Different diets provide nutrients in different proportions and affect the transcription of metabolic genes in different ways.

Dramatic changes in gene expression occur following dietary shifts in *C. elegans*, *D. melanogaster* and *M. musculus* [29] [65, 66].

Ensuring optimal metabolic tuning to complex dietary signals requires integration of nutrient sensors and their downstream targets to produce a coherent response. Studies in yeast have revealed co-expression of metabolic enzymes as a central mechanism of nutrient response. For example, the yeast TF Gcn4 activates enzymes involved in amino acid synthesis upon amino acid starvation [67]. This type of coordinated, need-based metabolic transcriptional response to nutrients is an important mechanism in yeast, but the extent to which it occurs in more complex multicellular organisms, remains largely unknown.

Inborn errors of metabolism are relatively rare recessive disorders that are characterized by a buildup of metabolites that cannot be processed and/or a lack of metabolites required for basic cellular processes [68]. Patients with such diseases can display a variety of symptoms such as failure to thrive, developmental delay and seizures [69]. These diseases are often clinically managed by altering the patient's diet to avoid buildup of toxic metabolites and to supplement limiting nutrients. For example, maple syrup urine disease, a disorder in which patients fail to catabolize the branched chain amino acids (BCAAs) leucine, isoleucine or valine, is managed by limiting the intake of protein-rich foods.

The nematode *C. elegans* is a free-living bacterivore that is a genetically tractable model instrumental in understanding mechanisms relating to human

disease. For instance, genome-scale RNA interference (RNAi) resources have been used to identify essential genes [7, 70], genes affecting fat storage [71], and other processes. Further, the animal is transparent, which has enabled the use of the green fluorescent protein (GFP) to monitor spatiotemporal gene expression in living animals [72-75]. The core metabolic networks and major nutrient sensing pathways, including insulin and TOR, are highly conserved between *C. elegans* and humans. However, the transcription factor (TF) family of nuclear hormone receptors (NHRs) that regulate metabolic gene expression has greatly expanded, with a total of 271 members, compared to 48 in humans [76, 77]. NHRs function as ligand-gated TFs and are postulated to provide the animal with a repertoire of responses to different environmental conditions [78, 79].

C. elegans exhibits an altered gene expression profile when fed a bacterial diet of *Comamonas* DA1877 compared to the standard laboratory diet of *E. coli* OP50, and these changes are accompanied by altered life-history traits such as developmental rate, number of offspring and lifespan [29]. The metabolic gene *acdh-1* exhibits the most dramatic change in expression between these diets. We developed a ‘dietary sensor’ strain comprising the *acdh-1* promoter driving the expression of GFP: when fed the standard laboratory diet of *E. coli* OP50 GFP expression is high, but on a *Comamonas* DA1877 diet GFP expression is dramatically reduced.

Here, we perform forward and reverse genetic screens to identify genes that can alter the transcriptional response to diet. We identify 184 genes,

including 146 ‘activators’ and 38 ‘repressors’. Most of the 38 repressors encode enzymes that function within four mitochondrial metabolic pathways: BCAA breakdown, methionine metabolism, glycine cleavage system, and the TCA cycle. Human orthologs of most of the dietary response repressors confer inborn diseases of amino acid metabolism when mutated. In addition to *acdh-1*, the transcription of several other metabolic genes from these four pathways is modulated in response to both diet and metabolic network perturbations. These genes represent two modules that exhibit reciprocal behavior – one module, which includes *acdh-1*, is repressed by *Comamonas* DA1877 but activated by specific metabolic network perturbations, while the other is activated by *Comamonas* DA1877 but repressed by these metabolic network perturbations. We identify the TFs SBP-1, NHR-10 and NHR-68 as candidate mediators of the response to metabolic perturbations. Taken together, we uncover extensive communication between mitochondrial metabolic networks and nuclear gene regulatory networks, which may serve to optimize metabolic flux under different dietary and/or metabolic conditions.

Results

A Forward Genetic Screen for Repressors of the Dietary Sensor *Pacdh-1::GFP*

Animals harboring the *Pacdh-1::GFP* dietary sensor display much lower levels of GFP expression when fed *Comamonas* DA1877 than when fed the standard laboratory diet of *E. coli* OP50 [29]. ACDH-1 has been annotated as an acyl-CoA dehydrogenase involved in beta-oxidation of short chain fatty acids [80], and as a

short branched chain acyl-CoA dehydrogenase involved in BCAA breakdown [81]. Sequence comparison of the ACDH-1 protein with the human ACADSB enzyme (which functions in BCAA breakdown) and the human SCAD enzyme (which functions in beta-oxidation) indicates that ACDH-1 more closely resembles ACADSB (**Figure 2.1**).

We performed a forward genetic screen to identify genes that, when mutated, cause activation of the *acdh-1* promoter on a *Comamonas* DA1877 diet. We mutagenized the dietary sensor strain, screened ~10,000 genomes and isolated 45 fertile F2 mutants that produced GFP positive offspring (**Figure 2.2a**). These mutants varied in both level and pattern of GFP expression. For example, some mutants displayed relatively broad expression in the intestine, hypodermis and muscle, while others express GFP only in the intestine (**Figure 2.2b, Table 2.1**). We mapped 20 mutations to four chromosomes. Five mutants were selected for whole genome sequencing, one from each linkage group and one additional mutant from linkage group IV. We identified five mutations in four genes: *mmcm-1*, *pccb-1*, F32B6.2 and F25B4.1, all of which encode mitochondrial metabolic enzymes: *mmcm-1* encodes methylmalonyl-CoA mutase, *pccb-1* encodes the beta subunit of propionyl-CoA carboxylase and F32B6.2 encodes an ortholog of alpha methylcrotonoyl-CoA carboxylase. These three proteins are all involved in BCAA breakdown. The fourth gene, F25B4.1, encodes the T-protein of the glycine cleavage system. We have named F32B6.2 '*mccc-1'* and F25B4.1 '*gcst-1'* to reflect these annotated biochemical functions.

By complementation tests and sequencing we identified additional alleles of three of the four genes (**Figure 2.2c**).

To verify that the mutations truly affect the expression of *acdh-1,* we examined endogenous mRNA levels in four mutants. When grown on *Comamonas* DA1877, all mutants showed an increase in *acdh-1* mRNA levels relative to wild type animals, which confirms the results obtained with the dietary sensor (**Figure 2.2d,** orange bars). We found similar changes in expression of two other diet-responsive genes, *acdh-2* and *ech-6* in these mutants (**Figure 2.2d**, and data not shown). When fed *E. coli* OP50, the expression of these genes was similar in wild type and mutant animals (**Figure 2.2d**, purple bars), demonstrating that the mutations do not cause a general increase in their expression. In three of the four mutants the expression of *acdh-1* was lower on *Comamonas* DA1877 than on *E. coli* OP50, indicating that, they are still somewhat able to respond to dietary cues (**Figure 2.2d**, compare orange and purple bars). The dietary response was completely impaired only in the *mmcm-1(ww5)* mutant (**Figure 2.2d**).

The *acdh-1* promoter not only responds to different bacterial diets, but is also repressed upon starvation [29, 80]. We tested the response to starvation in our mutants. When starved for 24 hours, *mccc-1(ww4)* mutant animals retain GFP expression, which indicates that the starvation response is impaired in these mutants as well. In contrast, in *mmcm-1*, *pccb-1* and *gcst-1* mutants GFP expression was reduced, indicating that the response to starvation is retained

(**Figure 2.2e**). *mmcm-1(ww5)* mutants are completely impaired in the dietary response (**Figure 2.2d**), but retain a starvation response, confirming our observation that these two responses are distinct [29]. Altogether, these observations show that the dietary sensor can respond not only to diet but also to endogenous metabolic network perturbations.

A Genome-Scale RNAi Screen For *Pacdh-1::GFP* Activators and Repressors

To identify additional genes that can affect the dietary sensor, we explored the use of RNAi by feeding, which is carried out in *E. coli* HT115 bacteria [82]. When fed *E. coli* HT115, the *Pacdh-1::GFP* animals express intermediate levels of GFP, enabling us to identify both dietary sensor repressors and activators. In addition, we took advantage of the fact that *Comamonas* DA1877 can be diluted and still repress the dietary sensor [29]. Adding a small amount of *Comamonas* DA1877 to the *E. coli* HT115 RNAi feeding lawn repressed the dietary sensor, while maintaining RNAi knockdown efficiency (**Figure 2.3a**). This enabled us to perform a genome-scale RNAi screen in the presence of *Comamonas* DA1877 (**Figure 2.3b**).

We screened the ORFeome RNAi library, which covers more than half of all predicted protein-coding genes [83]. After screening the library once in each dietary condition, we obtained 836 hits (8%, **Figure 2.3b**). These hits were re-arrayed and retested four times to remove false positives. The 554 genes that re-scored in at least two of four retests were considered further. This list of hits contained many genes involved in general protein expression that may not

specifically affect the dietary sensor. To identify such potential false positives, we screened the 554 hits against another transgene, *Pmir-63::GFP* that also expresses GFP in the intestine, but is not sensitive to *Comamonas* DA1877 (**Figures 2.3a, 2.3b**). We retained 179 high-confidence hits (~2% of the genes tested). Of these, 146 caused a decrease in GFP expression (activators), while 33 caused an increase (repressors) (**Table 2.2**).

We retrieved *nhr-10* and *mdt-15,* known activators of *acdh-1* [78], as well as two of the genes (*mccc-1* and *gcst-1*) found in the forward genetic screen. The other two genes (*mmcm-1* and *pccb-1*) were not retrieved, although they were present in the RNAi library. This could be due to the inherent variability and the relatively high false negative rate of RNAi experiments [7]. Indeed, when we retested these clones in a small-scale, directed RNAi experiment we found that their knockdown does increase GFP expression (data not shown).

RNAi Screen Validation

To verify that the genes found by RNAi affect endogenous *acdh-1* expression, we used quantitative RT-PCR (qRT-PCR) in wild type (N2) animals subjected to RNAi of 11 representative genes found in the screen. As shown in **Figure 2.3c**, the qRT-PCR recapitulated what was observed in the *Pacdh-1::GFP* dietary sensor strain for all 11 knockdowns.

We obtained *C. elegans* mutant strains for several genes found in the RNAi screen, including the TFs *nhr-68* and *hlh-11*, and the enzymes ZK669.4, *sams-5, sams-1* and *metr-1* (**Figure 2.4**). We introduced each mutation into the

Pacdh-1::GFP dietary sensor strain and examined GFP levels on *E. coli* OP50 and *Comamonas* DA1877 (**Figure 2.3d)**. These mutants exhibited GFP expression levels that recapitulate the effects observed by RNAi: mutations in the enzymes and *hlh-11* all activated GFP expression, whereas a deletion in *nhr-68* decreased GFP expression. Further, we confirmed the increased expression of endogenous *acdh-1* in animals fed *E. coli* OP50 and *Comamonas* DA1877 by qRT-PCR in Δ*hlh-11* and Δ*sams-5* mutant animals (**Figure 2.3e**).

To probe potential functional relationships among the genes discovered in the genetic screens, we assessed their connectedness in WormNet, a probabilistic functional gene network constructed through integration of different data types ([84]. The combined 181 genes found by both the forward and reverse genetic screens are significantly connected in WormNet and form a closely linked functional network (P = 1.97e-78)(**Figure 2.5**). Thus, these 181 genes are more functionally interrelated than would be expected for a random set of genes, supporting the overall quality of the RNAi screen.

Dietary Sensor Activators

The majority (74%) of the 146 activators are expressed in the intestine (**Figure 2.5**), suggesting that they may act cell-autonomously. Gene Ontology (GO) analysis revealed an enrichment for several terms, including ‘growth’, ‘sex differentiation’ and ‘ribosome biogenesis’ (**Figure 2.5**). Several of these genes are predicted to function in a number of biological processes, including general gene expression, splicing and translation, metabolism and the regulation of

transcription (**Figure 2.5**). Since *acdh-1* is also repressed in response to starvation, the dietary sensor strain cannot discriminate between genes involved in, or inducing, a starvation response and those involved in the dietary response. To identify which activators may mediate a starvation response and which may be more specific to the dietary response, we used two additional transgenic strains in which GFP expression is repressed by starvation, but not affected by bacterial diet (*Pgst-4::GFP* and *PC53A3.2::GFP*, **Figure 2.6**). We found 37 activators that affect at least one of these transgenes, 12 of which affected both, indicating that they may induce or mediate a starvation rather than dietary response (**Table 2.3**). The remaining 109 activators were specific to *Pacdh-1::GFP*.

Pacdh-1::GFP Repressors Function in Four Metabolic Pathways

The combined 35 dietary sensor repressors obtained in both screens are enriched for GO terms relating to metabolism, including 'mitochondrion', 'TCA cycle' and 'acetyl-CoA catabolic process' (**Figure 2.5**). Overall, 83% of these are annotated metabolic genes, compared to 15% of the activators, and the vast majority is expressed in the intestine (**Figure 2.5**). Interestingly, most (24) of the repressors encode enzymes specifically involved in four metabolic pathways: BCAA breakdown (n=8), methionine metabolism (n=5), the glycine cleavage system (n=2) and the TCA cycle (n=9)(**Figure 2.7**).

We wondered whether other genes in these pathways that were not retrieved in the genetic screens would affect the dietary sensor as well. We

obtained deletion mutants for two genes involved in BCAA breakdown (*mce-1* and *pcca-1*) and one from the methionine metabolism pathway (*cbl-1*) (**Figure 2.7**). These deletions were introduced into the *Pacdh-1::GFP* dietary sensor strain. Deletions in *mce-1* and *pcca-1* both caused increased GFP expression on all three diets and a deletion in *cbl-1* caused increased GFP on *Comamonas* DA1877 but not on *E. coli* OP50 (**Figure 2.8**). Altogether, these findings indicate that disrupting these four metabolic pathways affects the dietary response to *Comamonas* DA1877. The observation that loss of several individual genes within a common pathway can induce similar changes in the expression of *acdh-1* suggests that these perturbations may converge onto a common regulatory signal.

Interestingly, *acdh-1* itself was found as a repressor in the RNAi screen (**Table 2.2**). We obtained an *acdh-1* deletion mutant and introduced it into the *Pacdh-1::GFP* dietary sensor strain. We observed higher GFP levels in the Δ*acdh-1* mutant relative to the wild type dietary sensor strain when the animals were fed *E. Coli* OP50 or HT115 diets, but less of an increase on a *Comamonas* DA1877 diet. On the latter diet *acdh-1* expression is normally low (**Figure 2.9a**). Thus, feedback on the *acdh-1* promoter occurs mainly on diets where endogenous *acdh-1* levels are normally high, suggesting *acdh-1* expression is regulated according to need.

Cellular metabolic needs are unlikely to be met by modulating the expression of a single enzyme; rather enzymes within a metabolic pathway or

network may need to be coordinately regulated [85]. In addition to *acdh-1*, several other genes predicted to function within BCAA breakdown and methionine metabolism pathways are also transcriptionally regulated in response to diet (**Figure 2.7**) [29]. This suggests that these genes comprise (a) coordinately regulated module(s). We wondered whether these genes were also transcriptionally sensitive to metabolic network perturbation. We examined the expression of seven *Comamonas* DA1877-responsive genes (four from BCAA breakdown, two from methionine metabolism, and one NHR) by qRT-PCR in several mutant strains that exhibit altered *acdh-1* expression (Δ*metr-1,* Δ*sams-1,* Δ*mce-1,* Δ*acdh-1,* Δ*hlh-11* and Δ*nhr-68*). We found that several BCAA breakdown genes, as well as *nhr-68*, are co-induced with *acdh-1* in response to metabolic network perturbation (**Figure 2.9b**). This further supports the modular regulation of these functionally related genes, and indicates that this may perhaps be mediated by *nhr-68* (see below). The expression of *acdh-2,* a close homolog of *acdh-1*, is also increased in an *acdh-1* deletion mutant, which may indicate a compensation mechanism of *acdh-2* for the loss of *acdh-1* function. Interestingly, the *Comamonas* DA1877-induced gene *cbs-1* [29] exhibited opposite behavior compared to the *Comamonas* DA1877-repressed genes as it is repressed in the metabolic gene mutants.

To characterize the transcriptomic response to metabolic gene perturbations in more detail, we performed a microarray expression profiling experiment with two metabolic gene mutants on a *Comamonas* DA1877 diet.

One of these genes, *pcca-1*, functions in BCAA breakdown while the other, *metr-1*, is involved in methionine metabolism. The two mutations elicit highly similar changes in gene expression (**Figure 2.9c**), further suggesting that these two different metabolic mutations may cause similar metabolomic changes that may impinge on a common regulatory signal. Strikingly, most of the core genes that change in response to a *Comamonas* DA1877 diet also exhibited expression changes in one or both metabolic mutants [29] (**Figure 2.9d**). In fact, there are two modules of co-expressed genes that exhibit reciprocal behavior – one that is repressed by a *Comamonas* DA1877 diet but activated in the metabolic gene mutants, and one that is activated by a *Comamonas* DA1877 diet but repressed in the metabolic gene mutants (**Figure 2.9e, Table 2.4**).

Human Orthologs of *Pacdh-1::GFP* Repressors are Involved in Inborn Metabolic Disease

Many metabolic reactions are evolutionarily conserved, and most of the *C. elegans* enzymes found in our genetic screens have human orthologs (**Table 2.2**). Most of these are associated with inborn disorders of amino acid metabolism (**Figure 2.10**). For instance, we identified multiple orthologs of genes that, when mutated in humans, cause maple syrup urine disease, methylmalonic acidemia, homocystinuria or propionic acidemia. These diseases are characterized by toxic buildups of amino acids and intermediate metabolites, and are treated by limiting amino acid (protein) intake and supplementing vitamins and other cofactors (**Figure 2.10**). We also found orthologs of TCA cycle genes

that cause diseases such as lactic acidosis and pyruvate dehydrogenase deficiency. These may also result in the accumulation of intermediate metabolites, or in the inability to generate sufficient amounts of energy (ATP).

Mutations in two *C. elegans* metabolic genes (Δ*metr-1* and Δ*pcca-1*) cause highly similar changes in gene expression (**Figure 2.9c**). *metr-1* is the ortholog of human Methionine synthase (MTR), which when mutated, causes methylcobalamin (vitamin B12) deficiency. *pcca-1* is the ortholog of human PCCA in humans, which when mutated causes propionic acidemia. Our observations suggest that mutations in these genes may result in similar metabolic effects. The human disorders caused by mutations in these genes are treated in part by supplementation with vitamin B12, and both disorders can be revealed by elevated propionylcarnitine levels in newborn screening [86]. This suggests that, as in *C. elegans*, these two human diseases have at least partially overlapping molecular phenotypes.

Limited Involvement of TOR and Insulin Signaling Pathways in Response to Metabolic Network Perturbations

To determine whether known nutrient sensing pathways such as TOR or the Insulin signaling pathway are involved in upregulating *acdh-1* in response to metabolic network perturbations, we performed RNAi on a panel of genes from these pathways in metabolic mutants harboring the *Pacdh-1::GFP* transgene. Knockdown of *daf-2* or *daf-16* had no effect on GFP expression in any of the mutants. We also crossed the Δ*metr-1* and Δ*acdh-1* metabolic mutations into a

transgenic strain expressing a DAF-16::GFP fusion protein to determine whether these metabolic mutants affected DAF-16 nuclear localization, and found that neither had any effect (data not shown). Thus, insulin signaling does not mediate the response to metabolic network perturbations.

The TOR pathway is an attractive candidate for mediating the effects of metabolic perturbations because it affects *acdh-1* in wild type animals and is regulated by amino acid levels, specifically leucine [87]. We tested whether the TOR pathway is involved in mediating the response to endogenous metabolic network perturbations and found limited involvement (**Figures 2.11a, 2.11b**). Knockdown of *rheb-1* or *ruvb-1* reduced GFP levels in most metabolic gene mutants. However, in almost every case GFP was still higher in these mutant strains than in the wild type strain **(Figure 2.11a, 2.11b)**. Therefore it is likely that TOR signaling may be partially involved in, but not solely responsible for, mediating the induction of *acdh-1* in metabolic mutants

Multiple TFs Affect the Response to Metabolic Network Perturbations

In wild type animals, both *nhr-10* and *nhr-23* activate the dietary sensor [29, 78, 88]. In the RNAi screen, we identified additional TFs that affect *acdh-1* expression, most of which are NHRs (**Table 2.2**). We knocked down *nhr-10, nhr-23, nhr-68, nhr-173* and *nhr-74,* as well as *sbp-1* by RNAi in multiple metabolic gene mutants, and examined changes in GFP expression. We observed complex gene regulatory effects of different TFs (**Figures 2.11a, 2.11b**). First, *sbp-1* RNAi resulted in a dramatic decrease in GFP expression in all animals tested,

indicating that SBP-1 might function at the top of the metabolic gene regulatory hierarchy. However, *sbp-1* RNAi also reduced GFP expression in the two starvation-responsive transgenic strains (**Table 2.3**). Previously, SBP-1 has been shown to regulate genes involved methionine metabolism [89]. Altogether, these observations suggest that SBP-1 may be a general regulator of metabolic gene expression in the *C. elegans* intestine. Second, *nhr-23* RNAi has only mild effects on GFP expression in most mutants, whereas it has stronger effects in the wild type sensor strain, suggesting that it primarily controls *acdh-1* expression in response to diet. However, it is important to note that *nhr-23* RNAi was performed under dilute conditions to avoid larval arrest. Third, *nhr-10* and *nhr-68* knockdown dramatically reduces GFP expression in almost all mutants. For example, GFP levels in Δ*mce-1* and Δ*pcca-1* deletion animals are equivalent to those in wild type animals subjected to *nhr-10* or *nhr-68* knock down (**Figure 2.11b**). Therefore *nhr-10* and *nhr-68* may mediate the increase in *acdh-1* expression in response to specific metabolic network perturbations.

Knockdown of *nhr-10* in an *nhr-68* deletion mutant or *vice versa* had little additional effect on GFP expression, indicating that these two NHRs may function together (**Figure 2.11a**). Knockdown of the other NHRs tested, *nhr-173* and *nhr-74,* had mild effects on GFP expression in wild type animals, and had similarly mild effects in the context of metabolic network perturbations. However, knockdown of *nhr-173* further reduces GFP expression in an Δ*nhr-10* deletion mutant, indicating that these NHRs may function in parallel.

Conclusions

We have unraveled a complex network of genes that affect dietary gene expression in *C. elegans*. This network is likely not yet complete for several reasons. First, forward genetics identified mutations in four metabolic genes, and although we have multiple alleles for three of these genes, the screen is not yet saturated. Second, the reverse genetic RNAi screen has not revealed all genes involved, since the ORFeome RNAi library contains only half of all *C. elegans* protein-coding genes [83], and because RNAi screens are prone to a high false negative rate [7]. This is supported by the initial retrieval of only two of the four genes found by forward genetics, and the identification of additional genes through targeted analysis of mutants in the metabolic pathways involved.

We primarily focused on dietary sensor repressors, most of which encode mitochondrial enzymes. We found that these repressors function in an intricate feedback and compensation system that results in regulation of metabolic gene expression. This is perhaps best exemplified by the feedback in which deletion of *acdh-1* results in an increase in its own promoter activity under dietary conditions when *acdh-1* levels are normally high. We know that this feedback extends from *acdh-1* to other genes involved in BCAA breakdown because additional genes in this pathway either change in expression in response to a *Comamonas* DA1877 diet, confer an increase in *acdh-1* promoter activity when perturbed, or both. Thus, as has been observed in simpler unicellular organisms such as bacteria and yeast [85], metabolic changes induced genetically or by diet, likely result in

disruption of metabolic flux that, in turn, elicit a compensatory transcriptional response of relevant metabolic genes. Altogether, our study reveals extensive communication between mitochondrial metabolic networks and nuclear gene regulatory networks that function to dial metabolic gene expression according to cellular or organismal need (**Figure 2.12**).

The mechanisms by which information is relayed from the mitochondria to the nucleus remain poorly understood. There are several shared metabolites among the four metabolic pathways found in the screens, including acetyl-CoA, succinyl-CoA, pyruvate, lipoamide, and the cofactor cobalamin (vitamin B12) (**Figure 2.7**). These shared metabolites represent points of convergence for metabolic flux through each of the individual pathways. Perturbing flux through methionine metabolism by mutating *metr-1,* for instance, may affect flux through BCAA breakdown due to buildup or depletion of shared metabolites. This could explain the observation that several genes from these two pathways are co-regulated in response to diet and metabolic perturbation in either pathway. These metabolites may mediate the communication from the mitochondria to the nucleus. It is well known that these metabolites have broad ranging effects on the cell. For instance, epigenetic effects can be mediated by histone acetylation, methylation and phosphorylation, which require acetyl-CoA, SAM and ATP, respectively. It is possible that overall or specific protein modification levels are affected by metabolic network perturbations, and result in changes in gene

expression. Further, these metabolites may directly or indirectly target TFs such as NHRs (see below).

Interestingly, there was a high degree of overlap in both upregulated and downregulated genes in the gene expression profiles of two metabolic gene mutants, Δ*metr-1* and Δ*pcca-1*. This suggests that the functional defects caused by perturbing either the BCAA breakdown pathway or methionine metabolism may elicit similar metabolomic shifts in the animal, which may impinge upon a common regulatory signal. Both metabolic gene mutations reverse many of the gene expression changes conferred by a *Comamonas* DA1877 diet in wild type animals. Two modules of co-expressed genes exhibit reciprocal 'see-saw' behavior: one module is repressed by a *Comamonas* DA1877 diet but activated in the metabolic mutants, while another is activated by a *Comamonas* DA1877 diet but repressed in the metabolic gene mutants. This implies that both metabolic network perturbations and a *Comamonas* DA1877 diet converge onto the same regulatory network to elicit converse effects on the two modules, perhaps via two opposing regulatory signals (**Figure 2.12**).

NHR-10 directly binds the *acdh-1* promoter [78] and mediates the induction of *acdh-1* in response to metabolic network perturbations in several mutants, particularly those that function within BCAA breakdown. In addition, NHR-68 and several other NHRs either function together or in parallel with NHR-10. Epistasis experiments with additional NHRs, as well as other TFs, will further illuminate their function in metabolic gene regulation. NHRs are ligand-regulated

TFs that may be able to directly sense metabolite accumulation and regulate genes accordingly. For instance, NHR ligands may be produced as a result of specific metabolic network perturbations. Alternatively, NHRs may be inactivated by a metabolite, and depletion of that metabolite upon network perturbation might result in NHR activation. Perturbation of different metabolic pathways may result in the accumulation or depletion of metabolites that may be sensed by different NHRs with overlapping downstream targets. Previously, we found functional modularity of NHRs in a *C. elegans* gene regulatory network [78]. Here, we find a modular organization at the level of metabolic gene expression. Together, these findings support a model in which gene regulatory network modules facilitate rapid responses to physiological and environmental cues.

Most dietary sensor repressors encode enzymes involved in inborn disorders of amino acid metabolism in humans. These diseases are usually treated by dietary interventions that are designed to avoid build-up of toxic metabolites, to supplement patients with metabolites that are depleted, and/or with cofactors that may improve residual enzyme activity (**Figure 2.10**)[69]. In *C. elegans* mutations in genes from different pathways within the metabolic network (BCAA and methionine metabolism) can cause highly similar changes in gene expression. Thus, it may be that a dietary regimen used to mitigate one type of metabolic disease may also be beneficial for another. *C. elegans* presents an attractive model with which transcriptomic changes in response to different diets

and metabolic network perturbations can be compared, and potentially can be used in screens for drugs or other small molecules that affect these changes.

Our study establishes *C. elegans* as a powerful model to dissect the mechanisms of dietary responses, inborn metabolic diseases and the connections between them. It is likely that other parts of the metabolic network respond to different cues. We provide a framework to identify candidate sensors to these cues, and to combine these sensors with genetic screens and epistasis to dissect the mechanisms involved.

Figures

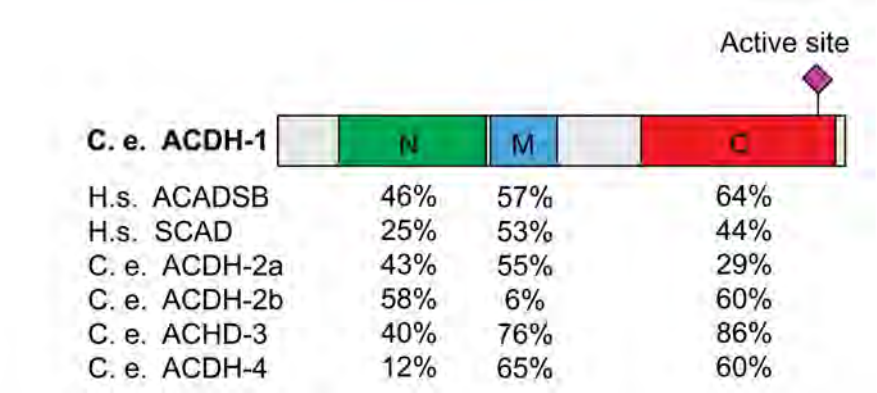

Figure 2.1 – Cartoon of Homology with ACDH-1 protein

Cartoon depicting the ACDH-1 protein with percent sequence identity with human and *C. elegans* enzymes in the acyl-CoA dehydrogenase N-terminal (N), Middle (M) and C-terminal (C) domains indicated.

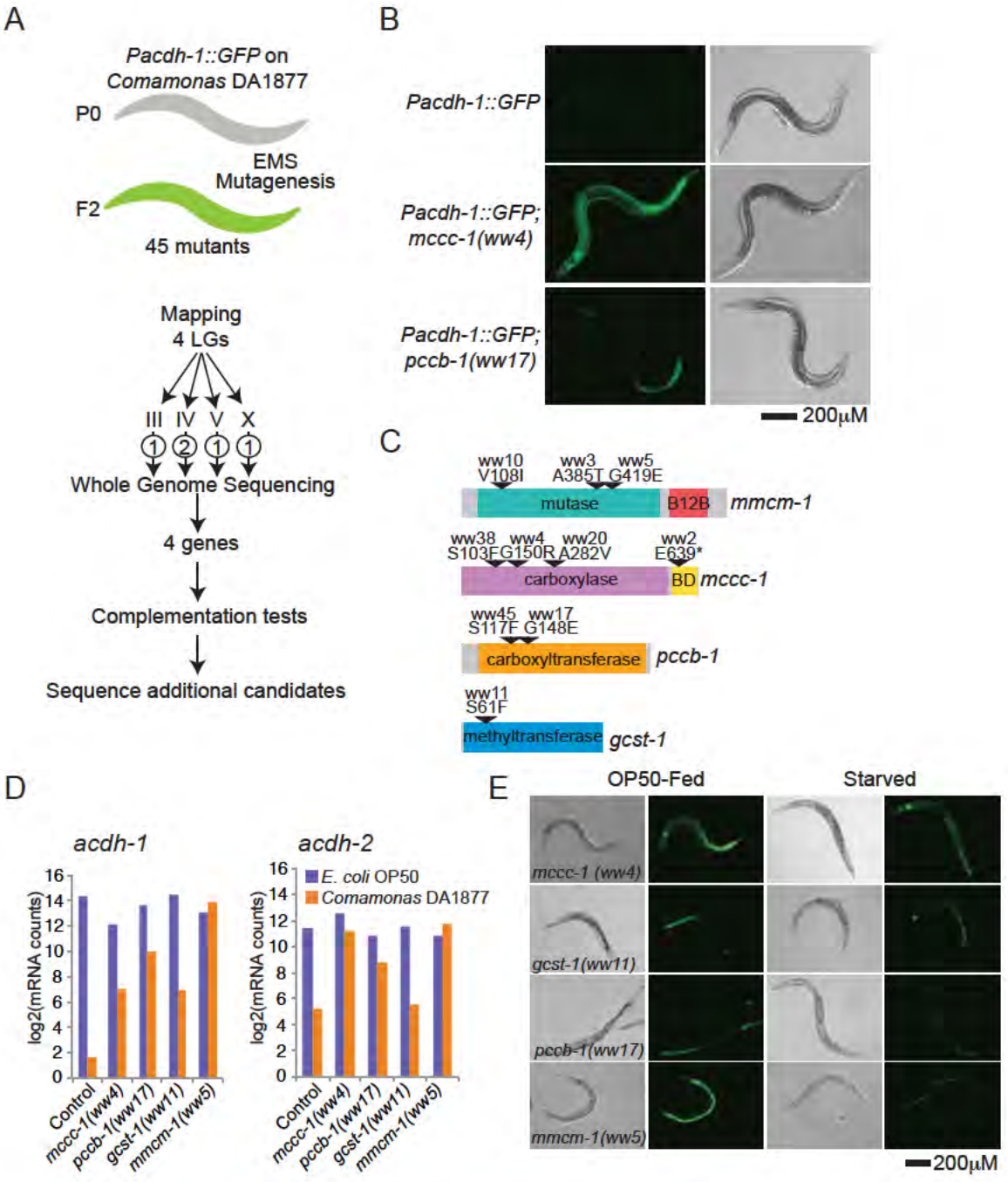

Figure 2.2 – Forward Genetic Screen For *Pacdh-1::GFP* Regulators

(A) Flow chart of EMS mutagenesis screen. (B) Examples of GFP expression in wild type animals and two mutant strains. (C) Cartoon illustrating amino acid changes in four proteins identified in the forward genetic screen. BD – biotin binding domain; B12B – vitamin B12 binding domain. (D) Endogenous *acdh-1* and *acdh-2* levels in mutants as measured by nCounter assays and normalized to *ama-1*. (E) Mutants exhibit different responses to starvation.

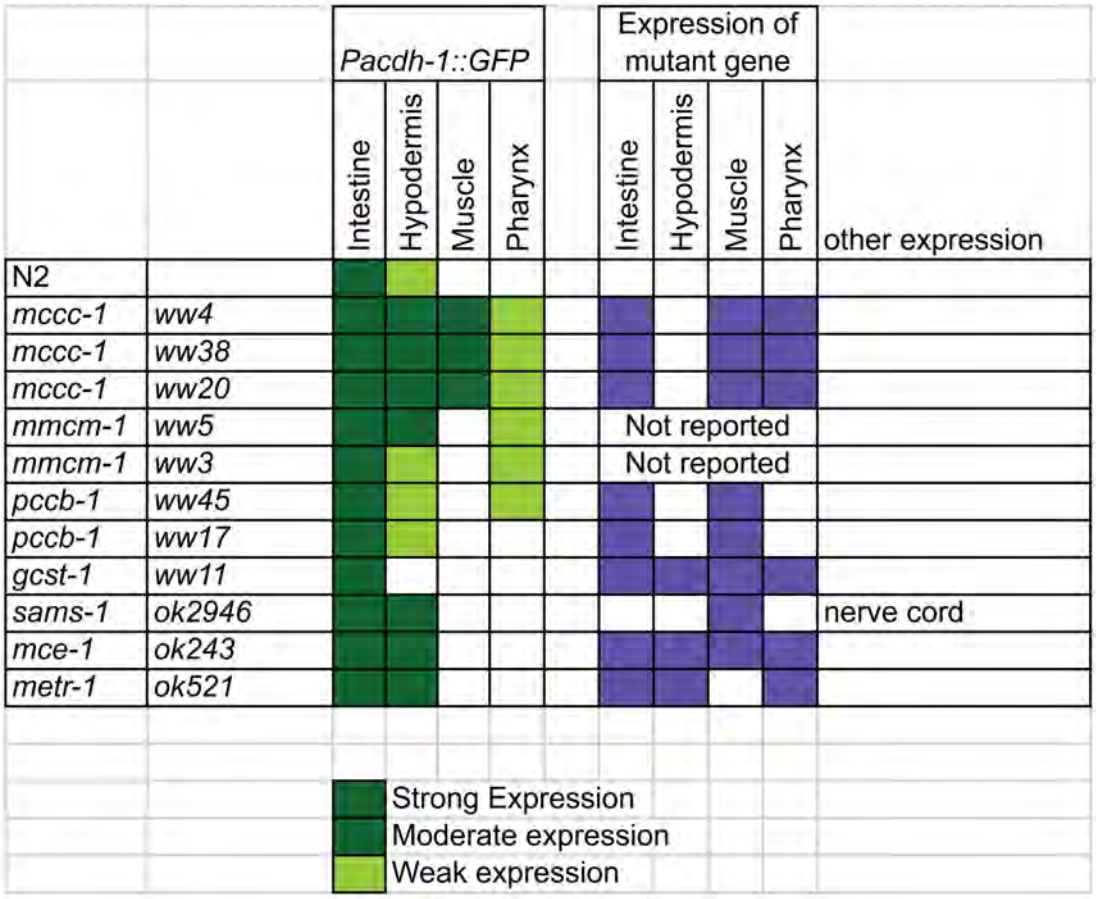

Table 2.1 – Effects of various metabolic mutations on *Pacdh-1::GFP expression*.
Levels of GFP expression within each compartment are shown (Green). In addition, the reported expression pattern according to Wormbase (WS234) of the mutated genes is shown (Purple).

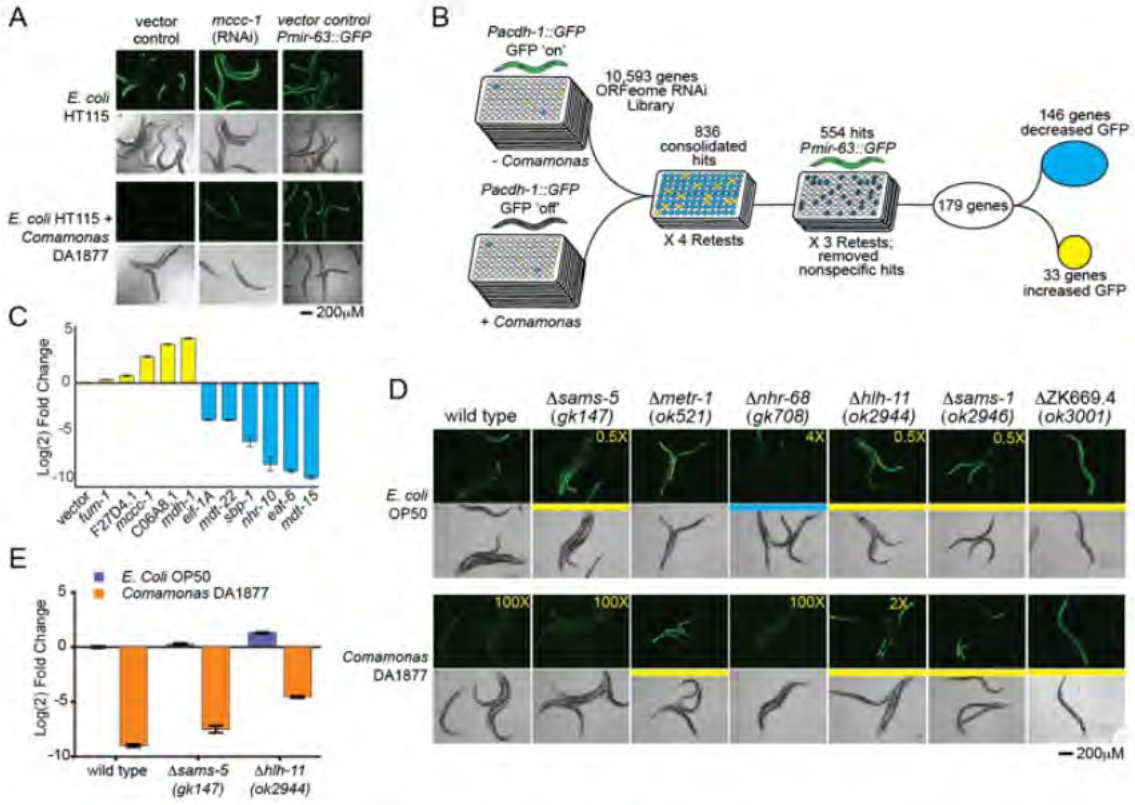

Figure 2.3 – Reverse Genetic Screen For *Pacdh-1::GFP* Regulators

(A) RNAi knockdown works efficiently in the presence of *Comamonas* DA1877. *Pacdh-1::GFP* animals were fed *E. coli* HT115 producing either dsRNA directed against *mccc-1* (which was found in the forward genetic screen) or no dsRNA (vector control) in the presence and absence of *Comamonas* DA1877. The intestinally-expressed transgene *Pmir-63::GFP*, which does not respond to *Comamonas*, is shown for comparison. (B) Flow chart of genome-scale RNAi screen. Initial hits were screened against *Pmir-63::GFP* to filter out genes that non-specifically affected intestinal transgene expression. (C) qRT-PCR of endogenous *acdh-1* mRNA in wild type animals subjected to RNAi of 11 genes found in the RNAi screen. Values were normalized to expression in a vector only control (which was set to equal 0) and plotted as $\log_2$ fold change. Yellow bars indicate genes whose knockdown caused increased GFP expression and blue bars indicate genes whose knockdown caused decreased GFP expression. Error bars indicated the standard error in three technical repeats. (D) Validation of RNAi results using mutant animals. Bright field and fluorescent images of *Pacdh-1::GFP* animals with wild type or mutant backgrounds, fed either *E. coli* OP50 or *Comamonas* DA1877. Yellow indicates increases in GFP expression and blue indicates decreased GFP expression compared to wild type *Pacdh-1:GFP* dietary sensor animals. Exposure times that are different from *Pacdh-1:GFP* dietary

sensor animals fed *E. coli* OP50 are indicated in the top-right corner of the respective panel. (E) qRT-PCR of endogenous *acdh-1* mRNA in Δ*sams-5* and Δ*hlh-11* mutant compared to wild type animals fed *E. coli* OP50, *E. coli* HT115, or *Comamonas* DA1877. Changes in *acdh-1* expression were plotted as $\log_2$ fold change compared to *acdh-1* levels in wild type animals fed *E. coli* OP50, which was set to equal 0. Error bars indicated the standard error in three technical repeats.

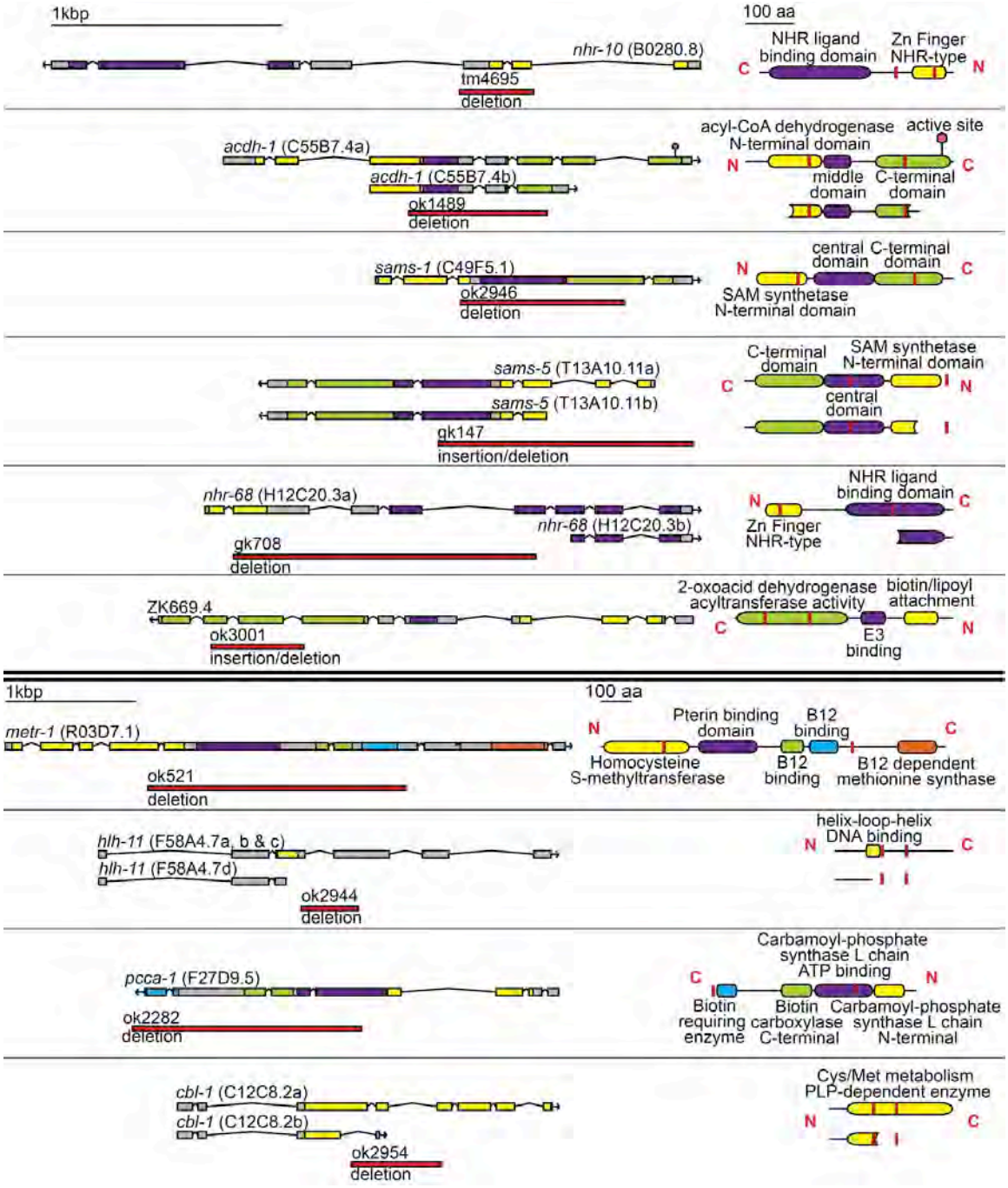

Figure 2.4 – Cartoon of Deletion Mutants

Cartoons depicting gene structures of deletion mutants used in these studies, with the exception of the Δ*mce-1* mutant for which the deletion has not been precisely mapped. Arrows indicate direction of transcription. Proteins are diagrammed to the right of the gene structures with N and C termini relative to depicted gene directionality. Color blocks on genes correspond to colored protein

domains, which were determined using PFAM. Red lines on protein cartoons indicate the region affected by the deletion. Bold double lines separate two sections with different scales, indicated by the 1kb scale lines at the tops of each section.

Table 2.2 – List of all genes found to affect *Pacdh-1::GFP* from both genetic screens.

ACTIVATORS

Gene	ORF	Overall category	Molecular function	Pos. Retests (x/4)	*Pacdh-1* GFP	Phenotype (Wormbase WS232)	Expression	Human Ortholog	Human disease	Additional observed phenotypes
B0261.1	B0261.1	general gene expression	RNA pol III subunit	4	off	Emb	ND	BDP1	No	slow grow
C16A3 6	C16A3.6	general gene expression	ribosome biogenesis	4	down	Emb	ND	MAK16	No	slow grow
C16C10 2	C16C10 2	general gene expression	ribosome biogenesis	4	down	Emb	ND	UTP11L	downregulated in Alzheimer's	slow grow
C36E8.1	C36E8.1	general gene expression	RNA pol I	4	down	Let	ND	RRN3	No	
C43E11.9	C43E11.9	general gene expression	ribosome	4	down	Lva	ND	N P7	No	slow grow
C53H9.2	C53H9.2	general gene expression	GTPase, ribosome biogenesis	2	down	Emb	ND	LSG1	No	
cars-2	Y23H5A.1	general gene expression	Cysteinyl Amino-acyl tRNA Synthetase	2	down	Yes	ND	CARS	Fused to ALK in some anaplastic large-cell lymphoma	
D1043.1	D1043.1	general gene expression	spliceasome processing	2	down	Emb	ND	INTS7	No	
D1054.14	D1054.14	general gene expression	pre-mRNA splicing factor 38A	4	down	Emb	ND	PRPF38A	No	thin, slow grow
eef-1G	F17C11.9	general gene expression	translation elongation factor	4	off	Emb	ND	EEF1G	overexpressed in pancreatic tumors; loss of contact inhibition?	slow grow
eef-2	F25H5.4	general gene expression	translation elongation factor	4	off	Emb	ND	EEF2	No	thin, slow grow
eif-1.A	H06H21 3	general gene expression	translation initiation	4	off	Emb	Intestine et al	E F1AX	No	slow grow
F14B4.3	F14B4 3	general gene expression	RNA pol I	4	off	Emb	Intestine et al	POLR1B	No	slow grow
F23B12.7	F23B12.7	general gene expression	CCAAT-binding	3	down	Emb	ND	CEBPZ	No	
fars-2	Y60A3A.13	general gene expression	Phenylalanyl Amino-acyl tRNA Synthetase (mitochondrial)	2	down	None	ND	FARS2	No	
K12H4 3	K12H4.3	general gene expression	ribosome	4	down	Emb	ND	BRIX1	No	slow grow
mdt-15	R12B2.5	general gene expression	Mediator	4	down	Emb	Intestine et al	MED15	deleted in DiGeorge Syndrome (not necessarily causal)	slow grow
mdt-22	ZK970 3	general gene expression	Mediator	2	down	Emb	ND	MED22	No	
mrpl-2	F56B3 8	general gene expression	mitochondrial ribosomal protein	2	down	Lva	ND	MRPL2	No	
mrpl-28	T25D3 2	general gene expression	ribosome	4	down	Emb	ND	MRPL28	No	slow grow

Gene	ORF	Overall category	Molecular function	Pos. Retests (x/4)	*Pacdh-1* ::GFP	Phenotype (Wormbase WS232)	Expression	Human Ortholog	Human disease	Additional observed phenotypes
taf-1	W04A8.7	general gene expression	TAF	2	down	Emb	ND	TAF1L	yes	
tag-345	F55F8.5	general gene expression	ribosome biogenesis	3	down	Emb	ND	WDR12	No	
W06E11.1	W06E11.1	general gene expression	RNA pol III	3	down	Emb	ND	POLR3E	No	
W07E6.2	W07E6.2	general gene expression	ribosome biogenesis	2	down	Lva	ND	NLE1	No	
W09C5.1	W09C5.1	general gene expression	ribosome biogenesis	4	down	Lva	Intestine et al	NSA2	No	slow grow
Y37E11AM.3	Y37E11AM.3	general gene expression	RNase P	2	down	None	ND	RPP14	No	
Y39A1A.14	Y39A1A.14	general gene expression	ribosome biogenesis	3	down	Emb	ND		No	
Y48B6A.1	Y48B6A.1	general gene expression	ribosome	4	down	Emb	ND	BOP1	misregulated in 39% of colorectal cancers	slow grow
Y48G1A.4	Y48G1A.4	general gene expression	ribosome	4	down	Emb	ND	NOP14	No	slow grow
Y52B11A.10	Y52B11A.10	general gene expression	ribosome	4	down	Lva	ND	NOM1	No	slow grow
Y53C12B.2	Y53C12B.2	general gene expression	ribosome	4	off	Emb	ND	PNO1	No	slow grow
Y54E10A.10	Y54E10A.10	general gene expression	ribosome	4	down	Lva	ND	RPF-2	No	slow grow
ZC376.6	ZC376.6	general gene expression	spliceasome processing	3	down	Emb	ND	INTS2	No	
ZK1127.5	ZK1127.5	general gene expression	ribosome	3	down	Emb	Intestine et al	RCL1	No	
ZK430.7	ZK430.7	general gene expression	ribosome	4	down	Emb	ND	DCAF13	No	slow grow
ZK856.10	ZK856.10	general gene expression	RNA pol III	4	down	Lva	ND	POLR3H	No	slow grow
asg-1	K07A12.3	metabolism	ATP synthesis	2	down	Emb	ND	ATP5L	No	
cyc-1	C54G4.8	metabolism	cytochrome c1	2	down	Emb	Not intestine	CYC1	No	thin, slow grow
cyc-2.1	E04A4.7	metabolism	cytochrome c	3	down	Emb	ND	CYCS	Thrombo-cytopenia 4	slow grow
cyp-33C3	F41B5.4	metabolism	cytochrome P450	3	down	Weak	ND	CYP2J2	No	
dph-1	C14B1.5	metabolism	Diphthamide biosynthesis protein 1	4	off	Let	ND	DPH1	mutated in 90% of ovarian cancers	slow grow
elo-3	D2024.3	metabolism	polyunsaturated fatty acid (PUFA) elongase	3	down	Yes	Not intestine	ELOVL6	No	
F14B6.4	F14B6.4	metabolism	beta-galactosaminyl-transferase	2	down	None	ND	B3GALT1	No	
F37C12.3	F37C12.3	metabolism	acyl carrier protein	3	down	Emb	ND	NDUFAB1	No	slow grow

Gene	ORF	Overall category	Molecular function	Pos. Retests (x/4)	*Pacdh-1* ::GFP	Phenotype (Wormbase WS232)	Expression	Human Ortholog	Human disease	Additional observed phenotypes
mrpl-4	T23B12.2	general gene expression	mitochondrial ribosomal protein	2	down	Emb	ND	MRPL4	No	
ncbp-1	F37E3.1	general gene expression	CAP binding complex	4	down	Emb	ND	NCBP1	No	gonad
pabp-2	C17E4.5	general gene expression	polyA binding protein	3	off	Emb	Intestine et al	PABPN1	autosomal dominant oculopharyngeal muscular dystrophy disease	
ppp-1	C15F1.4	general gene expression	translation initiation	2	down	Emb	ND	EIF2B3	Leuko-encephalopathy with vanishing white matter	
prp-4	C36B1.5	general gene expression	U4/U6 small nuclear riboprotein; splicing	4	down	Emb	ND	PRPF4	No	slow grow
rars-1	F26F4.10	general gene expression	Arginyl-tRNA synthetase, cytoplasmic	3	down	Emb	ND	RARS	No	slow grow
rpc-1	C42D4.8	general gene expression	RNA pol III	4	down	Emb	ND	POLR3A	No	slow grow
rpl-24.2	C03D6.8	general gene expression	ribosome biogenesis	4	off	Emb	ND	RSL24D1	No	thin, slow grow
rps-29	B0412.4	general gene expression	ribosome	3	down	Emb	Not intestine	RPS29	No	slow grow
rps-4	Y43B11AR.4	general gene expression	ribosome	4	off	Emb	Intestine et al	RPS4	No	thin, slow grow
rrbs-1	C15H11.9	general gene expression	ribosome biogenesis	4	down	Emb	ND	RRS1	No	slow grow
rsp-2	W02B12.2	general gene expression	splicing factor	2	down	Emb	ubiquitous	SRSF4	No	
sap-49	C08B11.5	general gene expression	splicing factor	4	off	Emb	ND	SF3B4	No	slow grow
sna-2	T13F2.7	general gene expression	snRNP protein	4	down	Emb	ND		No	
suf-1	F28C6.6	general gene expression	Poly-adenylation	4	down	Emb	ND	CSTF3	No	slow grow
T02H6.1	T02H6.1	general gene expression	pre-rRNA processing	2	down	None	ND	RRP9	No	slow grow
T04A8.6	T04A8.6	general gene expression	ribosome biogenesis	4	down	Lva	Not intestine	MKI67IP	No	slow grow
T07A9.9	T07A9.9	general gene expression	ribosome biogenesis	4	off	Emb	ND	GTPBP4	No	slow grow
T11G6.8	T11G6.8	general gene expression	RNA binding protein; splicing?	2	down	Emb	ND	RBM22	No	
T22H9.1	T22H9.1	general gene expression	ribosome	3	down	Emb	Intestine	RRP36	No	
T26G10.1	T26G10.1	general gene expression	RNA helicase	4	down	Emb	ND	DDX47	No	slow grow

Gene	ORF	Overall category	Molecular function	Pos. Retests (x/4)	*Pacdh-1* ::GFP	Phenotype (Wormbase WS232)	Expression	Human Ortholog	Human disease	Additional observed phenotypes
F42G8.10	F42G8.10	metabolism	NADH: ubiquinone oxidoreductase	2	down	Emb	ND	NDUFB11	No	
F44G4.2	F44G4.2	metabolism	NADH dehydrogenase	3	down	Emb	ND	NDUFB2	No	slow grow
K09C4.5	K09C4.5	metabolism	sugar transporter	2	down	High fat	ND	GLUT1	GLUT1 deficiency syndrome 1	
nduf-5	Y54E10BL.5	metabolism	NADH: ubiquinone oxidoreductase 15 kDa subunit mitochondrial	3	down	Reduced brood size	ND	NDUFS5	No	
nduf-7	W10D5.2	metabolism	NADH dehydrogenase ubiquinone iron-sulfur protein 7	3	down	Emb	Not intestine	NDUFS7	Leigh syndrome	slow grow
nstp-3	ZC250.3	metabolism	nucleotide sugar transporter	2	down	Emb	ND	SLC35A3	No	
nuo-1	C09H10.3	metabolism	mitochondrial complex I	3	down	Emb	ND	NDUFV1	Mitochondrial complex I deficiency	slow grow
nuo-4	K04G7.4	metabolism	NADH: Ubiquinone Oxidoreductase	2	down	Emb	ND	NDUFA10	Leigh syndrome	
pho-1	EGAP2.3	metabolism	intestinal acid phosphatase	2	down	Emb	Intestine	ACP2	No	
pyp-1	C47E12.4	metabolism	pyro-phosphatase	3	down	Emb	Intestine et al	PPA1	No	
T08B1.1	T08B1.1	metabolism	sugar transporter	2	down	Emb	ND	SLC22A4	GWAS associations with IBS and rheumatoid arthritis	
T25B9.9	T25B9.9	metabolism	6-phospho-gluconate dehydrogenase, decarboxylating pentose phosphate pathway	4	down	Emb	ND	PGD	6-phospho-gluconate dehydrogenase deficiency, autosomal dominant	
vha-14	F55H2.2	metabolism	V-ATPase	2	down (up coma)	Emb	ND	ATP6V1D	No	
Y24D9A.8	Y24D9A.8	metabolism	transaldolase, pentose phosphate pathway, cytoplasmid	4	down	None	ND	TALDO1	transaldolase deficiency	
Y51H1A.3	Y51H1A.3	metabolism	NADH: ubiquinone oxidoreductase	3	down	Emb	ND	NDUFB8	No	slow grow
B0336.3	B0336.3	ND	RBP	2	down	Yes	ubiquitous	RBM26	No	
C14C10.4	C14C10.4	ND	mito nucleoid associated	3	down	Emb	ND	LRPPRC	Leigh syndrome, French-Canadian type	
C23G10.8	C23G10.8	ND	ND	2	down	Emb	Intestine et al	SRRM5	No	
C50D2.1	C50D2.1	ND	ND	4	down	Emb	ND		No	slow grow
cab-1	C23H4.1	ND	ND	2	down (up on Coma?)	Emb	ND	NPDC1	No	
dre-1	K04A8.6	ND	works with DAF-12	4	down	Lva, molting	Intestine et al	FBXO11	downregulated in vitiligo; mutated in multiple diffuse large B-cell lymphoma	slow grow

Gene	ORF	Overall category	Molecular function	Pos. Retests (x/4)	*Pacdh-1* ::GFP	Phenotype (Wormbase WS232)	Expression	Human Ortholog	Human disease	Additional observed phenotypes
F11C7.2	F11C7.2	ND	transmembrane	2	down	None	ND	BAI2	No	
F16C3.2	F16C3.2	ND	ND	2	down	None	ND		No	
F29B9.11	F29B9.11	ND	ND	4	down	Emb	ND		No	slow grow
F52C6.3	F52C6.3	ND	polyubiquitin	3	down	Emb	ND	UBC	No	
F55F8.2	F55F8.2	ND	DEAD box helicase	4	down	Lva	ND	DDX24	No	slow grow
fbxb-119	B0462.3	ND	F-box protein	2	down	Emb	ND		No	
hsp-3	C15H9.6	ND	heast shock protein	2	down	Emb	Intestine et al	HSPA5	No	
K04G7.1	K04G7.1	ND	ND	4	down	Emb	ND		No	slow grow
lev-10	Y105E8A.7	ND	vitamin B12 transport	4	down	Low fat	ND	CUBN	Megaloblastic anemia-1, Finnish type	
nath-10	F55A12.8	ND	N-acetyl transferase; histone or microtubule	4	down	Emb	Intestine et al	NAT10	No	slow grow
R05D7.4	R05D7.4	ND	Abhydrolase domain; mitp	2	down	None	ND	ABHD11	deleted in Williams-Beuren Syndrome	
ril-2	C14C10.3	ND	trans membrane; transporter	3	down	Emb	ND	CLN3	mutated in Batten disease	slow grow
T10C6.7	T10C6.7	ND	F-box protein	2	down	None	ND		No	
tag-267	W06E11.2	ND	ND	2	down	Emb	ND		No	
ubc-13	Y54G2A.31	ND	E2 ubiquitin conjugating enzyme	4	down	Emb	ND	UBE2N	No	slow grow
wdr-46	F28D1.1	ND	ND	4	down	Emb	ND	WDR46	upregulated in melanoma cell lines	slow grow
Y110A7A.19	Y110A7A.19	ND	ND	2	down	Emb	ND	PTCD3	No	slow grow
Y39B6A.33	Y39B6A.33	ND	ND	3	down	Lva	ND	GLTSCR2	low expression correlated with survival in colorectal and esophageal cancers; regulates p53	slow grow
Y42G9A.1	Y42G9A.1	ND	ND	3	down	Sick	ND		No	
Y57A10A.27	Y57A10A.27	ND	ND	2	down	Emb	ND		No	
ZK1127.4	ZK1127.4	ND	ND	3	down	Emb	ND	BCCIP	No	slow grow
ZK355.2	ZK355.2	ND	ND	2	down	None	ND		No	
ZK418.5	ZK418.5	ND	trans membrane	2	down	Yes	ND	TMEM147	No	
baf-1	B0464.7	other	Chromsome structure	2	down	Emb	ubiquitous	BANF1	Nestor-Guillermo progeria syndrome	
cdk-1	T05G5.3	other	CDK	2	down	Emb	ubiquitous	CDK1	No	
cle-1	C36B1.1	other	Collagen	2	down	Weak	Not intestine	COL15A1	No	
csp-2	Y73B6BL.7	other	Caspase	4	off	None	Not intestine	CASP7	mutated in small percent of colon and esophageal cancers	thin, slow grow
eat-6	B0365.3	other	Na+,K(+)-ATPase	4	off	Emb	Intestine et al	ATP1A3	dystonia-12	thin, slow grow
epc-1	Y111B2A.11	other	enhancer of polycomb	2	down	Emb	Intestine et al	EPC2	No	
gei-4	W07B3.2	other	intermediate filament	3	down	Emb	ND	LOC283685	No	
ifa-4	K05B2.3	other	intermediate filament	3	down	None	Intestine et al (dauer only)	LMNB1	Leukodystrophy, adult-onset, autosomal dominant	

Gene	ORF	Overall category	Molecular function	Pos. Retests (x/4)	*Pacdh-1* ::GFP	Phenotype (Wormbase WS232)	Expression	Human Ortholog	Human disease	Additional observed phenotypes
mig-6	C37C3.6	other	ND	3	down	Emb	Intestine et al	PAPLN	No	
nap-1	D2096.8	other	nucleosome assembly protein	4	down	Emb	ND	NAP1L1	No	
pst-2	F54E7.1	other	Adenosine 3'-phospho 5'-phosphosulfate transporter 2	3	down	weak	Intestine et al	SLC35B3	No	
rmd-1	T05G5.7	other	microtubule dynamics	2	down	Emb	Not intestine	FAM82B	No	
sca-1	K11D9.2	other	Sarcoplasmic/ endoplasmic reticulum calcium ATPase 3	2	down	Emb	Not intestine	ATP2A1	Brody myopathy	slow grow
scpl-4	T21C9.12	other	Mitochondrial import inner membrane translocase subunit TIM50	3	down	Emb	ND	TIMM50	No	
T09B4.9	T09B4.9	other	Mitochondrial import inner membrane translocase subunit TIM44	4	down	Emb	Intestine et al	TIMM44	No	
T14G10.5	T14G10.5	other	COPI complex	3	off	Let	ND	COPG2	No	slow grow/sick
tomm-40	C18E9.6	other	Translocase of Outer Mitochondrial Membrane	3	down	Emb	ubiquitous	TOMM40	No	slow grow
unc-87	F08B6.4	other	myofilament maintenance	3	down	Let	Not intestine	CNN1	No	slow grow
xpf-1	C47D12.8	other	NER, nuclease	3	off	Emb	Intestine et al	ERCC4	Xeroderma pigmentosum, XFE progeroid syndrome	slow grow
Y67A10A.9	Y67A10A.9	other	claudin	2	down	None	ND		No	slow grow
osm-7	T05D4.4	other	ND	3	down	Yes	Not intestine		No	
plk-1	C14B9.4	other	polo-like kinase	3	down	Emb	Not intestine	PLK2	No	
pri-1	F58A4.4	other	DNA primase	3	down	Emb	ND	PRIM1	No	
pri-2	W02D9.1	other	DNA primase	4	down	Emb	ND	PRIM2	No	sick
rheb-1	F54C8.5	other	Rheb GTPase, TOR	3	down	Let	ND	RHEB	No	
ruvb-1	C27H6.2	other	TOR pathway ATPase	3	down	Emb	Intestine et al	RUVBL1	No	
ceh-86	F42G2.6	transcription	TF	4	down	Emb	Intestine	PAX4	Diabetes Mellitus, Type 2	slow grow
hmg-4	T20B12.8	transcription	TF	3	down	Emb	Intestine et al	SSRP1	No	
nhr-10	B0280.8	transcription	TF	4	off	High fat	ND	RXRB	No	
nhr-17	C02B4.2	transcription	TF	2	down	None	Intestine et al	RXRB	No	
nhr-173	C56E10.1	Transcription	TF	3	down (intestine only)	None	ND	HNF4A	Diabetes mellitus, noninsulin-dependent	
nhr-44	T19A5.4	transcription	TF	3	down	Let	Intestine et al	HNF4A	No	
nhr-68	H12C20.3	Transcription	TF	3	down (intestine only)	Other	Intestine	HNF4G	Diabetes mellitus, noninsulin-dependent	
nhr-74	C27C7.3	transcription	TF	3	down	None	ND	ESR1	No	

Gene	ORF	Overall category	Molecular function	Pos. Retests (x/4)	*Pacdh-1* ::GFP	Phenotype (Wormbase WS232)	Expression	Human Ortholog	Human disease	Additional observed phenotypes
pop-1	W10C8.2	transcription	TF	3	down	Emb	Intestine et al (E blastomere)	TCF7L2	Diabetes mellitus, type 2, susceptibility to	exploded through vulva
R151.8	R151.8	transcription	TF	2	down	None	ND	CRAMP1L	No	
sbp-1	Y47D3B.7	transcription	TF	4	off	Emb	Intestine	SREBF2	No	

REPRESSORS

Gene	ORF	Overall category	Molecular function	Pos. Retests (x/4)	*Pacdh-1* ::GFP	Phenotype (Wormbase WS232)	Expression	Human Ortholog	Human disease	Additional observed phenotypes
acdh-1	C55B7.4	Metabolism	acyl-CoA dehydrogenase	3	up	Other	Intestine et al	ACADSB	2-Methylbutyryl-glycinuria	
C30H6.7	C30H6.7	Metabolism	Dihydrolipoyllysine-residue acetyltransferase; component of pyruvate dehydrogenase complex, mitochondrial	4	up	None	ND	DLAT	Pyruvate dehydrogenase E2 deficiency	
cts-1	T20G5.2	Metabolism	Citrate synthase, mitochondrial	4	up	Emb	Intestine et al	CS	No	
dhs-19	T11F9.11	Metabolism	Short chain dehydrogenase, mitochondrial	4	up	None	Intestine et al	HSD17B3	No	
dlat-1	F23B12.5	Metabolism	Dihydrolipoamide dehydrogenase, acetyl transferase component mitochondrial	4	up	Emb	Intestine et al	DLAT	Pyruvate dehydrogenase E2 deficiency	
ech-6	T05G5.6	Metabolism	Enoyl-CoA Hydratase, mitochondrial	4	up	Lva	ND	AUH	3-methylglutaconic aciduria, type I	
F09F7.4	F09F7.4	Metabolism	3-hydroxyisobutyryl-CoA hydrolase, mitochondrial	3	up	Emb	ND(?)	HIBCH	3-hydroxyisobutryl-CoA hydrolase deficiency	
F23C8.5	F23C8.5	Metabolism	Electron transfer flavoprotein subunit beta	4	up	Emb	ND	ETFB	Glutaricaciduaria type IIB	
F27D4.1	F27D4.1	Metabolism	Electron transfer flavoprotein subunit alpha, mitochondrial	4	up	Emb	Intestine	ETFA	Glutaricaciduaria type IIA	
F52A8.5	F52A8.5	Metabolism	Glycine cleavage system H-protein, mitochondrial	3	up	Emb	ND	GCSH	glycine encephalopathy	
F54D5.7	F54D5.7	Metabolism	Glutaryl-coenzyme A dehydrogenase, mitochondrial	4	up (hypodrm)	None	ND	GCDH	Glutaricaciduaria type I	
fum-1	H14A12.2	Metabolism	Fumarase, mitochondrial, TCA cycle	3	up (on coma)	Emb	ND	FH	Fumarase deficiency; Leiomyomatosis and renal cell cancer	
gcst-1	F25B4.1	Metabolism	Glycine cleavage system T-protein, mitochondrial, aminomethyl-transferase	2	up (on coma)	None	Intestine et al	AMT	glycine encephalopathy (aka nonketotic hyperglycinemia)	
let-721	C05D11.12	Metabolism	Electron transfer flavoprotein-ubiquinone oxidoreductase, mitochondrial	4	up	Emb	Intestine et al	ETFDH	Glutaricaciduaria type IIC	
mccc-1	F32B6.2	Metabolism	Methylcrotonoyl-CoA carboxylase subunit alpha, mitochondrial	3	up	None	Intestine et al	hypermethioninemia	beta methylcrotonoyl-glycinuria	
mdh-2	F20H11.3	Metabolism	Malate dehydrogenase, mitochondrial	3	up	Emb	Intestine et al	MDH2	No	
metr-1	R03D7.1	Metabolism	methionine synthase	4	up	Other	Intestine et al	MTR	homocystinuria	
mev-1	T07C4.7	Metabolism	Succinate dehydrogenase cytochrome B subunit, mitochondrial	2	up	Emb	ND	SDHC	Paragangliomas 3	

Gene	ORF	Overall category	Molecular function	Pos. Retests (x/4)	*Pacdh-1* ::GFP	Phenotype (Wormbase WS232)	Expression	Human Ortholog	Human disease	Additional observed phenotypes
mthf-1	C06A8.1	Metabolism	Methylene-tetrahydrofolate reductase	4	up	Other	Intestine et al	MTHFR	homocystinuria	
pdha-1	T05H10.6	Metabolism	Pyruvate dehydrogenase, mitochondrial	3	up	Emb	ND	PDHA1	Leigh syndrome; pyruvate decarboxylase deficiency	
sams-1	C49F5.1	Metabolism	S-Adenosyl Methionine Synthetase	4	up	Let	not intestine	MAT1A	hyper-methioninemia	
sams-3	C06E7.1	Metabolism	S-Adenosyl Methionine Synthetase	3	up	Other	Intestine et al	MAT1A	hyper-methioninemia	
sams-5	T13A10.11	Metabolism	S-Adenosyl Methionine Synthetase	3	up	Emb	Intestine et al	MAT1A	hyper-methioninemia	
sdhb-1	F42A8.2	Metabolism	Succinate dehydrogenase [ubiquinone] iron-sulfur subunit, mitochondrial	2	up	Emb	Intestine et al	SDHB	paragangliomas-4	
suca-1	F47B10.1	Metabolism	Succinyl-CoA ligase, mitochondrial	2	up (on coma)	None	ND	SUCLA2	mitochondrial DNA depletion syndrome 5 (encephalo-myopathic with methylmalonic aciduria)	
tag-173	F27D4.5	Metabolism	2-oxoisovalerate dehydrogenase subunit beta, mitochondrial	3	up	Emb	ND	BCKDHB	maple syrup urine disease, type Ia	
ZK669.4	ZK669.4	Metabolism	Lipoamide acyltransferase component of branched-chain alpha-keto acid dehydrogenase complex, mitochondrial	4	up (hypodrm)	Emb	ND	DBT	maple syrup urine disease, type II	
C23H5.8	C23H5.8	ND	ND	3	up (on coma)	None	ND		No	
C34B2.4	C34B2.4	ND	Lim domain	2	up (on coma)	Yes	ND	LDB3	myofibrillar myopathy, Cardiomyopathy dilated 1C, Left ventricular noncompaction 3	
eel-1	Y67D8C.5	ND	E3 ubiquitin ligase	3	up	Emb	Intestine et al	HUWE1	Mental retardation, X-linked syndromic, Turner type	
clu-1	F55H2.6	Other	Directs cytoplasmic distribution of mitochondria	3	up (on coma)	Emb	ND	KIAA0664	No	
hsp-60	Y22D7AL.5	Other	Mitochondrial specific chaperone	4	up	Emb	ND	HSPD1	Spastic paraplegia, leukodystrophy	
hlh-11	F58A4.7	Transcription	TF	3	up (on coma)	Emb	Intestine et al	TFAP4	No	

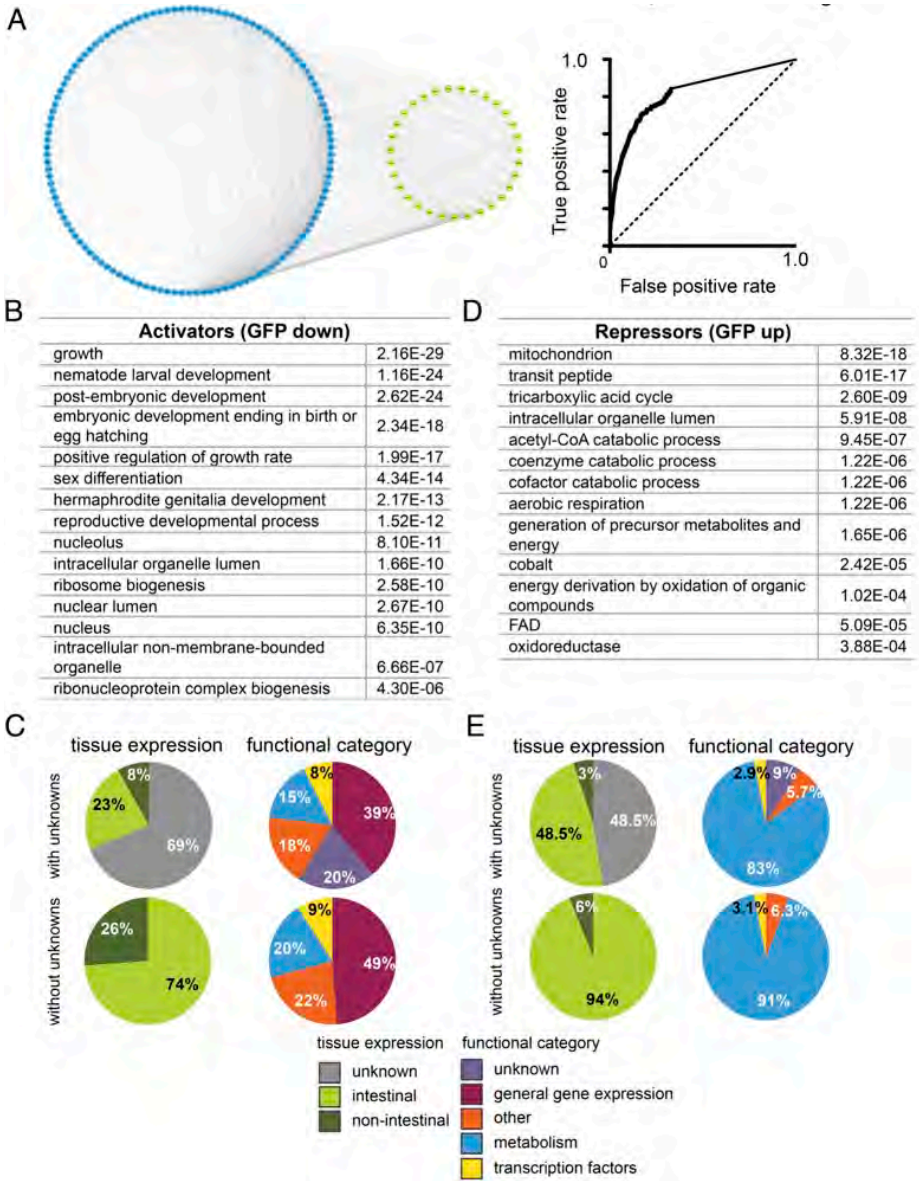

Figure 2.5 – Functional Annotation of *Pacdh-1::GFP* Regulators

(A) Left – network indicating predicted functional connections between dietary sensor regulators in WormNet. Blue indicates dietary sensor activators and yellow indicates dietary sensor repressors. Right – receiver operator curve illustrating significance of connections shown on left. The dashed line on the diagonal indicates random associations. (B) Significantly enriched GO terms for dietary sensor activators. (C) Tissue expression and functional category distribution of dietary sensor activators, with and without 'unknown' (in grey). (D) Significantly enriched GO terms for dietary sensor repressors. (E) Tissue expression and functional category distribution for dietary sensor repressors, with and without 'unknown' (in grey).

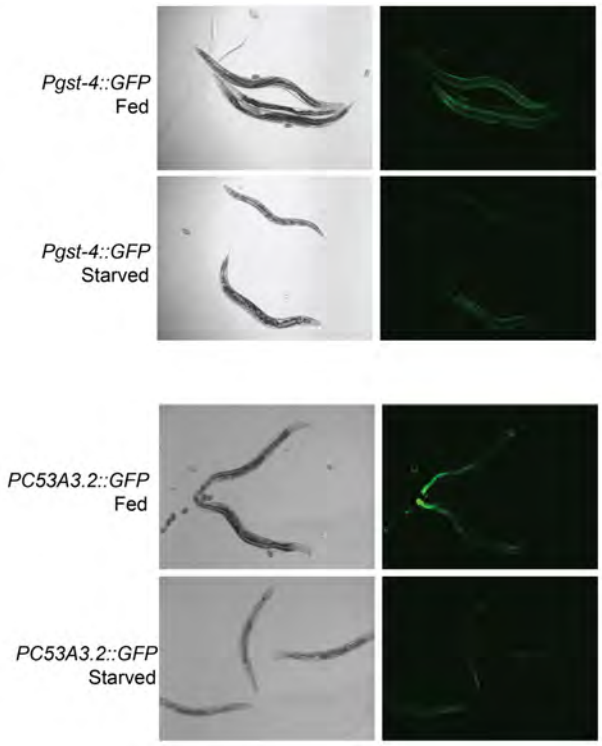

Figure 2.6 – Two Transgenic Reporters That Respond to Starvation
Two additional transgenic reporters, *Pgst-4::GFP* and *PC53A3.2::GFP* exhibit decreased GFP expression in response to starvation. The high confidence *Pacdh-1::GFP* activators identified in the RNAi screen were also screened against these two reporters to identify genes that are generally required to activate starvation-repressed genes under fed conditions, or that when knocked down trigger a starvation-like response in the animal. The results are listed in **Table S3**.

gst-4::GFP	*C53A3.2::GFP*	Both
W02D9.1	C08B11.5	*csp-2*
T11G6.8	B0336.3	T14G10.5
F54E7.1	*gei-4*	*epc-1*
C36B1.5	*nduf-7*	*nstp-3*
nhr-74	*nuo-1*	ZC376.6
ZK355.2	T09B4.9	Y42G9A.1
Y54G2A.31	F14B6.4	*nhr-17*
T08B1.1	F37C12.3	*mdt-15*
hmg-4	Y51H1A.3	*sbp-1*
T25B9.9	cyc-2.1	D1054.14
	F44G4.2	*dre-1*
	cyc-1	*elo-3*
	asg-1	
	eat-6	
	F56B3.8	

Table 2.3 – *Pacdh-1::GFP* activators that also activate other starvation reporters
Pacdh-1::GFP activators from RNAi screen that caused decreased GFP expression when knocked down by RNAi in either the *Pgst-4::GFP* strain, the *PC53A3.2::GFP* strain, or both.

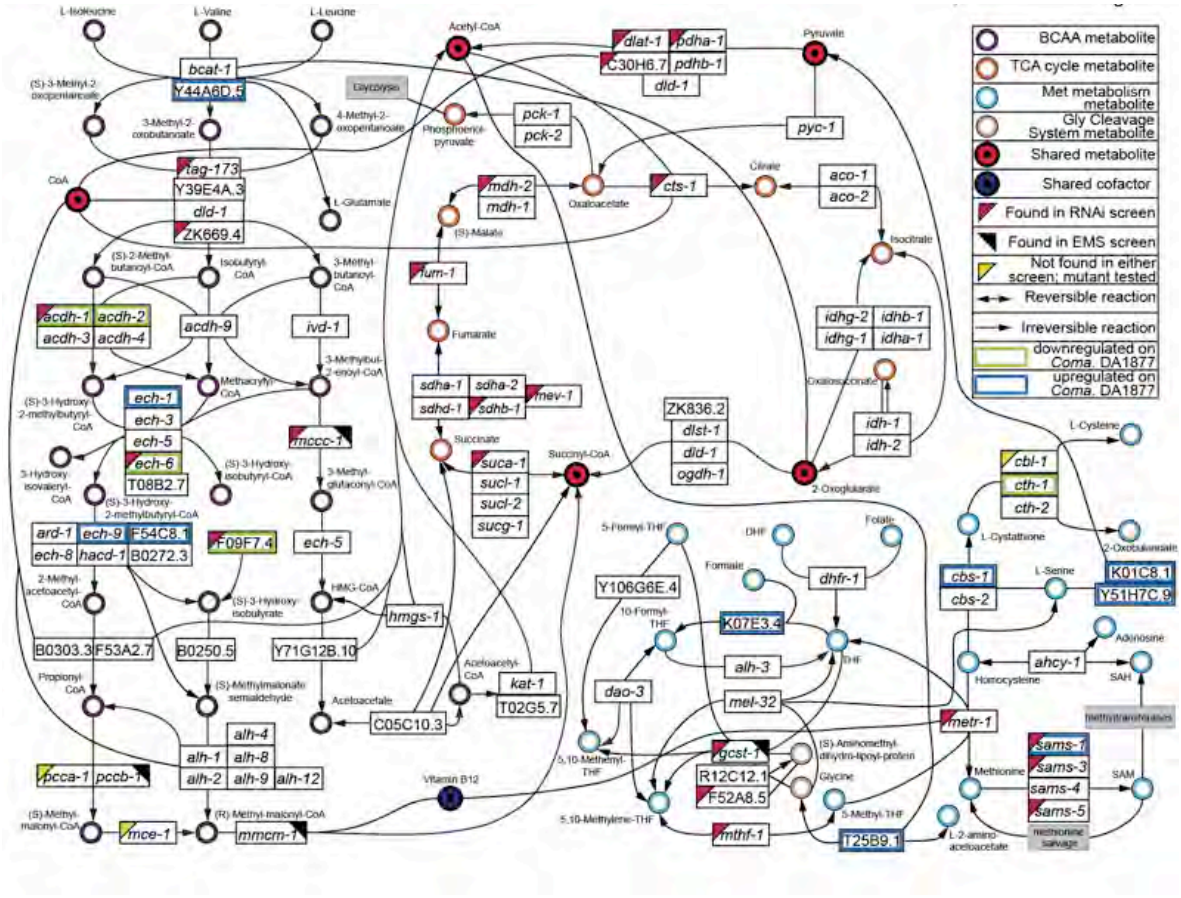

Figure 2.7 – *Pacdh-1::GFP* Repressors are Enriched in Four Metabolic Pathways
Cartoon of a metabolic map showing *C. elegans* BCAA breakdown, methionine metabolism, glycine cleavage system and TCA cycle. Rectangles indicate genes; circles are metabolites.

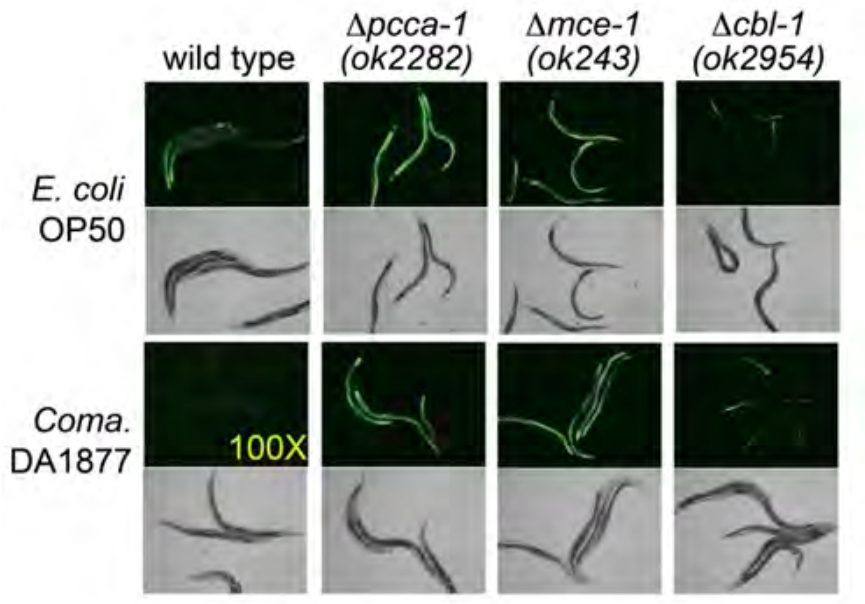

Figure 2.8 – Additional Mutants from Propionate and Methionine Metabolic Pathways.

Differential interference contrast (DIC) and fluorescent images of wild type animals compared to Δ*mce-1*, Δ*pcca-1* and Δ*cbl-1* mutant animals harboring the dietary sensor, grown on either *E. Coli* OP50, *E. Coli* HT115 or *Comamonas* DA1877.

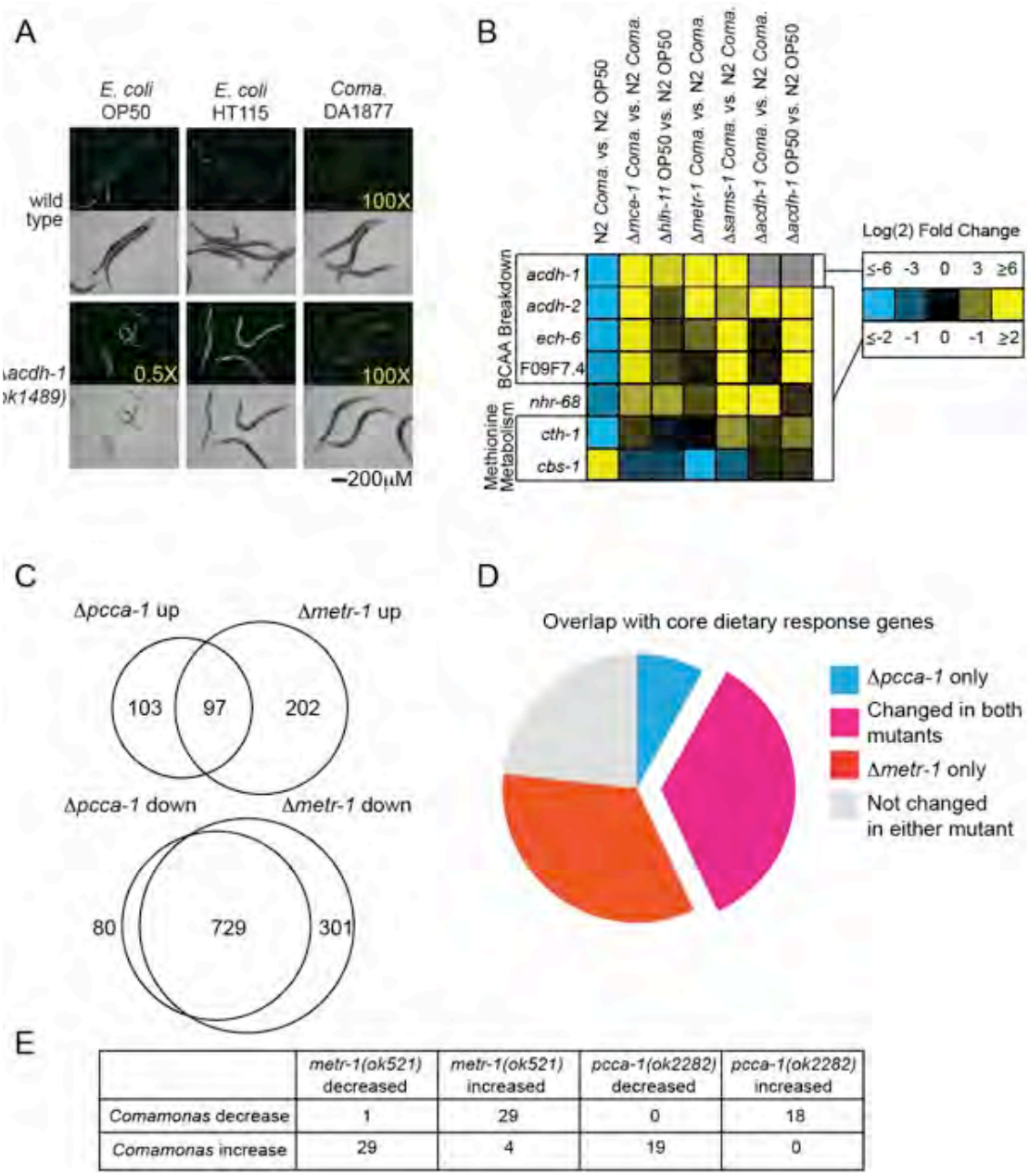

E

	metr-1(ok521) decreased	*metr-1(ok521)* increased	*pcca-1(ok2282)* decreased	*pcca-1(ok2282)* increased
Comamonas decrease	1	29	0	18
Comamonas increase	29	4	19	0

Figure 2.9 – Metabolic Feedback and Transcriptional Compensation

(A) Increased *acdh-1* promoter activity in Δ*acdh-1* mutants identifies feedback control. (B) qRT-PCR of seven genes (rows) in different strains (columns). (C) Overlap in gene expression changes between two metabolic gene mutants. (D) Overlap between genes that change in expression in the two metabolic gene mutants and those that change in response to a *Comamonas* DA1877 diet. (E) Opposite changes in gene expression in response to a *Comamonas* DA1877 diet versus metabolic network perturbations. See also **Figure 2.4 and Table S4.**

Table 2.4 – Gene expression changes in Δ*metr-1* and Δ*pcca-1* mutants

Core *Comamonas* response genes [29] that exhibit expression changes in the Δ*metr-1* and Δ*pcca-1* mutants.

Core genes		*Comamonas* DA1877 effect	*metr-1 (ok521)*	*pcca-1 (ok2282)*
Y53G8AM.5	Y53G8AM.5	increased	-41.22	-21.51
C45B2.2	C45B2.2	increased	-9.54	-7.47
F15E11.12	F15E11.12	increased	-289.03	-7.19
F15E11.15	F15E11.15	increased	-302.72	-6.75
T28D6.3	T28D6.3	increased	-7.89	-6.27
W10G11.3	W10G11.3	increased	-8.29	-5.70
Y43F8C.2	*nlp-26*	increased	-9.28	-5.01
C05E4.1	*srp-2*	increased	-4.50	-4.39
F35D11.10	*clec-139*	increased	-4.96	-4.14
D1086.3	D1086.3	increased	-7.87	-3.62
T24B8.5	T24B8.5	increased	-4.08	-3.57
T01B10.1	*grd-4*	increased	-2.96	-3.48
F35E8.8	*gst-38*	increased	-4.31	-3.00
F20D6.5	F20D6.5	increased	-4.68	-2.78
T05B11.4	T05B11.4	increased	-2.54	-2.76
C10C5.5	C10C5.5	increased	-2.66	-2.75
Y106G6D.6	Y106G6D.6	increased	-2.77	-2.69
F45E4.1	*arf-1.1*	increased	4.75	-2.12
W10G11.2	W10G11.2	increased	-3.14	NS*
F55G11.5	*dod-22*	increased	-8.07	NS*
ZK896.5	ZK896.5	increased	-2.36	NS*
C32H11.4	C32H11.4	increased	-9.93	NS*
Y45G5AM.1	*nhr-114*	decreased	5.48	NS*
C08B6.1	*ugt-17*	decreased	2.91	NS*
ZC373.1	ZC373.1	increased	NS	NS*
T05G5.6	*ech-6*	decreased	2.66	2.57
T28F3.4	T28F3.4	decreased	2.17	2.60
F46G10.6	*mxl-3*	decreased	5.42	3.43
F32D8.12	F32D8.12	decreased	2.27	3.79
DH11.2	DH11.2	decreased	7.72	3.92
T09F5.9	*clec-47*	decreased	23.76	4.96
F37B4.7	*folt-2*	decreased	3.36	5.90
Y38F1A.6	Y38F1A.6	decreased	7.12	9.50
C17C3.12	*acdh-2*	decreased	2.15	10.66
F15E6.4	F15E6.4	decreased	6.48	18.83
F28F8.2	*acs-2*	decreased	3.10	22.59
C55B7.4	*acdh-1*	decreased	305.36	255.25
K03H6.2	K03H6.2	increased	-29.31	NS
K11D2.2	*asah-1*	increased	-16.29	NS
F46B6.8	*lipl-2*	increased	-13.56	NS

F09A5.1	F09A5.1	increased	-6.39	NS
F01D5.3	F01D5.3	increased	-5.46	NS
K12G11.3	*sodh-1*	increased	-5.12	NS
Y41C4A.11	Y41C4A.11	increased	-2.15	NS
C02F5.11	*tsp-2*	increased	NS*	NS
T19C9.8	T19C9.8	increased	NS	NS
F28A12.4	F28A12.4	decreased	2.12	NS
F10E7.8	*farl-11*	decreased	2.20	NS
F59B1.8	F59B1.8	decreased	2.40	NS
T15B7.1	T15B7.1	decreased	2.68	NS
C30G12.2	C30G12.2	decreased	3.34	NS
F58B3.1	*lys-4*	decreased	3.68	NS
F44A6.5	F44A6.5	decreased	6.42	NS
T10H9.5	*pmp-5*	decreased	6.81	NS
F43E2.5	*msra-1*	decreased	7.30	NS
ZK593.3	ZK593.3	decreased	8.29	NS
F21C10.9	F21C10.9	decreased	8.66	NS
F58B3.3	*lys-6*	decreased	10.02	NS
Y34F4.2	Y34F4.2	decreased	23.90	NS
C09B8.4	C09B8.4	decreased	NS	NS
C14F11.6	C14F11.6	decreased	NS	NS
C23H5.8	C23H5.8	decreased	NS	NS
C34G6.6	*noah-1*	decreased	NS	NS
C35A5.3	C35A5.3	decreased	NS	NS
C44H4.3	*sym-1*	decreased	NS	NS
F09F7.4	F09F7.4	decreased	NS	NS
F15B9.8	F15B9.8	decreased	NS	NS
F22B8.6	*cth-1*	decreased	NS	NS
F22B8.7	F22B8.7	decreased	NS	NS
F23H12.4	*sqt-3*	decreased	NS	NS
F54D5.12	F54D5.12	decreased	NS	NS
K10D3.4	K10D3.4	decreased	NS	NS
M03A1.7	*dao-2*	decreased	NS	NS
R08E5.3	R08E5.3	decreased	NS	NS
T14B4.7	*dpy-10*	decreased	NS	NS
T22H6.2	*alh-13*	decreased	NS	NS
B0213.2	*nlp-27*	increased	NS	NS
C32H11.12	*dod-24*	increased	NS	NS
F09A5.1	F09A5.1	increased	NS	NS
F17C11.11	F17C11.11	increased	NS	NS
F44G3.10	F44G3.10	increased	NS	NS
K08D8.5	K08D8.5	increased	NS	NS
Y105C5B.5	Y105C5B.5	increased	NS	NS

Y43F8C.1	*nlp-25*	increased	NS	NS
ZK637.13	*glb-1*	increased	NS	NS
Y48E1B.10	*gst-20*	increased	-4.48	NS
W06D12.3	*fat-5*	decreased	7.23	NS
T05E12.6	T05E12.6	decreased	14.54	NS

NS - not significant
NS* - not significant at 2 fold, but => 1.5 fold change

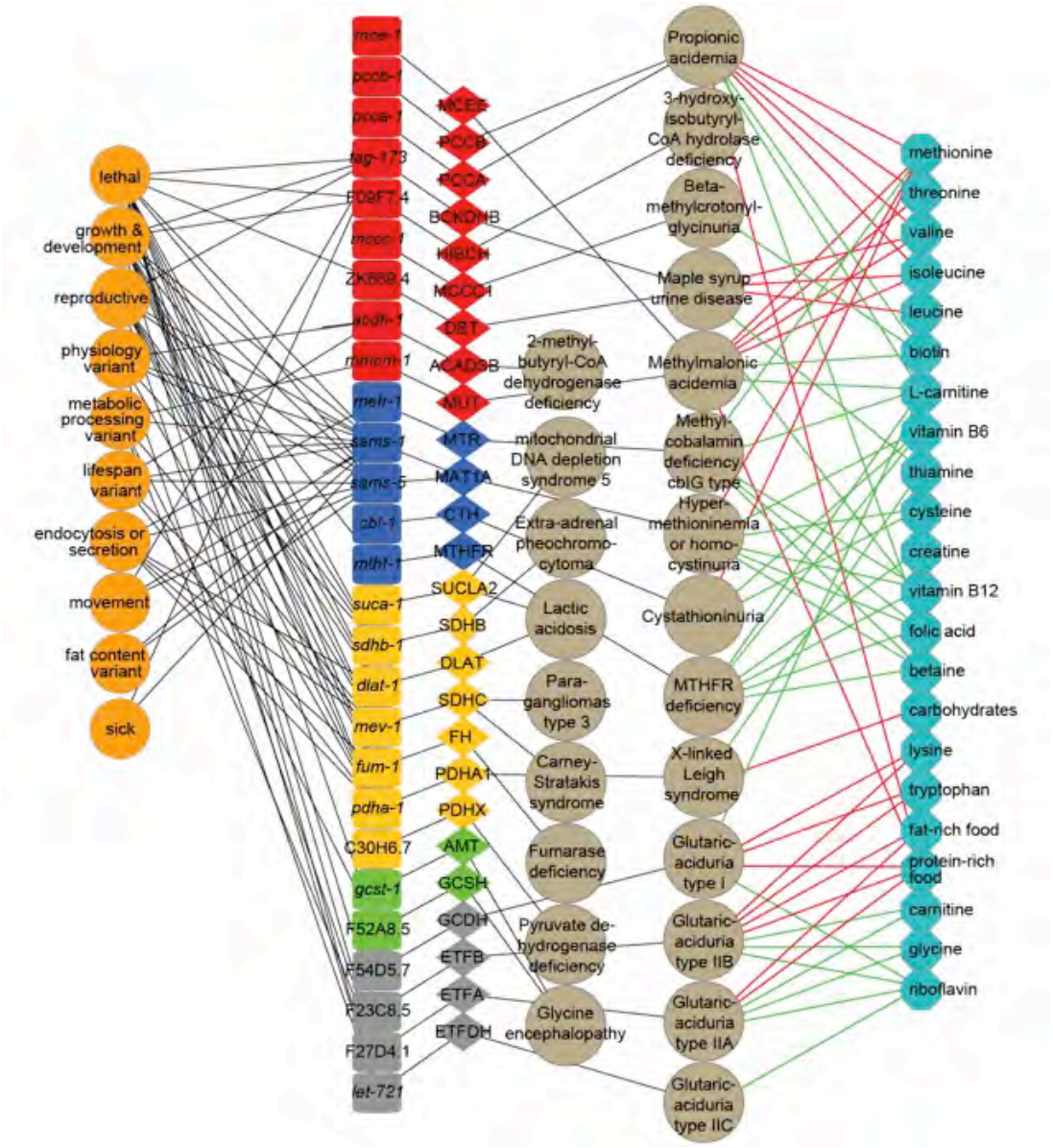

Figure 2.10 – Mutations in Orthologs of *acdh-1* Repressors Confer Human Inborn Metabolic Disorders Relating to Amino Acid Metabolism.

Network connecting dietary sensor repressors, *C. elegans* phenotypes, human orthologs, human inborn metabolic diseases and dietary treatments. Orange nodes – *C. elegans* phenotypes; colored squares – *C. elegans* genes found in the screen; diamonds – human orthologs/homologs; gray circles – human diseases; hexagons – nutrients. Red edges indicate dietary avoidance; green edges indicate dietary supplementation. Red – genes from BCAA breakdown & propionate metabolism; Blue – genes from methionine metabolism; Yellow – genes from the TCA cycle; Green – genes from glycine cleavage system; Gray – genes involved in harvesting electrons from reduced $FADH_2$.

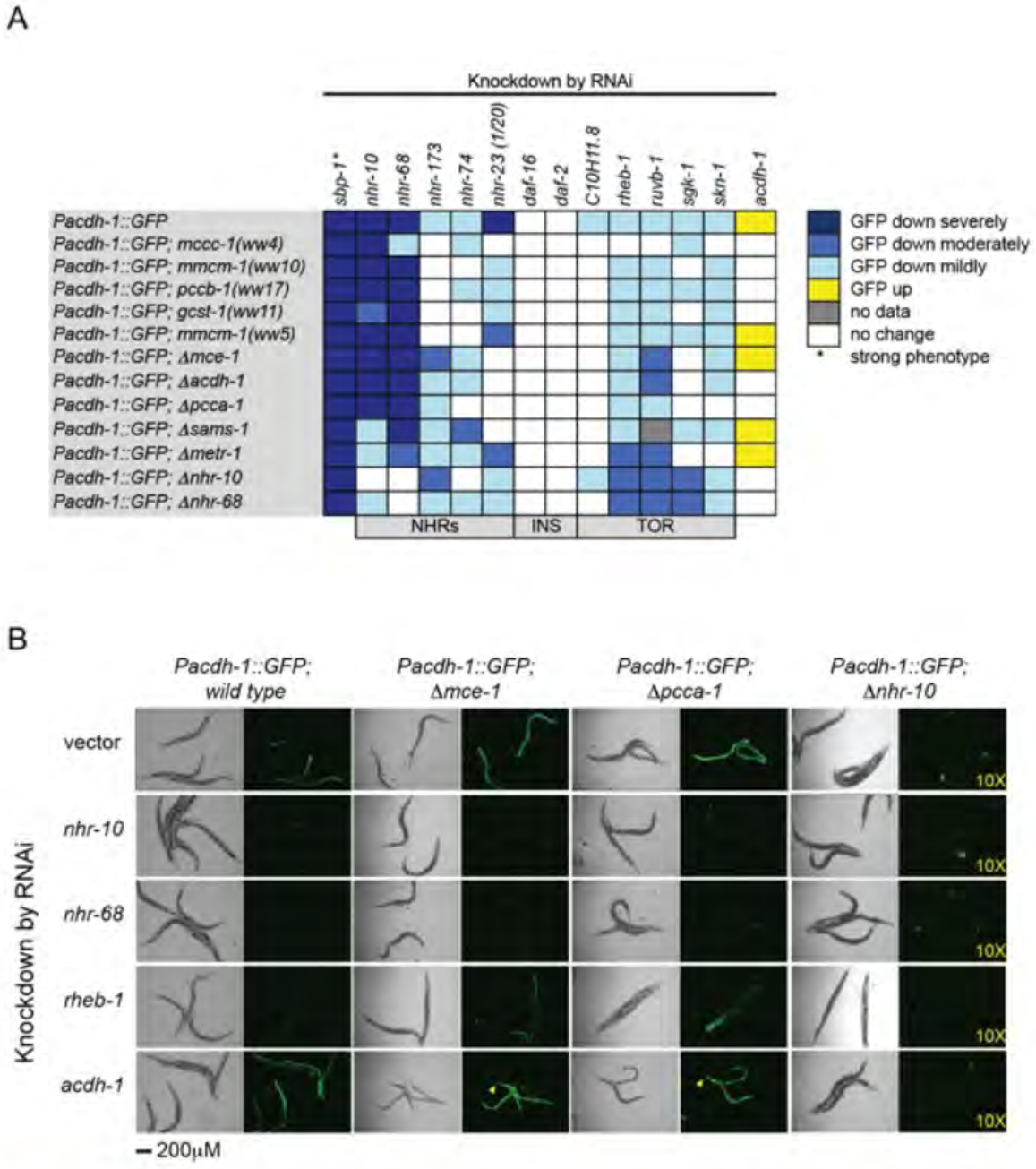

Figure 2.11 – Mediators of the Response to Metabolic Network Perturbation

(A) Summary of RNAi knockdown analysis in different mutant strains. INS – insulin signaling pathway components. The colors indicate visually examined changes in GFP expression in *Pacdh-1::GFP* dietary sensor animals. (B) DIC and fluorescent images of indicated strains (columns) exposed to different RNAi knockdowns (rows). Yellow arrowheads indicate an increase in GFP expression in the head hypodermis in *acdh-1* RNAi knockdown animals.

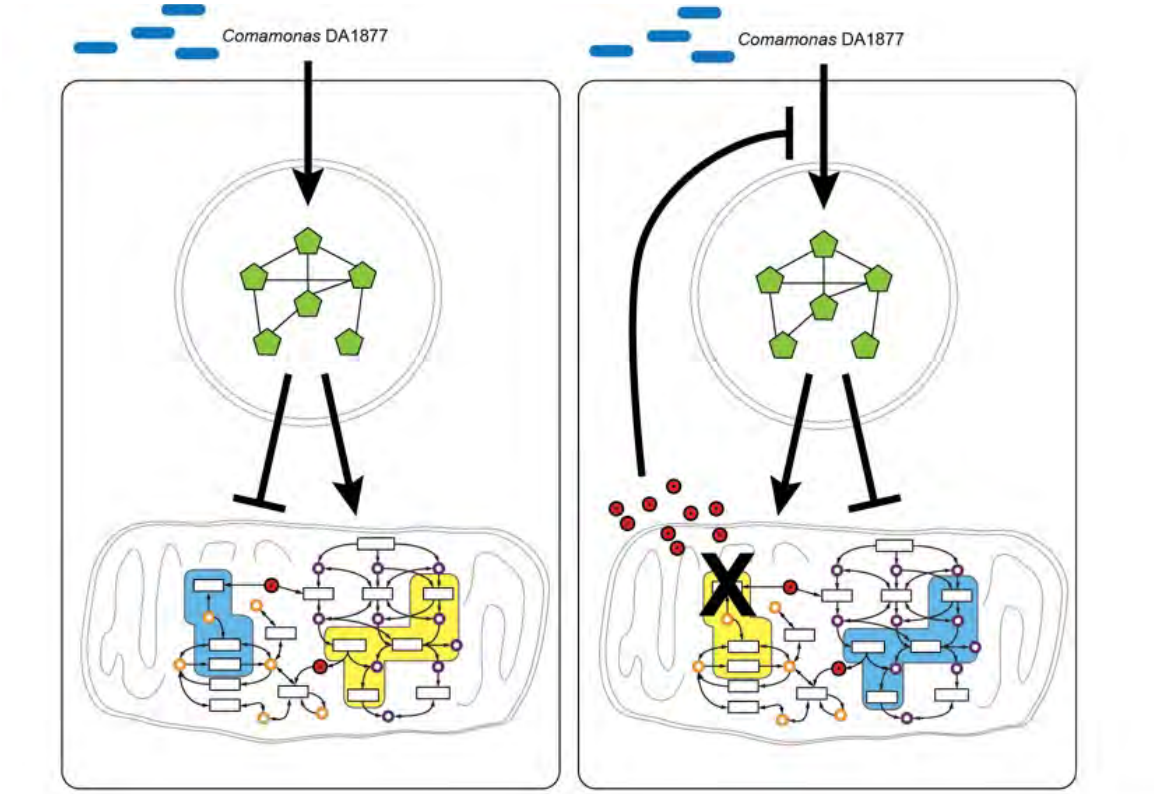

Figure 2.12 – Model Reflecting Feedback Between Mitochondrial Metabolic Networks and Nuclear Gene Regulatory Networks

qPCR primer sequences

Gene	Forward Primer	Reverse Primer
act-1	CTCTTGCCCCATCAACCATG	CTTGCTTGGAGATCCACATC
ama-1	AATATCTCGCAGGTTATCGC	GTGTACGATGACGGAAACC
cth-1	CACTTTGGAACTGATGCAGTC	CATACTAATTGGTGGAACTACCTG
cbs-1	AACAAGTTCAACCCAGAAAGG	TTGAAGCTTGACGAGTGGA
ech-6	TCGGAGCAATTGTGATTACTG	CGAACTCGTTATTGGTCATCTC
F09F7.4	CACAATGGAGTATCGTCTCAC	TTGTCAACGAGAATGGCTC
acdh-1	GCAAATGCAGATCCTAGCC	GTTTGTCTTCCTCCTTATCTACAG
acdh-2	GATGATAATCTTGGAATGCGTGC	CTTCAATAGCGTATTTGTATCCTTTTCC

nCounter probe sequences

Gene	Sequence	Target Region	Probe Sequence
acdh-2	C17C3_12a.1	659-759	ATGAAGGAGTCGTTCTTGGGGAACAAGATGATAATCTTGGAATGCGTGCAGGA ACCATTGCTCAAGTGCATTTGAATAGTGTGAGAGTTCCAAAAACATC
acdh-1	C55B7_4a.1	1020-1120	GCCGCACGTCTACTAGTGTATAATGCTGCCCGTATGAAAGAATATGGAATACCAT ATGTACGAGAAGCTGCAATGGCGAAACTGTTTGCATCACAGGTTG
ech-6	T05G5_6_1.1	734-834	CAATCTCCACTGATTGTTCAAATGGCAAAGGAGGCCGTTAACAAAGCTTATGAG CTTACTCTTCAAGAGGGACTTCACTTCGAAAGACGACTTTTCCATG
ama-1	F36A4_7.1	3528-3628	TGAAAAAGGTAACATGCAATACAGCGATCTACTACGATCCTGACCCAAAGAACA CGGTGATCGCCGAAGACGAGGAATGGGTATCGATTTTCTACGAGAT

Table 2.5 – RT-qPCR primers and Nanostring probe sequences.

Experimental Procedures

Strains

C. elegans strains were grown as described [90]. N2 (Bristol) was used as the wild type strain. The following mutant strains were provided by the *C. elegans* Gene Knockout Consortium (CGC): *nhr-68(gk708), sams-1(ok2946), cbl-1(ok2954), mce-1(ok243), pcca-1(ok2282), metr-1(ok521)*, ZK669.4(*ok3001*), *sams-5*(*gk147*) and *hlh-11*(*ok2944*). The *nhr-10*(*tm4695*) mutant strain was provided by the National Bioresource Project, Japan. The *Pacdh-1::GFP* strain (VL749) is described in [29]. VL405 [*Pmir-63::GFP* + *unc-119(+)*] is described in [74]. BC12350 *dpy-5(e907)*; *sIs12119* [rCesC53A3.2::GFP + pCeh361] is described [91]. CL2166 *dvIs19*[pAF15(*Pgst-4::GFP::NLS*)] [92].

EMS Screen

VL749 animals were treated with 0.5% EthylMethylSulfoxide (EMS) for four hours. Mutagenized animals were transferred to Nematode Growth media (NGM) plates seeded with *Comamonas* DA1877 and allowed to lay eggs. Eggs were collected and 100 10 cm *Comamonas* DA1877-NGM plates were seeded with 50 F1 animals each. F2 animals were screened for visible GFP. A single GFP-positive F2 animal was picked from each F1 plate and transferred to individual plates. Of the 100 mutants, 45 were fertile and produced GFP-positive offspring when fed *Comamonas* DA1877.

Mutant Mapping

Chromosomal assignment was done by crossing mutants carrying the *Pacdh-1::GFP* reporter into the CB4856 (Hawaiian) strain followed by SNP mapping of GFP positive pools of F2 animals as described [93]. Mutants that produced GFP positive F1 males were assigned to linkage group (LG) X. Primers used for chromosomal assignment are as described [94]. Following chromosomal assignment, fine mapping was undertaken for five mutants using chromosomal primers as described [93, 94]. We created *him-5(e1467)* lines carrying the *Pacdh-1::GFP* transgene and the mutation of interest to perform complementation tests. These *him-5* lines were used to generate males that were crossed into mutant hermaphrodites carrying *Pacdh-1::GFP,* and assessed GFP expression in F1 animals grown on *Comamonas* DA1877.

Whole Genome Sequencing

Before sequencing, mutants were outcrossed three times to N2 wild type animals. Total genomic DNA was prepared for mutants *ww2*, *ww4*, *ww10*, *ww11* and *ww17* as described [95]. Libraries were made and barcoded using the NextFlex barcoding system and library construction kits (Bio Scientific). Samples were sequenced by the IIGB Genomic Core facility, UC Riverside, using Illumina's HiSeq2000 platform (51 bp reads). After filtering out low-quality reads using the default Illumina pipeline quality filter, we recovered 184.8 million reads representing an 18X average coverage. Reads were mapped onto the *C. elegans* genome sequence (WS201) and variants were identified using

MAQgene with default parameter setting except that minimum fraction of non-wildtype reads was set to 0.8, minimum span of uncovered bases to report as uncovered region was set to 1 and maximum sum of error qualities was set to 150 [96]. Mismatches were compared between all five mutants. Basepair changes common to all mutants were ignored, as these were likely present in our starting strain. Variants were validated by PCR and sequencing. Additional alleles were identified by PCR amplification followed by sequencing of targeted genes.

RNAi Screen

RNAi screening was performed on 96-well plates using NGM agar containing 5 mM IPTG. *E. coli* HT115 RNAi cultures were grown in LB containing 100 µg/mL ampicillin to log phase in 96-well deep well dishes. Bacteria were centrifuged and resuspended in 1/20 volume of M9. 10 mL of the resuspended cultures was added to the RNAi screening plates. For the *Comamonas* DA1877 condition screen, *Comamonas* DA1877 was grown overnight to saturation in LB, then sonicated and diluted 1/10 with LB containing 100 µg/mL ampicillin. 10 mL drops were added to each well of the *E. coli* HT115-RNAi seeded plates. VL749 animals were synchronized by hypochlorite bleaching, washed in M9 media, and approximately 25 eggs were added to each well. After 60 hours animals reached the early adult stage and were visually screened for GFP expression. RNAi clones found to affect GFP in the first pass of the screen (856 clones) were re-arrayed and retested four times. 554 genes retested at least 2 out of 4 times and

were re-arrayed again. These clones were tested three times for specificity using strain VL405, which contains an integrated *Pmir-63::GFP* construct [74]. 192 genes did not affect *Pmir-63::GFP* in any of the three tests and were considered specific for *Pacdh-1::GFP*. All final hits were sequence-verified.

Mutant Validation

nhr-68(gk708), sams-1(ok2946), cbl-1(ok2954), mce-1(ok243), pcca-1(ok2282), metr-1 (ok521), ZK669.4 (*ok3001*), *sams-5* (*gk147*), *nhr-10* (*tm4695*) and *hlh-11* (*ok2944*) mutants were outcrossed three times to the wild type N2 strain, homozygosed, with the exception of the *ok3001* allele, a deletion in the gene ZK669.4, which produced sterile homozygotes. Pictures of sterile ZK669.4(*ok3001*) homozygotes from heterozygous parents were taken and animals were retrospectively genotyped. RNA was isolated from the *hlh-11* and *sams-5* deletion mutant strains grown on *E. coli* OP50, *E. coli* HT115 or *Comamonas* DA1877 for qRT-PCR analysis. All outcrossed mutant strains were also crossed to VL749 and homozygosed.

qRT-PCR

Animals were synchronized and grown on *E. coli* OP50, *E. coli* HT115, or *Comamonas* DA1877 and approximately 1000 adult animals were harvested for each condition. Animals were thoroughly washed in M9 buffer, and total RNA was isolated using Trizol (Invitrogen) followed by DNAseI treatment and cleanup using Qiagen RNeasy columns. cDNA was prepared from 1 mg of RNA using

oligo-dT and Mu-MLV enzyme (NEB). Primer sequences for quantitative RT-PCR (qRT-PCR) were generated using the GETprime database [97] and are listed in **Table S5**. qRT-PCR was performed in triplicate using the Applied Biosystems StepOnePlus Real-Time PCR system and Fast Sybr Green Master Mix (Invitrogen). Relative transcript abundance was determined using the ΔΔCt method, and normalized to averaged *ama-1* and *act-1* mRNA expression levels [98].

nCounter Analysis

RNA was extracted as described above. nCounter analysis was performed as per manufacturers instructions (Nanostring technologies) using 300 ng of total RNA, and expression between samples was normalized to *ama-1* mRNA levels. Probes used are listed in **Table 2.5**.

Functional Annotation

GO analyses were performed using David [99]. WormNet v.2 was used as described [100]. Genes found to affect *Pacdh-1::GFP* in the screens were subjected to functional categorization based on manual curation. Gene descriptions in WormBase were used to assign genes to categories when available, or the described function for the closest human homolog was used. If no functional annotation could be assigned to a gene, it was placed in the 'unknown' category. If a gene's described function was not within one of the major categories, it was placed in the 'other' category. Tissue expression was

assigned based on WormBase WS232 annotations and was categorized into intestinal, non-intestinal, and unknown groups. If the subset of tissues in which a gene is expressed included the intestine, it was placed in the intestinal group. If the tissue expression for a gene was described but did not include the intestine, it was placed in the non-intestinal group. If no expression patterns were described, it was placed in the unknown group.

Metabolic Map

Annotations for *C. elegans* BCAA breakdown, methionine metabolism and the TCA pathway were obtained from the KEGG database [101] and from WormBase.

Microarray Expression Profiling

Mutant animals were grown on *Comamonas* DA1877 on standard NGM plates for two generations prior to egg collection. Eggs were collected and synchronized in L1 stage and grown until they reached the gravid adult stage. Animals were washed twice in M9 buffer, pelleted by centrifugation and frozen at -80^{o}C in Trizol. RNA was collected using Trizol extraction followed by DNAse I treatment and cleanup using RNeasy prep kit (Qiagen). Three biological replicates were prepared for each condition. Microarray expression profiling was performed by the Genomics Core facility at University of Massachusetts Medical School using *C. elegans* genome arrays (Affymetrix). The RMA method in the Affy package

from Bioconductor was used in R to summarize the probe level data and normalize the dataset to remove across-array-variation. Log transformed data were used in subsequent analyses. Moderated T statistics in Limma (Smyth et al., 2004) was used to calculate significance. Significance was determined using an adjusted p-value [102]. Changes in gene expression that were 2-fold ($p < 0.001$) or greater were considered significantly changed. Microarray data was submitted to GEO (GSE43952).

Starvation Experiments

Animals were first grown to L4 on *E. coli* OP50 bacteria. L4 animals were washed five times in M9, and then transferred to unseeded peptone-free NGM plates. After 24 hours, animals were collected and examined for GFP expression.

CHAPTER III: INTERSPECIES SYSTEMS BIOLOGY UNCOVERS METABOLITES AFFECTING *C. ELEGANS* GENE EXPRESION AND LIFE HISTORY TRAITS

Preface

This research chapter derives from work that I started shortly after submitting our 2013 paper. We published this follow-up work in 2014, also in *Cell*, with the title "Interspecies systems biology uncovers metabolites affecting *C. elegans* gene expression and life history traits." In this work, I am the first author, Lesley MacNeil is the second author, and the others on the paper are Ashlyn Ritter, Safak Yilmaz, Adam Rosebrock, Amy Caudy, and Marian Walhout.

Lesley MacNeil generated and screened the transposon-based Comamonas mutant library, and contributed Figure 3.1b, and Table 3.1. Safak Yilmaz analyzed the *Comamonas* whole-genome sequencing data and assembled the genome, and contributed Figure 3.2a. Adam Rosebrock and Amy Caudy developed the mass spec methods for measuring Ado-Cbl and Me-Cbl from bacteria, and generated the data that went into Figure 3.4a. Ashlyn Ritter performed the lifespan assays and is responsible for Figure 3.8a.

Abstract

Diet greatly influences gene expression and physiology. In mammals, elucidating the effects and mechanisms of individual nutrients is challenging due

to the complexity of both the animal and its diet. Here we used an interspecies systems biology approach with *Caenorhabditis elegans* and two if its bacterial diets, *Escherichia coli* and *Comamonas aquatica,* to identify metabolites that affect the animal's gene expression and physiology. We identify vitamin B12 as the major dilutable metabolite provided by *Comamonas aq.* that regulates gene expression, accelerates development and reduces fertility, but does not affect lifespan. We find that vitamin B12 has a dual role in the animal: it affects development and fertility via the methionine/S-Adenosylmethionine (SAM) cycle and breaks down the short-chain fatty acid propionic acid preventing its toxic buildup. Our interspecies systems biology approach provides a paradigm for understanding complex interactions between diet and physiology.

Introduction

Our diet provides building blocks for development and reproduction, as well as energy to sustain daily cellular and organismal activities. Complex diets consist of macronutrients such as carbohydrates, fats and proteins, but also provide micronutrients such as vitamins that function as cofactors in metabolic reactions. In mammals, nutrients are provided not only by diet but are also synthesized by the gut microbiota [103]. A major challenge is to unravel the contributions of individual metabolites to cellular and organismal physiology, and to dissect the metabolic and genetic underpinnings of physiological responses to changing diets.

The nematode *C. elegans* is an emerging model to study the effects of diet on life history traits such as developmental rate, fertility and aging [104-106]. *C. elegans* is a relatively simple model organism composed of fewer than 1000 somatic cells. It lives in temperate climates around the globe and subsists on diets of various bacterial species growing on rotting vegetation. These bacteria also inhabit the *C. elegans* intestine to serve as its microbiota [107]. In the laboratory, *C. elegans* are grown monoxenically on *E. coli* OP50, but many other bacterial strains and species have been fed to worms as well [30, 104, 105, 108, 109]. Bacteria supply *C. elegans* with metabolites that can greatly affect its life history traits. For instance, bacterially derived nitric oxide and folate extend and limit the lifespan of the animal, respectively [37, 110]. The effects of these metabolites were identified by a hypothesis-driven approach (nitric oxide) or serendipitously by a mutation in the bacteria (folate). Since both *C. elegans* and its bacterial diet are genetically tractable, we reasoned that this predator-prey combination could be used for the unbiased identification of nutrients that drive transcriptional and physiological responses in the animal.

We previously found that, relative to *E. coli* OP50, a diet of *Comamonas* DA1877 accelerates *C. elegans* development and decreases fertility and lifespan [105]. These physiological effects are accompanied by dramatic changes in gene expression [105]. For instance, the acyl-CoA dehydrogenase-encoding gene *acdh-1* is repressed several hundred fold on the *Comamonas* DA1877 diet relative to *E. coli* OP50. We created transgenic animals harboring the *acdh-1*

promoter driving expression of the green fluorescent protein (GFP) to generate a transgenic “dietary sensor” strain with which the transcriptional response to the *Comamonas* DA1877 diet can be readily monitored in living animals [105]. Remarkably, the effects of *Comamonas* DA1877 on *C. elegans* gene expression and development persist even when these bacteria are mixed in small amounts with the *E. coli* OP50 diet, indicating that *Comamonas* DA1877 generates one or more dilutable compounds to which *C. elegans* responds. Using the dietary sensor strain, we identified a *C. elegans* network consisting of metabolic and regulatory genes that, when perturbed, interferes with the transcriptional response to *Comamonas* DA1877 [64].

Here, we used an interspecies systems biology approach to identify bacterial metabolites that affect *C. elegans* gene expression and life history traits. We performed genetic screens in *E. coli* and *Comamonas* to identify bacterial genes that, when mutated, result in aberrant repression or activation of *Pacdh-1::GFP* in *C. elegans*. We performed a secondary metabolite screen by supplementing 25 candidate metabolites to *Pacdh-1::GFP* animals. Eight compounds activated the dietary sensor, including branched chain amino acids, threonine and propionic acid. Two compounds repressed the sensor – methyl-cobalamin (Me-Cbl) and adenosyl-cobalamin (Ado-Cbl), the two biologically active forms of vitamin B12. We demonstrate that vitamin B12 is generated by *Comamonas* DA1877 but not by *E. coli*, and that it drives many of the gene expression and physiological changes in *C. elegans* induced by the *Comamonas*

diet. Interestingly all eight activating metabolites are closely connected in the *C. elegans* metabolic network to the two enzymes that require vitamin B12 as a cofactor. We find that vitamin B12 fulfills two important physiological roles in *C. elegans*: it regulates development through the synthesis of the major methyl donor SAM, and alleviates toxic buildup of the short-chain fatty acid propionic acid. Our interspecies systems biology approach provides a powerful paradigm for gaining insight into the complex interactions between diet, metabolic regulation and physiology.

Results

Genetic Screens in Bacterial Diets

We previously determined that *Comamonas* DA1877 bacteria must produce a dilutable compound to which *C. elegans* responds with altered gene expression programs, accelerated development, reduced fertility and reduced lifespan [105]. We reasoned that we could discover bacterial metabolites that affect *C. elegans* by identifying bacterial genes involved in the generation, processing or transport of these small molecules. We used the *C. elegans Pacdh-1*::*GFP* dietary sensor as a reporter for diet-induced gene expression changes: GFP expression is high when the animals are fed *E. coli* OP50, but barely detectable when they are fed *Comamonas* DA1877. We performed genetic screens in each of these bacteria to identify mutant strains that, when fed to *C. elegans* alter GFP expression.

First, we fed dietary sensor animals the Keio *E. coli* BW25113 collection, which contains deletion mutants for 3,985 of the 4,290 protein-coding genes [38]. We visually examined whether GFP expression was decreased or increased relative to animals fed the wild type strain (**Figure 3.1a)**. In total, 70 mutant *E. coli* strains decreased GFP expression, and seven caused an increase compared to the parent strain (**Table 3.1**). Second, we performed a transposon-based mutagenesis screen of *Comamonas* DA1877 bacteria (**Figure 3.1b**). Using a non-replicating transposon, we generated 5,760 *Comamonas* DA1877 mutants each with a single transposon insertion. Five mutant *Comamonas* DA1877 strains failed to repress GFP expression when fed to the sensor strain.

To facilitate the mapping of transposon insertions and identification of the disrupted genes, we sequenced the *Comamonas* DA1877 genome and annotated protein-coding sequences and RNA genes (**Figure 3.2a**). Since there was no systematic report on the taxonomic identity of *Comamonas* DA1877 before this study, we first used the single 16S rRNA gene to identify this strain at the species level as *Comamonas aquatica*, and we will henceforth refer to *Comamonas* DA1877 as *Comamonas aq.* DA1877.

We reasoned that bacterial mutants identified affect *C. elegans* gene expression due to either the buildup or reduction in particular metabolites. A total of 77 *E. coli* and 5 *Comamonas aq.* DA1877 genes (**Table 3.2**) were identified in the bacterial screens. We focused on bacterial genes encoding metabolic enzymes, transporters, and transcription factors known to regulate metabolic

operons. Mapping these genes onto bacterial metabolic networks revealed that perturbation of several different pathways affected GFP expression in *C. elegans* (**Figure 3.1c**). For instance, mutations in enzymes from *E. coli* purine metabolism, propionic acid metabolism, the TCA cycle, and the biosynthesis of siderophores (iron scavengers) decreased dietary sensor activity. Conversely, *E. coli* and *Comamonas* mutations in branched chain amino acid biosynthesis and vitamin B12 biosynthesis/import resulted in increased *C. elegans* dietary sensor activity.

A Metabolite Screen in *C. elegans* Identifies Vitamin B12 as a Candidate *Comamonas*-Provided Molecule

We selected a subset of metabolites implicated by the bacterial screens for use in a secondary screen in which their effect on the *C. elegans* dietary sensor was tested by direct supplementation to either diet. We focused on 18 metabolites implicated by bacterial genes encoding metabolic enzymes, transporters, and transcription factors known to regulate metabolic operons. We included 7 additional metabolites that were implicated from our earlier *C. elegans* genetic screens [64]. We supplemented the metabolites at various concentrations to the *Pacdh-1::GFP* sensor strain fed either bacterial diet (**Figure 3.3a**). Six metabolites caused mild, dose-dependent increases in GFP expression when supplemented to the *Comamonas aq.* DA1877 diet, including the amino acids valine, isoleucine, threonine and glycine, as well as homocysteine and vitamin B6. Two metabolites, α-ketobutyrate and propionic

acid, more dramatically increased GFP expression when supplemented to *Comamonas aq.* DA1877 and also further increased GFP expression on the *E. coli* OP50 diet (**Figure 3.3b, Table 3.3**).

Only two metabolites mimicked the strong repressive effect of the *Comamonas aq.* diet on the *Pacdh-1::GFP* sensor when supplemented to *E. coli* OP50: the two biologically active forms of vitamin B12, Ado-Cbl Me-Cbl (**Figure 3.3c**). Vitamin B12 is an attractive candidate to be the dilutable molecule produced by *Comamonas aq.* DA1877 [105] for several reasons. First, two of five *Comamonas aq.* DA1877 genes identified in the transposon screen encode vitamin B12 biosynthetic enzymes (*cbiA* and *cbiB*, **Table 3.2** and **Figure 3.2b**). Second, vitamin B12 was also implicated by the *E. coli* deletion collection screen, even though they do not synthesize this cofactor (see below). A deletion in *tonB*, which encodes a protein required for vitamin B12 import [111], resulted in even greater levels of GFP expression when fed to the sensor strain (**Figure 3.2c**). Third, Ado- and Me-Cbl were the only repressors identified in the chemical screen, and both robustly repress *Pacdh-1::GFP* in low (nM) doses. This fits with the observation that mixing small amounts of the *Comamonas aq.* DA1877 diet into the *E. coli* OP50 diet is sufficient to exert gene expression and physiological changes [29]. Finally, mutations in the two *C. elegans* enzymes that use vitamin B12 interfere with the transcriptional response to the *Comamonas aq.* DA1877 diet [64]. Vitamin B12 is an essential nutrient for most animals, but is only synthesized by some species of bacteria [112]. It is used as a cofactor by the

same two enzymes in all vitamin B12-dependent animals: methylmalonyl-CoA mutase (MUT; MMCM-1 in *C. elegans*), which is involved in propionyl-CoA breakdown, and methionine synthase (MS; METR-1 in *C. elegans*), which is involved in the methionine/SAM cycle. Methylmalonyl-CoA mutase uses Ado-Cbl whereas methionine synthase uses Me-Cbl (**Figure 3.2d**). We previously found that both of these vitamin B12-dependent enzymes, as well as others in their respective pathways, are required for *Comamonas* DA1877-induced gene expression changes [64]. Taken together, these results suggest that vitamin B12 may be the dilutable molecule provided by the *Comamonas aq.* DA1877 diet that represses *Pacdh-1::GFP*.

Vitamin B12-Producing Bacteria Repress *Pacdh-1::GFP*

Our results predict that vitamin B12 levels are dramatically higher in the *Comamonas aq.* DA1877 than the *E. coli* OP50 diet. To directly compare the amounts of vitamin B12 we measured Ado-Cbl by mass spectrometry. Ado-Cbl levels are much higher in *Comamonas aq.* DA1877 than *E. coli* OP50 (**Figure 3.4a**), but are reduced to background in the *Comamonas aq. cbiA* mutant, indicating that this mutant indeed fails to synthesize vitamin B12.

We fed additional bacterial species to *Pacdh-1::GFP* dietary sensor animals and correlated their effect on GFP expression with the presence or absence of a vitamin B12 biosynthesis pathway. Four of these seven bacterial species have the capacity to synthesize vitamin B12 and three do not (**Figure 3.4b**). We found that the presence or absence of a vitamin B12 biosynthetic

pathway in the bacterial diet correlates perfectly with the repression or activation of the *acdh-1* promoter in *C. elegans*, respectively (**Figure 3.4b**).

Vitamin B12 Processing and Utilization System is Required For Its Affects on *Pacdh-1::GFP*

Vitamin B12 repressed GFP expression equally well whether supplemented to live or UV-killed *E. coli* OP50 diets, indicating that its effects do not depend on *E. coli* modification or metabolism (**Figure 3.5a**). We wondered why Ado-Cbl and Me-Cbl repress the dietary sensor equally well (**Figure 3.3**). From studies of human cobalamin deficiency disorders, it is known that after vitamin B12 is imported into the cell, it is stripped of its upper axial ligand, undergoes several processing steps, is modified into Ado-Cbl and Me-Cbl, and distributed to the two enzymes that use it (**Figure 3.5b**). Our supplementation experiments likely cannot discriminate between individual effects of these two forms of vitamin B12 because they can be interconverted. We wondered whether vitamin B12 processing and/or distribution in *C. elegans* are required for its repressive effect on *Pacdh-1::GFP*. In our previous *C. elegans* genetic screens, we did not retrieve any vitamin B12 import and processing genes [64], potentially due to inherently high false negative rates in RNA interference (RNAi) screens [7]. We predicted *C. elegans* vitamin B12 processing genes based on homology with known human genes (**Figure 3.5b**). RNAi of each of two genes tested, *mtrr-1* and Y76A2B.5, resulted in failure of both Me-Cbl and Ado-Cbl to repress the dietary sensor (**Figure 3.5c**). This indicates that supplemented vitamin B12 must

be properly processed and regenerated into its active forms within *C. elegans* to repress *Pacdh-1::GFP*.

We previously found that enzymes in propionyl-CoA breakdown and the methionine/SAM cycle are required for the repressive effect of the *Comamonas aq.* DA1877 diet on the dietary sensor [64]. Thus, one would predict that these enzymes are also required for the repressive effects of vitamin B12 supplementation. We used two deletion mutants in each of these pathways to test whether they are also involved in mediating the response to vitamin B12. Indeed supplemention of vitamin B12 to either propionyl-CoA breakdown or methionine/SAM cycle mutants failed to repress *acdh-1* promoter activity. (**Figure 3.5d**). Taken together, vitamin B12 processing/distributing genes and intact vitamin B12-dependent metabolic pathways are required for the effect of this cofactor on *C. elegans*.

Propionic Acid Can Override Vitamin B12 to Activate the Sensor

Vitamin B12 represses the dietary sensor, while vitamin B6, homocysteine, glycine, threonine, isoleucine, valine, α-ketobutyrate and propionic acid activate the *acdh-1* promoter (**Figure 3.3a**). Interestingly, the breakdown of each of these amino acids as well as α-ketobutyrate and propionic acid involves conversion to propionyl-CoA (**Figure 3.6a**). Vitamin B6 functions as a cofactor in two reactions that lead to the production of propionyl-CoA (**Figure 3.6a**). Since vitamin B12 increases flux through the propionyl-CoA breakdown pathway, we hypothesized that the balance between vitamin B12 and propionyl-

CoA levels may be the driving force controlling *acdh-1* promoter activity. To test this hypothesis, we performed a chemical epistasis experiment and found that excess propionic acid can override the repressive effects of vitamin B12 on the dietary sensor in a dose-dependent manner (**Figure 3.6b**). This suggests that the effects of vitamin B12 on the *acdh-1* promoter may depend on its capacity to repress the buildup of an activator, propionic acid.

Vitamin B12 Mimics Broad *Comamonas aq.* DA1877 Mediated Gene Expression Changes

The *Comamonas aq.* DA1877 diet affects the expression of many *C. elegans* genes, including *acdh-1* [105]. To assess whether vitamin B12 can elicit similar broad effects on gene expression, we used quantitative RT-PCR (qRT-PCR) to determine relative expression levels of 14 representative *Comamonas*-downregulated genes and 14 representative *Comamonas*-upregulated genes in wild type animals fed *E. coli* OP50 with or without three doses of supplemented Me-Cbl or Ado-Cbl. All but one of the genes tested changed in expression on the *Comamonas aq.* DA1877 diet as described previously. Most of the *Comamonas*-downregulated genes were also downregulated when animals were fed *E. coli* OP50 supplemented with either form of vitamin B12 (**Figure 3.6c**). Likewise, most *Comamonas*-upregulated genes were also activated by supplementation of vitamin B12 (**Figure 3.6c**). Thus, vitamin B12 supplementation to the *E. coli* OP50 diet induces similar gene expression changes as those elicited by the *Comamonas aq.* DA1877 diet.

Six vitamin B12-downregulated genes, including *acdh-1,* were upregulated in response to propionic acid (**Figure 3.6c**). Further, propionic acid could override the repressive effect of vitamin B12 on these genes. Interestingly, a subset of the vitamin B12-downregulated genes did not respond to propionic acid. A similar trend was observed among the vitamin B12-activated genes; while some responded to propionic acid, others did not. Therefore, we determined that there are at least two classes of vitamin-B12 responsive genes: those that respond to propionic acid (hereafter referred to as type 1) and those that do not (type 2).

Vitamin B12 Accelerates *C. elegans* Developmental Rate and Egg Laying Timing and Requires the Methionine/SAM Cycle

Since vitamin B12 mimics the effects of the *Comamonas aq.* DA1877 diet on *C. elegans* gene expression, we next tested whether it also mimics the accelerated development, reduced fertility and accelerated aging induced by this bacterial diet [105]. Vitamin B12 supplementation affected neither the mean nor the maximum lifespan of *C. elegans* (**Figure 3.8a**). This indicates that another factor must be responsible for the *Comamonas aq.* DA1877 effect on aging, which is in agreement with the observation that a diet consisting of *E. coli* OP50 supplemented with a small amount of *Comamonas aq.* DA1877 does not shorten lifespan [105].

Addition of vitamin B12 to the *E. coli* OP50 diet did accelerate development, although it did not fully recapitulate the extent of developmental

rate increase elicited by the *Comamonas* diet (**Figure 3.7a**). This indicates that additional growth enhancing bacterial factors may be provided by *Comamonas*. Propionic acid supplementation to the *E. coli* OP50 diet slowed *C. elegans* development, and supplementation of both propionic acid and vitamin B12 resulted in intermediate growth rates (**Figure 3.7b**). Based on this observation we hypothesized that propionic acid levels may dictate developmental rate: low concentrations caused by high vitamin B12 would accelerate development, whereas high propionic acid levels that occur when vitamin B12 is limiting would slow development. To test this hypothesis, we measured developmental timing in four metabolic gene mutants, two from each vitamin B12-dependent pathway: Δ*mce-1* and Δ*pcca-1* from propionyl-CoA metabolism and Δ*metr-1* and Δ*sams-1* from the methionine/SAM cycle. When fed *E. coli* OP50, all four mutants exhibited slow growth compared to wild type animals (**Figure 3.7c**). Surprisingly, supplementation of vitamin B12 accelerated development in Δ*mce-1* and Δ*pcca-1* mutant animals, but failed to increase developmental rate in Δ*metr-1* and Δ*sams-1* mutants (**Figure 3.7c**). Thus, vitamin B12-induced developmental acceleration requires a functional methionine/SAM cycle, but not the propionyl-CoA breakdown pathway. Δ*mce-1* and Δ*pcca-1* mutants fail to catabolize propionyl-CoA [113], likely resulting in a buildup of propionic acid. Neither Δ*mce-1* nor Δ*pcca-1* mutants can break down propionic acid even when vitamin B12 is present; yet supplementation of this cofactor does accelerate development in these mutants. These data suggest that the levels of propionic acid are not the

driving force behind developmental rate, but rather that development is accelerated via the methionine/SAM cycle, as a result of buildup or lack of specific metabolites therein.

To further test this model, we first focused on *metr-1* (methionine synthase), which converts homocysteine to methionine by using vitamin B12 as a cofactor. In this reaction, 5-methyl-tetrahydrofolate is also converted to the biologically active form of folate, tetrahydrofolate (**Figure 3.6a**). Loss of METR-1 function can be caused either by a mutation in the corresponding gene or as a result of vitamin B12 deficiency. In humans, loss of the corresponding enzyme leads to depletion of tetrahydrofolate and methionine, and buildup of homocysteine. Folate supplementation (which is converted to tetrahydrofolate *in vivo*) did not rescue the slow growth of Δ*metr-1* mutants (**Figure 3.7d**). Thus, tetrahydrofolate depletion is not a primary cause of developmental rate reduction. Methionine supplementation, on the other hand, largely rescued the developmental rate defect of Δ*metr-1* mutants (**Figure 3.7d**). Interestingly, methionine supplementation did not accelerate development of Δ*sams-1* mutant animals, which are impaired in converting methionine to SAM (**Figure 3.7d**) [89]. This suggests that the developmental acceleration by methionine depends on its conversion to SAM. Taken together, these data suggest that vitamin B12 accelerates *C. elegans* development primarily through its role as a cofactor in the methionine/SAM cycle, rather than in propionyl-CoA breakdown. However, excess propionic acid slows development, which is likely due to toxic effects.

Supplementing *E. coli* with vitamin B12 reduced total brood size and therefore mimics the *Comamonas aq.* DA1877 diet in regard to this phenotype as well (**Figure 3.8b**). Both the *Comamonas aq.* DA1877 diet and vitamin B12 supplementation altered the dynamics of egg laying; animals laid almost all of their eggs (93% and 96% respectively) within the first two days. In contrast, animals fed *E. coli* OP50 laid only 70% in the first two days (**Figure 3.8c**). This vitamin B12-induced shift to early egg laying was still observed in Δ*pcca-1* mutants, but the effect was lost in Δ*metr-1* mutant animals (**Figure 3.8b**). Together, these results indicate that vitamin B12 both accelerates development and shifts egg-laying dynamics via its role in the methionine/SAM cycle.

Vitamin B12 Protects Against Propionic Acid Toxicity and Requires the Propionyl-CoA Breakdown Pathway

The developmental acceleration induced by vitamin B12 did not rely on its role in propionyl-CoA breakdown, however vitamin B12 did prevent some of the developmental deceleration induced by high doses of propionic acid (**Figure 3.7b**). At such high doses, propionic acid is toxic to the animal (**Figures 2A, 6A**). We asked whether vitamin B12 supplementation could alleviate the toxic effects of excess dietary propionic acid in wild type and Δ*pcca-1* mutant animals. Vitamin B12 increased tolerance to propionic acid in wild type animals, but not in Δ*pcca-1* mutant animals, which are much more sensitive to propionic acid supplementation in general (**Figure 3.9a**). This is in agreement with the notion that animals lacking *pcca-1* accumulate propionic acid and cannot utilize vitamin

B12 to metabolize it. Interestingly, wild type animals fed *Comamonas aq.* DA1877 are much more resistant to propionic acid than those fed *E. coli OP50* supplemented with 64 nM vitamin B12 (**Figure 3.9a**). This indicates that *Comamonas aq.* DA1877 may provide additional compounds that alleviate propionic acid toxicity, or that these bacteria metabolize more propionic acid, thus lowering the effective concentration delivered to the animal.

We wondered whether loss of *metr-1* would also increase sensitivity to propionic acid toxicity. Surprisingly, Δ*metr-1* mutants tolerated excess propionic acid slightly better than wild type animals, although this difference was lost when vitamin B12 was in ample supply (**Figure 3.9b**). When vitamin B12 is limiting it is conceivable that MMCM-1 and METR-1 compete for this cofactor. As a result, MMCM-1 might be able to utilize more of the vitamin B12 pool for the breakdown of propionic acid when METR-1 is absent.

Transcription of *acdh-1* is strongly activated in response to propionic acid supplementation, vitamin B12-deficient diets, or mutations in any of the four enzymes required for vitamin B12-dependent propionic acid breakdown. We wondered what the physiological role of this activation could be, and reasoned that *acdh-1* may function in response to propionic acid buildup, perhaps to help dampen its toxic effects. We tested the sensitivity of Δ*acdh-1* mutants to propionic acid and found that they are much more sensitive than wild type animals (**Figure 3.9b**). Unlike Δ*pcca-1* mutants, however, Δ*acdh-1* mutants survived better on propionic acid when vitamin B12 was supplemented to the

diet. This is likely because, unlike in Δ*pcca-1* mutants, the vitamin B12-dependent propionyl-CoA breakdown pathway is still intact in Δ*acdh-1* mutant animals. Taken together, type 1 vitamin B12 response genes that are activated by propionic acid may help to rewire flux through the metabolic network, thereby enabling the breakdown, excretion, or conversion of this metabolite, or alleviating its toxic effects indirectly.

Conclusions

Using an interspecies systems biology approach with *C. elegans* and two of its bacterial diets, we uncovered metabolites that affect gene expression and life history traits. We identified vitamin B12 as the major dilutable compound produced by *Comamomas aq.* DA1877 that regulates gene expression, accelerates development and affects fertility [105]; this study). Further, we determined that the balance between vitamin B12 and propionyl-CoA is likely the main driving force in the regulation of type 1 vitamin B12-response genes. This finding may reconcile a puzzling observation, namely that both vitamin B12 supplementation and starvation repress the dietary sensor [105]. How can supplementation of a compound and the absence of a compound have the same effect? In rats, starvation lowers levels of short chain fatty acids, including propionic acid, as animals catabolize their fat stores [114]. In worms starvation and vitamin B12 supplementation may have the same repressive effect on the dietary sensor by reducing the levels of propionyl-CoA.

We identified different physiological functions for the two vitamin B12-dependent pathways in *C. elegans*: the methionine/SAM cycle affects development and fertility, whereas the propionyl-CoA breakdown pathway mitigates propionic acid-induced toxicity (**Figure 3.10**). The observation that the methionine/SAM cycle affects development is compatible with the notion that this is an anabolic pathway that generates SAM, the major methyl donor used to modify proteins such as histones [115], and to synthesize phosphatidylcholine [89], which is vital for the production of cell membranes during development.

Vitamin B12 represses *acdh-1* expression at the level of transcription, though it is unclear whether it acts directly or indirectly. We previously identified several nuclear hormone receptors that control the response of the acdh-1 promoter to nutritional and metabolic conditions [64, 105]. Fat-soluble vitamins A and D are direct ligands for nuclear hormone receptors [116]. The *C. elegans* genome encodes 274 nuclear hormone receptors [117]. It is tempting to speculate that vitamin B12 directly interacts with one or more of these nuclear hormone receptors. However, our data indicate that vitamin B12 can only repress *Pacdh-1* when it can efficiently be used to break down propionyl-CoA because metabolic perturbations that block propionyl-CoA breakdown, or supplementation of excess propionic acid to wild type animals can override the repressive effect of vitamin B12 on *acdh-1* expression. We speculate that propionic acid may directly interact with one or more nuclear hormone receptors to regulate type 1 vitamin B12-response genes.

C. elegans is likely to encounter many different bacterial food sources in the wild [107]. Not all bacterial species synthesize vitamin B12 and *C. elegans* may have evolved an optimal gene expression program to help the animal cope with diets low in vitamin B12-producing bacteria. One consequence of this gene expression program may be metabolic rewiring; the expression levels of several metabolic genes predicted to function in vitamin B12-dependent pathways are sensitive to dietary vitamin B12 content [64, 105]. Turning various enzymes on or off at the level of gene expression may help to optimize metabolic flux. *acdh-1* expression is induced dramatically when vitamin B12 levels are low and propionic acid levels are high. While the exact metabolic functions of the ACDH-1 enzyme are unknown, we suspect that it may serve to re-route flux around propionyl-CoA within the metabolic network when vitamin B12 is limited to prevent toxic buildup of propionic acid in the animal. This notion is supported by our observation that Δ*acdh-1* mutants are sensitive to propionic acid toxicity.

Our findings suggest that *C. elegans* development, as it has been studied in the laboratory for decades using *E. coli* OP50, which is low in vitamin B12, only reflects one natural state. It will be interesting to study other characteristics of the animal such as behavior, mating and movement under ample vitamin B12 conditions.

Vitamin B12 deficiencies in humans can have severe impacts on health, causing anemias and neuropathies, as well as low birth weight, developmental retardation and defects in cognitive abilities in children of vitamin B12-deficient

mothers [118]. Such deficiencies can lead to propionic and methylmalonic acidemias, homocystinuria, methionine/SAM deficiency or a combination thereof, and it is not yet fully understood which of these metabolic imbalances lead to physiological and pathological consequences in humans. Each of these different diseases can also be caused by inborn errors in metabolic genes; for instance propionic acidemia is caused by mutations in the human ortholog of *pcca-1* [119]. Altogether, the interspecies paradigm we present provides a model to further characterize vitamin B12-dependent processes, and may provide a platform for the development of dietary or drug treatments to vitamin B12-related deficiencies.

Vitamin B12 is an essential cofactor in mammals and *C. elegans* [120], but is not used at all by plants, yeast or many insect species. The uneven distribution of vitamin B12 use among eukaryotes is interesting, as is the uneven distribution of vitamin B12 biosynthetic capability among bacterial species. Considering that many species of enteric bacteria can synthesize this essential vitamin suggests that the chemical outsourcing of vitamin B12 production may be an important keystone of a mutually beneficial relationship between gut microbiota and host [121-123]. The microbiota greatly affects its host's metabolism [124]. For instance, bacteria in the gut break down dietary fiber, which results in the production of short-chain fatty acids such as propionic acid that are absorbed by intestinal epithelia and used to generate energy [119]. Altogether, the microbiota facilitate digestion, affect xenobiotic response to drugs and other chemicals [125,

126], and are critically important in the immunological defense [127]. The fact that both *C. elegans* and its bacterial diets are genetically tractable provides a powerful system to further unravel the complex interactions between diet, microbiota, metabolism, physiology and pathology, and the molecular mechanisms involved.

Figures

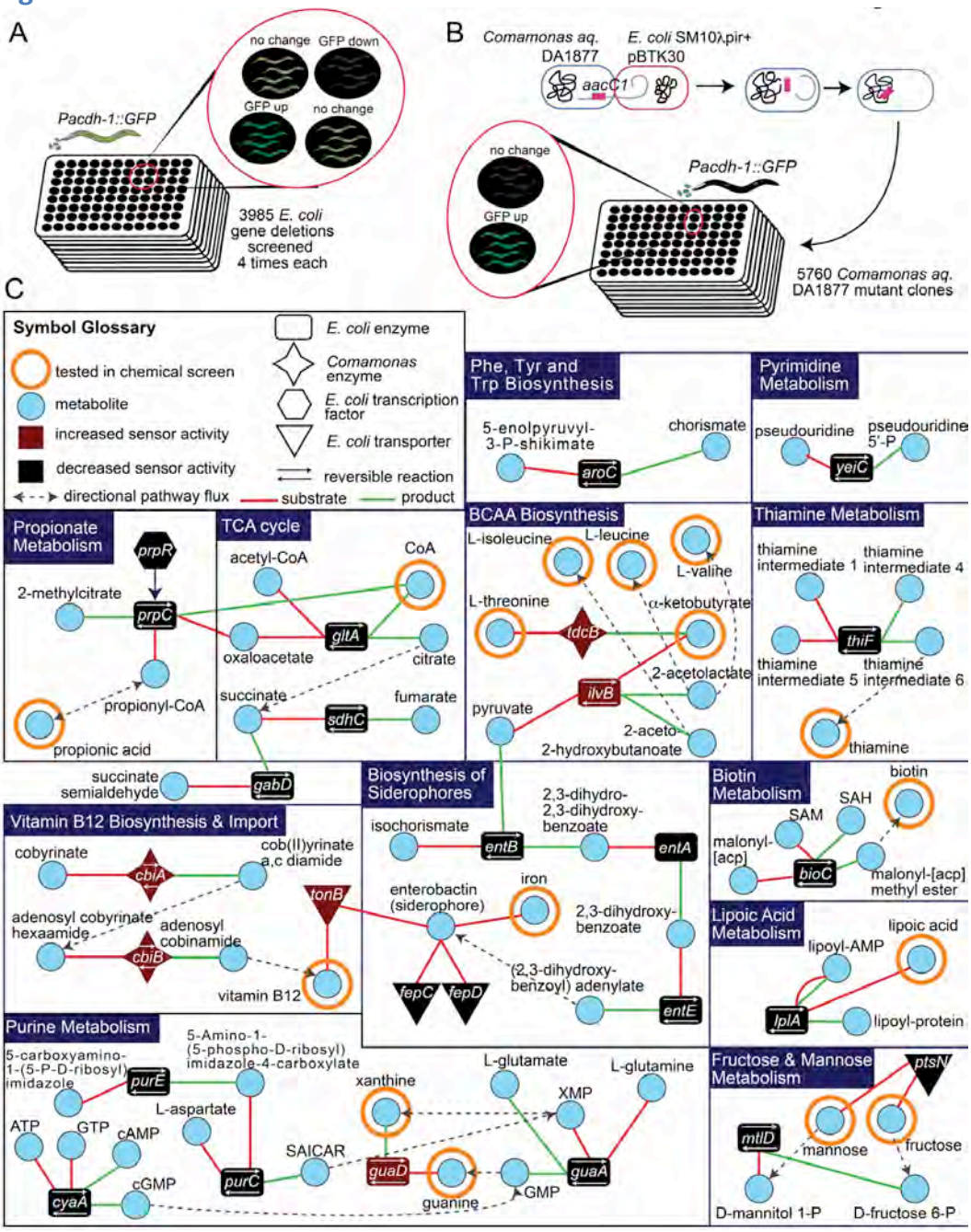

Figure 3.1 – Bacterial Screens

(A) Diagram of the Keio *E. coli* deletion collection screen. (B) Diagram of *Comamonas* DA1877 transposon mutagenesis screen. (C) Network of metabolites implicated by bacterial screens. SAICAR = 5-Amino-4-imidazole-N-succinocarboxamide ribonucleotide; [acp] = acyl carrier protein.

Table 3.1 – *E. coli* Deletion Mutants that Affect *Pacdh-1::GFP*

GFP up

gene	confidence	functional category	function	EC number	metabolites substrates	metabolites products	metabolic pathway
tonB	4	TNSP	provides the energy source required for the import of iron-siderophore complexes and vitamin B12 across the outer membrane	NA	NA	NA	Vitamin B12 import
guaD	2	EN	guanine deaminase; purine degradation	EC 6.3.2.6	C00242	C00385	Purine Metabolism
lit	2	TF?	cell death peptidase, inhibitor of T4 late gene expression	NA	NA	NA	NA
yjbQ	2	EN?	weak thiamin phosphate synthase activity	NA	NA	NA	NA
cchB	4	STRUC	Ethanolamine catabolic microcompartment shell protein	NA	NA	NA	NA
ilvB	2	EN	Component of acetohydroxybutanoate synthase I	EC 2.2.1.6	C00109; C00022	C06010; C06006	Isoleucine and Valine Biosynthesis
cybC	2	MISC	cytochrome b562 (soluble); heme-binding	NA	NA	NA	NA

Red: genes affecting bacterial metabolism included in Fig 1C network

EN	enzyme
TNSP	transporter
TF	transcription factor
UN	unknown
SIG	signalling
RB	ribosomal
MISC	miscellaneous
CHAP	chaperone
STRUC	structural protein

GFP down

gene	confidence	functional category	function	EC number	metabolites substrates	metabolites products	metabolic pathway
guaA	2	EN	GMP synthetase (glutamine aminotransferase); purine biosynthesis	EC 6.3.5.2	C00655; C00064	C00144; C00025	Purine Metabolism
purC	2	EN	SAICAR synthase converts 4-carboxy-5-aminoimidazole ribonucleotide (CAIR) to 4-(N-succinylcarboxamide)-5-aminoimidazole ribonucleotide (SAICAR)	EC 6.3.2.6	C04751; C00049	C04823	Purine Metabolism
purE	2	EN	the sixth step of de novo purine biosynthesis.	EC 5.4.99.18	C15667	C04751	Purine Metabolism
cyaA	2	EN	Adenylate cyclase	EC 4.6.1.1	C00002; C00044	C00575; C00942	Purine metabolism
aroC	2	EN	chorismate synthase; Trp, Try, Phe synthesis	EC 4.2.3.5	C01269	C00251	Phenylalanine, tyrosine and tryptophan biosynthesis
entB	2	EN	Isochorismatase	EC 3.3.2.1	C00885	C04171	Biosynthesis of siderophore group nonribosomal peptides
thiF	2	EN	thiamin (thiazole moiety) biosynthesis protein	EC 2.7.7.73	C15810; C15814	C15813; C15815	Thiamine metabolism
lplA	2	EN	lipoate-protein ligase A… lipoate cofactor for BCDH and BCOADC in bcaa breakdown	EC 2.7.7.63	C00725; C16238	C16238; C16237	Lipoic acid metabolism
entE	2	EN	2,3-dihydroxybenzoate-AMP ligase component of enterobactin synthase	EC 2.7.7.58	C00196	C04030	Biosynthesis of siderophore group nonribosomal peptides
yeiC	2	EN	pseudouridine kinase	EC 2.7.1.83	C02067	C01168	Pyrimidine metabolism
prpC	4	EN	2-Methylcitrate synthase; propionate catabolism via 2-methlycitrate cycle	EC 2.3.3.5	C02225; C00010	C00100; C00036	Propanoate metabolism
gltA	2	EN	Citrate synthase	EC 2.3.3.1	C00158; C00010	C00024; C00036	TCA cycle
bioC	2	EN	biotin biosynthesis; reaction prior to pimeloyl CoA; S-adenosylmethionine-dependent methyltransferases; malonyl-CoA methyltransferase	EC 2.1.1.197	C00019; C01209	C00021; C19673	Biotin metabolism
entA	3	EN	2,3-dihydro-2,3-dihydroxybenzoate dehydrogenase; Biosynthesis of siderophore group; iron?	EC 1.3.1.28	C04171; C00003	C00196; C00004	Biosynthesis of siderophore group nonribosomal peptides
gabD	2	EN	succinate-semialdehyde dehydrogenase I; glutamate and butyrate metabolism	EC 1.2.1.16	C00232; C00003	C00042; C00004	Alanine, aspartate and glutamate metabolism
mtlD	2	EN	Mannitol-1-phosphate dehydrogenase	EC 1.1.1.17	C00644; C00003	C00085; C00004	Fructose and mannose metabolism
sdhC	2	EN	succinate dehydrogenase membrane protein	EC 1.3.99.1	C00042	C00122	TCA cycle; Butanoate metabolism
nanK	2	EN	N-acetylmannosamine kinase	EC 2.7.1.60	C00625(general)	C00686(general)	sugar metabolism; general reaction
agaD	2	EN	N-acetylgalactosamine-specific enzyme IID	EC 2.7.1.69	NA	NA	general reaction; many pathways
fepC	2	TNSP	Ferrienterobactin transporter, membrane ATP protein	NA	NA	NA	siderophore import
fepD	2	TNSP	Ferrienterobactin transporter, membrane permease	NA	NA	NA	siderophore import
prpR	2	TF	Transcriptional regulator of prp operon; propionate catabolism via 2-methlycitrate cycle	NA	NA	NA	Propanoate metabolism
ptsN	2	TNSP	PTS system sugar-specific transporter subunit IIA; fructose/mannose	NA	NA	NA	fructose and mannose metabolism
cyoB	2	EN	cytochrome bo terminal oxidase subunit I	NA	NA	NA	Oxidative Phosphorylation
cyoD	2	EN	cytochrome bo terminal oxidase subunit IV	NA	NA	NA	Oxidative Phosphorylation
glpR	2	TF	Transcriptional repressor of the glycerol-3-phosphate regulon	NA	NA	NA	Glycerolipid metabolism
yheV	3	UN	hypothetical protein	NA	NA	NA	NA
ygeP	2	UN	hypothetical protein	NA	NA	NA	NA
yrfD	2	UN	required for utilization of DNA as the sole source of carbon and energy; pilus assembly?	NA	NA	NA	NA
ompX	2	UN	mutants show impaired motility, increased EPS production, and increased tolerance to SDS	NA	NA	NA	NA
yohC	2	UN	inner membrane protein	NA	NA	NA	NA
yfhL	2	UN	predicted 4Fe-4S cluster-containing protein	NA	NA	NA	NA
yadM	2	UN	fimbrial-like adhesin protein; motility?	NA	NA	NA	NA
uidC	2	UN	putative outer membrane porin protein;	NA	NA	NA	NA

yggE	2	UN	unknown	NA	NA	NA	NA
ygjV	2	UN	inner membrane protein[	NA	NA	NA	NA
ydjH	2	UN	predicted sugar kinase	NA	NA	NA	NA
hyfD	3	UN	predicted hydrogenase 4, membrane subunit	NA	NA	NA	NA
pbl	3	UN	predicted peptidoglycan-binding enzyme	NA	NA	NA	NA
tolB	2	UN	hypothetical protein	NA	NA	NA	NA
wzxE	2	TNSP	O-antigen translocase	NA	NA	NA	NA
gspD	2	TNSP	general secretory pathway component, protein export; cryptic	NA	NA	NA	NA
yohG	2	TNSP	Putative multidrug resistance outer membrane protein	NA	NA	NA	NA
ybhR	2	TNSP	transporter of unknown function; ATP-depended efflux	NA	NA	NA	NA
yhdP	2	TNSP	transporter of unknown function	NA	NA	NA	NA
trkA	2	TNSP	NAD-binding component of TrK potassium transporter	NA	NA	NA	NA
yojI	2	TNSP	multidrug ABC transporter ATP-binding protein/membrane protein	NA	NA	NA	NA
fiu	2	TNSP	putative outer membrane receptor for iron transport	NA	NA	NA	NA
gntP	2	TNSP	fructuronate transporter	NA	NA	NA	NA
yneL	2	TF	transcriptional regulator	NA	NA	NA	NA
rob	2	TF	right oriC-binding transcriptional activator, AraC family	NA	NA	NA	NA
hns	2	TF	H-NS transcriptional dual regulator	NA	NA	NA	NA
ygfI	2	TF	DNA-binding transcriptional regulator	NA	NA	NA	NA
ycgG	2	SIG	putative membrane-anchored cyclic-di-GMP phosphodiesterase	NA	NA	NA	NA
yhjH	2	SIG	c-di-GMP phosphodiesterase involved in regulation of the switch from flagellar motility to sessile behavior and curli expression at the end of exponential growth	NA	NA	NA	NA
rimM	2	RB	16S rRNA processing protein	NA	NA	NA	NA
rpsF	2	RB	30S ribosomal protein S6	NA	NA	NA	NA
rbfA	3	RB	30s ribosome binding factor	NA	NA	NA	NA
yeiW	2	MISC	Flagellin N-methylase	NA	NA	NA	NA
yceF	2	MISC	Maf-like; Maf is a nucleotide-binding protein implicated in inhibition of septum formation	NA	NA	NA	NA
cspH	2	MISC	cold shock protein	NA	NA	NA	NA
yeeU	2	MISC	antitoxin of the YeeV-YeeU toxin-antitoxin system	NA	NA	NA	NA
clpX	2	MISC	ATPase subunit of ClpXP protease	NA	NA	NA	NA
hlyE	2	MISC	Hemolysin E; causes lysis of mammalian cells	NA	NA	NA	NA
ygiU	2	MISC	RNase interferase	NA	NA	NA	NA
crcB	2	MISC	protein involved in resistance to camphor-induced chromosome decondensation	NA	NA	NA	NA
csgG	2	MISC	curli production component	NA	NA	NA	NA
atpD	2	MISC	F1 sector of membrane-bound ATP synthase	NA	NA	NA	NA
mdoG	2	MISC	glucan biosynthesis protein, periplasmic	NA	NA	NA	NA
ibpB	2	CHAP	heat shock chaperone	NA	NA	NA	NA

Red: genes affecting bacterial metabolism included in Fig 1C network

EN	enzyme
TNSP	transporter
TF	transcription factor
UN	unknown
SIG	signalling
RB	ribosomal
MISC	miscellaneous
CHAP	chaperone
STRUC	structural protein

Table 3.2 – *Comamonas aq.* DA1877 Mutants Identified in Transposon Screen.
Related to **Figure 3.1** and **Figure 3.2.**

Transposon-disrupted gene	Function
cbiA/cobB	EC 6.3.5.9/6.3.5.11; cobyrinic acid a,c-diamide synthase
cbiB	EC 6.3.1.10; adenosylcobinamide-phosphate synthase
threonine dehydratase	EC 4.3.1.19; converts threonine to 2-oxobutanoate and ammonia
RND efflux system protein	unknown
hypothetical protein with helix-turn-helix	unknown

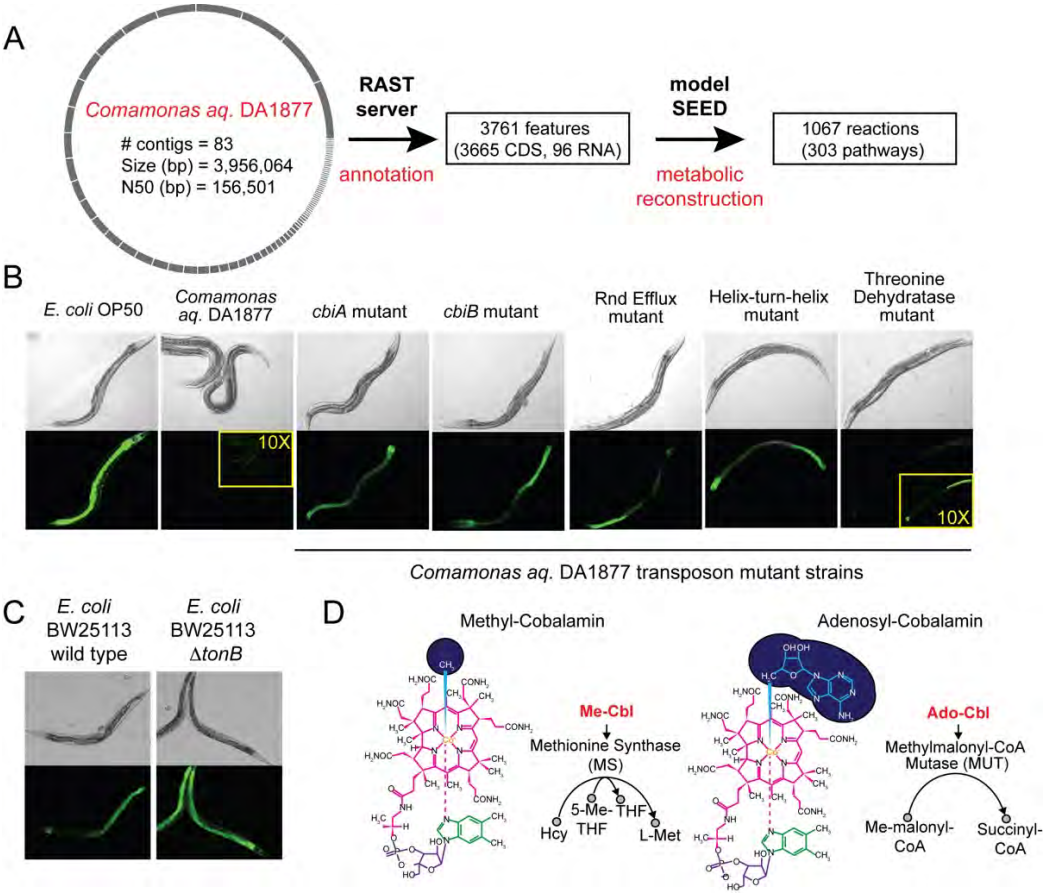

Figure 3.2 – *Comamonas aq.* DA1877 Genome Assembly and Vitamin B12 Import/Biosynthesis Mutants.

(A) Genome sequencing and analysis for *Comamonas* DA1877. The circle represents the assembled genome sequence with segments showing contig lengths. Half of the assembled genome resides in contigs of 156.5 kb or longer. The assembly served as the input to the RAST server for the annotation of coding sequences and RNA genes, which in turn was used by the model SEED for the reconstruction of metabolic pathways including vitamin B12 biosynthesis. (B) DIC and fluorescence images of *Pacdh-1::GFP* animals fed *E. coli* OP50, *Comamonas aq.* DA1877, and five *Comamonas aq.* DA1877 mutants identified in the transposon screen that increase GFP expression. Inset images were taken at 10x exposure time. (C) DIC and fluorescence images of *Pacdh-1::GFP* animals fed the Keio *E. coli* parent strain (left) or the Keio *E. coli* Δ*tonB* mutant (right). The mutant confers increased GFP expression in *C. elegans*. (D) Left: chemical structure of Me-Cbl and diagram of the Me-Cbl-dependent reaction catalyzed by methionine synthase (*metr-1*). Right: chemical structure of Ado-Cbl and diagram of the Ado-Cbl-dependent reaction catalyzed by methylmalonyl-CoA mutase (*mmcm-1*). Hcy = homocysteine; 5-Me-THF = 5-methyl-tetrahydrofolate; THF = tetrahydrofolate; L-Met = L-methionine; Me-malonyl-CoA = methylmalonyl-CoA.

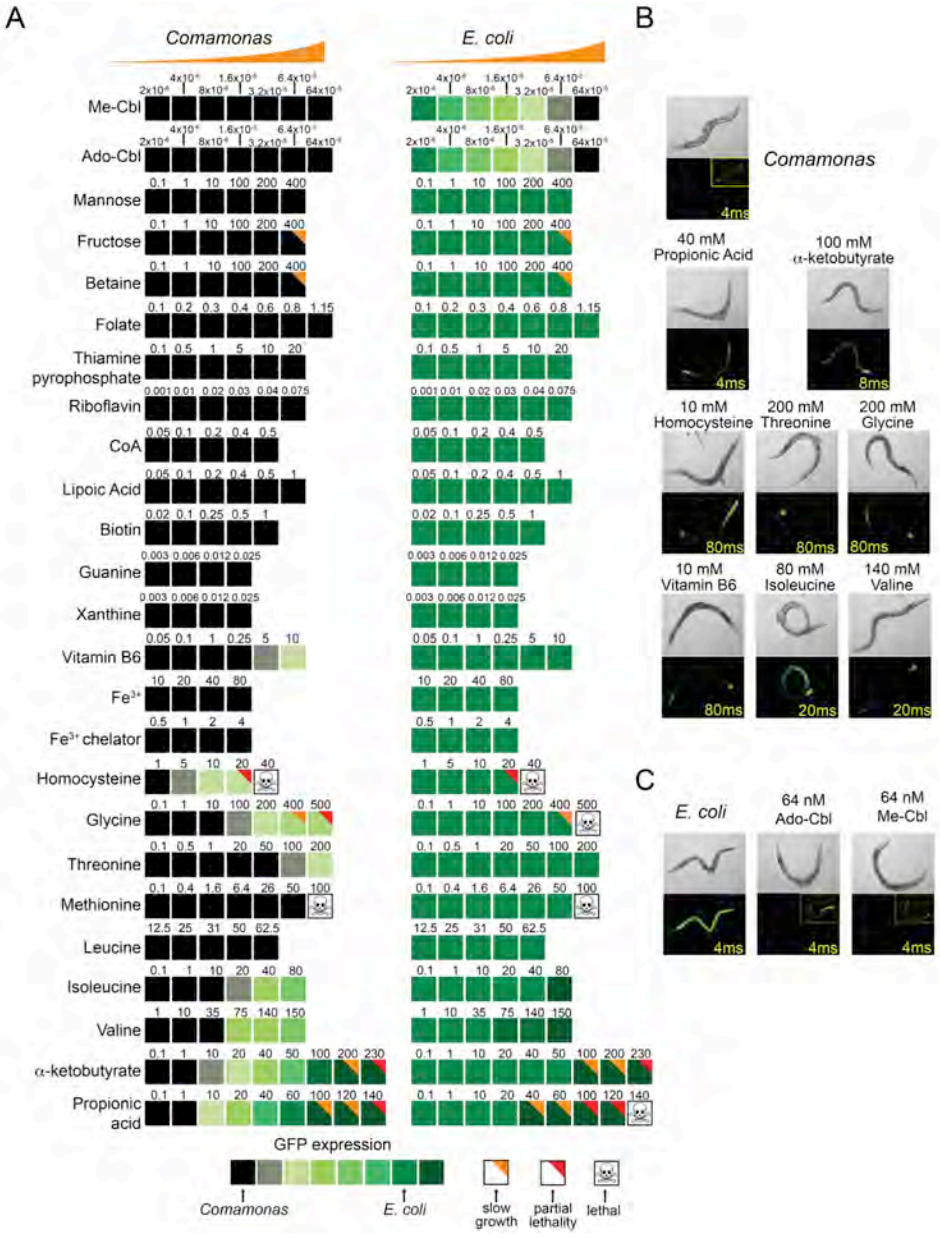

Figure 3.3 – Metabolite Screen

(A) Effects of supplementing metabolites to *Pacdh-1::GFP* animals fed either *Comamonas aq.* DA1877 (left column) or *E. coli* OP50 (right column). Shades of green represent relative GFP expression. Numbers indicate metabolite concentrations (in mM). (B) *Pacdh-1::GFP* animals fed *Comamonas aq.* DA1877 bacteria alone or supplemented with the indicated compounds that activate GFP expression. Exposure time is indicated in yellow. Exposure time for inset images is 400 ms. (C) *Pacdh-1::GFP* animals fed *E. coli* OP50 bacteria supplemented with the indicated compounds that repress GFP expression. Exposure time is indicated in yellow. Exposure time for inset images is 400 ms.

Compound	Implicated In *E. coli* Screen	Implicated in Comamonas Screen	Implicated in Watson, MacNeil et al 2013
alpha-ketobutyrate	yes	yes	yes
Threonine	yes	yes	yes
Ado-Cbl	yes	yes	yes
Me-Cbl	yes	yes	yes
L-Isoleucine	yes		yes
L-Valine	yes		yes
Propionate	yes		yes
L-Leucine	yes		yes
CoA	yes		yes
Biotin	yes		
Thiamine Pyrophosphate	yes		
Lipoic acid	yes		
Guanine	yes		
Xanthine	yes		
Fructose	yes		
Mannose	yes		
Ammonium iron(III) citrate	yes		
Deferoxamine mesylate salt	yes		
Betaine monohydrate			yes
Vitamin B6 (PLP)			yes
Homocysteine			yes
Riboflavin			yes
Glycine			yes
Folate			yes
Methionine			yes

Decreases *Pacdh-1::*GFP expression in *C. elegans*
Weakly increases *Pacdh-1::*GFP expression in *C. elegans*
Increases *Pacdh-1::*GFP expression in *C. elegans*

Table 3.3 – Compounds Tested in Chemical Screen for Effects on *Pacdh-1::GFP*.

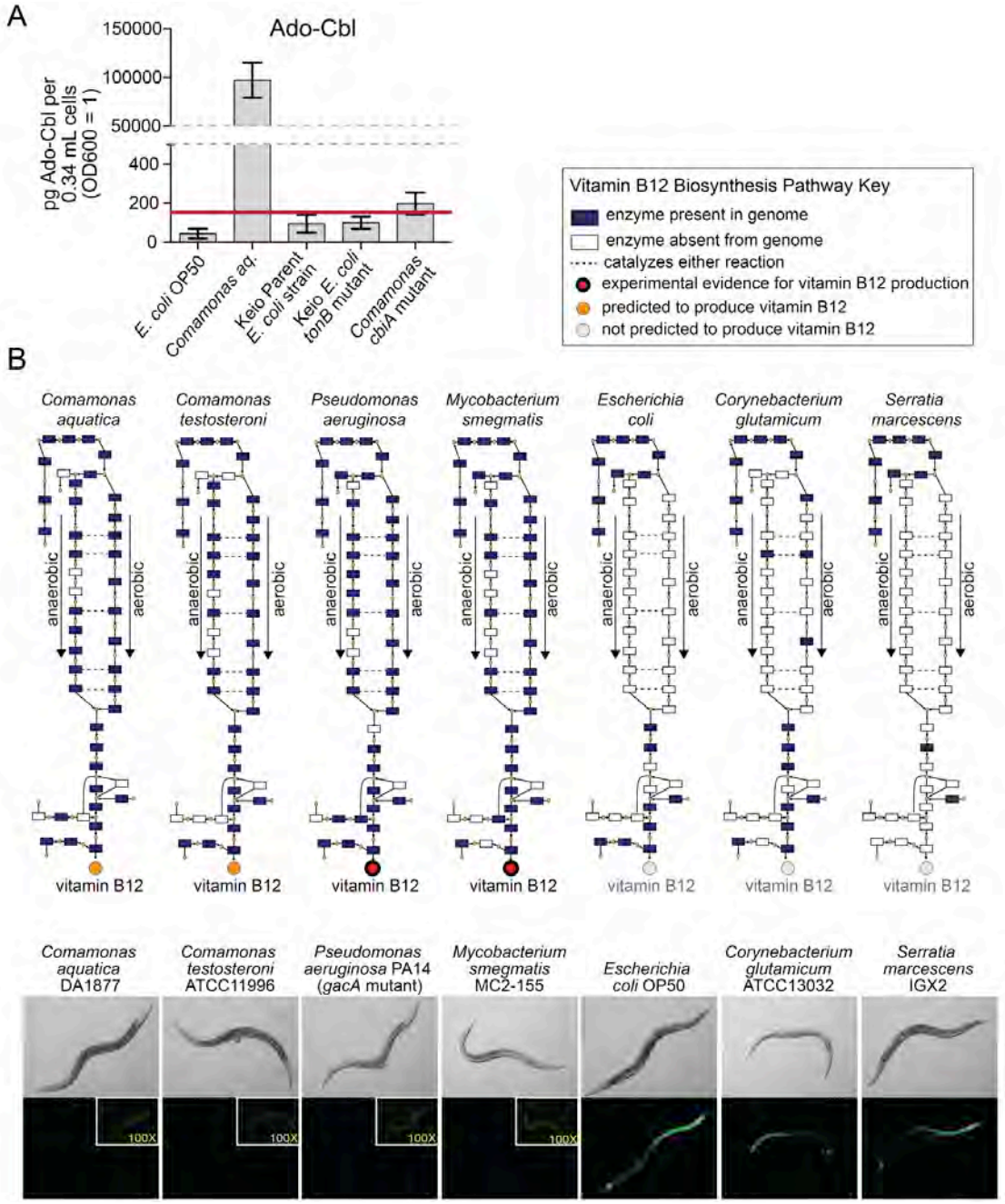

Figure 3.4 – Correlation Between Bacterial B12 Biosynthesis and Repression of *Pacdh-1::GFP*

(A) Ado-Cbl content measured by mass spectrometry in indicated bacterial strains. The red line indicates background levels of Ado-Cbl in the bacteria-free control. (B) Correlation between vitamin B12 biosynthesis pathway presence and dietary sensor repression. Images of *Pacdh-1::GFP* animals fed various bacterial strains are located below a cartoon that indicates pathway status. Differences in exposure times for the inset images are indicated in yellow.

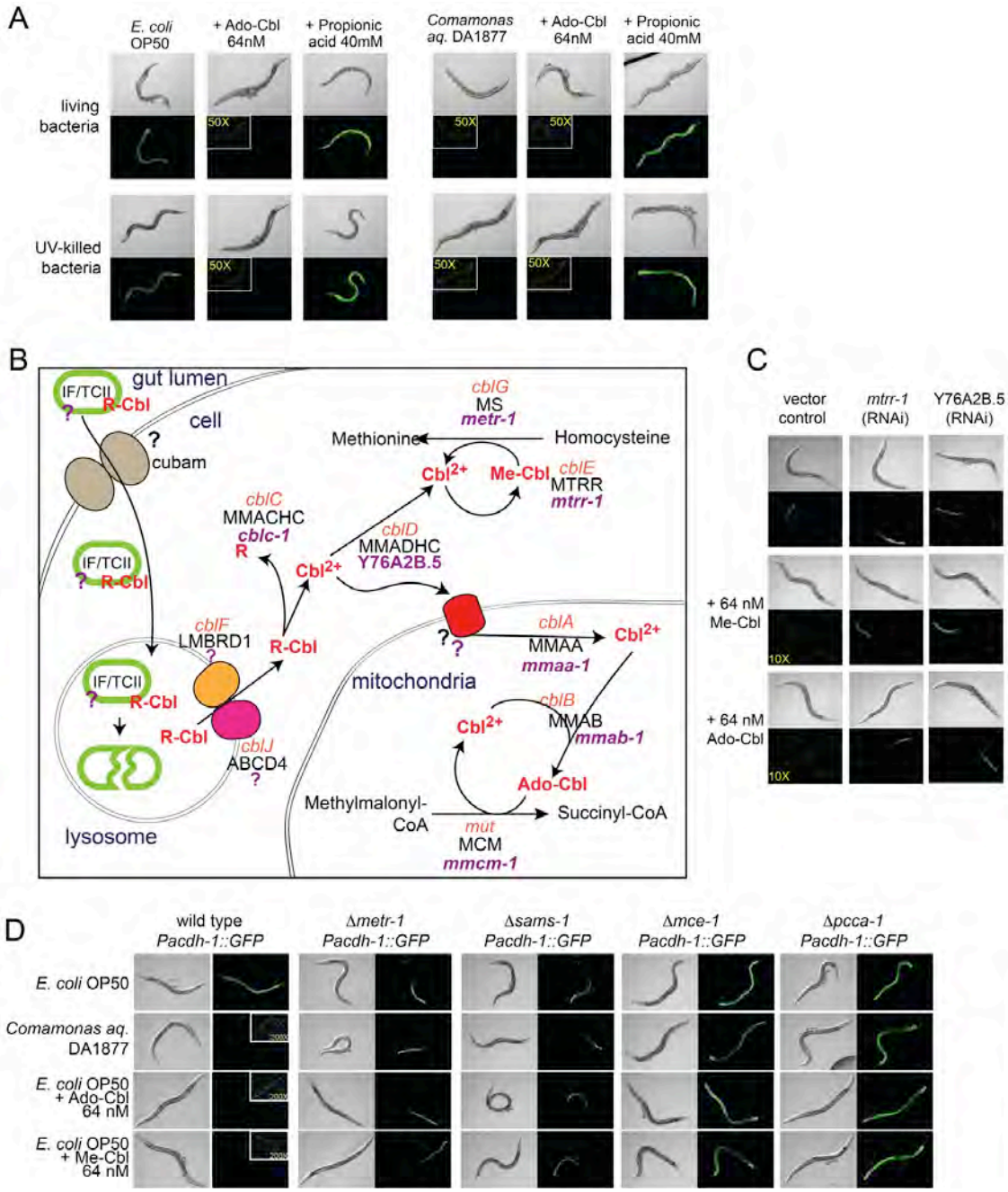

Figure 3.5 – Vitamin B12 Processing Genes and Dependent Pathways are Required for Repression of *Pacdh-1::GFP*.

(A) DIC and fluorescence images of *Pacdh-1::GFP* animals fed live and UV-killed *E. coli* OP50 (left set of images) or live and UV-killed *Comamonas aq.* DA1877 (right set of images). Addition of Ado-Cbl 64nM is sufficient to repress GFP expression on both living and killed *E. coli* OP50. Addition of 40mM propionic acid is sufficient to activate GFP expression on both live and killed *Comamonas*

aq. DA1877. (B) Cartoon of vitamin B12 processing and processes. Orange text indicates complementation groups of human genetic cobalamin deficiencies, black and purple indicate human and *C. elegans* genes, respectively, and red indicates different forms of vitamin B12 (Cbl). Question marks indicate vitamin B12 processing/distribution factors that have yet to be identified. (C) DIC and fluorescence images of *Pacdh-1::GFP* animals subjected to RNAi knockdown of *mtrr-1* and Y76A2B.5 compared to control knockdowns, in the presence and absence of supplemented Me-Cbl or Ado-Cbl (64nM each). (D) DIC and fluorescence images of *Pacdh-1::GFP* animals in a wild type background compared to metabolic mutant backgrounds (Δ*metr-1*, Δ*sams-1,* Δ*pcca-1* and Δ*mce-1*) fed *Comamonas aq.* DA1877, *E. coli* OP50, or *E. coli* OP50 supplemented with 64 nM Ado-Cbl or 64 nM Me-Cbl.

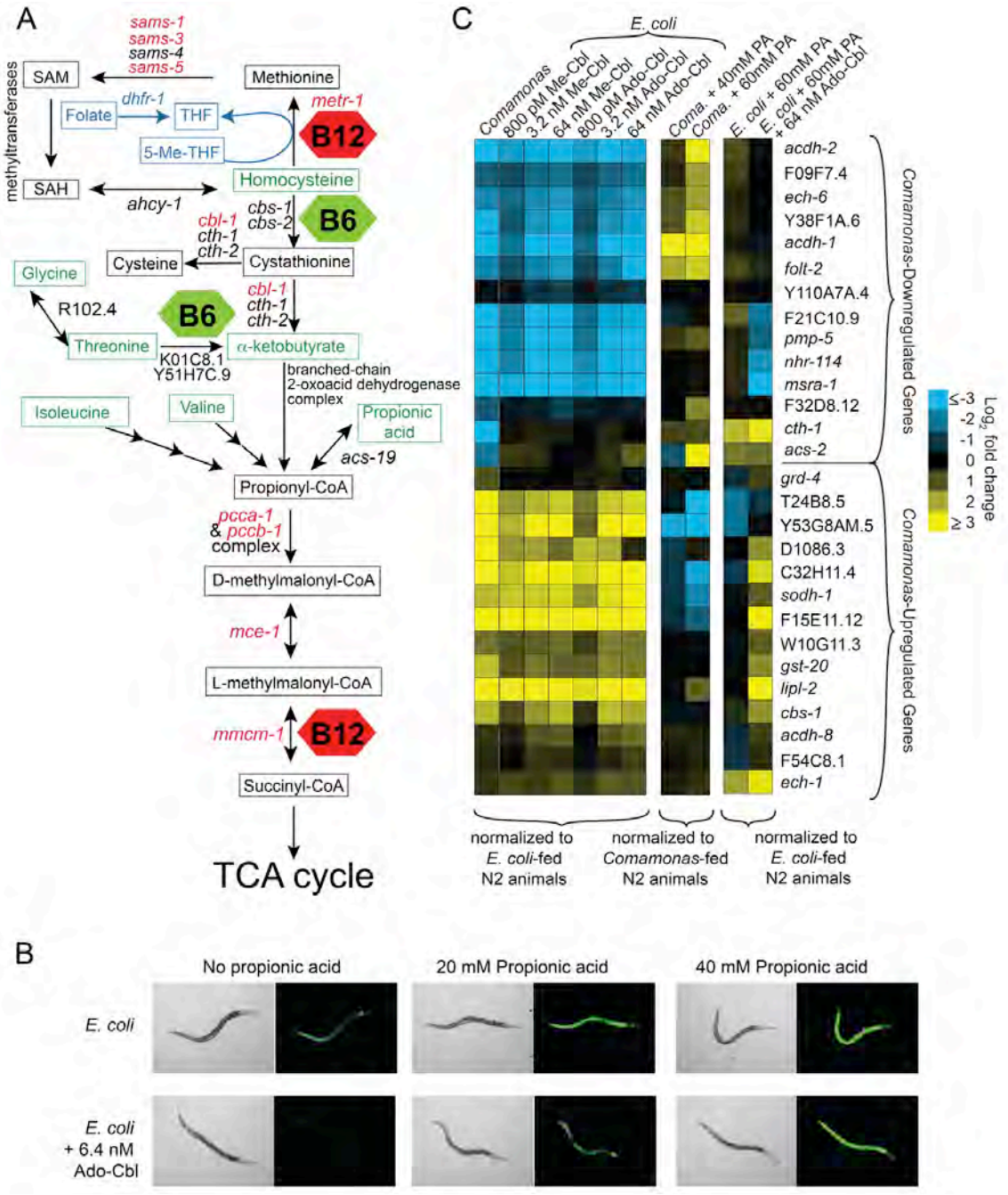

Figure 3.6 – Chemical Epistasis Between Vitamin B12 and Propionic Acid With Respect to *C. elegans* Gene Expression

(A) Network of the two vitamin B12-dependent pathways. Metabolites are indicated in rectangles. Green metabolites activate the dietary sensor when supplemented to the bacterial diet. Genes encoding the metabolic enzymes involved are indicated with arrows between metabolites. Genes that, when mutated, activate the dietary sensor are indicated in red. Red hexagons – vitamin

B12; green hexagons – vitamin B6; blue indicates folate metabolism. 5-Me-THF = 5-methyltetrahydrofolate; THF = tetrahydrofolate, the biologically active form of folate. (B) Chemical epistasis of combined supplementation of Ado-Cbl and propionic acid on *Pacdh-1::GFP* dietary sensor animals fed the *E. coli* OP50 diet. (C) qRT-PCR of 14 *Comamonas*-upregulated and 14 *Comamonas*-downregulated genes in wild type animals fed indicated diets and supplemented metabolites. PA = propionic acid. N2 = wild type animals. Changes in expression for each gene are plotted as $\log_2$ fold change compared to respective mRNA levels in wild type animals fed *E. coli* OP50 (first and third columns) or *Comamonas aq.* DA1877 (middle column).
See **Table 3.4** for qPCR primer sequences.

Primer	Forward Seq	Reverse Seq
Comamonas-upregulated genes		
cbs-1	AACAAGTTCAACCCAGAAAGG	TTGAAGCTTGACGAGTGGA
acdh-8	TGTCATTTGAACTGTCCGA	CATTTGGCACAAGAACGTC
F15E11.12	AGTATGCTGGAAAGGATGGA	TCCATTTGGCGAGTAGTCC
grd-4	CAGAACACTACGATGTTAACGG	CGGATGGAATACGAAGTTTGTC
D1086.3	CGTGCAAAGACACCATGGAATG	GAGCACGACCACAGAAGTCG
gst-20	CTAGACAGCTCTTCGCCCTATCC	GGCATTTGGCCAAAGGGC
ech-1	CTGAGGCTAAGGCATTTGG	CATTAGTCGATCCTTCGAACAG
sodh-1	GCTGGAGTCAAGCTCATGAACTTC	CGATCGAACCCATAGTTCTGGATG
Y53G8AM.5	GGAAGCAGCTACTACTCGT	GTAGTCGAAGGCATTTCCC
T24B8.5	TACACTGCTTCAGAGTCGTG	CGACAACCACTTCTAACATCTG
C32H11.4	GAATGGGCTCCGTATACCACCC	GTCTGAACTGAAATCGGCCGC
W110G11.3	GAGGCATGTGATAACCTTTTCGGG	GCTAGAGTGTTCTTCCGGAACC
F54C8.1	GCATCAATGACCGACATCG	TCGAGACCAATGTAGTCGG
lipl-2	GCATTGGCACCGATTGGTG	CGTACCAACCATCAAATTCGGGAG
Comamonas-downregulated genes		
msra-1	GAAAGAAGCAATACCAATCTGC	ATGTCTCCATGCTTGTCCT
Y38F1A.6	GATATTCCGAACAATGCCAG	TCCAAAGTCTCGCATATAACC
acs-2	TCCGGATAAGGAGTTCTGTG	ATTTGACGGACGTCATGGT
folt-2	CTTTGAATAGTCAGGTGTACCC	ATACATCGGTGAGTAGGAACG
pmp-5	CGCATTCTACTTCATCTACCT	TACGAATTCGCTCACTCTC
F21C10.9	TGGCTTAAGAGGAGTCGTC	CCCAATCTGTTTCAGATAAGTCTC
nhr-114	ATTACAGCTATCGCCTCCAC	GTTTGTAGGATGCAGCGAC
Y110A7A.4	ACAATGTGTCAGTTCTATGTGG	AACTCCGAGACCCATATCTC
F32D8.12	AGGGCAACTTTATGGAAAGC	TGTCGTGAATCCTCTTGCT
acdh-1	GCAAATGCAGATCCTAGCC	GTTTGTCTTCCTCCTTATCTACAG
acdh-2	GATGATAATCTTGGAATGCGTGC	CTTCAATAGCGTATTTGTATCCTTTTCC
ech-6	TCGGAGCAATTGTGATTACTG	CGAACTCGTTATTGGTCATCTC
F09F7.4	CACAATGGAGTATCGTCTCAC	TTGTCAACGAGAATGGCTC
cth-1	CACTTTGGAACTGATGCAGTC	CATACTAATTGGTGGAACTACCTG

Table 3.4 – qRT-PCR primers.
Related to **Figure 3.6**.

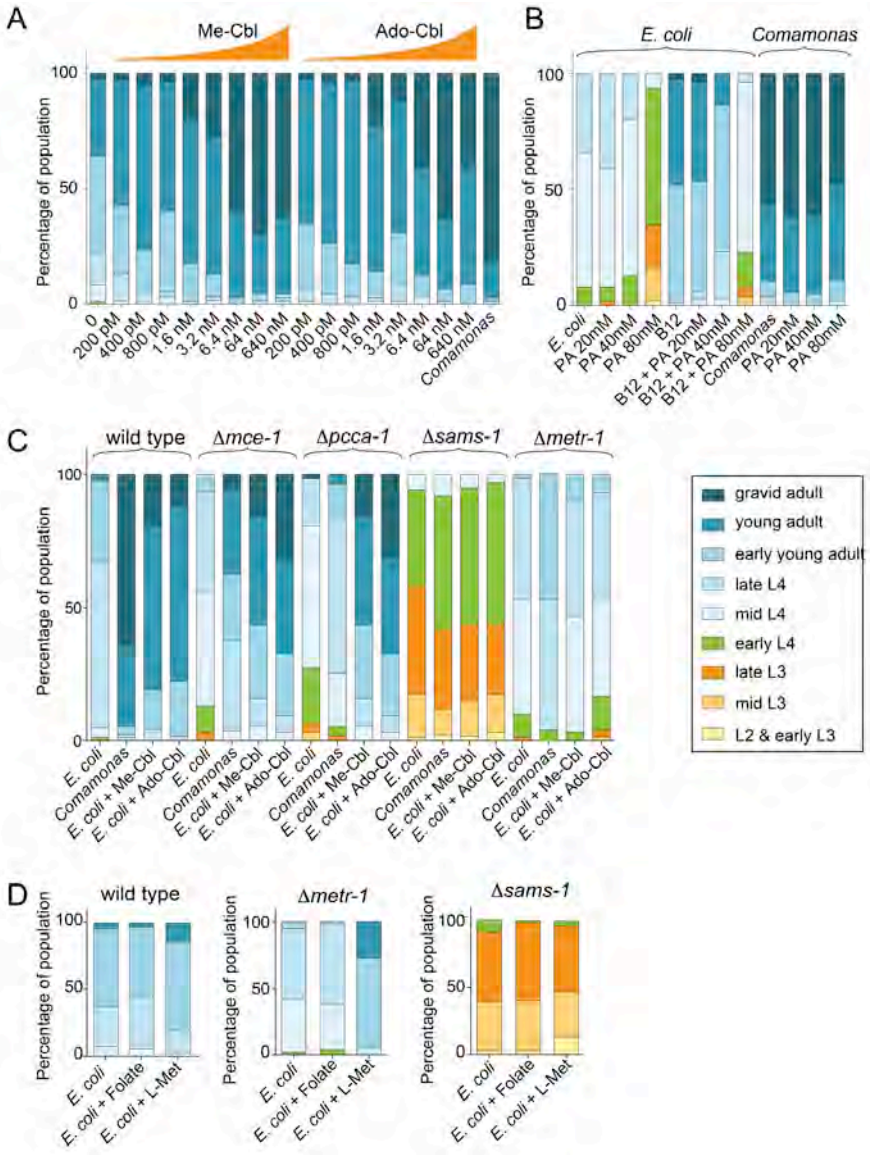

Figure 3.7 – Effects of Metabolite Supplementation on *C. elegans* Development

(A) Developmental progression of synchronized wild type populations of animals fed indicated diets and supplemented metabolites. The parental generation was cultivated on *E. coli* OP50. (B) Developmental progression of synchronized wild type populations of animals fed indicated diets and supplemented metabolites. PA = propionic acid. Vitamin B12 = 64 nM Ado-Cbl. The parental generation was cultivated on *E. coli* OP50. (C) Developmental progression of synchronized wild type and mutant populations of animals fed indicated diets and supplemented metabolites. 64 nM of each variant of vitamin B12 was used. (D) Developmental progression of synchronized wild type and mutant populations of animals fed indicated diets and supplemented metabolites. L-Met = 4 mM methionine. Folate = 56 mM.

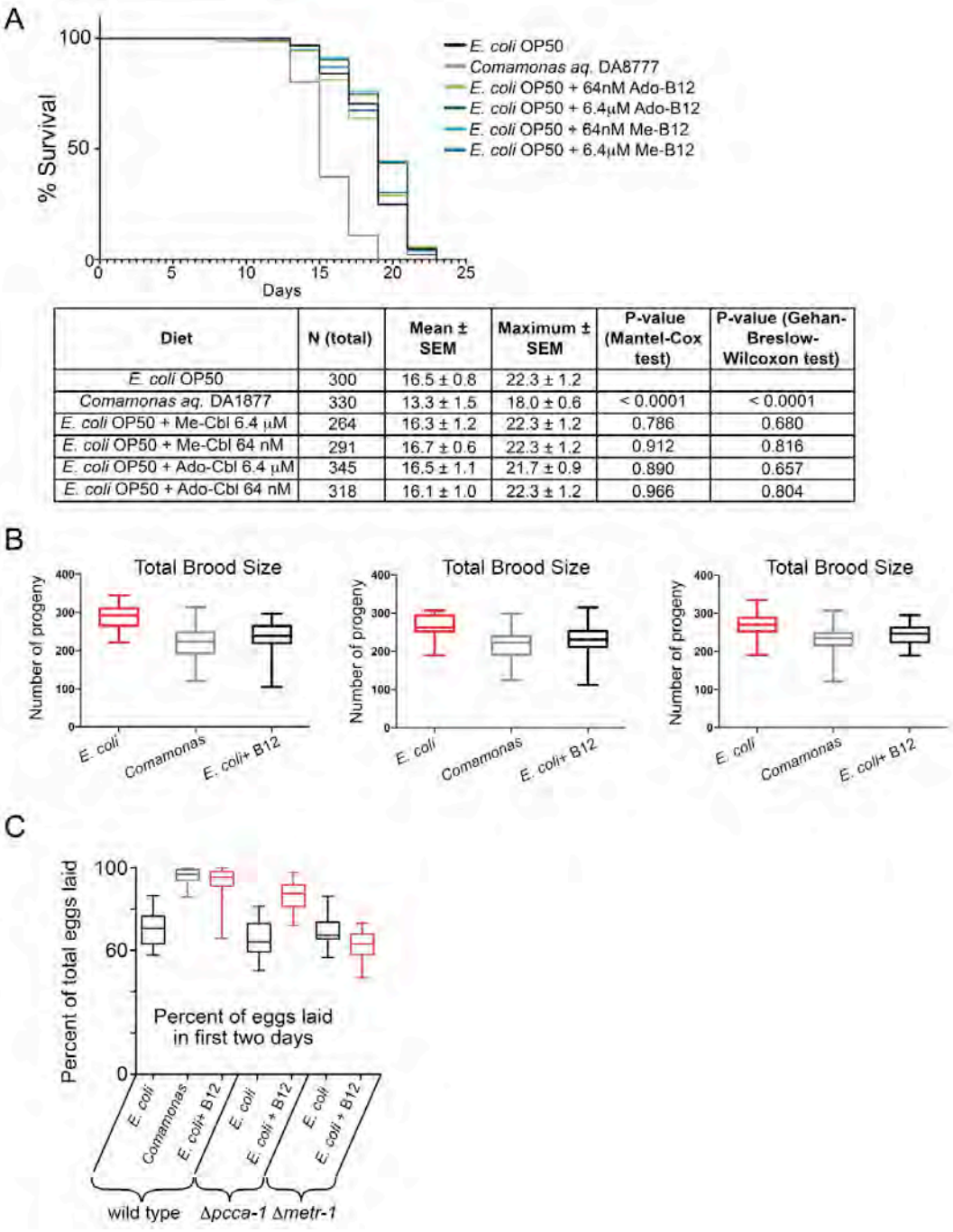

Diet	N (total)	Mean ± SEM	Maximum ± SEM	P-value (Mantel-Cox test)	P-value (Gehan-Breslow-Wilcoxon test)
E. coli OP50	300	16.5 ± 0.8	22.3 ± 1.2		
Comamonas aq. DA1877	330	13.3 ± 1.5	18.0 ± 0.6	< 0.0001	< 0.0001
E. coli OP50 + Me-Cbl 6.4 μM	264	16.3 ± 1.2	22.3 ± 1.2	0.786	0.680
E. coli OP50 + Me-Cbl 64 nM	291	16.7 ± 0.6	22.3 ± 1.2	0.912	0.816
E. coli OP50 + Ado-Cbl 6.4 μM	345	16.5 ± 1.1	21.7 ± 0.9	0.890	0.657
E. coli OP50 + Ado-Cbl 64 nM	318	16.1 ± 1.0	22.3 ± 1.2	0.966	0.804

Figure 3.8 – Vitamin B12 Affects *C. elegans* Egg Laying but not Lifespan.
Related to Figure 3.7. (A) Lifespan analysis of wild type animals fed *E. coli* OP50, *Comamonas aq.*, or *E. coli* OP50 supplemented with either 64 nM or 6.4 μM Ado-Cbl or Me-Cbl. A representative lifespan experiment is shown at the top. The table summarizes mean and maximum lifespans from three combined experiments. (B) Three independent brood size measurements of wild type

animals fed *E. coli* OP50, *Comamonas aq.* DA1877, or *E. coli* OP50 supplemented with 64 nM Ado-Cbl. (C) Percentage of total eggs laid in the first two days of adulthood by wild type animals fed *E. coli* OP50, *Comamonas aq.* DA1877, or *E. coli* OP50 supplemented with 64 nM Ado-Cbl. Included also is the percentage of total eggs laid in the first two days of adulthood by Δ*pcca-1* and Δ*metr-1* mutants fed either *E. coli* OP50 or *E. coli* OP50 supplemented with 64 nM Ado-Cbl. Vitamin B12 fails to shift egg laying in Δ*metr-1* mutants.

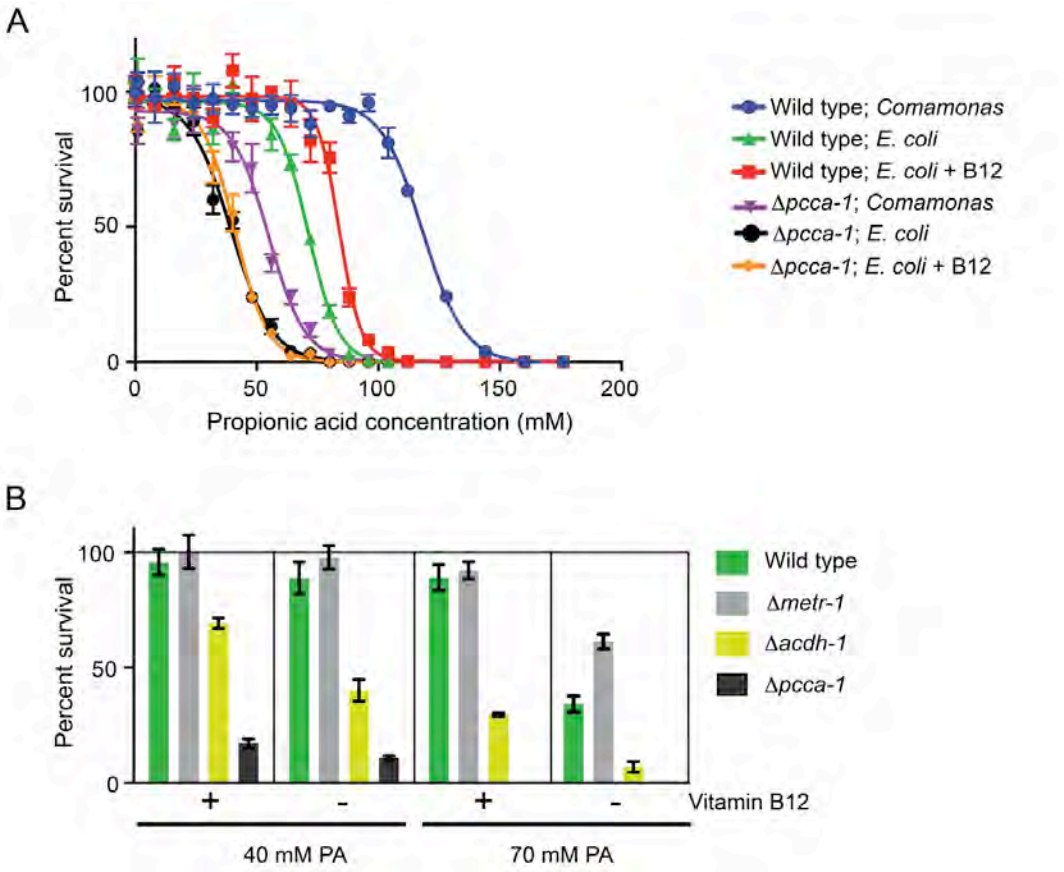

Figure 3.9 – Effects of Vitamin B12 on Propionic Acid Toxicity

(A) Toxicity analysis of incremental doses of propionic acid on wild type and Δ*pcca-1* mutant *C. elegans* in the absence and presence of 64 nM Ado-Cbl (B12). Mean +/- SEM is plotted from three combined experiments. (B) Percent survival of different *C. elegans* strains fed *E. coli* OP50 at two concentrations of propionic acid (PA) in the absence or presence of 64 nM Ado-Cbl. Mean +/- SEM is plotted from four combined experiments.

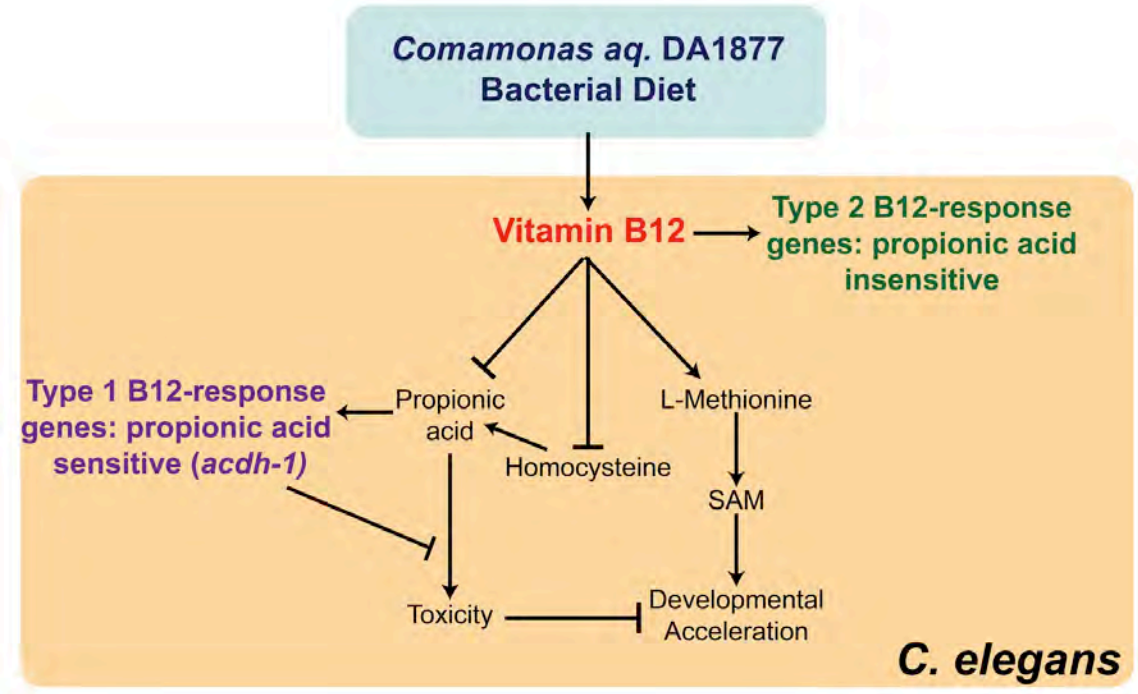

Figure 3.10 – Model

Our findings demonstrate that the *Comamonas aq.* DA1877 diet provides high levels of vitamin B12, whereas the *E. coli* OP50 diet is low in this cofactor. Vitamin B12 acts through two different pathways: it lowers levels of propionyl-CoA, thereby preventing propionic acid toxicity, and enables the synthesis of methionine and SAM, thereby accelerating development and reducing fertility. Methionine synthesis reduces levels of homocysteine and likely propionyl-CoA levels. Our data suggest that vitamin B12 may affect these processes by regulating the expression of different sets of genes (type 1 and type 2); some that respond oppositely to propionyl-CoA and others that are insensitive to this metabolite.

Experimental Procedures

C. elegans Strains

N2 (Bristol) was used as the wild type strain and animals were maintained as described at 20^{o}C [90]. *sams-1(ok2946), mce-1(ok243), pcca-1(ok2282), metr-1(ok521)* and *acdh-1(ok1489)* strains were provided by the *C. elegans* Gene Knockout Consortium and back-crossed as described [64]. We previously described the *Pacdh-1::GFP* strain (VL749) [105].

Bacterial Strains

E. coli OP50, *Serratia marcescens* IGX2 and *Comamonas aq.* DA1877 were obtained from the CGC. *Pseudomonas aeruginosa* PA14 (*gacA* mutant) was a gift from Victor Ambros (UMMS), *Corynebacterium glutamicum* ATCC13032 and *Comamonas testosteroni* ATCC11996 were obtained from ATCC. *Mycobacterium smegmatis* MC2-155 was a gift from Chris Sassetti (UMMS). For the killed bacteria experiment, *E. coli* OP50 and *Comamonas aq.* DA1877 cultures were grown to log phase in LB, then harvested and washed, irradiated with UV (254nm, 5 J/cm^2), concentrated, and added to NGM plates.

E. coli Deletion Collection Screen

Keio *E. coli* deletion collection clones (Thermo Scientific) were grown overnight in Luria Broth (LB) containing 50 mg/mL kanamycin in 96-well deep well dishes. 15 mL of this overnight culture was seeded onto 96-well nematode growth media (NGM) agar plates containing 50 mg/mL kanamycin. *Pacdh-1::GFP* gravid

adults fed the Keio parent strain were bleached to harvest embryos, which were subsequently washed in M9 media and allowed to hatch overnight to synchronize the population by L1 arrest. Approximately 25 synchronized L1 animals were added to each well of the seeded plates. After incubating 48 hours at 20°C, animals were visually screened for GFP expression. Each plate from the Keio collection was screened twice, thus each *E. coli* gene was screened four times. Deletion mutants that affected GFP expression in at least two out of four experiments were considered hits.

Comamonas aq. DA1877 Transposon-Based Mutagenesis Screen

Random insertions into the *Comamonas aq.* DA1877 genome were generated using a Mariner transposon introduced via conjugation with *E. coli*. Briefly, fresh cultures of *E. coli* SM10λpir+ carrying the pBTK30 transposon delivery vector [128] and *Comamonas aq.* DA1877 were scraped from plates and transferred to an LB plate where they were mixed together in a ratio of approximately 10:1 (*E. coli* : *Comamonas*). Bacteria were conjugated at 37°C for one hour, recovered from the plate, resuspended in LB and plated onto LB plates containing 10 µg/mL gentamycin and 100 µg/mL streptomycin to select for the transposon and against *E. coli*, respectively. Following overnight incubation, individual colonies were picked into 96 well plates and grown overnight at 37C in LB supplemented with 10 µg/mL gentamycin. NGM plates were inoculated from overnight cultures and allowed to grow for 2-3 days at room temperature. Plates were then seeded with

approximately 20 *Pacdh-1::GFP* eggs prepared by hypochlorite bleaching, and GFP expression was examined in adult animals. Positive scoring wells were streaked for single colonies. A single colony was picked and used for re-testing and further characterization. In total, 5,760 colonies (60 96-well plates) were screened for their effect on GFP expression.

Transposon insertion sites were identified by arbitrary PCR or by cloning of genomic fragments into pUC19 and selecting for gentamycin-resistant colonies. Arbitrary PCR was performed as described in [129] with a few modifications. Two separate PCR reactions were performed for each mutant using one of ARB1 (GGCCACGCGTCGACTAGTACNNNNNNNNNNAGAG), or ARB3 (GGCCACGCGTCGACTAGTACNNNNNNNNNNGATAT) primers along with Rnd1-TnM30 (CACCGCTGCGTTCGGTCAAGGTTC). A second round of PCR was done using ARB Rnd2 (GGCCACGCGTCGACTAGTAC) and BTK30 Rnd2 (CGAACCGAACAGGCTTATGTCAATTC) primers. Unique bands were gel purified and reamplified for sequencing. Target genes were identified by comparing sequences proximal to the transposon to the *Comamonas aq.* DA1877 genome using BLAST.

Comamonas aq. DA1877 Genome Sequencing, Assembly, and Annotation

Bacterial pellets from a centrifuged *Comamonas* DA1877 culture were submitted to Genewiz, Inc. (South Plainfield, NJ) for DNA isolation and whole genome sequencing with Illumina-Miseq technology. A library of ca. 30.5 million short

reads (150-bp, paired-end) was obtained and de novo assembled using Edena [130], version 3.130110. The assembly resulted in an overall length of 3,956,064 basepairs arranged in 83 contigs with N50=156,501 bp (i.e., 50% of the assembly was included in contigs of this size and greater). The genome sequence was annotated and analyzed using the SEED pipeline [131, 132]. First, contigs were uploaded to the rapid annotation using subsystem technology (RAST) server [133], which determined 3,665 protein-coding sequences and 96 RNA genes. The web-based Bayesian classifier tool of Ribosomal Database Project [134] placed the 16S rRNA sequence in the *Comamonas* genus under *Betaproteobacteria* at 100% confidence level. The SEQMATCH tool of the same website determined the nearest type strain as *Comamonas aquatica* [135] with a sequence similarity of 99.6%; no other type strain had a match with >99% similarity. A draft metabolic reconstruction was generated using the model SEED [132] for the systematic analysis of metabolic pathways.

Vitamin B12 Biosynthesis Pathway Analysis

To determine the presence or absence of vitamin B12 biosynthesis pathway in bacterial species used in this study, we first gathered EC numbers from KEGG [136] and MetaCyc [137] for all reactions comprising this pathway. For *Comamamonas aq*. DA1877, we cross-referenced these EC numbers against all EC numbers annotated in the draft metabolic network reconstruction from SEED and determined which vitamin B12 biosynthesis enzymes were encoded in the genome. For other bacterial species, we determined the presence or absence of

vitamin B12 biosynthesis genes based on the same EC numbers, but used KEGG and Metacyc databases to guide annotation. If an EC number in the vitamin B12 biosynthesis pathway was annotated as present for a particular species in either or both of these databases, we called it present.

Metabolite Screen

Metabolites were purchased from Sigma-Aldrich and dissolved in water to the maximum soluble concentration. Dilutions were made in water as indicated in Figure 3.3. For each stock solution, pH was adjusted to 6.0 with sodium hydroxide or hydrochloric acid. Stock solutions were added to NGM in various doses just prior to plate pouring.

Mass-Spectrometry

Bacterial strains were grown in NGM medium, with peptone supplied by American International Chemical. 30 mL bacterial cultures were centrifuged, washed twice with 50 mM sodium citrate buffer (pH = 7.2) and frozen at -80^{o}C until extraction. Washed cells were extracted on a roller drum at 37^{o}C for 3 hours using 3 mL of 100 mM sodium acetate buffer (pH = 4.0) containing 2 mg porcine pepsin (Sigma). The extract was clarified by centrifugation and purified using a gravity drip C18 100 mg column (Biotage). The column was preconditioned with 3 mL methanol, followed by 3 mL water; following sample application, the column was washed with 3 mL water and eluted with 1.5 mL methanol. The samples

were dried down under vacuum and resuspended in water corresponding to 0.096 OD600 units of cells per ml of solution.

Instrumentation for LC-MS analysis was an Agilent UHPLC system, HTS PAL autosampler, and an Agilent 6490 QQQ using an Agilent Eclipse Plus phenyl-hexyl UHPLC column (2.1 x 100 mm, 1.8 um particle size). Mobile phase A was 20 mM ammonium formate with 0.1% formic acid in water. Mobile phase B was 20 mM ammonium formate and 0.1% formic acid in methanol. The gradient was 0 min, 10% B, 0.5 min 33% B, 3 min 50% B, 3.1 min 90%B, 3.5 min 90% B, 4 min 10%A, supplied throughout at 0.5 mL/min. The column temperature was maintained at 35^{o}C and the autosampler at 4^{o}C. The injection loop volume as 2 ml. The QQQ was run in positive ionization mode. Instrument run parameters were: nebulizer pressure 20 psi, source gas temp 290 ^{o}C, source gas flow 13 LPM, sheath gas temp 400^{o}C, sheath gas flow 12 LPM, capillary voltage 3000 V, nozzle voltage 1000V, high pressure funnel RF 190V, low pressure funnel RF 100V. Monitored parent/product ions (collision energy) was 790.6/147.2 (50). Ado-Cbl was separated with a retention time of 2.3 minutes. Standards were purchased from Sigma-Aldrich and prepared fresh in water for analysis.

RNAi Experiments

RNAi feeding clones were obtained from the ORFeome RNAi library [8]. *E. coli* HT115 strains expressing dsRNA directed against the *C. elegans* genes *mtrr-1* and Y76A2B.5 and a control vector-only strain were grown in LB containing 100

µg/mL ampicillin to log phase, then concentrated and added to NGM agar plates containing 5 mM IPTG plus or minus Ado-Cbl or Me-Cbl. *Pacdh-1::GFP* embryos harvested by hypochlorite bleaching were added to the RNAi plates. Progeny of these RNAi-treated animals were transferred to fresh RNAi plates so that RNAi treatment could extend through an additional generation after which GFP was observed.

qRT-PCR

Embryos from N2 wild type gravid adults grown on *E. coli* OP50 were harvested, washed and hatched overnight in M9 to synchronize the population. Synchronized L1s were added to plates containing various concentrations of Me-Cbl or Ado-Cbl (both from Sigma), and/or propionic acid, seeded with *E. coli* OP50 or *Comamonas* DA1877. Animals were harvested for each condition when the majority of the population reached young adult stage. Total RNA was isolated using Trizol (Invitrogen), then purified of contaminating DNA by DNAseI treatment followed by cleanup using Qiagen RNeasy columns. cDNA was reverse-transcribed from RNA using oligo(dT)12-18 primer and Mu-MLV reverse transcriptase (NEB). Primer sequences for quantitative RT-PCR (qRT-PCR) were generated using the GETprime database [97] and are listed in **Table 3.4**. qRT-PCR reactions were performed in triplicate using the Applied Biosystems StepOnePlus Real-Time PCR system and Fast Sybr Green Master Mix (Invitrogen). Relative transcript abundance was determined using the ΔΔCt method, and normalized to averaged *ama-1* and *act-1* mRNA levels [98].

Developmental Rate, Fertility and Lifespan Assays

For all experiments, animals were grown at 20^{o}C. We measured the developmental state of a population by synchronizing animals by L1 arrest in M9 for 20 hr, then allowing animals to develop for 45 hours at 20^{o}C under various dietary conditions. For L-methionine and folate supplementations, solutions (5 mg/mL L-Met in water or 0.1 mg/mL folate in 20% ethanol) were added on top of plain NGM plates and dried prior to bacterial seeding. After 45 hours, ~35–80 animals were mounted on agarose pads and visually categorized on a compound microscope into age groups based on the development of the vulva and germline as described [105].

Brood sizes were determined by transferring 30 L4 animals onto individual plates containing *E. coli* OP50, *Comamonas aq.* DA1877, or *E. coli* OP50 supplemented with 64 nM Ado-Cbl. Animals were transferred to new individual plates daily and the number of viable offspring on the plates was counted after hatching.

For the lifespan assays, ~125 L4 animals were transferred onto NGM plates containing 0.1 mg/ml FUDR, with or without vitamin B12, seeded with either *E. coli* OP50 or *Comamonas aq*. DA187. Animals were checked for body movement or pharyngeal pumping every two days. If no pumping was observed, animals were lightly tapped with a sterile platinum wire, and if animals failed to respond to the touch stimulus they were considered dead.

Propionic Acid Toxicity Assay

Approximately 100 starved L1 animals were placed on NGM media with increasing concentrations of propionic acid (pH 6.0). After 48 hours, live animals were counted. Each dose of propionic acid was analyzed in triplicate.

CHAPTER IV: A PROPIONATE BREAKDOWN SHUNT IN *C. ELEGANS* ENABLES SURVIVAL ON LOW B12 DIETS

Preface

This research chapter derives from work that I started shortly after submitting our 2014 paper detailing the discovery that bacterially-provided vitamin B12 represses *acdh-1* expression. This chapter is an adaptation of a manuscript that is in the process of being submitted for publication, with the title "A propionate breakdown shunt in *C. elegans* enables survival on low B12 diets." In this work, I am the first author, Viridiana Olin-Sandoval is the second author, and the others on the paper are Michael Hoy, Chi-Hua Li, Timo Louisse, Vicky Yao, Amy Holdorf, Olga Troyanskaya, Markus Ralser, and Marian Walhout.

Viridiana Olin-Sandoval and Markus Ralser developed the mass spec protocols for measuring 3-hydroxypropionate and propionyl-CoA in *C. elegans*, and Maria generated the mass spec data displayed in Figure 4.6 c, d, and e, and Figure 4.9. Timo Louisse helped screen the metabolic RNAi library, and contributed to Figure 4.3b and Table 4.3. Vicky Yao and Olga Troyanskaya contributed their unpublished WISP tool for building tissue-specific gene co-expression networks, and thus contributed to Figure 4.3e. Akihiro Mori helped with the quantification of GFP expression in *C. elegans* by contributing his

unpublished IPPOME tool, and thus contributed to Figure 4.8b. Amy Holdorf constructed Table 4.4.

Abstract

Inborn errors of human metabolism are rare and often severe genetic disorders characterized by an inability to convert or breakdown cellular metabolites. Patients with inborn errors in vitamin B12 (B12)-dependent propionate breakdown build up high levels of propionate or methylmalonate (propionic acidemia or methylmalonic acidemia), depending on which enzyme in the pathway is mutated [138]. These diseases are diagnosed when unique aberrant metabolites such as 3-hydroxypropionate (3-HP) are observed in newborn screening [139]. The appearance of 3-HP, a propionate oxidation product, suggests that alternative propionate breakdown mechanisms may be utilized when the canonical pathway is perturbed [140]. However, the genetic pathway(s) that generate these metabolites and the biological significance of these pathways remains largely unknown. Using genetic interaction screening, metabolomics and ^{13}C propionate tracing, we identify a 3-HP-producing β-oxidation-like propionate breakdown shunt in the model organism *Caenorhabditis elegans*. This pathway is composed of five genes: *acdh-1*, *ech-6*, *hach-1*, *hphd-1* and *alh-8*, which have clear human orthologs. All five genes are transcriptionally activated when dietary B12 levels are low and/or when propionate levels are high. The capacity to

switch between the canonical propionate breakdown pathway and the oxidation shunt provides *C. elegans* with metabolic flexibility to adapt to B12 availability.

Results and Discussion

Humans and most animals, including *C. elegans*, require bacterially synthesized vitamin B12, or cobalamin, to support two essential metabolic pathways: the methionine/SAM cycle (or one-carbon cycle), and the breakdown of propionyl-CoA to succinyl-CoA [113, 141] (**Figure 4.1a**). Propionyl-CoA is produced from odd chain fatty acid and branched chain amino acid breakdown, and is readily interconverted via acyl-CoA synthases with propionate, a short chain fatty acid produced by bacterial fermentation. *C. elegans* has clear orthologs of the human B12-dependent propionyl-CoA breakdown genes [113], as well as a highly conserved B12-processing system [41], and therefore provides a genetically tractable model to characterize metabolic network rewiring relevant to B12 deficiency, and propionic and methylmalonic acidemias.

C. elegans inhabits temperate climates across the globe, and feeds on a wide variety of bacteria found in rotting vegetation [107]. WIthin microbial communities studied to date, bacterial species with B12-synthesizing capacity are in the minority [142] and there is evidence that other community members compete for B12 uptake [143]. It is likely that *C. elegans* encounters some bacterial diets in its natural habitat that do not provide B12, and it is unlikely that *C. elegans* obtains B12 from other sources within its environment since plants,

fungi and yeasts do not synthesize or use it [144]. We previously found that supplementing B12 to bacterial diets lacking B12 biosynthesis capacity, such as *E. coli* OP50, induces robust metabolic gene expression changes in *C. elegans* [41]. This transcriptional response to B12 may lead to metabolic network rewiring, however the functionality of such rewiring remains unknown.

Expression of *C. elegans* acyl-CoA dehydrogenase 1, *acdh-1*, is dramatically downregulated by dietary B12, and this repression occurs transcriptionally through its 1.5 kb promoter [41]. However, B12 supplementation is not sufficient to downregulate *acdh-1* expression, as its repressive effects depend on the canonical B12-dependent propionate breakdown pathway, and can also be overridden with excess propionate supplementation [41]. Thus, *acdh-1* expression may be activated when levels of propionate or propionyl-CoA increase, such as when the canonical breakdown pathway is genetically inactivated, or when dietary B12 intake is insufficient.

What is the function of the transcriptional upregulation of *acdh-1* by propionate? Like mutations in canonical propionate breakdown pathway genes, a null mutation in *acdh-1* renders animals sensitive to propionate-induced toxicity, a phenotype that is completely rescued by B12 supplementation (**Figure 4.1b**). Furthermore, *acdh-1* mutants exhibit conditional embryonic lethality on low-B12 diets, which can be rescued by supplementing B12 (**Figure 4.1c**). Based on these observations, we conclude that *acdh-1* is required by *C. elegans* to survive B12 deficiency, and may function in propionate breakdown or detoxification.

To test the relationship between *acdh-1* and the canonical B12-dependent propionate breakdown pathway, we attempted to generate a Δ*acdh-1*/Δ*pcca-1* double null mutant. *pcca-1* encodes the alpha subunit of the first enzyme in the canonical pathway (**Figure 4.1a**). A cross between Δ*pcca-1* and Δ*acdh-1* null mutants yielded no viable double homozygous mutant offspring (**Figure 4.1d** and **Table 4.1**). Since there were many dead eggs laid by the *pcca-1*-/-; *acdh-1*+/- hermaphrodites (**Figure 4.2** and **Table 4.1**), we conclude that the double null mutant is synthetic embryonic lethal. As synthetic relationships are often observed between genes in redundant pathways [145, 146], we hypothesized that *acdh-1* may function in a propionate breakdown shunt, transcriptionally activated when flux through the canonical pathway is inadequate, such as when B12 intake is suboptimal.

To identify additional *C. elegans* genes that may function with *acdh-1* in an alternate propionate breakdown pathway, we designed a synthetic lethality screen using Δ*pcca-1* mutants and an RNAi library of *C. elegans* metabolic genes. In contrast to the combination of null mutants, *acdh-1* knockdown by dsRNA feeding in the Δ*pcca-1* mutant only resulted in complete lethality in the presence of 30mM propionate (**Figure 4.3a**), indicating that RNAi likely results in incomplete knockdown. Therefore, we screened for knockdowns that led to non-viable offspring in the *pcca-1* mutant with 30mM propionate, with less severe or no phenotypes in the other conditions (**Figure 4.3b**). The library targeted 836 predicted metabolic genes (**Table 4.2**). After retesting first-pass hits from the

initial screen three times, we obtained three high-confidence hits: *acdh-1,* which validates the screening conditions, *ech-6*, an enoyl-CoA hydratase 6, and F09F7.4, which we will refer to henceforth as *hach-1*, a hydroxyacyl-CoA hydrolase. Seven lower-confidence hits were also retrieved from the screen that resulted in increased sensitivity to propionate when knocked down by RNAi, but displayed inconsistent or incomplete synthetic lethality with *pcca-1.* (**Figure 4.4 and Table 4.3**). We confirmed that RNAi knockdown of *ech-6* and *hach-1* in a wild type background results in sensitivity to propionate-induced toxicity. Similar to *acdh-1* perturbation, this sensitivity is alleviated by B12 supplementation, supporting the hypothesis that these three genes may function together in a genetic pathway (**Figure 4.4**).

The B12 independent yeast, *Candida albicans*, utilizes a β-oxidation-like propionate breakdown pathway rather than the B12-dependent carboxylation pathway. Recently, the *C. albicans* ortholog of HACH-1 was associated to the reaction 3-hydroxypropionyl-CoA → 3-HP + CoA (E.C. 3.1.2.4) in the β-oxidation-like propionate breakdown pathway [147]. Additionally, HACH-1 is predicted by KEGG [148] to catalyze the E.C. 3.1.2.4 reaction. While ACDH-1 and ECH-6 do not share sequence homology with the *C. albicans* proteins proposed to catalyze the first two reactions in the pathway, they are predicted to catalyze highly similar reactions. The human ortholog of ACDH-1, ACADSB, catalyzes the dehydrogenation of the C4 branched-chain substrate isobutyryl-CoA in valine breakdown, which is structurally similar to propionyl-CoA. Dehydrogenation of

both isobutyryl-CoA and propionyl-CoA involves a mono-substituted β-carbon, which is unique feature among acyl-CoA dehydrogenation reactions. ECH-6 is one of several *C. elegans* enzymes associated with the second reaction of the β-oxidation-like propionate breakdown pathway by KEGG, which uses the E.C. number 4.2.1.17 to describe this and several similar reactions in BCAA breakdown. We therefore hypothesized that ACDH-1, ECH-6, and HACH-1 function in a β-oxidation-like propionate breakdown shunt in *C. elegans* analogous to the *Candida* pathway that converts propionyl-CoA to acetyl-CoA (**Figure 4.3c**).

The first reaction in the propionate oxidation shunt produces acrylyl-CoA that can be readily hydrolyzed to acrylate, both of which are highly reactive and toxic molecules [149, 150]. Acrylyl-CoA is the predicted substrate for ECH-6, our predicted second enzyme in the propionate oxidation shunt. Therefore, we hypothesized that *ech-6* perturbation would result in more severe phenotypes than mutation in *acdh-1* due to toxic acrylyl-CoA or acrylate buildup. Indeed, knockdown of *ech-6* results in extremely slow growth and a “clear” phenotype (**Figure 4.3d**). Similar, albeit less severe, effects were observed with *hach-1* knockdown. The addition of B12 partially alleviates the detrimental effects caused by *ech-6* or *hach-1* knockdown. The partial rescue of *ech-6* and *hach-1* knockdowns by B12 depends on the canonical B12 dependent pathway, as B12 has no beneficial effect in *pcca-1* mutants (**Figure 4.3d**). Importantly, Δ*acdh-1* mutation largely suppressed the phenotypic effects of *ech-6* and *hach-1*

knockdown, likely due to the lack of acrylyl-CoA production in the absence of *acdh-1* (**Figure 4.3d**). This genetic buffering supports the placement of *ech-6* downstream of *acdh-1*.

In KEGG, the β-oxidation-like propionate breakdown pathway includes two additional reactions that convert 3-HP into acetyl-CoA and CO_2 (**Figure 4.3c**). To identify enzymes that may catalyze these reactions, we utilized WISP, a server for tissue-specific functional networks in *C. elegans* constructed from the integration of a large compendium of diverse datasets (Yao et al, in preparation; http://wisp.princeton.edu). The intestinal functional network centered on *acdh-1*, *ech-6* and *hach-1* and included high-confidence functional connections to Y38F1A.6 and *alh-8* (**Figure 4.3e**), neither of which were screened in the RNAi library (**Table 4.2**). These genes are excellent candidates to catalyze the fourth and fifth reactions in the propionate oxidation pathway, respectively. Y38F1A.6 is orthologous to the human gene ADHFE1, a hydroxyacid-oxoacid transhydrogenase that has been shown to metabolize γ-hydroxybutyrate (GHB)[151]. GHB is a structural analog of 3-HP produced by γ-aminobutyric acid (GABA) breakdown and is commonly known for its use as a recreational drug [152]. We will henceforth refer to Y38F1A.6 as *hphd-1* (3-hydroxypropionate-oxoacid transhydrogenase). *alh-8* is associated by KEGG to both E.C. 1.2.1.27, a reaction in branched chain amino acid breakdown, and E.C. 1.2.1.18, the fifth reaction in the propionate oxidation pathway, reactions that involve structurally similar substrates and products. Mutations in the human ortholog of *alh-8*,

ALDH6A1, result in 3-HP accumulation [153], which supports the placement of *alh-8* in the propionate shunt. Like *acdh-1*, *ech-6* and *hach-1*, the expression of *hphd-1* and *alh-8* is repressed by B12-synthesizing bacteria, *Comamonas aquatica* [29], as well as by B12 supplementation to the *E. coli* OP50 diet (**Figure 4.3f**). Further, qRT-PCR experiments revealed that all five genes are activated by propionate (**Figure 4.3f**). These data demonstrate that *hphd-1* and *alh-8* are co-regulated with *acdh-1*, *ech-6* and *hach-1* in response to metabolic cues.

We obtained an *hphd-1* deletion mutant from the *Caenorhabditis* Genetics Center (CGC), and generated an *alh-8* deletion mutant by CRISPR/Cas9-mediated genome editing [154] (**Figure 4.5**). Both mutants exhibit decreased propionate tolerance and partial larval lethality on a low-B12 diet, and both phenotypes were at least partially rescued by B12 supplementation (**Figure 4.6 a, b**). The B12-mediated rescue of the partial lethality exhibited by the Δ*hphd-1* mutant was dependent on a functional canonical propionate breakdown pathway, as B12 failed to rescue the partial larval lethality exhibited by the double mutant Δ*hphd-1*;Δ*pcca-1* (**Figure 4.6b**). The double mutant Δ*hphd-1*;Δ*pcca-1* also exhibited increased propionate sensitivity compared with either single mutant, indicating a genetic interaction between *hphd-1* and *pcca-1,* and supporting the placement of *hphd-1* in the same pathway as *acdh-1* (**Figure 4.7**). We previously found that the *acdh-1* promoter is activated by impaired propionate breakdown or by propionate supplementation [41, 64]. Knockdown of *acdh-1, ech-6* and *hach-1* all activate the *acdh-1* promoter [64]. Similarly, the loss-of-function mutant

Δ*hphd-1* activates the *acdh-1* promoter, further supporting its role in propionate breakdown (**Figure 4.8**).

3-HP is a unique metabolic intermediate produced by the propionate oxidation pathway – it is not produced by any other known metabolic pathway in any species [148]. Using liquid chromatography/selective reaction monitoring mass spectrometry (LC-SRM) we confirmed the presence of 3-HP in *C. elegans* (**Figure 4.6c**). 3-HP was detected in wild type animals, and we confirmed the peak identity by matching retention time, mass/charge ratio and MS/MS fragmentation spectra to a chemically synthesized 3-HP standard. We observed >4-fold increased 3-HP levels in Δ*pcca-1* mutants compared to wild type animals, supporting our hypothesis that the propionate oxidation shunt is activated when the canonical pathway is perturbed (**Figure 4.6 c, d**). This mirrors the elevated 3-HP observed in human patients with propionic acidemia caused by PCCA/PCCB mutations [155]. Finally, we detected a >200-fold increase in 3-HP concentration in Δ*hphd-1* mutants compared to wild type animals (**Figure 4.6 c, d**), supporting our prediction that 3-HP is a substrate for HPHD-1.

To verify that 3-HP is indeed derived from propionate, we performed carbon tracing by feeding Δ*hphd-1* mutant animals 20 mM ^{13}C-labeled propionate. We detected the formation of ^{13}C-3-HP, indicating *C. elegans* can indeed convert propionate to 3-HP (**Figure 4.6e**). Analysis of the *E. coli* OP50 diet used in these experiments revealed no detectable 3-HP, indicating that it is not derived from the bacterial diet (**Figure 4.6c**). We did however detect ample

propionyl-CoA in *E. coli* OP50 supplemented with propionate (3.38 nmol/mg protein), so the lack of 3-HP in *E. coli* was not simply due to lack of pathway substrate (**Figure 4.9**).

Taken together, our data support a two-pathway solution for propionyl-CoA breakdown in *C. elegans*, which enables metabolic flexibility to withstand changes in dietary B12 availability. *E. coli* and other low-B12 bacterial diets transcriptionally activate expression of the shunt. On B12-replete bacterial diets, such as *Comamonas aq.*, the B12-dependent pathway is likely preferred, since expression of the propionate shunt pathway genes is repressed (or simply not activated). It is likely that when B12 is present, the B12-dependent pathway is more efficient at metabolizing propionyl-CoA compared to the β-oxidation pathway due to the high redox potential between propionyl-CoA and acrylyl-CoA, the first oxidation pathway intermediate [156]. Other advantages of the canonical pathway over the oxidation pathway include the use of fewer enzymes, and the lack of production of toxic intermediates or byproducts. Thus we propose that the propionate oxidation pathway serves as a backup route for the B12-dependent pathway, and that its transcriptional response to propionate has evolved to enable survival on B12 deficient diets.

The *C. elegans* genes that we have associated with propionate oxidation have clear human orthologs (**Table 4.4**), making it plausible that these genes are responsible for producing the propionate oxidation intermediate 3-HP observed in patients with propionic acidemia and methylmalonic acidemia. Recently another

propionate oxidation shunt intermediate, acrylyl-CoA, was detected in the urine metabolomes of patients with mutations in the human orthologs of *ech-6* and *hach-1*, ECHS1 and HIBCH, supporting a role for these human genes in propionate oxidation [157]. While originally thought of as an “aberrant” metabolite since it was only detected in patients with propionate breakdown disorders, 3-HP has more recently been detected in healthy individuals [158].

Human orthologs of our five *C. elegans* genes are each known to be involved in other pathways (**Table 4.4**), indicating that roles within propionate oxidation would be the result of promiscuous, or “moonlighting,” enzymatic activities. Enzymatic promiscuity is increasingly recognized as a common evolutionary mechanism to increase metabolic reaction space and to maintain metabolic flexibility [159]. It is unclear whether the *C. elegans* genes associated with propionate oxidation also serve in other metabolic pathways, though *ech-6*, *hach-1*, and *alh-8* are assigned to at least one additional pathway in the KEGG database [148]. Future studies will reveal whether an alternate propionate oxidation pathway is active in human tissues and subject to metabolite-driven regulation like the *C. elegans* pathway.

Figures

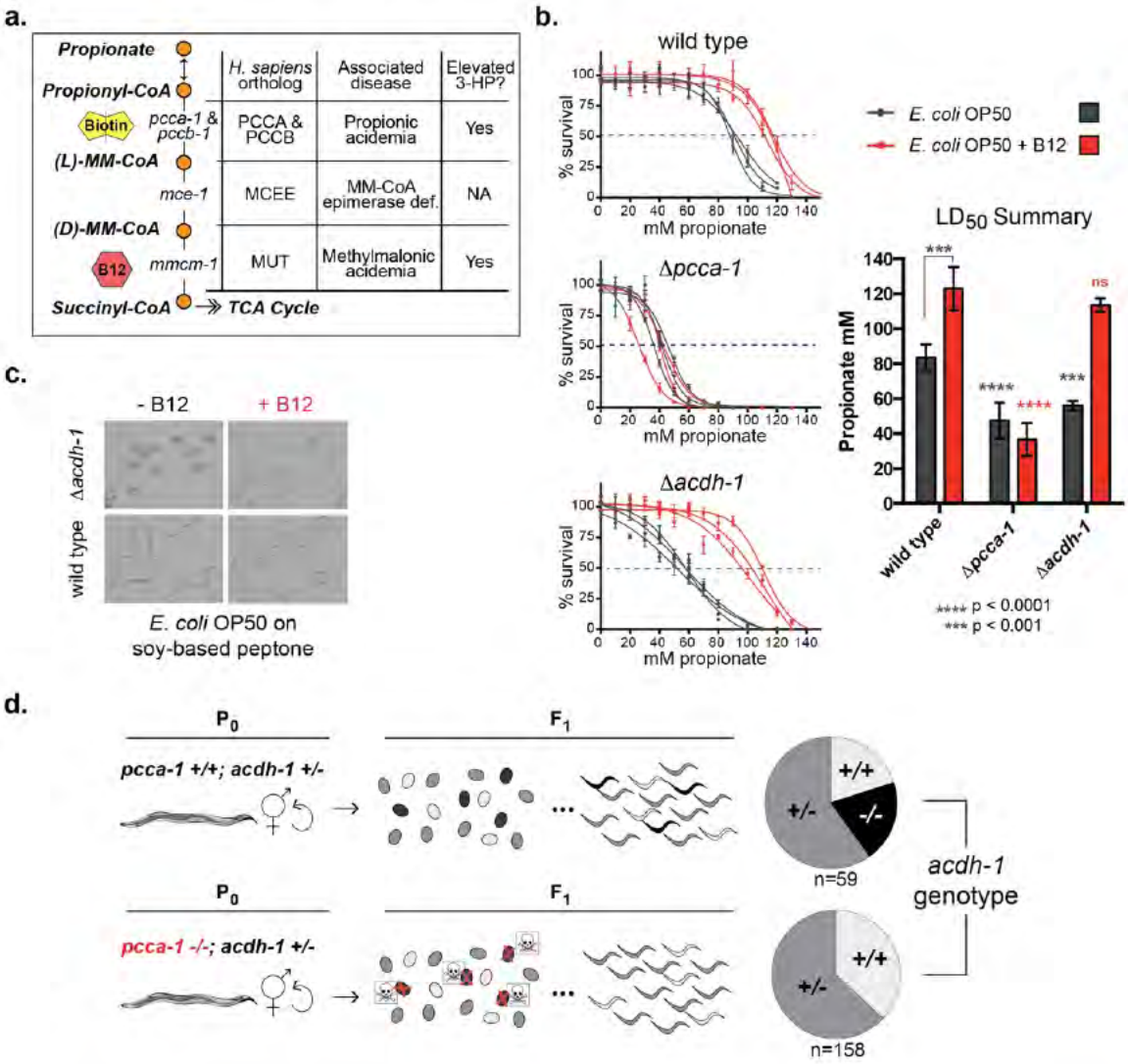

Figure 4.1 – The Δ*acdh-1* mutant is synthetic lethal with the canonical B12-dependent propionate breakdown pathway mutant Δ*pcca-1*.

a. Diagram of canonical B12-dependent propionyl-CoA breakdown pathway with associated *C. elegans* and human enzymes, as well as genetic human metabolic disorders caused by mutations in the human enzymes. 3-hydroxypropionate (3-HP) is elevated in patients with propionic acidemia (PA) and methylmalonic acidemia (MMA), but has not been assessed in methylmalonyl-CoA epimerase deficiency. **b.** Δ*pcca-1* and Δ*acdh-1* mutants both exhibit increased sensitivity to propionate compared to wild type animals. B12 increases propionate tolerance in *E. coli* OP50-fed wild type animals, and rescues the sensitivity phenotype of the

Δ*acdh-1* mutant, but has no effect in the Δ*pcca-1* mutant. Three biological replicate curves are shown on the left, with average LD_{50}'s +/- standard deviation on the right. Unpaired student's T tests were used to calculate p values. Black asterisks indicate significant difference compared to wild type, red asterisks indicate significant difference compared to wild type + B12. **c.** Δ*acdh-1* mutants cannot survive low B12 diets. Wild type animals and Δ*acdh-1* mutants were grown for one generation on media containing B12, and their F1 offspring were grown on soy peptone plates (that do not have B12), seeded with *E. coli* OP50, with or without 60nM B12. The F2 generation was collected and hatched overnight in the absence of food. Δ*acdh-1* mutant F2's from F1 parents grown without B12 fail to hatch. **d.** A cross between Δ*pcca-1* and Δ*acdh-1* mutants yields no viable double homozygous mutants. *pcca-1* +/+; *acdh-1* +/- animals and *pcca-1* -/-; *acdh-1* +/- animals were grown on *E. coli* OP50 seeded plates containing 60nM B12, and individual F1s were picked onto new plates, also containing 60nM B12. The distribution of *acdh-1* genotypes among the viable F1s picked from each P0 genotype is shown.

Table 4.1 – Summary of *acdh-1* genotypes in F1 generation of P0 *pcca-1 -/-; acdh-1 +/-* animals.

The *acdh-1* genotype (homozygous, heterozygous, or wild type) as determined by PCR for each F1 animal chosen from P0 *pcca-1* +/+; *acdh-1* +/- or *pcca-1* -/-; *acdh-1* +/- parents is shown, as well as an indication of whether the F1 animal laid non-viable embryos among the F2 offspring.

summary of acdh-1 genotypes

P0 pcca-1 -/-; acdh-1 +/-

F1:

animal	acdh-1 +/+	acdh-1 +/-	acdh-1 -/-	dead F2 eggs?
1		acdh-1 +/-		yes
2		acdh-1 +/-		yes
3		acdh-1 +/-		yes
4		acdh-1 +/-		yes
5		acdh-1 +/-		yes
6		acdh-1 +/-		yes
7	acdh-1 +/+			no
8		acdh-1 +/-		yes
9		acdh-1 +/-		yes
10		acdh-1 +/-		yes
11		acdh-1 +/-		yes
12		acdh-1 +/-		yes
13	acdh-1 +/+			no
14		acdh-1 +/-		yes
15		acdh-1 +/-		yes
16		acdh-1 +/-		yes
17		acdh-1 +/-		yes
18		acdh-1 +/-		yes
19	acdh-1 +/+			no
20		acdh-1 +/-		yes
21		acdh-1 +/-		yes
22	acdh-1 +/+			no
23		acdh-1 +/-		yes
24		acdh-1 +/-		yes
25	acdh-1 +/+			no
26		acdh-1 +/-		yes
27	acdh-1 +/+			no
28		acdh-1 +/-		yes
29		acdh-1 +/-		yes
30		acdh-1 +/-		yes
31		acdh-1 +/-		yes
32	acdh-1 +/+			no
33		acdh-1 +/-		yes
34	acdh-1 +/+			no
35		acdh-1 +/-		yes
36		acdh-1 +/-		yes
37	acdh-1 +/+			no
38		acdh-1 +/-		yes
39	acdh-1 +/+			no
40	acdh-1 +/+			no
41		acdh-1 +/-		yes
42	acdh-1 +/+			no
43	acdh-1 +/+			no
44	acdh-1 +/+			no
45		acdh-1 +/-		yes
46		acdh-1 +/-		yes
47		acdh-1 +/-		yes
48	acdh-1 +/+			no
49	acdh-1 +/+			no
50		acdh-1 +/-		yes
51		acdh-1 +/-		yes
52	acdh-1 +/+			no
53	acdh-1 +/+			no
54		acdh-1 +/-		yes
55	acdh-1 +/+			no

controls P0 pcca-1 +/+; acdh-1 +/-

F1:

animal	acdh-1 +/+	acdh-1 +/-	acdh-1 -/-	dead F2 eggs
1	acdh-1 +/+			no
2	acdh-1 +/+			no
3		acdh-1 +/-		no
4	acdh-1 +/+			no
5		acdh-1 +/-		no
6		acdh-1 +/-		no
7	acdh-1 +/+			no
8		acdh-1 +/-		no
9			acdh-1 -/-	no
10		acdh-1 +/-		no
11		acdh-1 +/-		no
12		acdh-1 +/-		no
13		acdh-1 +/-		no
14			acdh-1 -/-	no
15		acdh-1 +/-		no
16			acdh-1 -/-	no
17		acdh-1 +/-		no
18		acdh-1 +/-		no
19		acdh-1 +/-		no
20		acdh-1 +/-		no
21			acdh-1 -/-	no
22		acdh-1 +/-		no
23		acdh-1 +/-		no
24	acdh-1 +/+			no
25		acdh-1 +/-		no
26			acdh-1 -/-	no
27	acdh-1 +/+			no
28			acdh-1 -/-	no
29		acdh-1 +/-		no
30		acdh-1 +/-		no
31		acdh-1 +/-		no
32	acdh-1 +/+			no
33		acdh-1 +/-		no
34		acdh-1 +/-		no
35			acdh-1 -/-	no
36		acdh-1 +/-		no
37		acdh-1 +/-		no
38		acdh-1 +/-		no
39	acdh-1 +/+			no
40		acdh-1 +/-		no
41	acdh-1 +/+			no
42		acdh-1 +/-		no
43			acdh-1 -/-	no
44	acdh-1 +/+			no
45			acdh-1 -/-	no
46		acdh-1 +/-		no
47	acdh-1 +/+			no
48			acdh-1 -/-	no
49		acdh-1 +/-		no
50		acdh-1 +/-		no
51			acdh-1 -/-	no
52	acdh-1 +/+			no
53		acdh-1 +/-		no
54		acdh-1 +/-		no
55		acdh-1 +/-		no

P0 pcca-1 -/-; acdh-1 +/-

F1:

animal	acdh-1 +/+	acdh-1 +/-	acdh-1 -/-	dead F2 eggs?
56	acdh-1 +/+			no
57		acdh-1 +/-		yes
58		acdh-1 +/-		yes
59	acdh-1 +/+			no
60	acdh-1 +/+			no
61		acdh-1 +/-		yes
62		acdh-1 +/-		yes
63		acdh-1 +/-		yes
64		acdh-1 +/-		yes
65	acdh-1 +/+			no
66		acdh-1 +/-		yes
67		acdh-1 +/-		yes
68		acdh-1 +/-		yes
69		acdh-1 +/-		yes
70		acdh-1 +/-		yes
71		acdh-1 +/-		yes
72	acdh-1 +/+			no
73		acdh-1 +/-		yes
74	acdh-1 +/+			no
75		acdh-1 +/-		yes
76		acdh-1 +/-		yes
77	acdh-1 +/+			no
78		acdh-1 +/-		yes
79		acdh-1 +/-		yes
80		acdh-1 +/-		yes
81	acdh-1 +/+			no
82		acdh-1 +/-		yes
83	acdh-1 +/+			no
84		acdh-1 +/-		yes
85	acdh-1 +/+			no
86		acdh-1 +/-		yes
87	acdh-1 +/+			no
88		acdh-1 +/-		yes
89	acdh-1 +/+			no
90		acdh-1 +/-		yes
91		acdh-1 +/-		yes
92		acdh-1 +/-		yes
93		acdh-1 +/-		yes
94		acdh-1 +/-		yes
95		acdh-1 +/-		yes
96	acdh-1 +/+			no
97		acdh-1 +/-		yes
98		acdh-1 +/-		yes
99		acdh-1 +/-		yes
100	acdh-1 +/+			no
101		acdh-1 +/-		yes
102	acdh-1 +/+			no
103		acdh-1 +/-		yes
104		acdh-1 +/-		yes
105	acdh-1 +/+			no
106		acdh-1 +/-		yes
107		acdh-1 +/-		yes
108	acdh-1 +/+			no
109		acdh-1 +/-		yes
110		acdh-1 +/-		yes
111	acdh-1 +/+			no
112		acdh-1 +/-		yes

controls P0 pcca-1 +/+; acdh-1 +/-

F1:

animal	acdh-1 +/+	acdh-1 +/-	acdh-1 -/-	dead F2 eggs?
56		acdh-1 +/-		no
57		acdh-1 +/-		no
58			acdh-1 -/-	no
59		acdh-1 +/-		no

totals	12	35	12
percent	20.3389831	59.3220339	20.3389831

P0 pcca-1 -/-; acdh-1 +/-

F1:

animal	acdh-1 +/+	acdh-1 +/-	acdh-1 -/-	dead F2 eggs?
113	acdh-1 +/+			no
114		acdh-1 +/-		yes
115		acdh-1 +/-		yes
116		acdh-1 +/-		yes
117		acdh-1 +/-		yes
118	acdh-1 +/+			no
119		acdh-1 +/-		yes
120		acdh-1 +/-		yes
121		acdh-1 +/-		yes
122		acdh-1 +/-		yes
123	acdh-1 +/+			no
124	acdh-1 +/+			no
125	acdh-1 +/+			no
126		acdh-1 +/-		yes
127		acdh-1 +/-		yes
128		acdh-1 +/-		yes
129	acdh-1 +/+			no
130	acdh-1 +/+			no
131		acdh-1 +/-		yes
132		acdh-1 +/-		yes
133	acdh-1 +/+			no
134		acdh-1 +/-		yes
135	acdh-1 +/+			no
136	acdh-1 +/+			no
137	acdh-1 +/+			no
138		acdh-1 +/-		yes
139		acdh-1 +/-		yes
140	acdh-1 +/+			no
141	acdh-1 +/+			no
142	acdh-1 +/+			no
143	acdh-1 +/+			no
144		acdh-1 +/-		yes
145	acdh-1 +/+			no
146	acdh-1 +/+			no
147	acdh-1 +/+			no
148		acdh-1 +/-		yes
149	acdh-1 +/+			no
150		acdh-1 +/-		yes
151	acdh-1 +/+			no
152		acdh-1 +/-		yes
153	acdh-1 +/+			no
154		acdh-1 +/-		yes
155	acdh-1 +/+			no
156		acdh-1 +/-		yes
157		acdh-1 +/-		yes
158		acdh-1 +/-		yes
total	59	99	0	
percent	37.3417722	62.6582278	0	

controls P0 pcca-1 +/+; acdh-1 +/-

F1:

animal	acdh-1 +/+	acdh-1 +/-	acdh-1 -/-	dead F2 eggs?

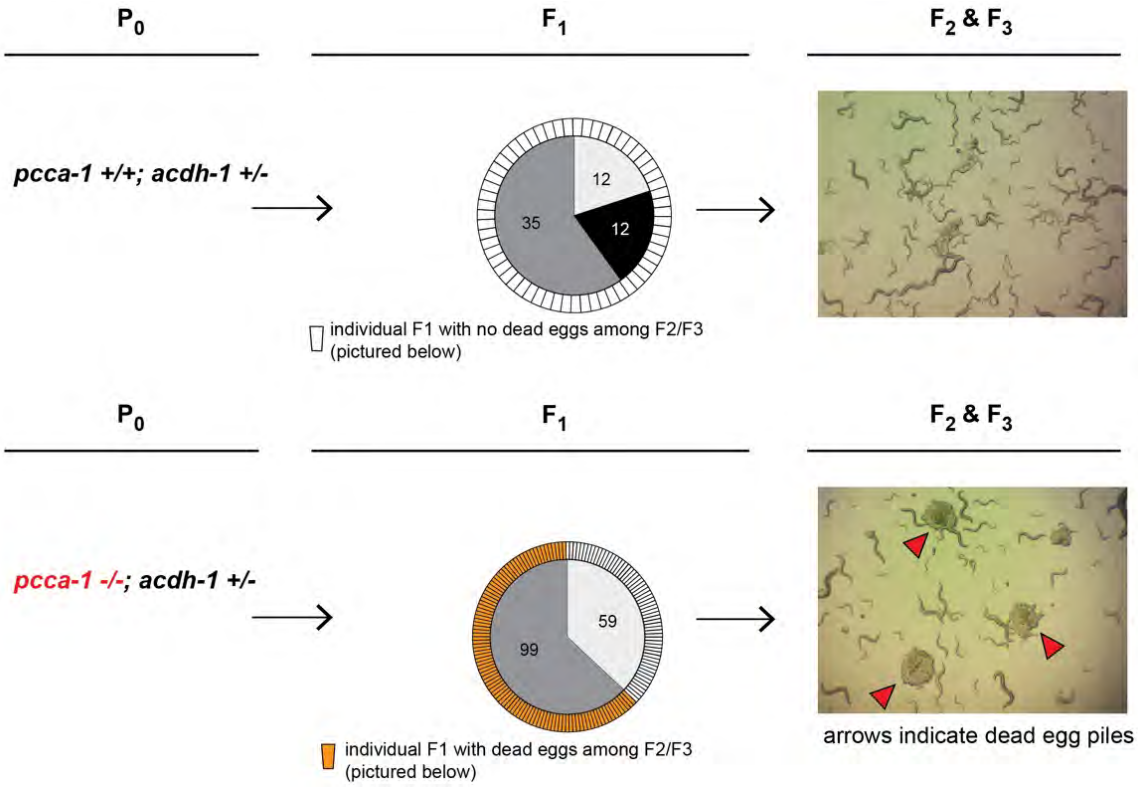

Figure 4.2 – Double Δ*acdh-1*; Δ*pcca-1* mutation is embryonically lethal.
Related to **Figure 4.1d**. *pcca-1* -/-; *acdh-1* +/- hermaphrodites produce ~63% viable *pcca-1* -/-; *acdh-1* +/-, ~37% viable *pcca-1* -/-; *acdh-1* +/+, and 0% viable *pcca-1* -/-; *acdh-1* -/- offspring. Dead eggs are abundant on plates with *pcca-1* +/+; *acdh-1* +/- parents, but not on plates with *pcca-1* -/-; *acdh-1* +/+ parents. It is likely that these dead eggs represent double homozygous mutants.

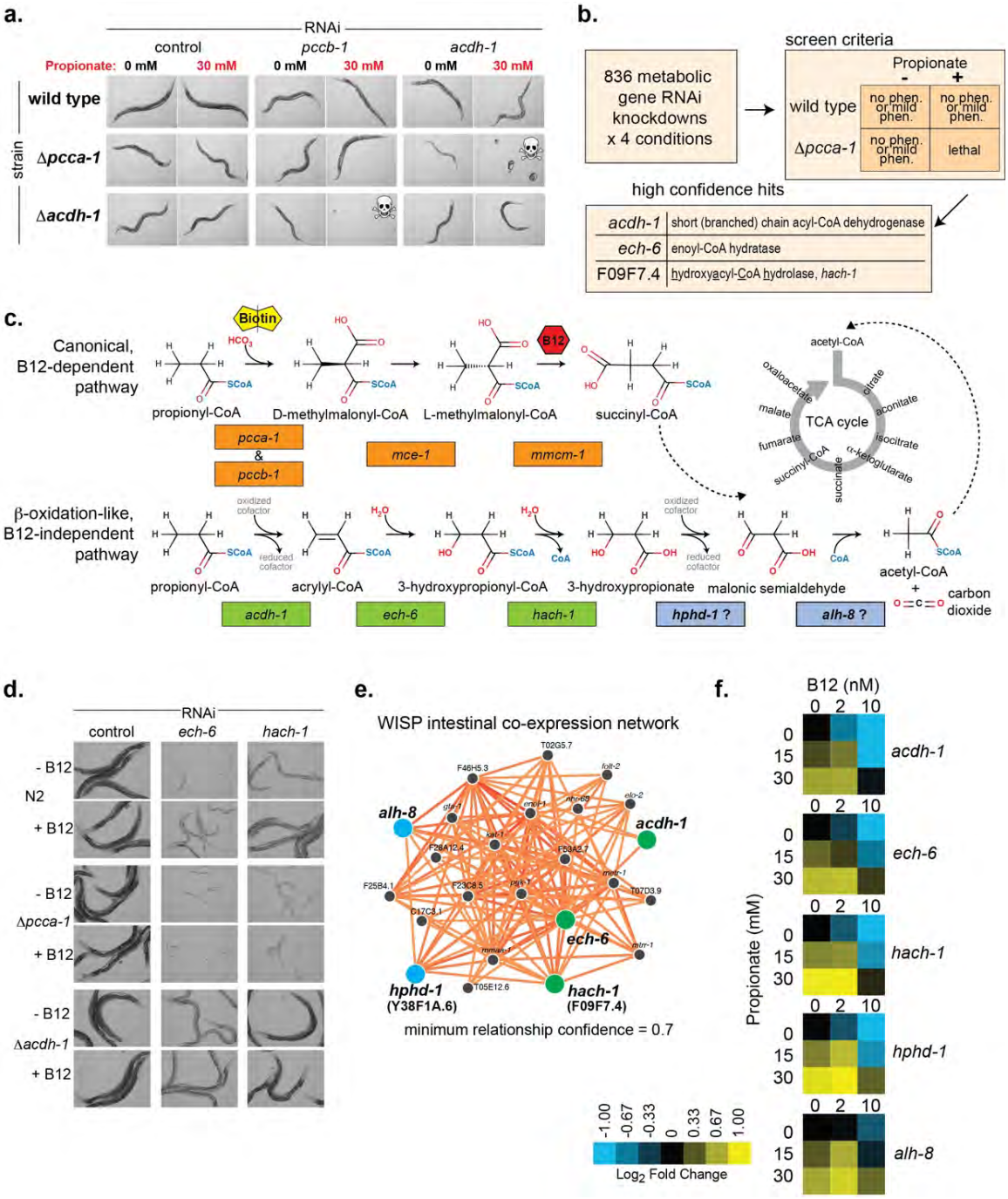

Figure 4.3 – An RNAi screen identifies candidate genes involved in alternate propionate breakdown shunt.

a. RNAi-mediated knockdown of *acdh-1* results in synthetic lethality with the Δ*pcca-1* mutant in the presence of 30 mM propionate. Synthetic lethality in the presence of propionate is also observed in the reciprocal experiment, in which *pccb-1*, the beta subunit of propionyl-CoA carboxylase, is knocked down in the

Δ*acdh-1* mutant. Lethality is only observed in the second generation of RNAi knockdown, shown in representative DIC images. Δ*acdh-1* animals were cultivated with 64nM B12 one generation prior to the first generation of knockdown to support survival of this mutant. **b.** RNAi-screen of 836 metabolic genes in presence or absence of added propionate and in wild type and Δ*pcca-1* mutant animals. Hits were retested three times. High-confidence hits, which retested all three times, are listed. Additional low-confidence hits are listed in **Table 4.3**. **c.** Enzymes that genetically interact with the canonical propionate-breakdown pathway may form a parallel, β-oxidation-like propionate breakdown pathway. Reactions and associated enzyme-encoding genes of the canonical B12-dependent pathway are shown on top (orange boxes). Reactions and candidate enzyme-encoding genes of the proposed oxidation shunt are shown on bottom (green boxes = genes identified in screen; blue boxes = candidate genes identified bioinformatically). **d.** Genetic buffering of severe *ech-6* and *hach-1* RNAi phenotypes by loss of *acdh-1* function. Representative DIC images of animals subjected to two generations of RNAi knockdown are shown. **e,** Candidates for the last two reactions in the proposed propionate oxidation shunt identified from an intestinal functional network around *acdh-1*, *ech-6* and *hach-1* in WISP (in preparation; http://wisp.princeton.edu), with a minimum relationship confidence score of 0.7. *hphd-1* and *alh-8* (blue) are both tightly connected to *acdh-1*, *ech-6* and *hach-1* (green), and are candidates to catalyze the 4^{th} and 5^{th} reactions of the pathway, respectively. **f,** The expression of all five candidate propionate oxidation pathway genes is repressed by B12 and activated by propionate. Condition matrices are shown for each gene. Expression is normalized to levels in the control (0nM B12, 0mM propionate) condition.

Table 4.2 – Metabolic gene lists

A manually curated list of putative metabolic genes in *C. elegans*. The 836 genes that were screened as part of the metabolic RNAi library are indicated.

ORF name	In Metabolic RNAi Library?	Clone source
T19B4.3	yes	ORFeome
F42F12.4	yes	ORFeome
D2063.1	yes	ORFeome
F20H11.3	yes	ORFeome
F25H9.6	yes	ORFeome
F39B2.3	yes	ORFeome
W02F12.5	yes	ORFeome
C44H4.6	yes	ORFeome
LLC1.3	yes	ORFeome
F23B12.6	yes	ORFeome
F43G9.1	yes	ORFeome
C03C10.3	yes	ORFeome
F53A2.7	yes	ORFeome
K01G5.5	yes	ORFeome
F40F8.1	yes	ORFeome
C36B1.7	yes	ORFeome
K05G3.3	yes	ORFeome
T03F6.1	yes	ORFeome
R07E5.2	yes	ORFeome
B0280.3	yes	ORFeome
C35D10.6	yes	ORFeome
F53F1.2	yes	ORFeome
F01G4.2	yes	ORFeome
K01A2.5	yes	ORFeome
F56H11.4	yes	ORFeome
T04G9.4	yes	ORFeome
M153.1	yes	ORFeome
F55A12.4	yes	ORFeome
F01D5.8	yes	ORFeome
B0272.3	yes	ORFeome
C25A1.5	yes	ORFeome
ZK430.2	yes	ORFeome
C07D8.6	yes	ORFeome
T21H3.1	yes	ORFeome
F53C11.3	yes	ORFeome
F13D12.2	yes	ORFeome
R05G6.4	yes	ORFeome
C05G5.4	yes	ORFeome
T08H10.1	yes	ORFeome
C30H6.7	yes	ORFeome
C47B2.6	yes	ORFeome
F08C6.2	yes	ORFeome
K11D2.2	yes	ORFeome
T05H10.6	yes	ORFeome
K12G11.3	yes	ORFeome
F54F3.3	yes	ORFeome
F41E6.5	yes	ORFeome
C53B4.7	yes	ORFeome
W04G3.5	yes	ORFeome
C05C10.4	yes	ORFeome
W02A2.1	yes	ORFeome
C14F11.1	yes	ORFeome
H24K24.3	yes	ORFeome
T06D8.3	yes	ORFeome
VF13D12L.3	yes	ORFeome
F47G4.3	yes	ORFeome
T02G5.7	yes	ORFeome

ORF name	In Metabolic RNAi Library?	Clone source
K08B12.1	yes	ORFeome
R06F6.9	yes	ORFeome
F54D5.7	yes	ORFeome
T03F1.3	yes	ORFeome
C04C3.3	yes	ORFeome
C37H5.3	yes	ORFeome
K04D7.3	yes	ORFeome
M03A8.1	yes	ORFeome
R03A10.4	yes	ORFeome
T25B9.9	yes	ORFeome
F02E9.7	yes	ORFeome
K02F2.2	yes	ORFeome
T27F6.6	yes	ORFeome
T13F2.1	yes	ORFeome
T03F1.1	yes	ORFeome
C46F11.2	yes	ORFeome
T21B10.2	yes	ORFeome
Y56A3A.13	yes	ORFeome
C34F6.8	yes	ORFeome
Y43F4B.5	yes	ORFeome
F57B10.3	yes	ORFeome
B0218.2	yes	ORFeome
T22G5.5	yes	ORFeome
Y45F3A.3	yes	ORFeome
T20B3.1	yes	ORFeome
F01G10.1	yes	ORFeome
F59G1.1	yes	ORFeome
F52E4.1	yes	ORFeome
F26D10.9	yes	ORFeome
ZK829.4	yes	ORFeome
R11F4.1	yes	ORFeome
H04M03.1	yes	ORFeome
F13D12.4	yes	ORFeome
R07H5.2	yes	ORFeome
T22H6.2	yes	ORFeome
T04A8.7	yes	ORFeome
C01F1.3	yes	ORFeome
F26H9.4	yes	ORFeome
F19H6.4	yes	ORFeome
ZC434.8	yes	ORFeome
C01G8.3	yes	ORFeome
C01G5.5	yes	ORFeome
D2085.6	yes	ORFeome
C28D4.3	yes	ORFeome
C50F7.4	yes	ORFeome
F27C8.6	yes	ORFeome
T07G12.11	yes	ORFeome
M18.3	yes	ORFeome
ZC410.3	yes	ORFeome
F22B3.4	yes	ORFeome
C34B2.7	yes	ORFeome
F07A11.2	yes	ORFeome
T23G5.1	yes	ORFeome
D2013.8	yes	ORFeome
K01A11.2	yes	ORFeome
F23H11.9	yes	ORFeome
B0524.2	yes	ORFeome

ORF name	In Metabolic RNAi Library?	Clone source
C16C10.10	yes	ORFeome
F54C8.1	yes	ORFeome
C40H1.4	yes	ORFeome
B0285.8	yes	ORFeome
R01H2.5	yes	ORFeome
F20H11.5	yes	ORFeome
Y56A3A.3	yes	ORFeome
Y48A6B.7	yes	ORFeome
ZC395.7	yes	ORFeome
ZC395.2	yes	ORFeome
ZK688.3	yes	ORFeome
Y49E10.18	yes	ORFeome
ZK1058.5	yes	ORFeome
T05G5.5	yes	ORFeome
Y56A3A.29	yes	ORFeome
T03F6.3	yes	ORFeome
T05G5.6	yes	ORFeome
Y44E3A.3	yes	ORFeome
F33A8.5	yes	ORFeome
T22D1.3	yes	ORFeome
B0395.3	yes	ORFeome
Y71H10A.1	yes	ORFeome
F32G8.6	yes	ORFeome
F44E7.2	yes	ORFeome
R04B5.5	yes	ORFeome
R02D3.1	yes	ORFeome
T20G5.2	yes	ORFeome
Y110A7A.6	yes	ORFeome
R12C12.1	yes	ORFeome
T22B11.5	yes	ORFeome
F26E4.12	yes	ORFeome
C16A3.10	yes	ORFeome
Y111B2A.8	yes	ORFeome
F23B12.5	yes	ORFeome
T07C4.1	yes	ORFeome
R05H10.5	yes	ORFeome
K01C8.1	yes	ORFeome
K11H3.1	yes	ORFeome
F25H2.5	yes	ORFeome
H19N07.4	yes	ORFeome
C47D2.2	yes	ORFeome
F28H7.2	yes	ORFeome
ZK1127.10	yes	ORFeome
C31C9.2	yes	ORFeome
C36A4.9	yes	ORFeome
T03G11.4	yes	ORFeome
ZC373.5	yes	ORFeome
C05C10.3	yes	ORFeome
R151.2	yes	ORFeome
Y62E10A.6	yes	ORFeome
F37C4.6	yes	ORFeome
M04B2.4	yes	ORFeome
C02D5.1	yes	ORFeome
F53C3.12	yes	ORFeome
F54G8.2	yes	ORFeome
E02H9.5	yes	ORFeome
C05D2.4	yes	ORFeome

ORF name	In Metabolic RNAi Library?	Clone source
F42G9.5	yes	ORFeome
VF13D12L.1	yes	ORFeome
E04F6.5	yes	ORFeome
ZK643.2	yes	ORFeome
ZK1058.3	yes	ORFeome
F01F1.10	yes	ORFeome
F35G12.1	yes	ORFeome
ZK370.5	yes	ORFeome
B0361.5	yes	ORFeome
F59B2.3	yes	ORFeome
C56G2.6	yes	ORFeome
F25B5.6	yes	ORFeome
F09F7.7	yes	ORFeome
B0285.9	yes	ORFeome
F57B9.4	yes	ORFeome
B0361.7	yes	ORFeome
F25B5.3	yes	ORFeome
B0303.3	yes	ORFeome
K03H1.1	yes	ORFeome
F37C12.7	yes	ORFeome
F01F1.6	yes	ORFeome
K02D10.1	yes	ORFeome
BE10.2	yes	ORFeome
F01F1.5	yes	ORFeome
K10D2.6	yes	ORFeome
C05D11.7	yes	ORFeome
B0285.7	yes	ORFeome
F17C8.1	yes	ORFeome
F53A2.8	yes	ORFeome
C48B4.1	yes	ORFeome
F37A4.1	yes	ORFeome
D2045.9	yes	ORFeome
ZK637.5	yes	ORFeome
ZK688.6	yes	ORFeome
T04A8.5	yes	ORFeome
ZK637.10	yes	ORFeome
Y71D11A.3	yes	ORFeome
ZK632.4	yes	ORFeome
T21C12.2	yes	ORFeome
W05G11.6	yes	ORFeome
F23H11.2	yes	ORFeome
ZK1058.1	yes	ORFeome
ZK112.1	yes	ORFeome
F23H11.2	yes	ORFeome
ZK370.4	yes	ORFeome
M88.1	yes	ORFeome
C27D8.4	yes	ORFeome
C06A12.5	yes	ORFeome
C43E11.7	yes	ORFeome
F41D3.5	yes	ORFeome
H23N18.4	yes	ORFeome
Y37H9A.6	yes	ORFeome
B0041.6	yes	ORFeome
D2030.5	yes	ORFeome
Y23H5A.8	yes	ORFeome
C06A5.4	yes	ORFeome
Y106G6E.4	yes	ORFeome
C32E8.9	yes	ORFeome

ORF name	In Metabolic RNAi Library?	Clone source
F32H2.6	yes	ORFeome
ZK909.3	yes	ORFeome
Y87G2A.14	yes	ORFeome
Y47G6A.22	yes	ORFeome
R119.3	yes	ORFeome
Y106G6H.4	yes	ORFeome
F09C3.2	yes	ORFeome
Y110A7A.7	yes	ORFeome
Y32H12A.6	yes	ORFeome
C54G6.1	yes	ORFeome
C24A11.9	yes	ORFeome
F36D1.1	yes	ORFeome
E01A2.1	yes	ORFeome
Y110A7A.4	yes	ORFeome
T05F1.10	yes	ORFeome
T01H8.2	yes	ORFeome
T28F2.3	yes	ORFeome
C31H5.1	yes	ORFeome
Y71F9B.9	yes	ORFeome
R05D7.4	yes	ORFeome
K07A3.1	yes	ORFeome
T27A3.6	yes	ORFeome
T26E3.2	yes	ORFeome
T10E9.9	yes	ORFeome
C30F12.7	yes	ORFeome
R06C1.2	yes	ORFeome
F27D4.5	yes	ORFeome
F57C9.1	yes	ORFeome
F10G8.9	yes	ORFeome
C46H11.2	yes	ORFeome
F56H6.5	yes	ORFeome
C32E8.6	yes	ORFeome
C15A11.7	yes	ORFeome
C55B7.4	yes	ORFeome
C32E12.2	yes	ORFeome
C15A11.4	yes	ORFeome
C44E4.3	yes	ORFeome
C37A2.3	yes	ORFeome
Y6B3B.5	yes	ORFeome
B0205.6	yes	ORFeome
T05E7.1	yes	ORFeome
F53F10.2	yes	ORFeome
C12C8.2	yes	ORFeome
C10H11.6	yes	ORFeome
Y110A7A.6	yes	ORFeome
F54D7.2	yes	ORFeome
W03D8.8	yes	ORFeome
F14B4.2	yes	ORFeome
R06C7.5	yes	ORFeome
F47G6.2	yes	ORFeome
C10H11.3	yes	ORFeome
F56C11.6	yes	ORFeome
T10B11.2	yes	ORFeome
F57B10.7	yes	ORFeome
R06C7.3	yes	ORFeome
Y87G2A.8	yes	ORFeome
C10H11.5	yes	ORFeome
C10H11.4	yes	ORFeome

ORF name	In Metabolic RNAi Library?	Clone source
F41D3.4	yes	ORFeome
D2030.1	yes	ORFeome
H25P06.1	yes	ORFeome
C53D5.5	yes	ORFeome
T09E11.7	yes	ORFeome
Y65B4BL.5	yes	ORFeome
F14B6.5	yes	ORFeome
R11A5.4	yes	ORFeome
Y48G9A.10	yes	ORFeome
T04D3.3	yes	ORFeome
Y40B1B.6	yes	ORFeome
F54C1.1	yes	ORFeome
F56H6.12	yes	ORFeome
C09D4.4	yes	ORFeome
C34G6.2	yes	ORFeome
Y106G6H.5	yes	ORFeome
C48E7.8	yes	ORFeome
Y4C6B.6	yes	ORFeome
T04D3.4	yes	ORFeome
C54G6.1	yes	ORFeome
C27A12.9	yes	ORFeome
K10B3.8	yes	ORFeome
Y54E10BR.1	yes	ORFeome
K02F2.1	yes	ORFeome
F11E6.1	yes	ORFeome
F55B11.1	yes	ORFeome
C05C8.7	yes	ORFeome
K06A4.5	yes	ORFeome
C27H5.1	yes	ORFeome
Y38A8.1	yes	ORFeome
F43E2.5	yes	ORFeome
F37H8.3	yes	ORFeome
R07G3.2	yes	ORFeome
Y46G5A.5	yes	ORFeome
F58A6.1	yes	ORFeome
Y17G7B.3	yes	ORFeome
T23F4.3	yes	ORFeome
Y38E10A.10	yes	ORFeome
D1022.3	yes	ORFeome
B0491.7	yes	ORFeome
F49E12.9	yes	ORFeome
B0228.7	yes	ORFeome
W01C9.4	yes	ORFeome
Y53F4B.2	yes	ORFeome
T13B5.5	yes	ORFeome
E04F6.3	yes	ORFeome
T02G5.13	yes	ORFeome
H41C03.2	yes	ORFeome
F13H8.9	yes	ORFeome
Y46G5A.19	yes	ORFeome
ZK1290.5	yes	ORFeome
F01D5.7	yes	ORFeome
E04F6.7	yes	ORFeome
Y39G8B.2	yes	ORFeome
B0432.5	yes	ORFeome
T25D3.3	yes	ORFeome
B0491.1	yes	ORFeome
C34C6.5	yes	ORFeome

ORF name	In Metabolic RNAi Library?	Clone source
F27E5.1	yes	ORFeome
C33F10.7	yes	ORFeome
K05F1.3	yes	ORFeome
T13B5.3	yes	ORFeome
M05D6.7	yes	ORFeome
Y46G5A.21	yes	ORFeome
C06A8.1	yes	ORFeome
Y53F4B.18	yes	ORFeome
Y46G5A.24	yes	ORFeome
F49E12.1	yes	ORFeome
Y46G5A.31	yes	ORFeome
C23H3.7	yes	ORFeome
R53.2	yes	ORFeome
K10B4.1	yes	ORFeome
F58G1.5	yes	ORFeome
F14E5.5	yes	ORFeome
Y25C1A.13	yes	ORFeome
F53C3.13	yes	ORFeome
C23H3.9	yes	ORFeome
C09E8.2	yes	ORFeome
C15F1.6	yes	ORFeome
C30G12.2	yes	ORFeome
T06D8.6	yes	ORFeome
Y110A2AL.14	yes	ORFeome
C32D5.12	yes	ORFeome
T05C12.3	yes	ORFeome
W09H1.5	yes	ORFeome
F57C2.5	yes	ORFeome
T14D7.1	yes	ORFeome
B0286.3	yes	ORFeome
ZK1320.9	yes	ORFeome
D2089.5	yes	ORFeome
T02G5.8	yes	ORFeome
ZK945.1	yes	ORFeome
M05D6.4	yes	ORFeome
F28A10.6	yes	ORFeome
C01G6.7	yes	ORFeome
M28.6	yes	ORFeome
E02H1.3	yes	ORFeome
W07A12.7	yes	ORFeome
ZK669.4	yes	ORFeome
R153.1	yes	ORFeome
Y48B6A.12	yes	ORFeome
C34C6.4	yes	ORFeome
C38C6.2	yes	ORFeome
C08H9.3	yes	ORFeome
K01C8.3	yes	ORFeome
R53.7	yes	ORFeome
K09E4.4	yes	ORFeome
ZK430.8	yes	ORFeome
F37B12.2	yes	ORFeome
R05F9.6	yes	ORFeome
C16C8.2	yes	ORFeome
ZK1127.2	yes	ORFeome
C33C12.3	yes	ORFeome
DH11.1	yes	ORFeome
C01G6.6	yes	ORFeome
ZK177.8	yes	ORFeome
R06A4.8	yes	ORFeome

ORF name	In Metabolic RNAi Library?	Clone source
F52H3.1	yes	ORFeome
W09B6.1	yes	ORFeome
F32A5.2	yes	ORFeome
R05F9.12	yes	ORFeome
C17G10.8	yes	ORFeome
R03D7.1	yes	ORFeome
C13B4.1	yes	ORFeome
Y48G10A.1	yes	ORFeome
D2013.9	yes	ORFeome
T25G3.4	yes	ORFeome
C45G3.3	yes	ORFeome
K01G5.9	yes	ORFeome
F56G4.5	yes	ORFeome
F54D5.12	yes	ORFeome
R09H10.3	yes	ORFeome
F49E8.4	yes	ORFeome
R10H10.6	yes	ORFeome
T09A12.2	yes	ORFeome
JC8.4	yes	ORFeome
C06E4.3	yes	ORFeome
ZK1251.3	yes	ORFeome
T04B2.6	yes	ORFeome
Y57G11C.21	yes	ORFeome
Y55F3BR.5	yes	ORFeome
C06E4.6	yes	ORFeome
Y57G11C.3	yes	ORFeome
F01G4.5	yes	ORFeome
ZK829.1	yes	ORFeome
F56H11.3	yes	ORFeome
ZK550.5	yes	ORFeome
F08G5.2	yes	ORFeome
B0035.16	yes	ORFeome
F38E11.3	yes	ORFeome
C45E5.1	yes	ORFeome
F33D4.4	yes	ORFeome
T25B9.1	yes	ORFeome
ZK617.2	yes	ORFeome
Y54G2A.17	yes	ORFeome
C50F7.6	yes	ORFeome
C06A6.4	yes	ORFeome
C10C5.3	yes	ORFeome
F01G10.3	yes	ORFeome
Y45F10D.11	yes	ORFeome
D2096.4	yes	ORFeome
Y37E11AR.4	yes	ORFeome
Y105C5B.28	yes	ORFeome
F01G10.2	yes	ORFeome
F01D4.8	yes	ORFeome
T25B9.7	yes	ORFeome
C47E12.8	yes	ORFeome
K08B4.3	yes	ORFeome
Y7A9A.1	yes	ORFeome
C01B10.4	yes	ORFeome
K08B4.4	yes	ORFeome
C08F11.8	yes	ORFeome
H23L24.5	yes	ORFeome
D2024.3	yes	ORFeome
R11A8.3	yes	ORFeome
H12I13.4	yes	ORFeome

ORF name	In Metabolic RNAi Library?	Clone source
K08F4.9	yes	ORFeome
T23G4.4	yes	ORFeome
K09E10.2	yes	ORFeome
ZK809.2	yes	ORFeome
B0001.4	yes	ORFeome
F37C4.3	yes	ORFeome
Y57G11C.11	yes	ORFeome
ZK550.6	yes	ORFeome
C33A12.7	yes	ORFeome
R07H5.8	yes	ORFeome
F38H4.8	yes	ORFeome
Y55F3AM.10	yes	ORFeome
T20D3.8	yes	ORFeome
F41H10.8	yes	ORFeome
D2024.2	yes	ORFeome
K02D7.1	yes	ORFeome
C06G3.5	yes	ORFeome
C06E7.1	yes	ORFeome
H04M03.3	yes	ORFeome
F13B12.4	yes	ORFeome
ZK829.7	yes	ORFeome
C55F2.1	yes	ORFeome
Y105C5B.9	yes	ORFeome
F30B5.4	yes	ORFeome
C10C5.4	yes	ORFeome
C10C5.5	yes	ORFeome
T13A10.11	yes	ORFeome
T12G3.4	yes	ORFeome
C06E7.3	yes	ORFeome
Y37E11B.5	yes	ORFeome
F01D4.2	yes	ORFeome
C50F7.10	yes	ORFeome
R09E10.3	yes	ORFeome
C24F3.4	yes	ORFeome
C33H5.18	yes	ORFeome
ZK593.1	yes	ORFeome
C28D4.2	yes	ORFeome
K08C7.2	yes	ORFeome
F21D5.1	yes	ORFeome
F58H7.2	yes	ORFeome
K08C7.5	yes	ORFeome
B0218.1	yes	ORFeome
ZC416.6	yes	ORFeome
W03G1.7	yes	ORFeome
B0035.5	yes	ORFeome
T14G10.1	yes	ORFeome
C06G3.9	yes	ORFeome
F21D5.3	yes	ORFeome
F32B6.2	yes	ORFeome
F58F9.7	yes	ORFeome
F36H1.6	yes	ORFeome
F13H10.4	yes	ORFeome
T26C12.1	yes	ORFeome
ZK829.2	yes	ORFeome
F15E6.6	yes	ORFeome
Y54E5A.1	yes	ORFeome
K11C4.4	yes	ORFeome
Y37E11C.1	yes	ORFeome
T16G1.10	yes	ORFeome

ORF name	In Metabolic RNAi Library?	Clone source
F45F2.9	yes	ORFeome
W02G9.1	yes	ORFeome
T20B3.7	yes	ORFeome
Y105E8B.5	yes	ORFeome
T01G6.10	yes	ORFeome
F44C4.5	yes	ORFeome
D1054.1	yes	ORFeome
Y105E8A.4	yes	ORFeome
K08B12.3	yes	ORFeome
C55A6.5	yes	ORFeome
F20G2.1	yes	ORFeome
F43H9.1	yes	ORFeome
C55A6.7	yes	ORFeome
C55A6.6	yes	ORFeome
C55A6.4	yes	ORFeome
F20G2.2	yes	ORFeome
R05D8.7	yes	ORFeome
D1054.8	yes	ORFeome
T05H4.4	yes	ORFeome
W03F9.9	yes	ORFeome
K07C5.2	yes	ORFeome
F26D2.15	yes	ORFeome
F25D1.5	yes	ORFeome
R05D8.9	yes	ORFeome
R08H2.1	yes	ORFeome
T01G6.1	yes	ORFeome
F11A5.12	yes	ORFeome
F59E11.2	yes	ORFeome
T05H4.5	yes	ORFeome
C06B3.4	yes	ORFeome
W02F12.2	yes	ORFeome
Y73C8B.1	yes	ORFeome
F22F7.6	yes	ORFeome
C47A10.5	yes	ORFeome
K12B6.3	yes	ORFeome
F59A7.9	yes	ORFeome
F10D2.9	yes	ORFeome
C50B8.3	yes	ORFeome
K07B1.4	yes	ORFeome
Y46H3D.6	yes	ORFeome
T05H4.1	yes	ORFeome
C53A3.2	yes	ORFeome
ZK262.3	yes	ORFeome
W01A11.2	yes	ORFeome
F22F7.5	yes	ORFeome
C37H5.2	yes	ORFeome
F46B6.8	yes	ORFeome
Y44A6D.5	yes	ORFeome
ZK6.7	yes	ORFeome
F49H6.5	yes	ORFeome
W06H8.2	yes	ORFeome
C12D8.5	yes	ORFeome
AC3.8	yes	ORFeome
T19H12.9	yes	ORFeome
F17C11.7	yes	ORFeome
T19H12.1	yes	ORFeome
K07B1.2	yes	ORFeome
C04F5.7	yes	ORFeome
D1054.13	yes	ORFeome

ORF name	In Metabolic RNAi Library?	Clone source
H23N18.3	yes	ORFeome
T03D3.1	yes	ORFeome
H23N18.2	yes	ORFeome
C24G6.6	yes	ORFeome
F39G3.1	yes	ORFeome
T19H12.10	yes	ORFeome
F29F11.1	yes	ORFeome
AC3.7	yes	ORFeome
F10D2.11	yes	ORFeome
ZC443.6	yes	ORFeome
M04G12.3	yes	ORFeome
C44H9.1	yes	ORFeome
T01G5.2	yes	ORFeome
F25G6.6	yes	ORFeome
R03H4.1	yes	ORFeome
ZC376.2	yes	ORFeome
B0238.1	yes	ORFeome
K11G9.2	yes	ORFeome
W02H5.8	yes	ORFeome
C50H11.1	yes	ORFeome
H23N18.1	yes	ORFeome
Y39H10A.2	yes	ORFeome
F08F3.2	yes	ORFeome
F10D2.6	yes	ORFeome
R03H4.6	yes	ORFeome
F43H9.2	yes	ORFeome
B0222.4	yes	ORFeome
F52F10.4	yes	ORFeome
T03D8.6	yes	ORFeome
Y105E8B.9	yes	ORFeome
T02B5.1	yes	ORFeome
F54F3.4	yes	ORFeome
Y105E8A.10	yes	ORFeome
C13C4.4	yes	ORFeome
R05D8.8	yes	ORFeome
R09B5.6	yes	ORFeome
Y73C8B.3	yes	ORFeome
Y60A3A.7	yes	ORFeome
C45B11.3	yes	ORFeome
F28H7.3	yes	ORFeome
C10F3.2	yes	ORFeome
K07B1.5	yes	ORFeome
C01G10.7	yes	ORFeome
K04A8.5	yes	ORFeome
T11F9.11	yes	ORFeome
F32D1.5	yes	ORFeome
F59A1.10	yes	ORFeome
R04B5.6	yes	ORFeome
ZK287.7	yes	ORFeome
F53F4.5	yes	ORFeome
R11G11.14	yes	ORFeome
F20D6.11	yes	ORFeome
K08H10.4	yes	ORFeome
C03A7.11	yes	ORFeome
F28F8.2	yes	ORFeome
W05E10.4	yes	ORFeome
T08B1.3	yes	ORFeome
H24K24.5	yes	ORFeome
W01A11.1	yes	ORFeome

ORF name	In Metabolic RNAi Library?	Clone source
F25B4.6	yes	ORFeome
R07B7.11	yes	ORFeome
ZC455.4	yes	ORFeome
C52A10.1	yes	ORFeome
F11A3.1	yes	ORFeome
F09F3.5	yes	ORFeome
ZC455.6	yes	ORFeome
F52F10.3	yes	ORFeome
W01A11.5	yes	ORFeome
AH10.1	yes	ORFeome
K07C11.4	yes	ORFeome
C50B6.7	yes	ORFeome
C52E4.5	yes	ORFeome
T08B1.6	yes	ORFeome
F25C8.4	yes	ORFeome
F09F3.9	yes	ORFeome
Y76A2B.3	yes	ORFeome
W03F9.4	yes	ORFeome
C29F3.1	yes	ORFeome
D2023.2	yes	ORFeome
PAR2.4	yes	ORFeome
C50F4.2	yes	ORFeome
B0365.1	yes	ORFeome
F45E1.4	yes	ORFeome
C31A11.5	yes	ORFeome
K09H11.1	yes	ORFeome
F58H1.1	yes	ORFeome
C39D10.3	yes	ORFeome
W06B3.1	yes	ORFeome
F27D9.6	yes	ORFeome
B0272.4	yes	ORFeome
F42F12.3	yes	ORFeome
F59F4.4	yes	ORFeome
F46H5.8	yes	ORFeome
F35C8.5	yes	ORFeome
F02C12.2	yes	ORFeome
C03F11.2	yes	ORFeome
F46G10.4	yes	ORFeome
T27A10.3	yes	ORFeome
ZC8.1	yes	ORFeome
C44C1.5	yes	ORFeome
F16F9.4	yes	ORFeome
R04B3.2	yes	ORFeome
Y41G9A.3	yes	ORFeome
F45E6.4	yes	ORFeome
K05B2.4	yes	ORFeome
C23H4.2	yes	ORFeome
T20F7.7	yes	ORFeome
F28H6.3	yes	ORFeome
C55B6.1	yes	ORFeome
F52H2.6	yes	ORFeome
Y71H10A.2	yes	ORFeome
F15A2.2	yes	ORFeome
F55F3.2	yes	ORFeome
B0310.5	yes	ORFeome
C03B1.7	yes	ORFeome
C44C1.2	yes	ORFeome
F56F10.3	yes	ORFeome
C29F7.3	yes	ORFeome

ORF name	In Metabolic RNAi Library?	Clone source
F09E10.3	yes	ORFeome
K07E3.3	yes	ORFeome
C37E2.1	yes	ORFeome
F46H5.3	yes	ORFeome
T08G2.3	yes	ORFeome
F08C6.4	yes	ORFeome
F53B1.4	yes	ORFeome
C01C10.3	yes	ORFeome
F42D1.2	yes	ORFeome
ZK455.4	yes	ORFeome
C49F5.1	yes	ORFeome
K10C2.4	yes	ORFeome
T25G12.5	yes	ORFeome
C54D1.4	yes	ORFeome
Y70D2A.2	yes	ORFeome
Y71H10B.1	yes	ORFeome
F01E11.1	yes	ORFeome
C54G7.2	yes	ORFeome
Y7A5A.1	yes	ORFeome
H13N06.4	yes	ORFeome
M02D8.4	yes	ORFeome
C17G1.3	yes	ORFeome
ZC506.3	yes	ORFeome
T03G6.3	yes	ORFeome
T24C12.3	yes	ORFeome
R07E4.4	yes	ORFeome
K03A1.5	yes	ORFeome
ZC506.1	yes	ORFeome
F15A8.6	yes	ORFeome
C46F4.2	yes	ORFeome
T14F9.3	yes	ORFeome
F47B10.2	yes	ORFeome
C42D8.3	yes	ORFeome
C52B9.9	yes	ORFeome
F49E10.2	yes	ORFeome
D1009.1	yes	ORFeome
F09B9.1	yes	ORFeome
F59F4.1	yes	ORFeome
ZK455.1	yes	ORFeome
D1005.1	yes	ORFeome
F39B1.1	yes	ORFeome
C33G3.4	yes	ORFeome
K09C8.5	yes	ORFeome
T26A5.7	yes	ORFeome
F42G8.6	yes	ORFeome
C02C2.5	yes	ORFeome
ZK637.9	yes	ORFeome
K02A4.1	yes	ORFeome
C29E4.8	yes	ORFeome
T24D1.4	yes	ORFeome
Y42G9A.4	yes	ORFeome
ZK484.6	yes	ORFeome
C32F10.8	yes	ORFeome
C26D10.3	yes	ORFeome
F30F8.2	yes	ORFeome
C49D10.4	yes	ORFeome
K10H10.6	yes	ORFeome
F55A12.3	yes	ORFeome
Y94H6A.4	yes	ORFeome

ORF name	In Metabolic RNAi Library?	Clone source
C17C3.12	yes	ORFeome
F11G11.9	yes	ORFeome
Y76B12C.6	yes	ORFeome
K04A8.10	yes	ORFeome
B0238.13	yes	ORFeome
F36G9.12	yes	ORFeome
F55C5.6	yes	ORFeome
T05H4.13	yes	ORFeome
ZC443.1	yes	ORFeome
F55A11.5	yes	ORFeome
ZC455.5	yes	ORFeome
C46C11.1	yes	ORFeome
C56G3.2	yes	ORFeome
C52B9.1	yes	ORFeome
R03G5.5	yes	ORFeome
C34F6.4	yes	ORFeome
B0285.5	yes	ORFeome
T07C4.4	yes	ORFeome
F21F3.1	yes	ORFeome
K07C5.7	yes	ORFeome
C10G11.5	yes	ORFeome
T24D1.1	yes	ORFeome
T08B2.7	yes	ORFeome
K10H10.3	yes	ORFeome
F12A10.3	yes	ORFeome
T02G5.4	yes	ORFeome
Y51H4A.7	yes	ORFeome
E04A4.4	yes	ORFeome
F13H10.4	yes	ORFeome
F55C5.2	yes	ORFeome
F10C2.5	yes	ORFeome
C14C11.3	yes	ORFeome
F35B12.2	yes	ORFeome
F13H6.4	yes	ORFeome
C03A3.3	yes	ORFeome
B0250.5	yes	Ahringer
C02B10.1	yes	Ahringer
C05C10.3	yes	Ahringer
C05D11.11	yes	Ahringer
C08B6.1	yes	Ahringer
C28C12.9	yes	Ahringer
D2063.1	yes	Ahringer
E04F6.5	yes	Ahringer
F08A8.1	yes	Ahringer
F08A8.3	yes	Ahringer
F08A8.4	yes	Ahringer
F08F3.4	yes	Ahringer
F08F8.2	yes	Ahringer
F09F7.4	yes	Ahringer
F11E6.5	yes	Ahringer
F18E3.7	yes	Ahringer
F22B8.6	yes	Ahringer
F23B12.5	yes	Ahringer
F25B4.1	yes	Ahringer
F29G9.6	yes	Ahringer
F41H10.7	yes	Ahringer
F42A8.2	yes	Ahringer
F45H10.1	yes	Ahringer
F46E10.10	yes	Ahringer

ORF name	In Metabolic RNAi Library?	Clone source
F47B10.1	yes	Ahringer
F53F1.3	yes	Ahringer
F54A3.4	yes	Ahringer
F54D8.3	yes	Ahringer
F56D1.5	yes	Ahringer
F56D12.1	yes	Ahringer
F59B8.2	yes	Ahringer
H14A12.2	yes	Ahringer
K04F1.15	yes	Ahringer
K06A5.6	yes	Ahringer
K10H10.2	yes	Ahringer
K12G11.4	yes	Ahringer
R05D8.10	yes	Ahringer
T15B7.2	yes	Ahringer
T25G12.7	yes	Ahringer
W06D12.3	yes	Ahringer
Y32H12A.3	yes	Ahringer
Y69F12A.2	yes	Ahringer
Y6B3B.11	yes	Ahringer

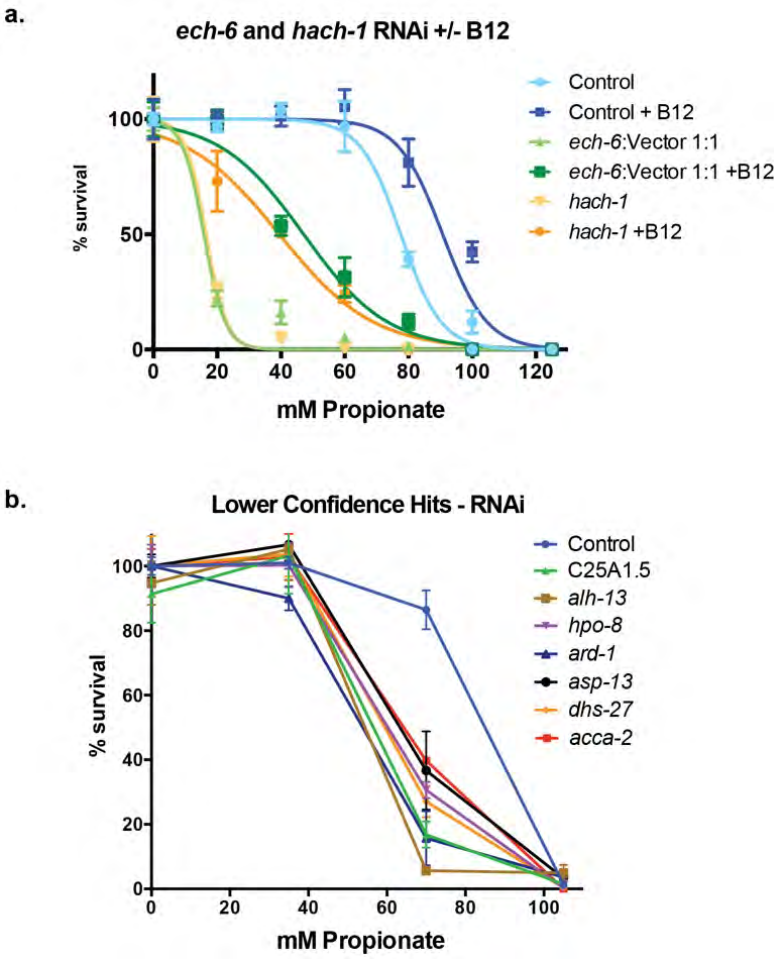

Figure 4.4 – Validation of hits from screen.

a, *ech-6* and *hach-1* knockdown in wild type animals results in sensitivity to propionate-induced toxicity compared to the control (vector alone) treatment. B12 supplementation partially rescues these phenotypes. Toxicity assays were performed with the respective gene-targeting dsRNA-expressing *E. coli* HT115 clone in the presence of 1mM IPTG to induce dsRNA expression. Animals used in this assay had been exposed to respective dsRNA-expressing clones for one generation prior. To obtain enough viable animals to perform the assay, the *ech-6* targeting dsRNA-expressing clone was diluted 1:1 with the vector control clone to reduce knockdown efficiency, reducing the severely detrimental effects of loss of *ech-6*. **b,** Lower confidence hits from the screen reduced propionate tolerance when knocked down in wild type animals. However, these hits did not result in synthetic lethality with the *pcca-1* mutant in the presence of 30mM propionate in every retest (see **Table 4.3**).

Gene	Retest Positives (out of 3)	General sensitivity to Propionate?	Confidence level
acdh-1	3	Yes	High
ech-6	3	Yes	High
F09F7.4	3	Yes	High
C25A1.5	1	Yes	Medium
acca-2	1	Yes	Medium
alh-13	0	Yes	Low
hpo-8	0	Yes	Low
ard-1	0	Yes	Low
asp-13	0	Yes	Low
dhs-27	0	Yes	Low

Table 4.3 – All hits from RNAi screen
Confidence levels are indicated.

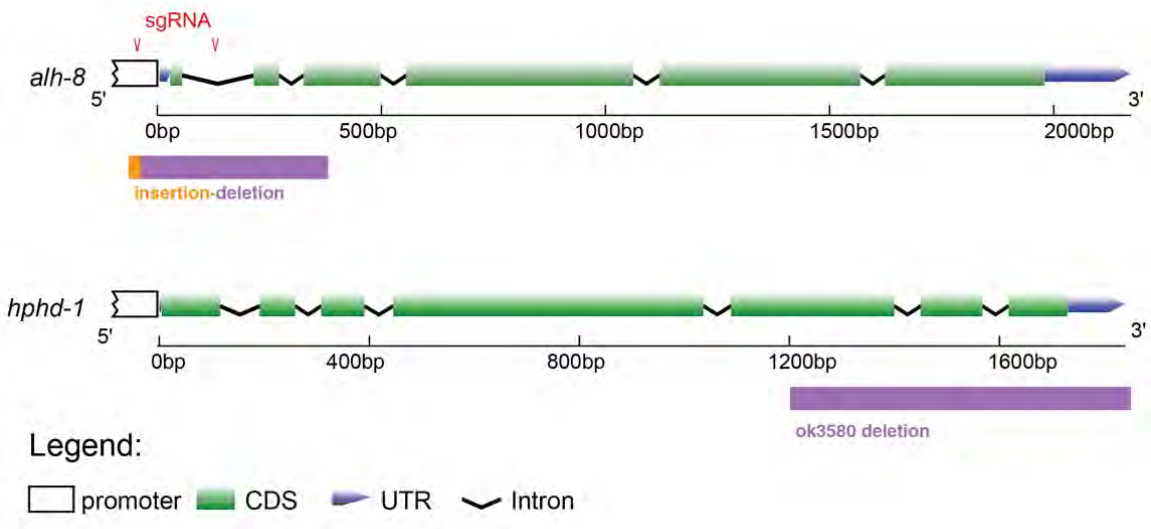

Figure 4.5 – Structure of Δ*hphd-1* mutant and CRISPR/Cas9-generated Δ*alh-8* mutant. Diagram of the mutation generated by CRISPR/Cas9-mediated genome editing using an sgRNA (red sequence) targeting *alh-8*. The mutation consists of a 23 bp indel and 399 bp deletion, and removes part of the 5'UTR, the start codon, the first and second exons, and part of the third exon. Also shown is the Δ*hphd-1* mutation.

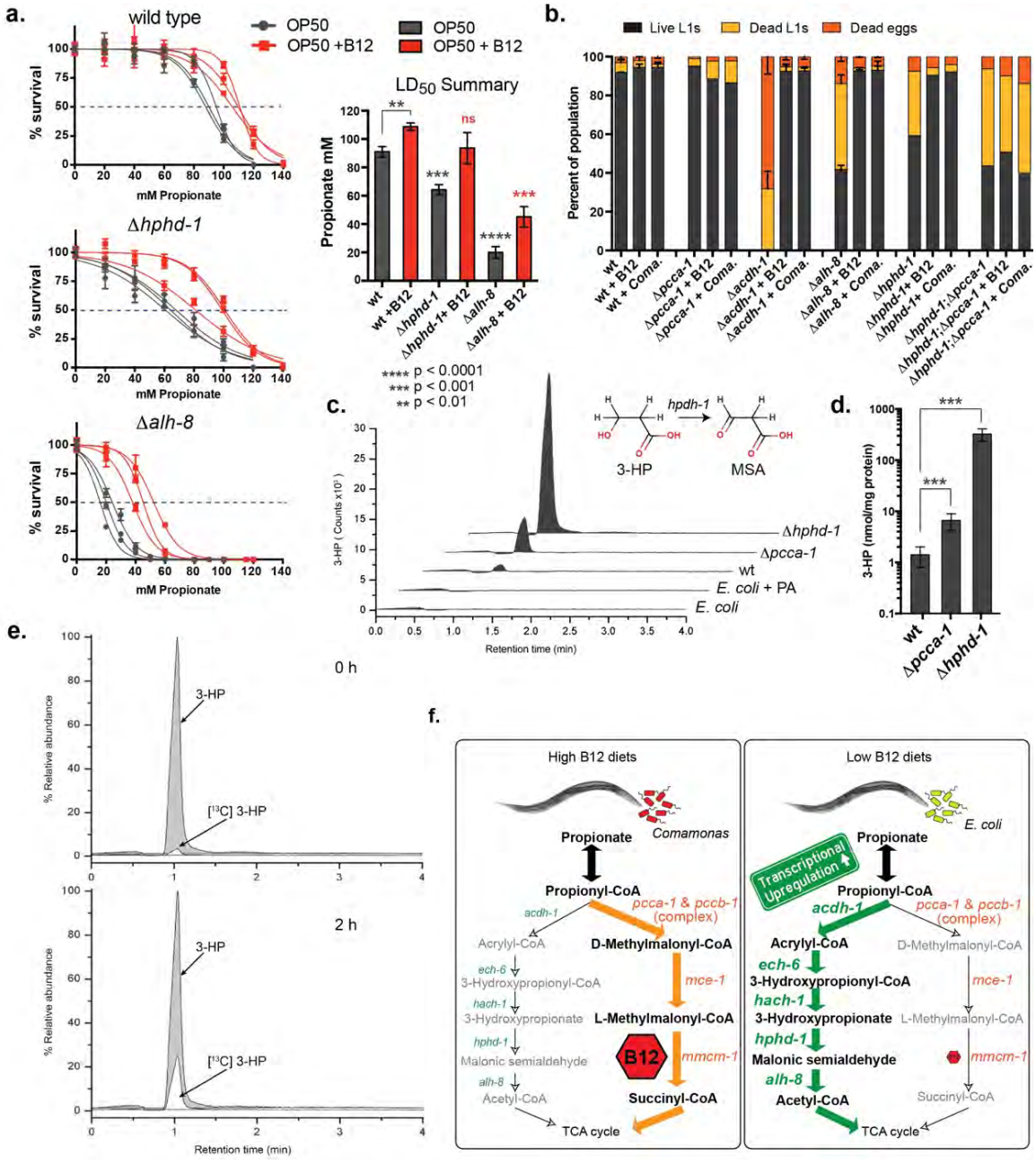

Figure 4.6 – Perturbation of predicted propionate breakdown shunt genes confers propionate-sensitivity phenotypes and result in buildup of 3-HP, a unique pathway intermediate.

a, Δ*hphd-1* and Δ*alh-8* mutants exhibit sensitivity to propionate in toxicity assays compared to wild type animals. B12 increases propionate tolerance in both mutants, but does not completely rescue the sensitivity phenotype of *alh-8* mutant. Three biological replicate curves are shown on the left, with average LD_{50}'s +/- standard deviation on the right. Unpaired student's T tests were used

to calculate p values. Black asterisks indicate significant difference compared to wild type, red asterisks indicate significant difference compared to wild type + B12. **b,** Δ*hphd-1* and Δ*alh-8* mutants exhibit partial lethality on low-B12 conditions. Animals were fed for one generation on *E. coli* OP50 supplemented with 60nM B12, then grown for one generation on the indicated diet. Offspring were harvested and live and dead L1s and embryos were quantified following an overnight arrest. Δ*acdh-1*, Δ*hphd-1* and Δ*alh-8* mutant phenotypes were rescued by 60nM B12 supplementation or by the B12-producing bacteria *Comamonas aquatic* DA1877. The partial lethal phenotype of the double mutant Δ*hphd-1*;Δ*pcca-1* was not rescued by B12. Error bars depict standard error of the mean (SEM) from three biological replicates. **c,** 3-HP detection by liquid chromatography – the 3-HP chromatogram (Q1/Q3: 91->73 m/z) corresponds to a 3-HP concentration of 11.6, 59.8 and 302.5 picomoles/mg protein for wild type, *Δpcca-1* and *Δhphd-1*, respectively. 3-HP was not present, or below the detection limit, of a selective reaction monitoring (LC-SRM) analysis of concentrated metabolite extract harvested from an *E. coli* pellet derived from 3L of saturated culture. **d,** Average 3-HP quantities normalized to total protein levels from four biological replicates, +/- SEM. Asterisks indicate p values < 0.001. Animals were grown in liquid culture seeded with *E. coli* OP50. **e,** ^{13}C-labeled propionate fed to Δ*hphd-1* mutant animals for 2 hours results in ^{13}C-labeled labeled 3-HP, indicating that *C. elegans* oxidizes propionate to 3-HP. Shown are SRM (MS^2) chromatograms specific for 3-HP. The peak corrsesponding to the natural ^{13}C isotope distribution (~ 1.1% of ^{12}C signal) is illustrated for comparison in t=0. **f**, Model describing two-pathway solution for propionate breakdown in *C. elegans*. When B12 is available from the diet, *C. elegans* engages the canonical, B12-dependent pathway and represses expression of genes in the oxidation shunt. On low-B12 diets such as *E. coli* and other bacteria that do not synthesize the vitamin, the oxidation shunt genes are transcriptionally upregulated and this pathway is relied upon for survival.

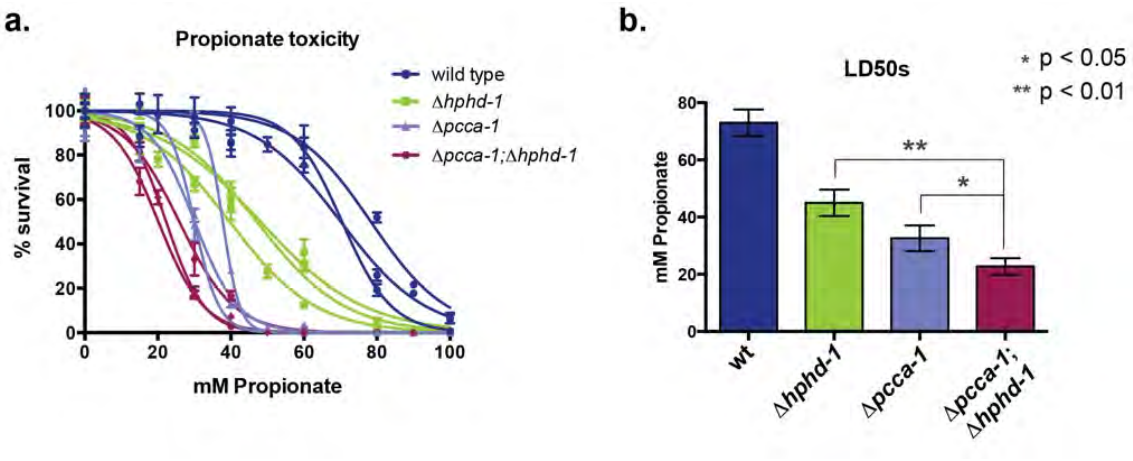

Figure 4.7 – The double mutant Δ*pcca-1*;Δ*hphd-1* is more sensitive to propionate.
a, Propionate toxicity assays were performed in biological triplicate for wild type, Δ*pcca-1*, Δ*hphd-1*, and a Δ*pcca-1*; Δ*hphd-1* double mutant. **b,** Summary of propionate LD50's indicate that the double mutant Δ*hphd-1*;Δ*pcca-1* is more sensitive to propionate-induced toxicity compared to either the Δ*pcca-1* or Δ*hphd-1* single mutant. Average LD50s derived from three biological replicates are shown +/- standard deviation. Unpaired student's T tests were used to calculate p values.

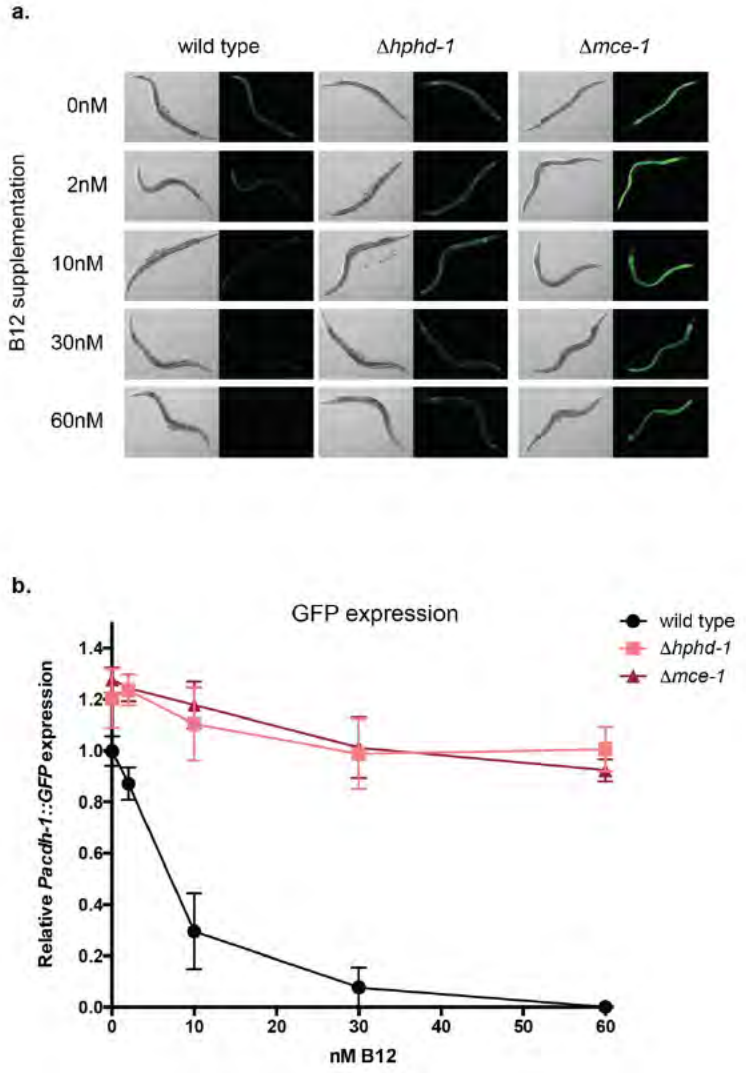

Figure 4.8 – Δ*hphd-1* mutation results in increased *acdh-1* promoter activity.

a, Δ*hphd-1* and Δ*mce-1* mutations result in increased expression of the *Pacdh-1::GFP* transgene despite the addition of B12. Representative DIC and corresponding GFP images of *C. elegans* grown on *E. coli* OP50 supplemented with the indicated dose of B12. *mce-1* encodes the second enzyme of the canonical propionate breakdown pathway. **b,** Quantification of GFP in Δ*hphd-1;Pacdh-1::GFP* and Δ*mce-1;Pacdh-1::GFP* animals across a range of doses of B12 using the program IPPOME (Mori et al, in preparation) and a minimum pixel intensity cutoff value of 25. The number of GFP-positive pixels is normalized to body size, and the average GFP/area score of wild type *Pacdh-1::GFP* animals with no B12 was set to equal one. Each data point represents the average relative GFP score of 5-6 animals, +/- standard deviation.

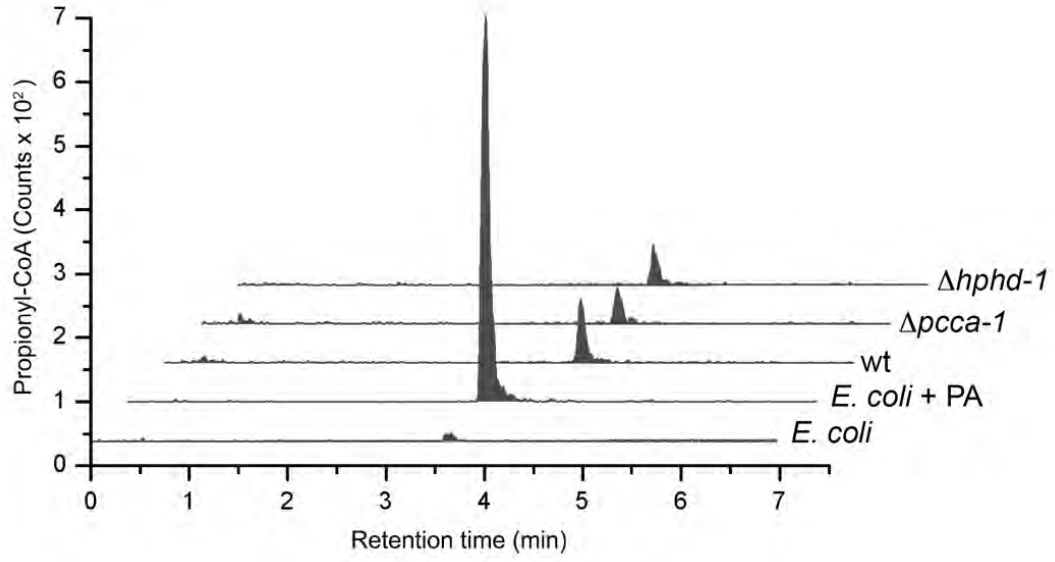

Figure 4.9 – Propionyl-CoA measurements in *E. coli* and *C. elegans.*

a, Despite the lack of 3-HP, we were readily able to measure propionyl-CoA in *E. coli*, suggesting the lack of 3-HP detection is not simply due to a lack of pathway substrate. The propionyl-CoA chromatogram correspond to 15.9, 2, 1.4 and 1.3 picomoles/mg protein for *E. coli*+PA, wild type, *Δpcca-1* and *Δhphd-1*, respectively.

	KEGG homologies with *C. albicans* genes										
	C. elegans	***H. sapiens***	***C. albicans***		***H. sapiens***	SW Score		***C. elegans***	SW Score		
Propionyl-CoA to Acrylyl-CoA	*acdh-1*	*acadsb*	*pox1-3*	fatty-acyl coenzyme A oxidase	*acox1*	994	acyl-CoA oxidase 1, palmitoyl	F59F4.1	985	acyl-CoA oxidase	
		acads	*pxp2*	no result							
			acd99	probable acyl-CoA dehydrogenase	*acad10*	1076	acyl-CoA dehydrogenase family, member 10	K09H11.1	1011	acyl-CoA dehydrogenase family member 10	
Acrylyl-CoA to 3-Hydroxypropionyl-CoA	ech-6	*echs-1*	*fox2*	peroxisomal trifunctional hydratase-dehydrogenase-epimerase	*hsd17b4*	1253	hydroxysteroid (17-beta) dehydrogenase 4	*dhs-28*	914	short chain dehydrogenase	
3-Hydroxypropionyl-CoA to 3-hydroxypropionate	F09F7.4a	*hibch*	*ehd3*	3-hydroxyisobutyryl-CoA hydrolase	*hibch*	763	3-hydroxyisobutyryl-CoA hydrolase	F09F7.4a	756		
3-hydroxypropionate to Malonate Semialdehyde	Y38F1A.6	*adhfe1*	*hpd1*	putative 3-hydroxyisobutyrate dehydrogenase	*hibadh*	514	3-hydroxyisobutyrate dehydrogenase	B0250.5	508	3-hydroxyisobutyrate dehydrogenase	
Malonate Semialdehyde to Acetyl-CoA	*alh-8*	*aldh6a1*	*ald5/ald99*	aldehyde dehydrogenase	*aldh1b1*	1557	aldehyde dehydrogenase 1 family, member B	*alh-2*	1626	aldehyde dehydrogenase	
			ald6	malonate-semialdehyde dehydrogenase	*aldh6a1*	1785	aldehyde dehydrogenase 6 family, member A1	*alh-2*	670		

Table 4.4 – Comparison of *C. albicans* propionate oxidation genes and *C. elegans* genes proposed to form propionate shunt, with human orthologs.

	genotyping primers	
gene	Forward	Reverse
acdh-1	CTTCCAGCTAATGGGTGTTCATGTTCC	CGCCATTGCAGCTTCTCGTAC
ech-6	-	-
hach-1	-	-
hphd-1	TCGACACGACGAAGGCTG	AAGCCGGCAATATTTAAACG
alh-8	TTCAATGTTCGCGTGTATTTTG	TCAGCGAGCTTCTTCATGT
pcca-1	GGGGCAACAAAACAGGGTGGTG	CGAGCTTGAGAAGGCTGGAGC

	qPCR primers	
gene	Forward	Reverse
acdh-1	GCAAATGCAGATCCTAGCC	GTTTGTCTTCCTCCTTATCTACAG
ech-6	TCGGAGCAATTGTGATTACTG	CGAACTCGTTATTGGTCATCTC
hach-1	CACAATGGAGTATCGTCTCAC	TTGTCAACGAGAATGGCTC
hphd-1	GATATTCCGAACAATGCCAG	TCCAAAGTCTCGCATATAACC
alh-8	TTTGAGAATGGAAACTTCGTGG	GAAGATTTCTTCTCTGTAGCAAGTC
pcca-1	-	-

Table 4.5 – Genotyping and qPCR primers

Experimental Procedures

C. elegans strains.

N2 (Bristol) was used as the wild type strain, and animals were maintained as described (Brenner, 1974). Δ*pcca-1*(ok2282), Δ*acdh-1*(ok1489), Δ*mce-1*(ok243) and Δ*hphd-1*(ok3580) strains were provided by the *C. elegans* Gene Knockout Consortium and were backcrossed 3 times against N2 prior to assays. The Δ*hphd-1*(ok3580) allele was genotyped and sequenced using the primers CTCTGTAATGACAACCGCAGTGGC and CGTAAGGGACTTCTCGTACAGAGTGC. This allele removes only part of the C terminus of the protein and may not be a complete loss-of-function mutation. For a diagram of deletion mutant loci, see **Figure 4.5** and for a full list of genotyping primers refer to **Table 4.5**.

Propionate toxicity assays.

Approximated 100 synchronized L1s (hatched overnight, 20hr post-bleach) were added to *E. coli* OP50-seeded 35mM NGM (bactopeptone) agar plates containing various concentrations of pH-neutralized propionic acid. Each dose tested included 4 technical replicates. After 72 hours, un-arrested survivors (animals that had developed past L1 stage) were counted. Dose response curves were fit to the raw data using the following equation:

Y=Bottom + (Top-Bottom)/(1+10^((LogLD50-X)*HillSlope))

The dose required to kill 50% of the population (LD50) was calculated according to the fitted dose response curves. Toxicity assays were performed in biological

triplicate, and the average LD50's are plotted +/- SEM. To obtain enough viable Δ*acdh-1* mutant animals for these assays, 64nM B12 was supplemented to animals two generations prior to assay.

RNAi screen with metabolic library.

A list of metabolic enzyme domain-containing genes was manually curated based on KEGG and WormBase databases, and available metabolic gene-targeting clones in the ORFeome RNAi library were re-arrayed in 96 well format. See **Table 4.2** for these gene lists. RNAi experiments were performed as follows: 24-well NGM (bactopeptone) agar plates containing 1mM IPTG and 1mM Ampicillin were seeded with one dsRNA-expressing *E. coli* HT115 clone per well the night before use. A separate set of plates containing 30mM pH-neutralized propionate was also prepared and seeded with the same HT115 clones. The HT115 cultures were prepared by seeding 1 mL fresh LB + Ampicillin with 50 uL overnight culture, growing at 37^{o}C for 6 hours, then centrifuged and resuspended in 150 uL LB + Ampicillin. 30 uL of this resuspended culture was placed in the center of NGM wells in the 24-well plates. Wild type and Δ*pcca-1* mutants were cultivated on *E. coli* OP50, and eggs were harvested by bleaching, and hatched overnight in M9 media (20 hours), and synchronized L1s were added to prepared plates. Animals were observed after 3 days to observe effects in the 1st generation, and after 6 days to observe lethality in the 2nd generation.

qPCR experiments

Animals were synchronized by L1 arrest and grown on plates containing bactopeptone and various doses of B12 and/or propionate, seeded with *E. coli* OP50. Approximately 1500 adult animals were harvested for each condition, in biological duplicate. Animals were washed in M9 buffer, and total RNA was isolated using Trizol (Invitrogen) followed by DNAseI treatment and cleanup using Qiagen RNeasy columns. cDNA was prepared from RNA using oligo-dT and Mu-MLV enzyme (NEB). Primer sequences for quantitative RT-PCR (qRT-PCR) were generated using the GETprime database [97] and are listed in **Table 4.5**. qPCR was performed in technical triplicate per gene per condition using the Applied Biosystems StepOnePlus Real-Time PCR system and Fast Sybr Green Master Mix (Invitrogen). Relative transcript abundance was determined using the ΔΔCt method [160], and normalized to averaged *ama-1* and *act-1* mRNA expression levels.

C. elegans liquid culture.

Synchronized animals were cultivated on 15cm NGM plates seeded with *E. coli* OP50, and bleached after 3 days. Bleached eggs were washed 3 times in M9, then allowed to hatch for 20 hrs. 1 million synchronized L1s were added to 400 mL liquid NGM in a 2L Erlenmeyer flask, containing concentrated *E. coli* OP50 bacteria from 500mL overnight LB culture, and total volume was adjusted to 450 mL with M9. Some flasks contained 20mM pH-neutralized propionic acid. Flasks were kept at 20C, shaking gently at 100rpm. Each day concentrated bacteria were added to the flasks to feed the worms. Adult animals were

collected (after 3 days of development for N2, and 4 days for the mutants) and washed 2 times in M9 in sterile Imhoff settling cones. The final pellet was flash-frozen and stored at -80^{o}C until extraction.

C. elegans metabolite extraction.

Cell extracts were obtained by re-suspending the frozen *C. elegans* or bacterial pellets in 4 mL of 5% trichloroacetic acid (TCA). Cell suspensions were homogenized in a Polytron PT 1300 for 2 min at 20,000 rpm and neutralized with 1 mL of 2M of potassium monoacid phosphate. The samples were centrifuged at high speed for 10 min at 4^{o}C and immediately injected for propionyl-CoA determination. The pellets were stored for protein quantification using the bicinchoninic acid method (Thermo Scientific Pierce Protein BCA Kit). For 3-HP measurements, the cell extract was desiccated in a Speedvac and the resulting pellet was resuspended in the same volume of methanol. Then, the samples were centrifuged at high speed for 10 min at 4^{o}C. For *E.coli* metabolite extraction, the cell extracts were obtained as mentioned above except that bacteria cells were disrupted by sonication for 2 min using intervals of 15 seconds of sonication followed by 15 seconds for cooling.

LC-MS/MS Quantification

The quantification of metabolites was performed using a LC-MS/MS system consisting of an ultra-high pressure LC system (Agilent 1290) online coupled to a Triple Quadrupole mass spectrometer equipped with an

electrospray ionization source (Agilent 6460). Propionyl-CoA was separated using a column Zorbax Eclipse Plus C18 Rapid Resolution HD 2.1x50 mm 1.8 Micron (Agilent) at 30 C. The mobile phase was composed of Buffer A: 10 mM tributylamine, 15 mM acetic acid and 5% methanol; and Buffer B: 100% methanol. The flow rate was 0.5 mL/min and the gradient method consisted of: 0-0.25 min, 2.5 %B; 0.25-0.5 min, 2.5-30 %B; 0.5-5 min, 30-70%B; 5-5.25 min, 70-100% B; 5.25-6.25 min, 100% B; 6.25-7 min, 2.5 %B; 7-8 min 2.5% B. The 3-hydroxypropanoic acid was separated using a column Zorbax Eclipse Plus C18 Rapid Resolution HD 2.1x100 mm 1.8 Micron (Agilent) at 30 C. The mobile phase was composed of Buffer A: 0.1% formic acid in water; and Buffer B: 100% methanol. The flow rate was 0.35 mL/min and the gradient consisted of: 0-3 min, 5 %B; 3-4 min, 5-70 %B; 4-5.25 min, 70%B; 5.25-5.5 min, 70-100% B; 5.5-6.5 min, 100% B; 6.5-7 min, 5 %B; 7-7.5 min 5% B. Q1/Q3 (MRM) transitions, ion source and collision energy settings were optimized according to the metabolites and were: 91->73, 25 eV; 824.2->317.1, 25 eV; and 92->74, 25 eV (in positive mode), for 3-HP, propionyl-CoA and ^{13}C labeled 3-HP, respectively . Ion source settings were as follows: gas temperature, 300 C: gas flow, 8L/min; nebulizer 50 psi (Nitrogen); sheath gas temperature, 200 C: sheath gas flow, 11 L/min, capillary 3500 V and nozzle voltage, 500 V.

CRISPR/Cas9 genome editing

The *alh-8* mutant was generated by dual sgRNA directed-deletion [161]. We used a co-CRISPR strategy, which includes *unc-22* as a CRISPR marker to

enhance detection of genome-editing events [154]. The target sequences were manually derived to conform to the sequence N19NGG near the 5' end of *alh-8*. Two target sequences were chosen: CCGCCCATCTCTTGTGATTTTC and CTGTGCGACAGTTGTCGTATGG. We designed forward and reverse oligomers containing the N19 sequence and ends of BsaI recognition sites. The forward and reverse oilgomers were annealed and ligated to BsaI-digested pRB1017 vector [162]. The *alh-8* sgRNA plasmids were prepared using a PureLink Quick Plasmid Miniprep Kit (Invitrogen). The other coinjected DNA vectors were purified using a Qiagen midiprep kit. The DNA mixture used in microinjection contained *Peft-3::Cas9* vector, *pRF4::rol-6(su1006)*, *unc-22* sgRNA vector (all gifts from the Mello lab) and two *alh-8* sgRNA vectors, each with a concentration of 40 ng/µl. Approximately 20 young adult hermaphrodite worms were injected. After recovering from injection, each worm was placed onto an individual *E. coli* OP50 plate. After 2-3 days, the F1 rollers (dominant phenotype indicating presence of the *pRF4::rol-6(su1006)* construct) were picked onto new plates. F1s with twitcher F2s were genotyped by PCR for mutations in *alh-8*. The PCR primers are outside of the sgRNA-targeted region. Forward primer: TTCAATGTTCGCGTGTATTTTG; Reverse primer: TCAGCGAGCTTCTTCATGT. The amplicons with smaller size than wild type amplicons were reconfirmed by sequencing. Forward primer: ATTCGAAACGTGATCAGTAATG; Reverse primer: CTCTCTTGATCAAGGCTTGA. A mutant animal with a ~400bp deletion (23 bp

indel and 399 bp deletion) was chosen for further analysis, and was outcrossed with N2 three times before use in phenotypic assays.

Network Analysis

The WISP tissue-specific functional networks were built using a semi-supervised regularized Bayesian approach that integrated 56,179 expression- and interaction-based measurements across 174 genome-level datasets [in preparation; http://wisp.princeton.edu]. Using the intestine network, we found genes that were tightly connected to *acdh-1*, *ech-6* and *hach-1* even after adjusting for average network connectivity, which improved the specificity of the retrieved genes to our seed genes.

CHAPTER V: CONCLUSIONS AND FUTURE DIRECTIONS

Preface

This conclusions chapter is partially adapted from a review written by myself, Safak Yilmaz, and Marian Walhout, to be published in the journal *Annual Review of Genetics* in 2015, titled, "Understanding Metabolic Regulation at a Systems Level: Metabolite Sensing, Mathematical Predictions, and Model Organisms." (Watson et al, in press)

Introduction

Most of what is known about the mammalian metabolic network comes from a century of enzymology research, in which enzyme activities were detected, functionally purified, and eventually genetically characterized. The current age of genomics has enabled the study of metazoan metabolism at a genome-wide, or systems-, level. Genome sequencing has revealed a predicted parts list of the metabolic network, and there are hundreds of enzyme-domain containing genes whose functions are yet to be determined. Transcriptomic and proteomic studies have revealed that metabolic networks exhibit great diversity between tissues, during proliferation versus senescence, and in health versus disease. This differential use of metabolic subnetworks or pathways is referred to as metabolic network rewiring. Today we are challenged with understanding

which metabolic pathways are employed in which tissues and under which conditions, and how control systems drive metabolic rewiring.

To explore metabolic network rewiring we must consider both the mechanisms and outputs of metabolic network regulation. Mechanistically, metabolic genes are extensively regulated at the levels of transcription [163], post-transcription [164-166], post-translation [167, 168] including allostery through direct interactions with metabolites [169-171], and subcellular localization [172, 173]. Further, the regulators are themselves regulated at multiple levels [174] and are connected to master endocrine signaling pathways that coordinate metabolism across tissues [175]. Understanding how metabolic network regulation affects global outputs (phenotypes) is another major challenge. Predictions about the output of metabolic network rewiring can be generated through stoichiometric metabolic network models, which are built by comprehensively annotating the collection of enzymes encoded by the genome and the reactions they are likely to catalyze. The power of this approach is that such models can provide nonintuitive metabolic and physiological hypotheses. An advantage of these models is that “omics” data can be integrated into the network model to investigate tissue- and condition-specific metabolic programs, such as metabolite and enzyme dependencies of cancer cells [176].

A complementary approach for exploring metabolic network function is to utilize forward and reverse genetics to identify the genes responsible for metabolic phenotypes or metabolic rewiring events *in vivo*. Metazoan model

organisms such as *Caenorhabditis elegans* offer a platform for high-throughput genetic screening to uncover novel functions and biological roles of metabolic enzymes, as well as the regulatory networks involved in metabolic network rewiring. *C. elegans* is particularly powerful because in addition to being genetically tractable itself, its bacterial diet can also be subjected to systematic mutagenesis.

We have taken advantage of this interspecies system to identify, in an unbiased fashion, the most important players in the orchestration of *C. elegans* metabolic states induced by different amounts of bacterially supplied vitamin B12. We serendipitously found an alternate metabolic shunt in *C. elegans* by studying these diet-responsive gene networks, which we believe is a target of metabolic rewiring induced by insufficient flux through the parallel (canonical) pathway. Our studies provide a blueprint for identifying other interspecies genetic interactions, which may dictate other metabolic or physiological states (**Figure 5.1**). This chapter will discuss the implications, unanswered questions, and future directions from the work presented in this thesis.

Metabolite Sensing and Transcriptional Regulation of Metabolic Enzymes

Many questions remain regarding the mechanisms behind the transcriptional regulation of *acdh-1* and other genes in response to vitamin B12 and propionate. Is vitamin B12 directly sensed to repress the *acdh-1* promoter, or is propionate (or some other derivative) the molecule that is sensed within the *acdh-1* regulatory system, or is it both? The fact that B12 fails to repress *acdh-1*

expression when the B12-dependent propionyl-CoA breakdown pathway is genetically inactivated [41], suggests that B12 alone is not sufficient to repress *acdh-1* under all conditions. If vitamin B12 is not sensed directly, its repressive effects occur entirely via enhancing flux through the canonical propionate breakdown pathway to reduce propionate/propionyl-CoA levels, thus lowering the activation signal. If vitamin B12 is sensed directly as part of the regulation of *acdh-1*, then sufficient levels of the propionate/propionyl-CoA activation signal can override the B12 repression signal. The latter system requires two sensing components, while the former system requires only one.

While there have been none discovered to date in animals, direct B12-binding riboswitches are prevalent in bacteria, where they regulate the translation of genes involved in B12 import and processing [177, 178]. The only mechanisms of cellular vitamin sensing that have been described in metazoans to date are the vitamin D and vitamin A sensing systems, both of which involve direct binding by a nuclear hormone receptor. Vitamin D, while technically a hormone rather than a vitamin given that it can be synthesized from cholesterol in the skin upon UV light exposure, regulates the uptake of calcium, iron, magnesium, and zinc [179]. This regulation occurs through Vitamin D receptor (VDR)-mediated transcriptional activation of the transporters of these micronutrients [180]. Vitamin A, a true vitamin derived from plant carotenoids that takes several forms, has a plethora of functions in diverse processes, including development, vision, and immunity [181]. Vitamin A does not function in anabolic

or catabolic processes as most other vitamins but rather serves as a light-sensing cofactor for rhodopsin and a signaling morphagen to regulate hox genes during development via retinoic acid receptor (RAR) binding [181]. There are enzymes that modify Vitamin A (retinol) to generate retinal (the form utilized by rhodopsin) and retinoic acid (the form that directly binds and activates RAR), as well as enzymes that degrade retinoic acid. Vitamin A metabolism is tightly regulated by positive and negative FBLs to maintain proper concentrations of the various forms of Vitamin A during development, given that dysregulation can lead to teratogenesis [182, 183]. For instance, the retinoic acid--degrading enzyme CYP26A1 is directly activated by RAR through binding of highly conserved retinoic acid response elements (RAREs) in its promoter [182]. Thus, retinoic acid activates its own degradation, preventing deleteriously high levels of retinoic acid from building up. Retinoic acid also represses the expression of the enzymes involved in its synthesis from retinol, although the mechanisms of this repression are unknown [182].

Less is known about the mechanisms employed by metazoan cells to sense other vitamins, if they do exist. However, gene expression studies in mammalian cells have revealed regulatory responses to vitamins B1 (thiamine) [184-186], B2 (riboflavin) [187], B3 (nicotinamide/niacin) [188-190], B6 (pyridoxal 5′ phosphate, PLP) [191, 192], B9 (folic acid) [193-195], C (ascorbic acid) [196-198], and E (tocopherol/tocotrienols) [199-201]. It will be interesting to know the mechanisms by which cells sense vitamin intake and regulate genes accordingly,

to determine whether vitamins are sensed directly or indirectly through monitoring flux through their dependent pathways, which we have shown may at least be part of the story with vitamin B12 sensing in *C. elegans*.

To understand whether *C. elegans* senses vitamin B12 intake directly, indirectly, or both, identification and interrogation of the metabolite-sensing components in the *acdh-1* regulatory system are required. We identified candidate metabolite-sensing system components in our genome-wide RNAi screen for effectors of *acdh-1* promoter activity [64]. Interestingly, two nuclear hormone receptors identified as *acdh-1* activators from the screen (*nhr-10* and *nhr-68*) were broadly required for the *acdh-1*-activating effect of canonical propionate breakdown pathway disruption [64]. In other words, when *nhr-10* or *nhr-68* was knocked down by RNAi, loss of *pcca-1, mce-1, and mmcm-1* all failed to activate *Pacdh-1::GFP* [64]. This suggests that *nhr-10* and/or *nhr-68* are involved in sensing propionate metabolism flux, which is dictated by vitamin B12 concentrations, and activating *acdh-1* accordingly. Since nuclear hormone receptors possess both DNA-binding and ligand-binding domains, they are excellent conduits through which small molecule signals can be transmitted to the genome to affect gene expression. Future experiments will reveal whether *nhr-10* and/or *nhr-68* are involved in the direct binding of metabolites from propionate metabolism, or perhaps propionate/propionyl-CoA itself, or whether they are the downstream targets of the actual metabolite sensor. Either way, they appear to be components of a metabolic homoestatic system centered on

propionate metabolism.

Metabolic homeostatic systems utilize negative feedback loops (nFBLs), which are known to confer the properties of robustness [202] and adaptability [22, 203] to biological networks. Oftentimes the goal of a metabolic nFBL is to maintain a metabolite within a certain concentration threshold, thus metabolic nFBLs center around metabolites. In these nFBLs, metabolites serve as both the currency of communication between the metabolic network and its regulators, and the commodities that are ultimately regulated. Metabolic nFBLs include additional components such as enzymes to modify metabolite concentrations, regulators to regulate enzyme expression or activity, and sensors to monitor metabolite levels [204]. For example, the cellular ATP control system operates as an nFBL to maintain appropriate energy levels (**Figure 5.2**). In this system, AMP:ATP ratios are sensed by AMPK, which serves both sensor and regulator functions. AMPK is activated when ATP levels drop relative to AMP levels, and in turn phosphorylates glycolytic enzymes among other metabolic targets to enhance glycolytic flux, ultimately increasing ATP production. As ATP levels increase, AMPK is inhibited, which completes the feedback loop. Other metabolic nFBLs are described in **Figure 5.2.**

Is there an nFBL in *C. elegans* to monitor and regulate propionate levels? The answer would appear to be Yes. We have obtained evidence that i) propionate activates the *acdh-1* promoter [41], ii) mutation of *acdh-1* also activates its own promoter [64], and iii) *acdh-1* likely functions in an oxidative

propionate breakdown shunt (Watson et al, in preparation; Chapter IV). Thus propionate would activate its own breakdown through a self-regulating nFBL (which includes *acdh-1* and its activators *nhr-10* and *nhr-68* as key components) to maintain cellular levels within a certain threshold. If propionate levels can be used as an inverse proxy for measuring vitamin B12 levels (since B12 dictates propionyl-CoA breakdown flux through the canonical pathway) then there may be no need for a direct vitamin B12 sensor. Monitoring and regulating propionate levels maybe be advantageous since its buildup can be toxic.

Propionate Metabolism

Metabolic networks evolve to maximize efficiency and flexibility, to enhance the system's robustness to changes in resource availability. In nature, multiple routes can arise to solve the same chemical problem, with more efficient routes evolving for instance if a chemical cofactor is available from the diet or environment. Thus, metabolic alliances exist between vitamin-synthesizing bacteria and vitamin auxotrophs, like humans [205, 206] and our model organism *C. elegans*. Propionate metabolism is an excellent example of this phenomenon. Several metabolic solutions exist in nature to breakdown this abundant C3-chain fatty acid: a carboxylation-based pathway that utilizes vitamin-derived cofactors, and several other pathways, including an oxidation pathway, that do not.

Propionate isn't efficiently broken down by β-oxidation like it's C4- and longer-chain fatty acid counterparts, likely due to a basic principle in organic chemistry summarized by Zaitsev's rule, which states that alkane elimination

reactions proceed to generate the most stable possible alkene, which is the alkene with the most highly substituted double bond carbons. The β-carbon of C3-chain propionyl-CoA is monosubstituted, while the β-carbon in C4 butyryl-CoA (and all longer chain acyl-CoAs) is disubstituted (**Figure 5.3**). This results in a high redox potential between propionyl-CoA and its unstable dehydrogenated form, acrylyl-CoA, rendering propionyl-CoA a poor substrate for β-oxidation [156]. Nature has solved this problem with a completely different C3-chain fatty acyl-CoA catabolic pathway. This pathway begins with the carboxylation of propionyl-CoA using bicarbonate as a co-substrate, which requires bacterially synthesized biotin. The next reaction is an epimerization, followed by a unique carbon skeleton rearrangement to form succinyl-CoA, which requires bacterially synthesized vitamin B12. Succinyl-CoA, when fully oxidized, yields more ATP than the products of direct propionyl-CoA oxidation, acetyl-CoA and CO_2, thus the B12-dependent pathway may be both more efficient and more energy yielding. Vitamin B12 auxotrophs, including *C. elegans* and mammals, encode enzymes for the vitamin-dependent pathway, while B12 non-users like *C. albicans* utilize the vitamin-independent β-oxidation-like pathway [147] or the methylcitrate cycle [207].

Efficient breakdown of propionate is not only advantageous from an energy generation perspective, but also from a toxicity prevention perspective, as propionate buildup can be highly toxic. Propionate inhibits core TCA cycle enzymes and poisons the mitochondrial electron transport chain (ETC) [208],

depletes vital CoA pools [209] and acts as a potent HDAC inhibitor leading to histone hyperacetylation [210]. Perhaps this is why B12-independent organisms such as *C. albicans* that rely on the less efficient β-oxidation-like propionate breakdown pathway have a relatively low tolerance for propionate in the environment [147]. In fact, propionate is used industrially as an anti-fungal food preservative [211]. The "advantage" that B12 auxotrophs have over yeast with respect to propionate breakdown applies only when there is ample B12 in the organism's diet. This begs the question, how do B12-dependent organisms avoid propionate-induced toxicity when B12 intake is suboptimal? We believe that for *C. elegans*, the answer to this question is that they maintain two pathways – one B12-dependent, and the other B12-independent. The B12-independent oxidative propionate breakdown shunt is transcriptionally upregulated upon B12 deficiency in an elegant example of metabolic rewiring as an adaptive response to diet. Mutating genes in the oxidative shunt renders animals more sensitive to B12 deficiency. The major question remains, do humans (and other B12 auxotrophs) also maintain this oxidative propionate breakdown shunt?

There are some tantalizing clues to suggest that humans directly oxidize propionate. In fact the oxidative shunt was first hypothesized to exist in humans over 40 years ago [140], however it has never been characterized at the genetic level, its existence in healthy individuals has remained unproven, and it's biological significance in mammals (if it does indeed exist) is unknown. The main support for the existence of a human propionate oxidation shunt is the detection

of 3-hydroxypropionate (3-HP), a unique intermediate in the pathway, in fluids from patients with propionic acidemia (PA), a condition of propionate buildup due to genetic mutations in the canonical B12-dependent breakdown pathway [140]. Elevated 3-HP is currently used as a diagnostic marker for PA in newborn screening [155]. More recently, global metabolomic profiling studies have revealed trace amounts of 3-HP in the urine of healthy subjects [158, 212]. Though it has been confirmed through carbon tracing experiments that the 3-HP observed in PA patients does in fact come directly from propionate [140], it is unclear whether humans truly have a devoted propionate oxidation pathway. To find the answer, the enzymes that contribute to the production of 3-HP in humans must be identified.

Humans have one-to-one orthologs (defined as reciprocal best BLAST hits) of our *C. elegans* oxidative shunt genes *acdh-1*, *ech-6*, *hach-1*, *hphd-1*, and *alh-8*. The closest human homolog of *acdh-1* is ACADSB, a short-branched chain acyl-CoA dehydrogenase that functions in valine and isoleucine breakdown. *acdh-1* also has high sequence similarity to the human ACADS gene, which functions in β-oxidation as a short-chain (C4-C6) acyl-CoA dehydrogenase. The human orthologs of *ech-6* and *hach-1*, ECHS1 and HIBCH respectively, are predicted to function primarily in branched chain amino acid (BCAA) breakdown, suggesting these enzymes would be required to “moonlight” if they indeed also function in the propionate shunt. Supporting this notion, HIBCH has been shown to metabolize structurally analogous intermediates from both BCAA breakdown

and the propionate oxidation shunt by *in vitro* biochemical assays [213, 214]. Recently, ECHS1 and HIBCH mutations were associated with acrylyl-CoA buildup in the urine of patients with inborn errors of metabolism [157].

Our candidate *C. elegans* 3-HP dehydrogenase *hphd-1* is the first gene to be associated with 3-HP dehydrogenase activity in a metazoan. The human ortholog of *hphd-1*, ADHFE1, is not assigned to any pathways in the human metabolic network by KEGG or BRENDA databases, but has been shown to metabolize the drug/neurotransmitter γ-hydroxybutyrate (GHB) [151], a structural analog of 3-HP derived from GABA breakdown. The ADHFE1 reaction is unique in that it uses the TCA cycle intermediate α-ketoglutarate (α-KG) as an electron acceptor, and in the process generates the "byproduct" (D)-2-hydroxyglutarate (D2HG) – an oncometabolite that is also produced by gain of function mutants of IDH1 and IDH2 frequently found in cancer [215, 216]. If ADHFE1 also has 3-HP dehydrogenase activity coupled to α-KG reduction and D2HG production, a novel link will be revealed between propionate metabolism and oncometabolite production. Future experiments will determine whether *C. elegans* HPHD-1 requires α-KG as a co-substrate, and whether it is also involved in GABA breakdown in *C. elegans*.

Figures

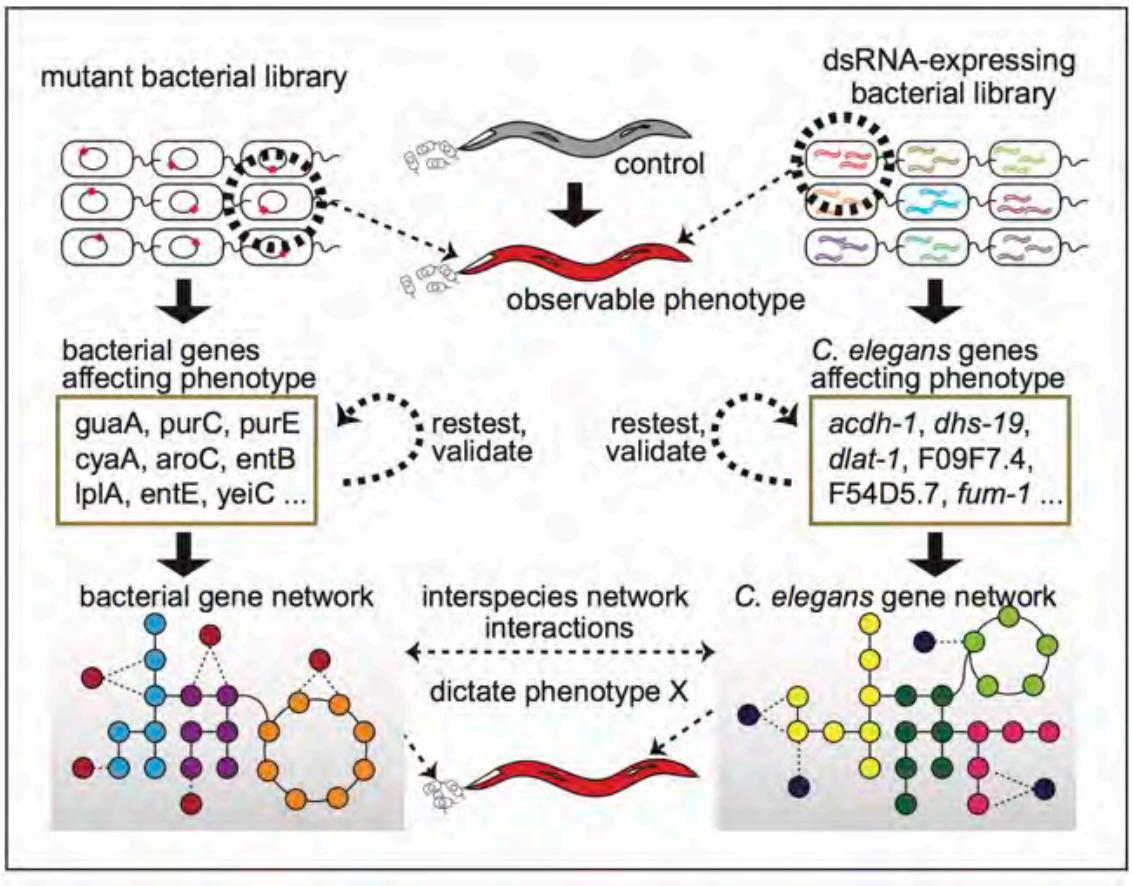

Figure 5.1 – Dissecting diet-related phenotypes in *Caenorhabditis elegans* with interspecies genetics.

To determine gene networks involved in diet-related phenotypes in *C. elegans*, genetic screens can be performed in both the bacterial diet and in the animal. *C. elegans* can be fed a library of mutant bacteria to determine bacterial genes that, when mutated, lead to a particular phenotype. To identify *C. elegans* genes that are involved in the diet-associated phenotype, animals can be fed a library of dsRNA-expressing bacteria targeting individual *C. elegans* genes. Hits from either screen should be retested and validated, and can be built into gene networks based on coexpression, co-complex formation, and/or genetic interaction data, or metabolic pathway annotations. Hypotheses about interspecies gene network interactions and their consequences with respect to the metabolic phenotype can be generated and further tested.

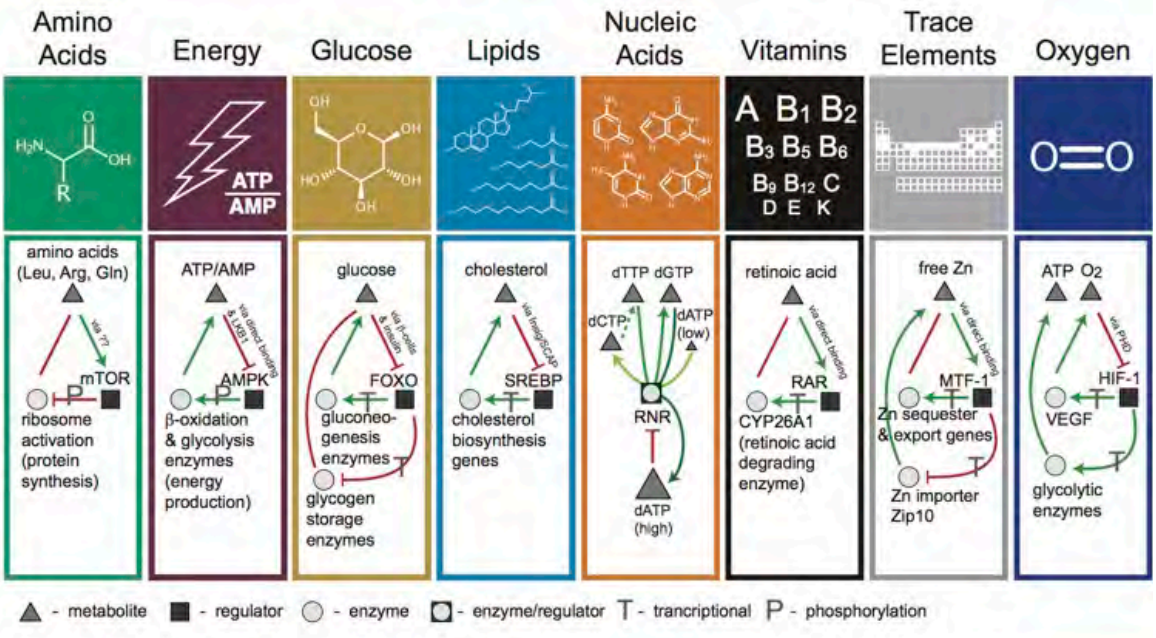

Figure 5.2 – Feedback loops in metabolic network regulation

Feedback loops can consist of small molecules (triangles), regulators (squares), and enzymes or other metabolic gene targets (circles). Edges from metabolites to regulators indicate a repressive (red) or activating (green) effect of a metabolite on regulator function, with the sensing mechanism noted along edge. Edges from regulators to enzymes or metabolic genes indicate a repressive (red) or activating (green) effect on target function. Edges are marked P to indicate phosphorylation or T to indicate transcription. Edges from enzymes/metabolic genes to metabolites indicate a consuming (red) or producing (green) relationship.

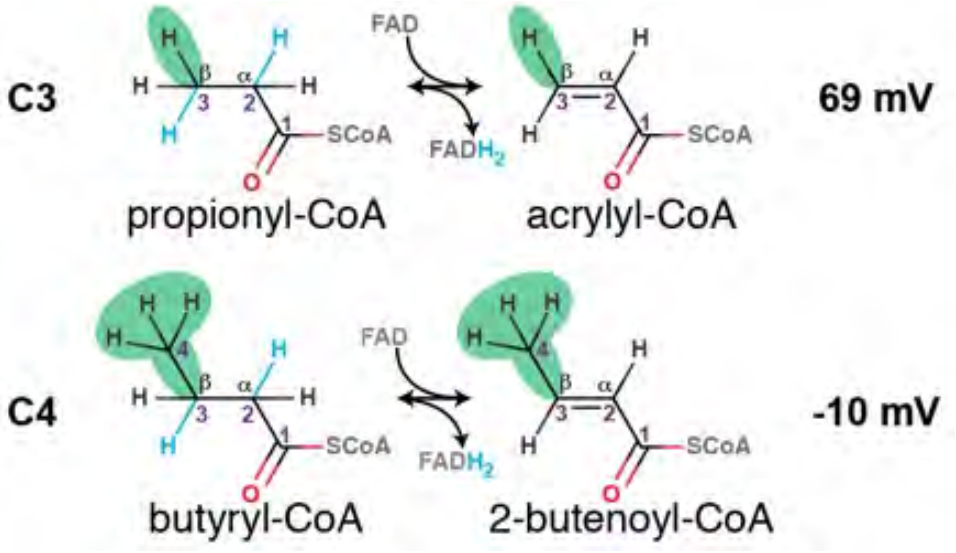

Figure 5.3 – C2-C3 dehydrogenation of propionyl-CoA vs. butyryl-CoA.
The high redox potential for the propionyl-CoA/acrylyl-CoA pair indicates that dehydrogenation of propionyl-CoA is thermodynamically less favorable than dehydrogenation of butyryl-CoA. Redox potentials are listed on the right.

BIBLIOGRAPHY

1. Watson E, Walhout AJ: **Caenorhabditis elegans metabolic gene regulatory networks govern the cellular economy**. *Trends in endocrinology and metabolism: TEM* 2014, **25**(10):502-508.
2. Sanderson S, Green A, Preece MA, Burton H: **The incidence of inherited metabolic disorders in the West Midlands, UK**. *Archives of disease in childhood* 2006, **91**(11):896-899.
3. Wild S, Roglic G, Green A, Sicree R, King H: **Global prevalence of diabetes: estimates for the year 2000 and projections for 2030**. *Diabetes care* 2004, **27**(5):1047-1053.
4. Pegklidou K, Nicolaou I, Demopoulos VJ: **Nutritional overview on the management of type 2 diabetes and the prevention of its complications**. *Current diabetes reviews* 2010, **6**(6):400-409.
5. Consortium CeS: **Genome sequence of the nematode C. elegans: a platform for investigating biology**. *Science* 1998, **282**(5396):2012-2018.
6. Stein L, Sternberg P, Durbin R, Thierry-Mieg J, Spieth J: **WormBase: network access to the genome and biology of Caenorhabditis elegans**. *Nucleic Acids Res* 2001, **29**(1):82-86.
7. Kamath RS, Fraser AG, Dong Y, Poulin G, Durbin R, Gotta M, Kanapin A, Le Bot N, Moreno S, Sohrmann M *et al*: **Systematic functional analysis of the *Caenorhabditis elegans* genome using RNAi**. *Nature* 2003, **421**(6920):231-237.
8. Rual JF, Ceron J, Koreth J, Hao T, Nicot AS, Hirozane-Kishikawa T, Vandenhaute J, Orkin SH, Hill DE, van den Heuvel S *et al*: **Toward improving Caenorhabditis elegans phenome mapping with an ORFeome-based RNAi library**. *Genome Res* 2004, **14**(10B):2162-2168.
9. Deplancke B, Mukhopadhyay A, Ao W, Elewa AM, Grove CA, Martinez NJ, Sequerra R, Doucette-Stamm L, Reece-Hoyes JS, Hope IA *et al*: **A gene-centered C. elegans protein-DNA interaction network**. *Cell* 2006, **125**(6):1193-1205.
10. Li S, Armstrong CM, Bertin N, Ge H, Milstein S, Boxem M, Vidalain PO, Han JD, Chesneau A, Hao T *et al*: **A map of the interactome network of the metazoan C. elegans**. *Science* 2004, **303**(5657):540-543.
11. Reece-Hoyes JS, Pons C, Diallo A, Mori A, Shrestha S, Kadreppa S, Nelson J, Diprima S, Dricot A, Lajoie BR *et al*: **Extensive rewiring and complex evolutionary dynamics in a C. elegans multiparameter transcription factor network**. *Molecular cell* 2013, **51**(1):116-127.
12. Tikhanovich I, Cox J, Weinman SA: **Forkhead box class O transcription factors in liver function and disease**. *Journal of gastroenterology and hepatology* 2013, **28 Suppl 1**:125-131.

13. Jewell JL, Russell RC, Guan KL: **Amino acid signalling upstream of mTOR**. *Nature reviews Molecular cell biology* 2013, **14**(3):133-139.
14. Mark M, Ghyselinck NB, Wendling O, Dupe V, Mascrez B, Kastner P, Chambon P: **A genetic dissection of the retinoid signalling pathway in the mouse**. *The Proceedings of the Nutrition Society* 1999, **58**(3):609-613.
15. Carlberg C, Campbell MJ: **Vitamin D receptor signaling mechanisms: integrated actions of a well-defined transcription factor**. *Steroids* 2013, **78**(2):127-136.
16. Contreras AV, Torres N, Tovar AR: **PPAR-alpha as a key nutritional and environmental sensor for metabolic adaptation**. *Advances in nutrition* 2013, **4**(4):439-452.
17. Desvergne B, Michalik L, Wahli W: **Transcriptional regulation of metabolism**. *Physiological reviews* 2006, **86**(2):465-514.
18. Taubert S, Ward JD, Yamamoto KR: **Nuclear hormone receptors in nematodes: evolution and function**. *Molecular and cellular endocrinology* 2011, **334**(1-2):49-55.
19. Motola DL, Cummins CL, Rottiers V, Sharma KK, Li T, Li Y, Suino-Powell K, Xu HE, Auchus RJ, Antebi A *et al*: **Identification of ligands for DAF-12 that govern dauer formation and reproduction in C. elegans**. *Cell* 2006, **124**(6):1209-1223.
20. Mahanti P, Bose N, Bethke A, Judkins JC, Wollam J, Dumas KJ, Zimmerman AM, Campbell SL, Hu PJ, Antebi A *et al*: **Comparative Metabolomics Reveals Endogenous Ligands of DAF-12, a Nuclear Hormone Receptor, Regulating C. elegans Development and Lifespan**. *Cell metabolism* 2014, **19**(1):73-83.
21. Arda HE, Taubert S, MacNeil LT, Conine CC, Tsuda B, Van Gilst M, Sequerra R, Doucette-Stamm L, Yamamoto KR, Walhout AJ: **Functional modularity of nuclear hormone receptors in a Caenorhabditis elegans metabolic gene regulatory network**. *Molecular systems biology* 2010, **6**:367.
22. Macneil LT, Walhout AJ: **Gene regulatory networks and the role of robustness and stochasticity in the control of gene expression**. *Genome Res* 2011, **21**(5):645-657.
23. Ravasz E, Somera AL, Mongru DA, Oltvai ZN, Barabasi AL: **Hierarchical organization of modularity in metabolic networks**. *Science* 2002, **297**(5586):1551-1555.
24. Babu MM, Luscombe NM, Aravind L, Gerstein M, Teichmann SA: **Structure and evolution of transcriptional regulatory networks**. *Curr Opin Struct Biol* 2004, **14**(3):283-291.
25. Ritter AD, Shen Y, Fuxman Bass J, Jeyaraj S, Deplancke B, Mukhopadhyay A, Xu J, Driscoll M, Tissenbaum HA, Walhout AJ: **Complex expression dynamics and robustness in C. elegans insulin networks**. *Genome research* 2013, **23**(6):954-965.

26. Felix MA, Braendle C: **The natural history of Caenorhabditis elegans**. *Current biology : CB* 2010, **20**(22):R965-969.
27. Shtonda BB, Avery L: **Dietary choice behavior in Caenorhabditis elegans**. *The Journal of experimental biology* 2006, **209**(Pt 1):89-102.
28. Avery L, Shtonda BB: **Food transport in the C. elegans pharynx**. *The Journal of experimental biology* 2003, **206**(Pt 14):2441-2457.
29. MacNeil LT, Watson E, Arda HE, Zhu LJ, Walhout AJ: **Diet-induced developmental acceleration independent of TOR and insulin in C. elegans**. *Cell* 2013, **153**(1):240-252.
30. Soukas AA, Kane EA, Carr CE, Melo JA, Ruvkun G: **Rictor/TORC2 regulates fat metabolism, feeding, growth, and life span in *Caenorhabditis elegans***. *Genes Dev* 2009, **23**(4):496-511.
31. Coolon JD, Jones KL, Todd TC, Carr BC, Herman MA: **Caenorhabditis elegans genomic response to soil bacteria predicts environment-specific genetic effects on life history traits**. *PLoS genetics* 2009, **5**(6):e1000503.
32. Jones LM, Rayson SJ, Flemming AJ, Urwin PE: **Adaptive and specialised transcriptional responses to xenobiotic stress in Caenorhabditis elegans are regulated by nuclear hormone receptors**. *PloS one* 2013, **8**(7):e69956.
33. Wang J, Robida-Stubbs S, Tullet JM, Rual JF, Vidal M, Blackwell TK: **RNAi screening implicates a SKN-1-dependent transcriptional response in stress resistance and longevity deriving from translation inhibition**. *PLoS genetics* 2010, **6**(8).
34. O'Rourke EJ, Ruvkun G: **MXL-3 and HLH-30 transcriptionally link lipolysis and autophagy to nutrient availability**. *Nat Cell Biol* 2013, **15**(6):668-676.
35. Handschin C, Meyer UA: **Induction of drug metabolism: the role of nuclear receptors**. *Pharmacological reviews* 2003, **55**(4):649-673.
36. Virk B, Correia G, Dixon DP, Feyst I, Jia J, Oberleitner N, Briggs Z, Hodge E, Edwards R, Ward J *et al*: **Excessive folate synthesis limits lifespan in the C. elegans: E. coli aging model**. *BMC Biol* 2012, **10**:67.
37. Gusarov I, Gautier L, Smolentseva O, Shamovsky I, Eremina S, Mironov A, Nudler E: **Bacterial nitric oxide extends the lifespan of *C. elegans***. *Cell* 2013, **152**(4):818-830.
38. Baba T, Ara T, Hasegawa M, Takai Y, Okumura Y, Baba M, Datsenko KA, Tomita M, Wanner BL, Mori H: **Construction of Escherichia coli K-12 in-frame, single-gene knockout mutants: the Keio collection**. *Molecular systems biology* 2006, **2**:2006 0008.
39. Yamamoto N, Nakahigashi K, Kakamichi T, Yoshino M, Takai Y, Touda Y, Furubayashi A, Kinjyo S, Dose H, Hasegawa M *et al*: **Update on the Keio collection of *Escherichia coli* single-gene deletion mutants.** *Molecular systems biology* 2009, **5**:335.

40. Pang S, Curran SP: **Adaptive capacity to bacterial diet modulates aging in C. elegans**. *Cell Metab* 2014, **19**(2):221-231.
41. Watson E, MacNeil LT, Ritter AD, Yilmaz LS, Rosebrock AP, Caudy AA, Walhout AJ: **Interspecies systems biology uncovers metabolites affecting C. elegans gene expression and life history traits**. *Cell* 2014, **156**(4):759-770.
42. Gracida X, Eckmann CR: **Fertility and germline stem cell maintenance under different diets requires nhr-114/HNF4 in C. elegans**. *Current biology : CB* 2013, **23**(7):607-613.
43. Magner DB, Wollam J, Shen Y, Hoppe C, Li D, Latza C, Rottiers V, Hutter H, Antebi A: **The NHR-8 nuclear receptor regulates cholesterol and bile acid homeostasis in C. elegans**. *Cell metabolism* 2013, **18**(2):212-224.
44. Castro C, Krumsiek J, Lehrbach NJ, Murfitt SA, Miska EA, Griffin JL: **A study of Caenorhabditis elegans DAF-2 mutants by metabolomics and differential correlation networks**. *Molecular bioSystems* 2013, **9**(7):1632-1642.
45. Martin FP, Spanier B, Collino S, Montoliu I, Kolmeder C, Giesbertz P, Affolter M, Kussmann M, Daniel H, Kochhar S *et al*: **Metabotyping of Caenorhabditis elegans and their culture media revealed unique metabolic phenotypes associated to amino acid deficiency and insulin-like signaling**. *Journal of proteome research* 2011, **10**(3):990-1003.
46. Schrier Vergano S, Rao M, McCormack S, Ostrovsky J, Clarke C, Preston J, Bennett MJ, Yudkoff M, Xiao R, Falk MJ: **In vivo metabolic flux profiling with stable isotopes discriminates sites and quantifies effects of mitochondrial dysfunction in C. elegans**. *Molecular genetics and metabolism* 2013.
47. An YJ, Xu WJ, Jin X, Wen H, Kim H, Lee J, Park S: **Metabotyping of the C. elegans sir-2.1 mutant using in vivo labeling and (13)C-heteronuclear multidimensional NMR metabolomics**. *ACS chemical biology* 2012, **7**(12):2012-2018.
48. Butler JA, Mishur RJ, Bhaskaran S, Rea SL: **A metabolic signature for long life in the Caenorhabditis elegans Mit mutants**. *Aging cell* 2013, **12**(1):130-138.
49. Butler JA, Ventura N, Johnson TE, Rea SL: **Long-lived mitochondrial (Mit) mutants of Caenorhabditis elegans utilize a novel metabolism**. *FASEB journal : official publication of the Federation of American Societies for Experimental Biology* 2010, **24**(12):4977-4988.
50. Castro C, Sar F, Shaw WR, Mishima M, Miska EA, Griffin JL: **A metabolomic strategy defines the regulation of lipid content and global metabolism by Delta9 desaturases in Caenorhabditis elegans**. *BMC genomics* 2012, **13**:36.

51. Butler JA, Mishur RJ, Bokov AF, Hakala KW, Weintraub ST, Rea SL: **Profiling the anaerobic response of C. elegans using GC-MS**. *PloS one* 2012, **7**(9):e46140.
52. Reinke SN, Hu X, Sykes BD, Lemire BD: **Caenorhabditis elegans diet significantly affects metabolic profile, mitochondrial DNA levels, lifespan and brood size**. *Molecular genetics and metabolism* 2010, **100**(3):274-282.
53. Brooks KK, Liang B, Watts JL: **The influence of bacterial diet on fat storage in C. elegans**. *PloS one* 2009, **4**(10):e7545.
54. Hochbaum D, Zhang Y, Stuckenholz C, Labhart P, Alexiadis V, Martin R, Knolker HJ, Fisher AL: **DAF-12 regulates a connected network of genes to ensure robust developmental decisions**. *PLoS genetics* 2011, **7**(7):e1002179.
55. McCormick M, Chen K, Ramaswamy P, Kenyon C: **New genes that extend Caenorhabditis elegans' lifespan in response to reproductive signals**. *Aging cell* 2012, **11**(2):192-202.
56. Van Gilst MR, Hadjivassiliou H, Jolly A, Yamamoto KR: **Nuclear hormone receptor NHR-49 controls fat consumption and fatty acid composition in C. elegans**. *PLoS biology* 2005, **3**(2):e53.
57. Pathare PP, Lin A, Bornfeldt KE, Taubert S, Van Gilst MR: **Coordinate regulation of lipid metabolism by novel nuclear receptor partnerships**. *PLoS genetics* 2012, **8**(4):e1002645.
58. Brock TJ, Browse J, Watts JL: **Genetic regulation of unsaturated fatty acid composition in C. elegans**. *PLoS genetics* 2006, **2**(7):e108.
59. Goudeau J, Bellemin S, Toselli-Mollereau E, Shamalnasab M, Chen Y, Aguilaniu H: **Fatty acid desaturation links germ cell loss to longevity through NHR-80/HNF4 in C. elegans**. *PLoS biology* 2011, **9**(3):e1000599.
60. Heestand BN, Shen Y, Liu W, Magner DB, Storm N, Meharg C, Habermann B, Antebi A: **Dietary restriction induced longevity is mediated by nuclear receptor NHR-62 in Caenorhabditis elegans**. *PLoS genetics* 2013, **9**(7):e1003651.
61. Pohludka M, Simeckova K, Vohanka J, Yilma P, Novak P, Krause MW, Kostrouchova M, Kostrouch Z: **Proteomic analysis uncovers a metabolic phenotype in C. elegans after nhr-40 reduction of function**. *Biochemical and biophysical research communications* 2008, **374**(1):49-54.
62. Brozova E, Simeckova K, Kostrouch Z, Rall JE, Kostrouchova M: **NHR-40, a Caenorhabditis elegans supplementary nuclear receptor, regulates embryonic and early larval development**. *Mechanisms of development* 2006, **123**(9):689-701.
63. Liang B, Ferguson K, Kadyk L, Watts JL: **The role of nuclear receptor NHR-64 in fat storage regulation in Caenorhabditis elegans**. *PloS one* 2010, **5**(3):e9869.

64. Watson E, MacNeil LT, Arda HE, Zhu LJ, Walhout AJM: **Integration of metabolic and gene regulatory networks modulates the *C. elegans* dietary response.** *Cell* 2013, **153**:253-266.
65. Carsten LD, Watts T, Markow TA: **Gene expression patterns accompanying a dietary shift in *Drosophila melanogaster.*** *Mol Ecol* 2005, **14**:3203-3208.
66. Du D, Shi YH, Le GW: **Microarray analysis of high-glucose diet-induced changes in mRNA expression in jejunums of C57BL/6J mice reveals impairment in digestion, absorption.** *Mol Biol Rep* 2010, **37**:1867-1874.
67. Hinnebusch AG: **Translational regulation of GCN4 and the general amino acid control of yeast**. *Annual review of microbiology* 2005, **59**:407-450.
68. Saudubray J-M, Sedel F, Walter JH: **Clinical approach to treatable inborn metabolic diseases: an introduction.** *Journal of inherited metabolic disease* 2006, **29**:261-274.
69. Acosta PB: **Nutrition management of patients with inherited metabolic disorders.** Sudbury, Massachusetts: Jones and Bartlett publishers; 2010.
70. Sonnichsen B, Koski LB, Walsh A, Marschall P, Neumann B, Brehm M, Alleaume AM, Artelt J, Bettencourt P, Cassin E *et al*: **Full-genome RNAi profiling of early embryogenesis in *Caenorhabditis elegans***. *Nature* 2005, **434**(7032):462-469.
71. Ashrafi K, Chang FY, Watts JL, Fraser AG, Kamath RS, Ahringer J, Ruvkun G: **Genome-wide RNAi analysis of *Caenorhabditis elegans* fat regulatory genes**. *Nature* 2003, **421**(6920):268-272.
72. Chalfie M, Tu Y, Euskirchen G, Ward WW, Prasher DC: **Green Fluorescent Protein as a marker for gene expression**. *Science* 1994, **263**:802-805.
73. Grove CA, deMasi F, Barrasa MI, Newburger D, Alkema MJ, Bulyk ML, Walhout AJ: **A multiparameter network reveals extensive divergence between *C. elegans* bHLH transcription factors.** *Cell* 2009, **138**:314-327.
74. Martinez NJ, Ow MC, Reece-Hoyes J, Ambros V, Walhout AJ: **Genome-scale spatiotemporal analysis of *Caenorhabditis elegans* microRNA promoter activity.** *Genome Res* 2008, **18**:2005-2015.
75. Hunt-Newbury R, Viveiros R, Johnsen R, Mah A, Anastas D, Fang L, Halfnight E, Lee D, Lin J, Lorch A *et al*: **High-throughput in vivo analysis of gene expression in *Caenorhabditis elegans.*** *PLoS Biol* 2007, **5**(9):e237.
76. Reece-Hoyes JS, Diallo A, Kent A, Shrestha S, Kadreppa S, Pesyna C, Lajoie B, Dekker J, Myers CL, Walhout AJM: **Enhanced yeast one-hybrid (eY1H) assays for high-throughput gene-centered regulatory network mapping.** *Nature Methods* 2011, **8**:1059-1064.

77. Reece-Hoyes JS, Barutcu AR, Patton McCord R, Jeong J, Jian L, MacWilliams A, Yang X, Salehi-Ashtiani K, Hill DE, Blackshaw S *et al*: **Yeast one-hybrid assays for high-throughput human gene regulatory network mapping.** *Nature Methods* 2011, **8**:1050-1052.
78. Arda HE, Taubert S, Conine C, Tsuda B, Van Gilst MR, Sequerra R, Doucette-Stam L, Yamamoto KR, Walhout AJM: **Functional modularity of nuclear hormone receptors in a *C. elegans* gene regulatory network.** *Molecular systems biology* 2010, **6**:367.
79. Taubert S, Ward JD, Yamamoto KR: **Nuclear hormone receptors in nematodes: evolution and function.** *Mol Cell Endocrinol* 2011, **334**:49-55.
80. Van Gilst MR, Hadjivassiliou H, Yamamoto KR: **A *Caenorhabditis elegans* nutrient response system partially dependent on nuclear receptor NHR-49**. *Proceedings of the National Academy of Sciences of the United States of America* 2005, **102**(38):13496-13501.
81. Murphy CT, McCarroll SA, Bargmann CI, Fraser A, Kamath RS, Ahringer J, Li H, Kenyon C: **Genes that act downstream of DAF-16 to influence the lifespan of *Caenorhabditis elegans.*** *Nature* 2003, **424**(6946):277-283.
82. Timmons L, Court DL, Fire A: **Ingestion of bacterially expressed dsRNAs can produce specific and potent genetic interference in *Caenorhabditis elegans*.** *Gene* 2001, **263**:103-112.
83. Rual J-F, Ceron J, Koreth J, Hao T, Nicot A-S, Hirozane-Kishikawa T, Vandenhaute J, Orkin SH, Hill DE, van den Heuvel S *et al*: **Toward improving *Caenorhabditis elegans* phenome mapping with an ORFeome-based RNAi library.** *Genome Res* 2004, **14**:2162-2168.
84. Lee I, Lehner B, Vavouri T, Shin J, Fraser AG, Marcotte EM: **Predicting genetic modifier loci using functional gene networks.** *Genome Res* 2010, **20**:1143-1153.
85. Gruning N-M, Lehrach H, Ralser M: **Regulatory crosstalk of the metabolic network.** *Trends Biochem Sci* 2010, **35**:220-227.
86. Weisfeld-Adams JD, Morrissey MA, Kirmse BM, Salveson BR, Wasserstein MP, McGuire PJ, Sunny S, Cohen-Pfeffer JL, Yu C, Caggana M *et al*: **Newborn screening and early biochemical follow-up in combined methylmalonic aciduria and homocystinuria, cblC type, and utility of methionine as a secondary screening analyte**. *Molecular genetics and metabolism* 2010, **99**(2):116-123.
87. Laplante M, Sabatini DM: **mTOR signaling in growth control and disease**. *Cell* 2012, **149**(2):274-293.
88. MacNeil LT, Watson E, Arda HE, Zhu LJ, Walhout AJM: **Nutrigenomics reveals nuclear hormone receptor-mediated life-strategy adjustment in response to diet.** submitted.
89. Walker AK, Jacobs RL, Watts JL, Rottiers V, Jiang K, Finnegan DM, Shioda T, Hansen M, Yang F, Niebergall LJ *et al*: **A conserved SREBP-**

1/phosphatidylcholine feedback circuit regulates lipogenesis in metazoans. *Cell* 2011, **147**(4):840-852.
90. Brenner S: **The genetics of *Caenorhabditis elegans.*** *Genetics* 1974, **77**(1):71-94.
91. McKay SJ, Johnsen R, Khattra J, Asano J, Baillie DL, Chan S, Dube N, Fang L, Goszczynski B, Ha E *et al*: **Gene expression profiling of cells, tissues, and developmental stages of the nematode C. elegans**. *Cold Spring Harb Symp Quant Biol* 2003, **68**:159-169.
92. Tawe WN, Eschbach ML, Walter RD, Henkle-Duhresen K: **Identification of stress-responsive genes in *Caenorhabditis elegans* using RT-PCR differential display.** *Nucleic Acids Res* 1998, **26**:1621-1627.
93. Wicks SR, Yeh RT, Gish WR, Waterston R, Plasterk RH: **Rapid gene mapping in *Caenorhabditis elegans* using a high density polymorphism map.** *Nat Genet* 2001, **28**:160-164.
94. Davis MW, Hammarlund M, Harrach T, Hullett P, Olsen S, Jorgensen EM: **Rapid single nucleotide polymorphism mapping in *C. elegans*.** *BMC genomics* 2005, **6**:118.
95. Sarin S, Bertrand V, Bigelow H, Boyanov A, Doitsidou M, Poole RJ, Narula S, Hobert O: **Analysis of multiple ethyl emthanesulfonate-mutagenized *Caenorhabditis elegans* strains by whole-genome sequencing.** *Genetics* 2010, **185**:417-430.
96. Bigelow H, Doitsidou M, Sarin S, Hobert O: **MAQGene: software to facilitate *C. elegans* mutant genome sequence analysis.** *Nat Methods* 2009, **6**:549.
97. Gubelmann C, Gattiker A, Massouras A, Hens K, David F, Decouttere F, Rougemont J, Deplancke B: **GETPrime: a gene- or transcript-specific primter database for quantitative real-time PCR.** *Database* 2011, **bar040**.
98. Livak KJ, Schmittgen TD: **Analysis of relative gene expression data using real-time quantitative PCR and the 2(-Delta Delta C(T)) method.** *Methods* 2001, **25**:402-408.
99. Huang dW, Sherman BT, Lempicki RA: **Systematic and integrative analysis of large gene lists uisng DAVID bioinformatics resources.** *Nat Protoc* 2009, **4**:44-57.
100. Lee I, Lehner B, Crombie C, Wong W, Fraser AG, Marcotte EM: **A single gene network accurately predicts phenotypic effects of gene perturbation in *Caenorhabditis elegans***. *Nat Genet* 2008, **40**(2):181-188.
101. Kanehisa M, Goto S, Furumichi M, Tanabe M, Hirakawa M: **KEGG for representation and analysis of molecular networks involving diseases and drugs.** *Nucleic Acids Res* 2010, **38**:D355-360.
102. Benjamini Y, Hochberg Y: **Controlling the false discovery rate: a practical and powerful approach to multiple testing.** . *Journal of the Royal Statistical Society Series B* 1995, **57**:289-300.

103. Hooper LV, Midtvedt T, Gordon JI: **How host-microbial interactions shape the nutrient environment of the mammalian intestine**. *Annu Rev Nutr* 2002, **22**:283-307.
104. Coolon JD, Jones KL, Todd TC, Carr BC, Herman MA: ***Caenorhabditis elegans* genomic response to soil bacteria predicts environment-specific genetic effects on life history traits**. *PLoS genetics* 2009, **5**(6):e1000503.
105. MacNeil LT, Watson E, Arda HE, Zhu LJ, Walhout AJM: **Diet-induced developmental acceleration independent of TOR and insulin in *C. elegans*.** *Cell* 2013, **153**:240-252.
106. Gracida X, Eckmann CR: **Fertility and germline stem cell maintenance under different diets requires nhr-114/HNF4 in *C. elegans***. *Current biology : CB* 2013, **23**(7):607-613.
107. Felix M-A, Duveau F: **Population dynamics and habitat sharing of natural populations of *Caenorhabditis elegans* and *C. briggsae*.** *BMC Biology* 2013, **10**:59.
108. Avery L, Shtonda BB: **Food transport in the *C. elegans* pharynx**. *J Exp Biol* 2003, **206**(Pt 14):2441-2457.
109. Shtonda BB, Avery L: **Dietary choice behavior in *Caenorhabditis elegans.*** *J Exp Biol* 2006, **209**(Pt 1):89-102.
110. Virk B, Correia G, Dixon DP, Feyst I, Jia J, Oberleitner N, Briggs Z, Hodge E, Edwards R, Ward J *et al*: **Excessive folate synthesis limits lifespan in the C. elegans: E. coli aging model**. *BMC Biology* 2012, **10**:67.
111. Kadner RJ: **Vitamin B12 transport in Escherichia coli: energy coupling between membranes**. *Mol Microbiol* 1990, **4**(12):2027-2033.
112. Bender DA: **Nutritional biochemistry of the vitamins.** Cambridge: Cambridge University Press; 2003.
113. Chandler RJ, Aswani V, Tsai MS, Falk M, Wehrli N, Stabler S, Allen R, Sedensky M, Kazazian HH, Venditti CP: **Propionyl-CoA and adenosylcobalamin metabolism in *Caenorhabditis elegans*: evidence for a role of methylmalonyl-CoA epimerase in intermediary metabolism**. *Molecular genetics and metabolism* 2006, **89**(1-2):64-73.
114. Illman RJ, Topping DL, Trimble RP: **Effects of food restriction and starvation-refeeding on volatile fatty acid concentrations in the rat**. *The Journal of nutrition* 1986, **116**(9):1694-1700.
115. Liu H, Galka M, Mori E, Liu X, Lin YF, Wei R, Pittock P, Voss C, Dhami G, Li X *et al*: **A method for systematic mapping of protein lysine methylation identifies functions for HP1beta in DNA damage response**. *Molecular cell* 2013, **50**(5):723-735.
116. Chawla A, Repa JJ, Evans RM, Mangelsdorf DJ: **Nuclear receptors and lipid physiology: opening the X-files.** *Science* 2001, **294**:1866-1870.
117. Reece-Hoyes JS, Deplancke B, Shingles J, Grove CA, Hope IA, Walhout AJM: **A compendium of *C. elegans* regulatory transcription factors: a**

resource for mapping transcription regulatory networks. *Genome Biol* 2005, **6**:R110.
118. Pepper MR, Black MM: **B12 in fetal development**. *Seminars in cell & developmental biology* 2011, **22**(6):619-623.
119. Al-Lahham SH, Peppelenbosch MP, Roelofsen H, Vonk RJ, Venema K: **Biological effects of propionic acid in humans; metabolism, potential applications and underlying mechanisms**. *Biochimica et biophysica acta* 2010, **1801**(11):1175-1183.
120. Bito T, Matsunaga Y, Yabuta Y, Kawano T, Watanabe F: **Vitamin B12 deficiency in Caenorhabditis elegans results in loss of fertility, extended life cycle, and reduced lifespan**. *FEBS Open Bio* 2013, **3**:112-117.
121. Albert MJ, Mathan VI, Baker SJ: **Vitamin B12 synthesis by human small intestinal bacteria**. *Nature* 1980, **283**(5749):781-782.
122. Goodman AL, McNulty NP, Zhao Y, Leip D, Mitra RD, Lozupone CA, Knight R, Gordon JI: **Identifying genetic determinants needed to establish a human gut symbiont in its habitat**. *Cell Host Microbe* 2009, **6**(3):279-289.
123. LeBlanc JG, Milani C, de Giori GS, Sesma F, van Sinderen D, Ventura M: **Bacteria as vitamin suppliers to their host: a gut microbiota perspective**. *Current opinion in biotechnology* 2013, **24**(2):160-168.
124. Tremaroli V, Backhed F: **Functional interactions between the gut microbiota and host metabolism.** *Nature* 2012, **489**:242-249.
125. Maurice CF, Haiser HJ, Turnbaugh PJ: **Xenobiotics shape the physiology and gene expression of the active human gut microbiome**. *Cell* 2013, **152**(1-2):39-50.
126. Haiser HJ, Gootenberg DB, Chatman K, Sirasani G, Balskus EP, Turnbaugh PJ: **Predicting and manipulating cardiac drug inactivation by the human gut bacterium Eggerthella lenta**. *Science* 2013, **341**(6143):295-298.
127. Kamada N, Seo SU, Chen GY, Nunez G: **Role of the gut microbiota in immunity and inflammatory disease**. *Nat Rev Immunol* 2013, **13**(5):321-335.
128. Goodman AL, Kulasekara B, Rietsch A, Boyd D, Smith RS, Lory S: **A signaling network reciprocally regulates genes associated with acute infection and chronic persistence in Pseudomonas aeruginosa**. *Developmental cell* 2004, **7**(5):745-754.
129. Chun KT, Edenberg HJ, Kelley MR, Goebl MG: **Rapid amplification of uncharacterized transposon-tagged DNA sequences from genomic DNA**. *Yeast* 1997, **13**(3):233-240.
130. Hernandez D, Francois P, Farinelli L, Osteras M, Schrenzel J: **De novo bacterial genome sequencing: millions of very short reads assembled on a desktop computer**. *Genome research* 2008, **18**(5):802-809.

131. Devoid S, Overbeek R, DeJongh M, Vonstein V, Best AA, Henry C: **Automated genome annotation and metabolic model reconstruction in the SEED and Model SEED**. *Methods Mol Biol* 2013, **985**:17-45.
132. Henry CS, DeJongh M, Best AA, Frybarger PM, Linsay B, Stevens RL: **High-throughput generation, optimization and analysis of genome-scale metabolic models**. *Nature biotechnology* 2010, **28**(9):977-982.
133. Aziz RK, Bartels D, Best AA, DeJongh M, Disz T, Edwards RA, Formsma K, Gerdes S, Glass EM, Kubal M *et al*: **The RAST Server: rapid annotations using subsystems technology**. *BMC genomics* 2008, **9**:75.
134. Cole JR, Wang Q, Cardenas E, Fish J, Chai B, Farris RJ, Kulam-Syed-Mohideen AS, McGarrell DM, Marsh T, Garrity GM *et al*: **The Ribosomal Database Project: improved alignments and new tools for rRNA analysis**. *Nucleic acids research* 2009, **37**(Database issue):D141-145.
135. Wauters G, De Baere T, Willems A, Falsen E, Vaneechoutte M: **Description of Comamonas aquatica comb. nov. and Comamonas kerstersii sp. nov. for two subgroups of Comamonas terrigena and emended description of Comamonas terrigena**. *Int J Syst Evol Microbiol* 2003, **53**(Pt 3):859-862.
136. Kanehisa M, Goto S, Sato Y, Furumichi M, Tanabe M: **KEGG for integration and interpretation of large-scale molecular data sets**. *Nucleic acids research* 2012, **40**(Database issue):D109-114.
137. Caspi R, Altman T, Dale JM, Dreher K, Fulcher CA, Gilham F, Kaipa P, Karthikeyan AS, Kothari A, Krummenacker M *et al*: **The MetaCyc database of metabolic pathways and enzymes and the BioCyc collection of pathway/genome databases**. *Nucleic acids research* 2010, **38**(Database issue):D473-479.
138. la Marca G, Malvagia S, Pasquini E, Innocenti M, Donati MA, Zammarchi E: **Rapid 2nd-tier test for measurement of 3-OH-propionic and methylmalonic acids on dried blood spots: reducing the false-positive rate for propionylcarnitine during expanded newborn screening by liquid chromatography-tandem mass spectrometry**. *Clinical chemistry* 2007, **53**(7):1364-1369.
139. Matsumoto I, and Kuhara, T.: **A new chemical diagnostic method for inborn errors of metabolism by mass spectrometry—rapid, practical, and simultaneous urinary metabolites analysis**. *Mass Spectrometry Reviews* 1996, **15**(1):43-57.
140. Ando T, Rasmussen K, Nyhan WL, Hull D: **3-hydroxypropionate: significance of -oxidation of propionate in patients with propionic acidemia and methylmalonic acidemia**. *Proceedings of the National Academy of Sciences of the United States of America* 1972, **69**(10):2807-2811.
141. Flavin M, Ortiz PJ, Ochoa S: **Metabolism of propionic acid in animal tissues**. *Nature* 1955, **176**(4487):823-826.

142. Sanudo-Wilhelmy SA, Gomez-Consarnau L, Suffridge C, Webb EA: **The role of B vitamins in marine biogeochemistry**. *Ann Rev Mar Sci* 2014, **6**:339-367.
143. Degnan PH, Taga ME, Goodman AL: **Vitamin B12 as a modulator of gut microbial ecology.** *Cell Metab* 2014, **20**:769-778.
144. Roth JR, Lawrence JG, Bobik TA: **Cobalamin (coenzyme B12): synthesis and biological significance**. *Annu Rev Microbiol* 1996, **50**:137-181.
145. Clark SG, Lu X, Horvitz HR: **The *Caenorhabditis elegans* locus *lin-15*, a negative regulator of a tyrosine kinase signaling pathway, encodes two different proteins.** *Genetics* 1994, **137**:987-997.
146. Costanzo M, Baryshnikova A, Bellay J, Kim Y, Spear ED, Sevier CS, Ding H, Koh JL, Toufighi K, Mostafavi S *et al*: **The genetic landscape of a cell**. *Science* 2010, **327**(5964):425-431.
147. Otzen C, Bardl B, Jacobsen ID, Nett M, Brock M: **Candida albicans utilizes a modified beta-oxidation pathway for the degradation of toxic propionyl-CoA**. *The Journal of biological chemistry* 2014, **289**(12):8151-8169.
148. Ogata H, Goto S, Sato K, Fujibuchi W, Bono H, Kanehisa M: **KEGG: Kyoto Encyclopedia of Genes and Genomes**. *Nucleic Acids Res* 1999, **27**(1):29-34.
149. Hellwig J, Deckardt K, Freisberg KO: **Subchronic and chronic studies of the effects of oral administration of acrylic acid to rats**. *Food Chem Toxicol* 1993, **31**(1):1-18.
150. Saillenfait AM, Bonnet P, Gallissot F, Protois JC, Peltier A, Fabries JF: **Relative developmental toxicities of acrylates in rats following inhalation exposure**. *Toxicol Sci* 1999, **48**(2):240-254.
151. Lyon RC, Johnston SM, Panopoulos A, Alzeer S, McGarvie G, Ellis EM: **Enzymes involved in the metabolism of gamma-hydroxybutyrate in SH-SY5Y cells: identification of an iron-dependent alcohol dehydrogenase ADHFe1**. *Chemico-biological interactions* 2009, **178**(1-3):283-287.
152. Wong CG, Bottiglieri T, Snead OC, 3rd: **GABA, gamma-hydroxybutyric acid, and neurological disease**. *Ann Neurol* 2003, **54 Suppl 6**:S3-12.
153. Marcadier JL, Smith AM, Pohl D, Schwartzentruber J, Al-Dirbashi OY, Consortium FC, Majewski J, Ferdinandusse S, Wanders RJ, Bulman DE *et al*: **Mutations in ALDH6A1 encoding methylmalonate semialdehyde dehydrogenase are associated with dysmyelination and transient methylmalonic aciduria**. *Orphanet J Rare Dis* 2013, **8**:98.
154. Kim H, Ishidate T, Ghanta KS, Seth M, Conte D, Jr., Shirayama M, Mello CC: **A co-CRISPR strategy for efficient genome editing in Caenorhabditis elegans**. *Genetics* 2014, **197**(4):1069-1080.

155. Carrillo-Carrasco N, Venditti C: **Propionic Acidemia**. In: *GeneReviews(R).* Edited by Pagon RA, Adam MP, Ardinger HH, Bird TD, Dolan CR, Fong CT, Smith RJH, Stephens K. Seattle (WA); 1993.
156. Sato K, Nishina Y, Setoyama C, Miura R, Shiga K: **Unusually high standard redox potential of acrylyl-CoA/propionyl-CoA couple among enoyl-CoA/acyl-CoA couples: a reason for the distinct metabolic pathway of propionyl-CoA from longer acyl-CoAs**. *Journal of biochemistry* 1999, **126**(4):668-675.
157. Peters H, Ferdinandusse S, Ruiter JP, Wanders RJ, Boneh A, Pitt J: **Metabolite studies in HIBCH and ECHS1 defects: Implications for screening**. *Molecular genetics and metabolism* 2015, **115**(4):168-173.
158. Bouatra S, Aziat F, Mandal R, Guo AC, Wilson MR, Knox C, Bjorndahl TC, Krishnamurthy R, Saleem F, Liu P *et al*: **The human urine metabolome**. *PloS one* 2013, **8**(9):e73076.
159. Pandya C, Farelli JD, Dunaway-Mariano D, Allen KN: **Enzyme promiscuity: engine of evolutionary innovation**. *The Journal of biological chemistry* 2014, **289**(44):30229-30236.
160. Schmittgen TD, Livak KJ: **Analyzing real-time PCR data by the comparative C(T) method**. *Nat Protoc* 2008, **3**(6):1101-1108.
161. Chen X, Xu F, Zhu C, Ji J, Zhou X, Feng X, Guang S: **Dual sgRNA-directed gene knockout using CRISPR/Cas9 technology in Caenorhabditis elegans**. *Sci Rep* 2014, **4**:7581.
162. Arribere JA, Bell RT, Fu BX, Artiles KL, Hartman PS, Fire AZ: **Efficient marker-free recovery of custom genetic modifications with CRISPR/Cas9 in Caenorhabditis elegans**. *Genetics* 2014, **198**(3):837-846.
163. Karagianni P, Talianidis I: **Transcription factor networks regulating hepatic fatty acid metabolism**. *Biochimica et biophysica acta* 2015, **1851**(1):2-8.
164. David CJ, Chen M, Assanah M, Canoll P, Manley JL: **HnRNP proteins controlled by c-Myc deregulate pyruvate kinase mRNA splicing in cancer**. *Nature* 2010, **463**(7279):364-368.
165. Ravi S, Schilder RJ, Kimball SR: **Role of Precursor mRNA Splicing in Nutrient-Induced Alterations in Gene Expression and Metabolism**. *The Journal of nutrition* 2015.
166. Rouault TA: **Post-transcriptional regulation of human iron metabolism by iron regulatory proteins**. *Blood cells, molecules & diseases* 2002, **29**(3):309-314.
167. Lushchak OV, Piroddi M, Galli F, Lushchak VI: **Aconitase post-translational modification as a key in linkage between Krebs cycle, iron homeostasis, redox signaling, and metabolism of reactive oxygen species**. *Redox report : communications in free radical research* 2014, **19**(1):8-15.

168. Munday MR: **Regulation of mammalian acetyl-CoA carboxylase**. *Biochemical Society transactions* 2002, **30**(Pt 6):1059-1064.
169. Ahmad MF, Dealwis CG: **The structural basis for the allosteric regulation of ribonucleotide reductase**. *Progress in molecular biology and translational science* 2013, **117**:389-410.
170. Liberles JS, Thorolfsson M, Martinez A: **Allosteric mechanisms in ACT domain containing enzymes involved in amino acid metabolism**. *Amino acids* 2005, **28**(1):1-12.
171. Wegner A, Meiser J, Weindl D, Hiller K: **How metabolites modulate metabolic flux**. *Current opinion in biotechnology* 2014, **34C**:16-22.
172. McKenna MC: **Glutamate dehydrogenase in brain mitochondria: do lipid modifications and transient metabolon formation influence enzyme activity?** *Neurochemistry international* 2011, **59**(4):525-533.
173. Menard L, Maughan D, Vigoreaux J: **The structural and functional coordination of glycolytic enzymes in muscle: evidence of a metabolon?** *Biology* 2014, **3**(3):623-644.
174. Berrabah W, Aumercier P, Lefebvre P, Staels B: **Control of nuclear receptor activities in metabolism by post-translational modifications**. *FEBS letters* 2011, **585**(11):1640-1650.
175. Kousteni S: **FoxO1, the transcriptional chief of staff of energy metabolism**. *Bone* 2012, **50**(2):437-443.
176. Folger O, Jerby L, Frezza C, Gottlieb E, Ruppin E, Shlomi T: **Predicting selective drug targets in cancer through metabolic networks**. *Molecular systems biology* 2011, **7**:501.
177. Nahvi A, Barrick JE, Breaker RR: **Coenzyme B12 riboswitches are widespread genetic control elements in prokaryotes**. *Nucleic Acids Res* 2004, **32**(1):143-150.
178. Johnson JE, Jr., Reyes FE, Polaski JT, Batey RT: **B12 cofactors directly stabilize an mRNA regulatory switch**. *Nature* 2012, **492**(7427):133-137.
179. Haussler MR, Haussler CA, Bartik L, Whitfield GK, Hsieh JC, Slater S, Jurutka PW: **Vitamin D receptor: molecular signaling and actions of nutritional ligands in disease prevention**. *Nutrition reviews* 2008, **66**(10 Suppl 2):S98-112.
180. Carlberg C, Seuter S: **A genomic perspective on vitamin D signaling**. *Anticancer research* 2009, **29**(9):3485-3493.
181. di Masi A, Leboffe L, De Marinis E, Pagano F, Cicconi L, Rochette-Egly C, Lo-Coco F, Ascenzi P, Nervi C: **Retinoic acid receptors: From molecular mechanisms to cancer therapy**. *Molecular aspects of medicine* 2015, **41C**:1-115.
182. D'Aniello E, Waxman JS: **Input overload: Contributions of retinoic acid signaling feedback mechanisms to heart development and teratogenesis**. *Dev Dyn* 2015, **244**(3):513-523.

183. Shenefelt RE: **Morphogenesis of malformations in hamsters caused by retinoic acid: relation to dose and stage at treatment**. *Teratology* 1972, **5**(1):103-118.
184. Fraser DA, Hessvik NP, Nikolic N, Aas V, Hanssen KF, Bohn SK, Thoresen GH, Rustan AC: **Benfotiamine increases glucose oxidation and downregulates NADPH oxidase 4 expression in cultured human myotubes exposed to both normal and high glucose concentrations**. *Genes Nutr* 2012, **7**(3):459-469.
185. Liu S, Stromberg A, Tai HH, Moscow JA: **Thiamine transporter gene expression and exogenous thiamine modulate the expression of genes involved in drug and prostaglandin metabolism in breast cancer cells**. *Mol Cancer Res* 2004, **2**(8):477-487.
186. Tanaka T, Sohmiya K, Kono T, Terasaki F, Horie R, Ohkaru Y, Muramatsu M, Takai S, Miyazaki M, Kitaura Y: **Thiamine attenuates the hypertension and metabolic abnormalities in CD36-defective SHR: uncoupling of glucose oxidation from cellular entry accompanied with enhanced protein O-GlcNAcylation in CD36 deficiency**. *Mol Cell Biochem* 2007, **299**(1-2):23-35.
187. Nakano E, Mushtaq S, Heath PR, Lee ES, Bury JP, Riley SA, Powers HJ, Corfe BM: **Riboflavin depletion impairs cell proliferation in adult human duodenum: identification of potential effectors**. *Dig Dis Sci* 2011, **56**(4):1007-1019.
188. Choi S, Yoon H, Oh KS, Oh YT, Kim YI, Kang I, Youn JH: **Widespread effects of nicotinic acid on gene expression in insulin-sensitive tissues: implications for unwanted effects of nicotinic acid treatment**. *Metabolism* 2011, **60**(1):134-144.
189. Couturier A, Keller J, Most E, Ringseis R, Eder K: **Niacin in pharmacological doses alters microRNA expression in skeletal muscle of obese Zucker rats**. *PloS one* 2014, **9**(5):e98313.
190. Giammona LM, Fuhrken PG, Papoutsakis ET, Miller WM: **Nicotinamide (vitamin B3) increases the polyploidisation and proplatelet formation of cultured primary human megakaryocytes**. *Br J Haematol* 2006, **135**(4):554-566.
191. Toya K, Hirata A, Ohata T, Sanada Y, Kato N, Yanaka N: **Regulation of colon gene expression by vitamin B6 supplementation**. *Mol Nutr Food Res* 2012, **56**(4):641-652.
192. Zhang P, Suidasari S, Hasegawa T, Yanaka N, Kato N: **Vitamin B(6) activates p53 and elevates p21 gene expression in cancer cells and the mouse colon**. *Oncol Rep* 2014, **31**(5):2371-2376.
193. Barua S, Chadman KK, Kuizon S, Buenaventura D, Stapley NW, Ruocco F, Begum U, Guariglia SR, Brown WT, Junaid MA: **Increasing maternal or post-weaning folic acid alters gene expression and moderately changes behavior in the offspring**. *PloS one* 2014, **9**(7):e101674.

194. Champier J, Claustrat F, Nazaret N, Fevre Montange M, Claustrat B: **Folate depletion changes gene expression of fatty acid metabolism, DNA synthesis, and circadian cycle in male mice**. *Nutr Res* 2012, **32**(2):124-132.
195. Lin YW, Wang JL, Chen HM, Zhang YJ, Lu R, Ren LL, Hong J, Fang JY: **Folic acid supplementary reduce the incidence of adenocarcinoma in a mouse model of colorectal cancer: microarray gene expression profile**. *J Exp Clin Cancer Res* 2011, **30**:116.
196. Canali R, Natarelli L, Leoni G, Azzini E, Comitato R, Sancak O, Barella L, Virgili F: **Vitamin C supplementation modulates gene expression in peripheral blood mononuclear cells specifically upon an inflammatory stimulus: a pilot study in healthy subjects**. *Genes Nutr* 2014, **9**(3):390.
197. Jun HJ, Kim S, Dawson K, Choi DW, Kim JS, Rodriguez RL, Lee SJ: **Effects of acute oral administration of vitamin C on the mouse liver transcriptome**. *J Med Food* 2011, **14**(3):181-194.
198. Takahashi K, Kishimoto Y, Konishi T, Fujita Y, Ito M, Shimokado K, Maruyama N, Ishigami A: **Ascorbic acid deficiency affects genes for oxidation-reduction and lipid metabolism in livers from SMP30/GNL knockout mice**. *Biochimica et biophysica acta* 2014, **1840**(7):2289-2298.
199. Landrier JF, Gouranton E, Reboul E, Cardinault N, El Yazidi C, Malezet-Desmoulins C, Andre M, Nowicki M, Souidi M, Borel P: **Vitamin E decreases endogenous cholesterol synthesis and apo-AI-mediated cholesterol secretion in Caco-2 cells**. *J Nutr Biochem* 2010, **21**(12):1207-1213.
200. Makpol S, Zainuddin A, Chua KH, Mohd Yusof YA, Ngah WZ: **Gamma-tocotrienol modulated gene expression in senescent human diploid fibroblasts as revealed by microarray analysis**. *Oxid Med Cell Longev* 2013, **2013**:454328.
201. Mustacich DJ, Gohil K, Bruno RS, Yan M, Leonard SW, Ho E, Cross CE, Traber MG: **Alpha-tocopherol modulates genes involved in hepatic xenobiotic pathways in mice**. *J Nutr Biochem* 2009, **20**(6):469-476.
202. Kitano H: **Biological robustness**. *Nat Rev Genet* 2004, **5**(11):826-837.
203. Ma W, Trusina A, El-Samad H, Lim WA, Tang C: **Defining network topologies that can achieve biochemical adaptation**. *Cell* 2009, **138**(4):760-773.
204. Kotas ME, Medzhitov R: **Homeostasis, Inflammation, and Disease Susceptibility**. *Cell* 2015, **160**(5):816-827.
205. LeBlanc JG, Milani C, de Giori GS, Sesma F, van Sinderen D, Ventura M: **Bacteria as vitamin suppliers to their host: a gut microbiota perspective**. *Current opinion in biotechnology* 2013, **24**(2):160-168.
206. Fischbach MA, Sonnenburg JL: **Eating for two: how metabolism establishes interspecies interactions in the gut**. *Cell host & microbe* 2011, **10**(4):336-347.

207. Limenitakis J, Oppenheim RD, Creek DJ, Foth BJ, Barrett MP, Soldati-Favre D: **The 2-methylcitrate cycle is implicated in the detoxification of propionate in Toxoplasma gondii**. *Mol Microbiol* 2013, **87**(4):894-908.
208. Schwab MA, Sauer SW, Okun JG, Nijtmans LG, Rodenburg RJ, van den Heuvel LP, Drose S, Brandt U, Hoffmann GF, Ter Laak H *et al*: **Secondary mitochondrial dysfunction in propionic aciduria: a pathogenic role for endogenous mitochondrial toxins**. *The Biochemical journal* 2006, **398**(1):107-112.
209. Matsuishi T, Stumpf DA, Seliem M, Eguren LA, Chrislip K: **Propionate mitochondrial toxicity in liver and skeletal muscle: acyl CoA levels**. *Biochemical medicine and metabolic biology* 1991, **45**(2):244-253.
210. Nguyen NH, Morland C, Gonzalez SV, Rise F, Storm-Mathisen J, Gundersen V, Hassel B: **Propionate increases neuronal histone acetylation, but is metabolized oxidatively by glia. Relevance for propionic acidemia**. *Journal of neurochemistry* 2007, **101**(3):806-814.
211. Suhr KI, Nielsen PV: **Effect of weak acid preservatives on growth of bakery product spoilage fungi at different water activities and pH values**. *International journal of food microbiology* 2004, **95**(1):67-78.
212. Guneral F, Bachmann C: **Age-related reference values for urinary organic acids in a healthy Turkish pediatric population**. *Clinical chemistry* 1994, **40**(6):862-866.
213. Hawes JW, Jaskiewicz J, Shimomura Y, Huang B, Bunting J, Harper ET, Harris RA: **Primary structure and tissue-specific expression of human beta-hydroxyisobutyryl-coenzyme A hydrolase**. *The Journal of biological chemistry* 1996, **271**(42):26430-26434.
214. Shimomura Y, Murakami T, Nakai N, Huang B, Hawes JW, Harris RA: **3-hydroxyisobutyryl-CoA hydrolase**. *Methods in enzymology* 2000, **324**:229-240.
215. Ward PS, Patel J, Wise DR, Abdel-Wahab O, Bennett BD, Coller HA, Cross JR, Fantin VR, Hedvat CV, Perl AE *et al*: **The common feature of leukemia-associated IDH1 and IDH2 mutations is a neomorphic enzyme activity converting alpha-ketoglutarate to 2-hydroxyglutarate**. *Cancer cell* 2010, **17**(3):225-234.
216. Kats LM, Reschke M, Taulli R, Pozdnyakova O, Burgess K, Bhargava P, Straley K, Karnik R, Meissner A, Small D *et al*: **Proto-oncogenic role of mutant IDH2 in leukemia initiation and maintenance**. *Cell stem cell* 2014, **14**(3):329-341.